4197

HEAT TRANSFER IN POLYMER MELT FLOWS

by

ENNO ERIC AGUR, B.A.Sc.

A Thesis
Submitted to the School of Graduate Studies
in Partial Fulfilment of the Requirements
for the Degree
Master of Engineering

McMaster University
April 1978

MASTER OF ENGINEERING (1978) McMASTER UNIVERSITY
(Chemical Engineering)

TITLE: Heat Transfer in Polymer Melt Flows

AUTHOR: Enno Eric Agur, B.A.Sc. (University of Waterloo)

SUPERVISOR: Dr. J. Vlachopoulos

NUMBER OF PAGES: xvi, 266

ABSTRACT

The heat transfer problem of polymer melts flowing through narrow channels and tubes has been studied. Four types of flow with constant temperature boundary conditions were examined:

(i) drag (or Couette) flow between parallel plates,

(ii) Poiseuille flow between parallel plates,

(iii) Poiseuille flow through a tube with circular cross-section, and

(iv) drag flow between converging plates.

In each case, the equations of conservation of mass, momentum and energy were solved simultaneously by the implicit finite difference method. A power-law temperature-dependent viscosity model was used and viscous dissipation was taken into account. Velocity and temperature profiles, pressure distributions, bulk temperatures and local Nusselt numbers have been calculated and are presented as a function of the axial distance along the channel. Results obtained by using the power-law temperature-dependent viscosity model were also compared with the power-law temperature-independent viscosity model and the Newtonian, constant viscosity model results.

ACKNOWLEDGEMENTS

It is a pleasure to acknowledge my gratitude to my research supervisor, Dr. John Vlachopoulos of the Department of Chemical Engineering. His patience, guidance and encouragement made this research project very interesting and enjoyable.

I would also like to express my appreciation to others who helped:

To the National Research Council of Canada which provided financial support in the form of a post graduate scholarship and research grants;

To Ms. Debbie Sanché who typed this manuscript, and

To my wife, Anne, for her patience and encouragement. It is to her that I dedicate this thesis.

CONTENTS

FIGURES

TABLES

NOTATION

Dimensions and units

The absolute system of dimensions (mass-length-time-temperature) is used, and the units are normally SI (Système International d'Unités) units:

m	mass, kg (kilograms)
L	length, m (metres)
t	time, s (seconds)
T	temperature, °C (Celsius) or K (Kelvin)
E	energy, J (joules)
F	force, N (newtons)

Variables

A	constant in constitutive equation (3.13), $Pa \cdot s^n$.
A_m	coefficient in finite difference equations, dimensionless.
a	inside radius of circular tube, cm.
B	constant in constitutive equation (3.13), K^{-1}.
B(X)	dimensionless distance between converging plates, Eq. (7.7).
B_m	coefficient in finite difference equations, dimensionless.
b,b(x)	distance between plates, cm.
C_m	coefficient in finite difference equations, dimensionless.
C_p	specific heat of fluid, J/(kg·K).
D	diameter, cm.
D_m	coefficient in finite difference equations, dimensionless.

E_m coefficient in finite difference equations, dimensionless.

F_m coefficient in finite difference equations, dimensionless.

G_m coefficient in finite difference equations, dimensionless.

$\overline{g}$ gravitational acceleration, m/s^2.

H_m coefficient in finite difference equations, dimensionless.

h heat transfer coefficient, W/(m$^2\cdot$K).

k thermal conductivity of fluid, W/(m$\cdot$K).

L length, cm.

M number of grid divisions perpendicular to the direction of flow on the finite difference grid.

N number of grid divisions in the direction of flow on the finite difference grid.

n power-law index, dimensionless.

P dimensionless pressure, Eqs. (5.7), (6.9) and (7.7).

P^n dimensionless pressure at column n on finite difference grid.

p pressure, Pa.

Q volumetric flow rate, cm^3/s.

q heat flux, W/m^2.

R dimensionless radial distance in tube, Eq. (6.9).

r radial distance in tube, cm.

T temperature of fluid, °C or K.

T_o temperature of fluid at the entrance of channel, °C.

T_{bulk} bulk temperature of fluid, °C.

T_m melting temperature of polymer, K.

T_w, T_{w1}, T_{w2} wall temperatures, °C.

t time, s.

U dimensionless axial velocity, Eqs. (4.6), (5.7), (6.9) and (7.7).

U_m^n, $U1_m^n$, $U2_m^n$ dimensionless axial velocities at node (m,n) on finite difference grid.

u axial velocity, cm/s.

u_{avg} average axial velocity of fluid, cm/s.

u_{max} velocity of moving plate in drag flow, cm/s.

V_m^n dimensionless axial velocity (obtained by interpolation).

$\overline{v}$ velocity of fluid, cm/s.

v velocity of fluid perpendicular to the axial direction (in Cartesian co-ordinates), cm/s.

$\overline{\overline{W}}$ sub-matrix in Eq. (7.20).

W_m coefficient in finite difference equations, dimensionless.

w mass flow rate, kg/s.

X dimensionless axial distance (in Cartesian co-ordinates), Eqs. (4.6), (5.7), (7.7).

X_m coefficient in finite difference equations, dimensionless.

x axial distance (in Cartesian co-ordinates), cm.

Y dimensionless distance perpendicular to axial direction (in Cartesian co-ordinates), Eqs. (4.6), (5.7), (7.7).

Z dimensionless axial distance in tube, Eq. (6.9).

Z_m coefficient in finite difference equations, dimensionless.

z axial distance in tube, cm.

$\overline{\overline{\Delta}}$ rate of deformation tensor, Eq. (3.10), s^{-1}.

Δa a_2-a_1, in which 1 and 2 refer to two control surfaces.

η shear viscosity, Pa·s.

η_m^n shear viscosity at node (m,n) on finite difference grid, Pa·s.

θ dimensionless temperature, Eqs. (4.6), (5.7), (6.9), (7.7).

θ_{bulk} dimensionless bulk temperature.

θ_m^n, $\theta 1_m^n$, $\theta 2_m^n$, θP_m^n, θQ_m^n dimensionless temperature at node (m,n) on finite difference grid.

ν $\frac{n+1}{n}$

π 3.14159...

ρ fluid density, kg/m^3.

$\overline{\overline{\tau}}$ viscous stress tensor, Pa.

τ_{yx} shear stress in the x-direction and acting on the plane perpendicular to the y-axis, Pa.

ϕ_m coefficient in finite difference equations, dimensionless.

ψ_m coefficient in finite difference equations, dimensionless.

Subscripts

a refers to an average heat transfer coefficient.

m refers to a row in the finite difference grid.

o refers to the entrance of the channel.

x, z refer to local heat transfer coefficients.

Superscripts

n refers to a column in the finite difference grid.

Overscripts

— refers to a vector.

═ refers to a tensor or matrix.

Dimensionless Groups

Gz Graetz number $\equiv \frac{wC_p}{kL}$.

Nu Nusselt number $\equiv \frac{hD}{k}$.

Re Reynolds number $\equiv \frac{\rho u D}{\eta}$.

Mathematical Conventions

$\frac{D}{Dt}$ substantial derivative; $\frac{DT}{Dt} = \frac{\partial T}{\partial t} + u\frac{\partial T}{\partial x} + v\frac{\partial T}{\partial y} + w\frac{\partial T}{\partial z}$.

∇ vector differential operator.

CHAPTER 1

INTRODUCTION

The heat transfer problem for fluids flowing through narrow channels and tubes has been studied quite extensively and many publications have appeared in the literature. Both Newtonian and non-Newtonian fluids have been treated by either approximate analytical or numerical methods. A large number of papers published thus far, however, report only velocity and temperature profiles inside the channel without any mention of the heat transfer coefficients involved. These analyses can be used for such things as the determination of temperature rise due to viscous dissipation, and the influence of the power-law index on velocity and temperature profile development. The publications that include heat transfer coefficients are mostly restricted to cases of limited applicability. For instance, some deal with dilute polymer solutions where the heat generated by viscous dissipation is negligible. Others do not include temperature dependent rheological laws. In most cases, average heat transfer coefficients have been reported. Local heat transfer coefficients are presented only in a few papers.

The objective of this thesis is to develop a systematic and comprehensive heat transfer analysis of polymer melts flowing through narrow channels and tubes. Four types of flow with different temperature boundary conditions will be examined:

1. drag (or Couette) flow between parallel plates,
2. Poiseuille flow between parallel plates,

3. Poiseuille flow through a tube with circular cross-section, and

4. drag flow between converging plates.

In each case, the equations of conservation of mass, momentum and energy are solved simultaneously by an implicit finite difference method. A temperature and shear rate dependent viscosity model is used and viscous dissipation is taken into account. The velocity and temperature profiles, bulk temperatures and local Nusselt numbers are calculated along the length of each channel.

CHAPTER 2

LITERATURE SURVEY

2.1 Laminar Flow through a Tube with Circular Cross-section

Most of the studies available in the literature on heat transfer to fluids flowing through narrow channels and tubes are for tubular geometry. Other flow geometries including flow between parallel and converging plates will be reviewed in the next section. Since the flow of polymer melts is laminar, this literature review is restricted to those publications dealing with laminar fluid flows. Also, since polymer melts are non-Newtonian, most of the papers reviewed deal with non-Newtonian fluids, with the exception of some earlier papers.

In the literature, the problem of heat transfer to fluids flowing through narrow channels is often referred to as the Graetz-Nusselt problem (33). It was Graetz (24) in 1885 and Nusselt (47) in 1910 who first presented solutions to the following problem: A fluid flows with a fully-developed laminar parabolic velocity profile in the +z-direction in a circular tube of constant radius R. In the region $z < 0$, the fluid is at a constant temperature T_o. At $z = 0$, the fluid passes into a region where the tube walls are held at a constant temperature T_w, greater or smaller than T_o, for all $z > 0$. The problem can be described by the following differential equations:

Momentum: $$\frac{-dp}{dz} + \frac{1}{r}\frac{d}{dr}(r\,\tau_{rz}) = 0 \qquad (2.1)$$

$$\text{Energy:} \qquad \underset{\text{convective term}}{\rho C_p u \frac{\partial T}{\partial z}} = \underset{\text{conductive term}}{\frac{k}{r}\frac{\partial}{\partial r}\left(r \frac{\partial T}{\partial r}\right)} + \underset{\text{viscous dissipation term}}{\tau_{rz} \frac{du}{dr}} \tag{2.2}$$

with the accompanying boundary conditions:

$$\begin{aligned} &\text{at } z = 0, \quad 0 \le r \le R \qquad T = T_o \\ &\text{at } z > 0, \quad r = R \qquad\quad\ \ T = T_w \end{aligned} \tag{2.3}$$

Both Graetz and Nusselt obtained the temperature profiles $T(r,z)$ in the flowing fluid by an approximate analytical method. They assumed that the viscosity was constant and ignored viscous dissipation. Graetz obtained the following expression for the average Nusselt number:

$$Nu_a = \frac{2wC_p}{\pi kL} \left[\frac{1-8\psi_1(X)}{1+8\psi_1(X)}\right] \tag{2.4}$$

where Nu_a = average Nusselt number

$\psi_1(X)$ = convergent infinite series of exponential functions in $\frac{\pi kL}{4wC_p}$

In 1951, Brinkman (7) presented an approximate analytical solution to the above problem, taking into account viscous dissipation. In addition to the constant wall temperature problem, he also solved the adiabatic wall problem. However, no Nusselt numbers were reported for either case. Bird (4) in 1955 extended Brinkman's solutions to include non-Newtonian fluids which obey the power-law relation. More recently, approximate analytical solutions for non-Newtonian fluids have been presented by

Lyche and Bird (33), Toor (67, 68), Schenk and Van Laar (57), Whiteman and Drake (72), Bird (5), Gill (22, 23), Foraboschi and Federico (15), Matsuhisa and Bird (37), Martin (36), Šesták and Charles (59), Mitsuishi and Miyatake (44), Smorodinskii and Froishteter (60), Sukanek (62), Koyama, Kanamaru and Wada (29), Galili, Rigbi and Takserman-Krozer (18), Sundaram and Nath (63), Faghri and Welty (13) and Pearson (51). Their work, in addition to others which will be discussed later, is summarized in Table 2-1.

The analytical solutions found in the literature are very complex, as they consist of converging infinite series of exponential functions. When the series are slow to converge, the solutions usually are not very accurate. However, with the advent of high-speed computers, it has become possible to solve the Graetz-Nusselt problem numerically. The finite difference method is most commonly used. Numerical solutions found in the literature include those by Gee and Lyon (20), Christiansen and Craig (8), McKillop (38), Christiansen, Jensen and Tao (9), Morrette and Gogos (45), Forsyth and Murphy (17), Kim and Collins (28), Forrest and Wilkinson (16), Vlachopoulos, Larocque and Ho (71), Mahalingam, Tilton and Coulson (34), Mahalingam, Chan and Coulson (35), Winter (74), Popovska and Wilkinson (53), and Nunn and Fenner (46). Their work is summarized in Table 2-1.

An alternative method which follows Lévêque's approximation has been used in several papers. The method is discussed here for the sake of completeness, since it is relevant to dilute polymer solutions and not to molten polymers. In 1922 Lévêque (32) solved the same Newtonian fluid flow problem as did Graetz and Nusselt, except that he assumed the velocity profile near the wall to be linear. His final result was:

$$Nu_a = 1.75\ Gz^{1/3} \tag{2.5}$$

where $Gz = \text{Graetz number} = \frac{wC_p}{kL}$

It should be noted that temperature profiles cannot be obtained from this method. Lévêque's approximation has been extended to non-Newtonian fluids by the use of empirical corrections to account for temperature dependence of viscosity and the effect of free convection. Solutions using this method have been presented by Pigford (52), Metzner, Vaughn and Houghton (39), Metzner and Gluck (40) and Oliver and Jenson (48). In all of the solutions, viscous dissipation has been neglected. For this reason, the derived equations are not relevant for molten polymers, but are acceptable only for dilute polymer solutions where the heat generated by viscous dissipation is negligible.

In addition to the papers discussed above, four review papers have appeared in the literature, namely those by Metzner (41), Porter (54), Astarita and Mashelkar (1) and Winter (75). A recently published book by Middleman (43) contains a discussion of heat and mass transfer to flowing polymer melts. There is also a discussion of heat generation and heat transfer in polymer melt flows in a paper by Pearson (50).

Few papers have been published which report experimentally measured temperature profiles of molten polymers flowing through circular tubes. These include papers by Griskey and Wiehe (25), Saltuk, Siskovik and

Griskey (56) and Bassett and Welty (2). Here, the experimental results obtained have been compared with theoretical predictions made by other investigators.

2.2 Other Flow Geometries

Studies involving flows through geometries other than circular tubes have been covered less extensively in the literature. Drag flow between parallel plates has been studied by Tien (65), Turian (69), Gavis and Laurence (19) and Winter (73, 74). Poiseuille flow between parallel plates has been studied by Prins, Mulder and Schenk (55), Tien (66), Suckow, Hrycak and Griskey (61), Vlachopoulos and Keung (70), Payvar (49), Vlachopoulos, Larocque and Ho (71), Cox and Macosko (11), Winter (74), Sundaram and Nath (63) and Pearson (51). Both approximate analytical and numerical solutions have been presented. They are summarized in Table 2-1.

Very little has been reported in the literature about drag flow between converging plates. Schlichting (58), Bergen (3) and Tadmor and Klein (64) have obtained analytical solutions for the velocity profiles and pressure distribution of a Newtonian fluid. Huebner (27) has obtained velocity and temperature profiles for a Newtonian fluid using the finite element method. As yet, no work on non-Newtonian fluids has been published in this area.

Table 2-1. Summary of Literature

Investigator(s)	Ref.	Fluid	Viscous Dissipation	Temperature Dependent Viscosity	Comments
Graetz (1885)	24	Newtonian	No	No	Tube with circular cross-section Approximate analytical solution Temperature profiles Average Nusselt numbers
Nusselt (1910)	47	Newtonian	No	No	Tube with circular cross-section Approximate analytical solution Temperature profiles Average Nusselt numbers
Lévêque (1922)	32	Newtonian	No	No	Tube with circular cross-section Lévêque's approximation Average Nusselt numbers
Brinkman (1951)	7	Newtonian	Yes	No	Tube with circular cross-section (i) Isothermal walls (ii) Adiabatic walls Approximate analytical solution Temperature profiles
Prins, Mulder and Schenk (1951)	55	Newtonian	No	No	Poiseuille flow-parallel plates Isothermal walls Approximate analytical solution Temperature profiles and local Nusselt numbers

Table 2-1. (continued)

Investigator(s)	Ref.	Fluid	Viscous Dissipation	Temperature Dependent Viscosity	Comments
Bird (1955)	4	Power-law	Yes	No	Tube with circular cross-section (i) Isothermal walls (ii) Adiabatic walls Approximate analytical solution Temperature profiles Experimental data (polymer melts)
Pigford (1955)	52	Power-law	No	No	Tube with circular cross-section Isothermal walls Lévêque's approximation Average Nusselt numbers
Lyche and Bird (1956)	33	Power-law	No	No	Tube with circular cross-section Isothermal walls Approximate analytical solution Temperature profiles and average Nusselt numbers
Gee and Lyon (1957)	20	Power-law	Yes	Yes	Tube with circular cross-section Isothermal walls Numerical integration Temperature profiles Experimental data (polymer melts)
Toor (1957)	67	Power-law	Yes	No	Tube with circular cross-section (i) Adiabatic flow (no conduction) (ii) Isothermal walls Approximate analytical solution Temperature profiles

Table 2-1. (continued)

Investigator(s)	Ref.	Fluid	Viscous Dissipation	Temperature Dependent Viscosity	Comments
Metzner, Vaughn and Houghton (1957)	39	Pseudo-plastic	No	Yes	Tube with circular cross-section Isothermal walls Lévêque's approximation Average Nusselt numbers Experimental data (polymer solutions)
Toor (1958)	68	Power-law	Yes	No	Tube with circular cross-section Isothermal walls Approximate analytical solution Temperature profiles and average Nusselt numbers
Schenk and Van Laar (1958)	57	Power-law, Prandtl-Eyring	Yes	No	Tube with circular cross-section Constant heat flux at walls Approximate analytical solution Temperature profiles and local Nusselt numbers
Whiteman and Drake (1958)	72	Power-law	No	No	Tube with circular cross-section Isothermal walls Approximate analytical solution Temperature profiles and Average Nusselt numbers

Table 2-1. (continued)

Investigator(s)	Ref.	Fluid	Viscous Dissipation	Temperature Dependent Viscosity	Comments
Bird (1959)	5	Power-law	No	No	Tube with circular cross-section Constant heat flux at walls Approximate analytical solution Temperature profiles and local Nusselt numbers
Bergen (1959)	3	Newtonian	No	No	Drag flow-converging plates Analytical solution Velocity profiles and pressure distribution
Metzner and Gluck (1960)	40	Pseudo-plastic	No	Yes	Tube with circular cross-section Isothermal walls Leveque's approximation Average Nusselt numbers Experimental data (polymer solutions)
Tien (1961)	65	Power-law	Yes	No	Drag flow-parallel plates No convective term Isothermal walls Analytical solution Temperature profiles

Table 2-1. (continued)

Investigator(s)	Ref.	Fluid	Viscous Dissipation	Temperature Dependent Viscosity	Comments
Gill (1962)	22	Power-law	Yes	No	Tube with circular cross-section (i) Isothermal walls (ii) Constant wall heat flux Approximate analytical solution Temperature profiles
Christiansen and Craig (1962)	8	Power-law	No	Yes	Tube with circular cross-section Isothermal walls Finite difference solution Average Nusselt numbers Experimental data (polymer solutions)
Tien (1962)	66	Power-law	No	No	Poiseuille flow-parallel plates Isothermal walls Approximate analytical solution Temperature profiles and local Nusselt numbers
Gill (1963)	23	Power-law	No	No	Tube with circular cross-section Isothermal walls Approximate analytical solution Temperature profiles and local Nusselt numbers

Table 2-1. (continued)

Investigator(s)	Ref.	Fluid	Viscous Dissipation	Temperature Dependent Viscosity	Comments
Foraboschi and Federico (1964)	15	Power-law	No	No	Tube with circular cross-section Arbitrary internal heat generation Isothermal walls Approximate analytical solution Temperature profiles and local Nusselt numbers
McKillop (1964)	38	Power-law	No	No	Tube with circular cross-section (i) Isothermal walls (ii) Constant heat flux at walls Finite difference solution Local Nusselt numbers
Oliver and Jenson (1964)	48	Pseudo-plastic	No	Yes	Tube with circular cross-section Isothermal walls Lévêque's approximation Average Nusselt numbers Experimental data (polymer solutions)
Matsuhisa and Bird (1965)	37	Ellis model	No	No	Tube with circular cross-section (i) Isothermal walls (ii) Constant heat flux at walls Approximate analytical solution Local Nusselt numbers

Table 2-1. (continued)

Investigator(s)	Ref.	Fluid	Viscous Dissipation	Temperature Dependent Viscosity	Comments
Turian (1965)	69	Power-law, Ellis model	Yes	Yes	Drag flow-parallel plates No convective term (i) Isothermal walls (ii) One isothermal, one adiabatic wall Perturbation solution Temperature profiles
Metzner (1965)	41				Review article (130 references)
Griskey and Wiehe (1966)	25				Experimental temperature profiles and average Nusselt numbers (polymer melts)
Christiansen, Jensen and Tao (1966)	9	Power-law	No	Yes	Tube with circular cross-section Isothermal walls Finite difference solution Average Nusselt numbers Experimental data (polymer solutions)

Table 2-1. (continued)

Investigator(s)	Ref.	Fluid	Viscous Dissipation	Temperature Dependent Viscosity	Comments
Martin (1967)	36	Power-law	Yes	Yes	(i) Tube with circular cross-section (ii) Tangential flow-concentric cylinder (iii) Drag flow-parallel plates No convective term Isothermal walls Approximate analytical solution Temperature profiles
Gavis and Laurence (1968)	19	Power-law	Yes	Yes	Drag flow-parallel plates No convective term (i) Isothermal walls (ii) One isothermal and one adiabatic wall Approximate analytical solution Temperature profiles
Morrette and Gogos (1968)	45	Power-law	Yes	Yes	Tube with circular cross-section (i) Isothermal walls (ii) Adiabatic walls Finite difference solution Temperature profiles
Sesták and Charles (1968)	59	Power-law	Yes	No	Tube with circular cross-section Constant heat flux at walls Approximate analytical solution Local Nusselt numbers

Table 2-1. (continued)

Investigator(s)	Ref.	Fluid	Viscous Dissipation	Temperature Dependent Viscosity	Comments
Schlichting (1968)	58	Newtonian	No	No	Drag flow-converging plates Analytical solution Velocity profiles and pressure distribution
Mitsuishi and Miyatake (1969)	44	Power-law	No	Yes	Tube with circular cross-section Constant heat flux at walls Approximate analytical solution Local Nusselt numbers
Forsyth and Murphy (1969)	17	Power-law	Yes	Yes	Tube with circular cross-section Isothermal walls Finite difference solution Temperature profiles Experimental data (polymer melts)
Tadmor and Klein (1970)	64	Newtonian	No	No	Drag flow-converging plates Analytical solution Velocity profiles and pressure distribution
Kim and Collins (1971)	28	Power-law	Yes	Yes	Tube with circular cross-section Isothermal walls Predictor-corrector, Euler methods Temperature profiles Experimental data (polymer melts)

Table 2-1. (continued)

Investigator(s)	Ref.	Fluid	Viscous Dissipation	Temperature Dependent Viscosity	Comments
Smorodinskii and Froishteter (1971)	60	Power-law with yield stress	Yes	No	Tube with circular cross-section Isothermal wall Approximate analytical solution Temperature profiles and local Nusselt numbers
Suckow, Hrycak and Griskey (1971)	61	Power-law	No	No	Poiseuille flow-parallel plates Isothermal walls Approximate analytical solution Temperature profiles
Sukanek (1971)	62	Power-law	Yes	Yes	Tube with circular cross-section No convective term Isothermal walls Analytical solution Temperature profiles
Porter (1971)	54				Review article (263 references)
Koyama, Kanamaru and Wada (1972)	29	Power-law	No	No	Tube with circular cross-section Isothermal walls Approximate analytical solution Temperature profiles Experimental data (polymer solutions)

Table 2-1. (continued)

Investigator(s)	Ref.	Fluid	Viscous Dissipation	Temperature Dependent Viscosity	Comments
Vlachopoulos and Keung (1972)	70	Power-law	Yes	No	Poiseuille flow-parallel plates Isothermal walls Finite difference solution Bulk temperatures and local Nusselt numbers
Saltuk, Siskovic and Griskey (1972)	56				Experimental measurement of temperature profiles and average Nusselt numbers (polymer melts)
Pearson (1972)	50				Discussion of heat generation, heat transfer in polymer melt flows
Winter (1972)	73	Power-law	Yes	Yes	Drag flow-parallel plates Isothermal walls Approximate analytical solution Temperature profiles
Payvar (1973)	49	Power-law, Ellis fluid	Yes	No	Poiseuille flow-parallel plates -circular tube Constant heat flux at walls Approximate analytical solution Temperature profiles and local Nusselt numbers

Table 2-1. (continued)

Investigator(s)	Ref.	Fluid	Viscous Dissipation	Temperature Dependent Viscosity	Comments
Griskey, Choi and Siskovic (1973)	26				Experimental measurement of temperature profiles (polymer melts)
Forrest and Wilkinson (1973)	16	Power-law	Yes	Yes	Tube with circular cross-section Isothermal walls Finite difference solution Average Nusselt numbers
Vlachopoulos, Larocque and Ho (1974)	71	Power-law	Yes	No	Poiseuille flow-parallel plates -circular tubes Isothermal walls Finite difference solution Bulk temperatures and local Nusselt numbers
Cox and Macosko (1974)	11	Pseudo-plastic	Yes	Yes	Poiseuille flow-circular die -slit die -annular die Constant heat transfer coefficient Finite difference solution Temperature profiles Experimental data (polymer melts)

Table 2-1. (continued)

Investigator(s)	Ref.	Fluid	Viscous Dissipation	Temperature Dependent Viscosity	Comments
Huebner (1974)	27	Newtonian	Yes	Yes	Drag flow-converging plates Adiabatic walls Finite element method Velocity and temperature profiles
Mahalingam, Tilton and Coulson (1975)	34	Power-law	No	Yes	Tube with circular cross-section Constant heat flux at walls Finite difference solution Local Nusselt numbers Experimental data (polymer solutions)
Mahalingam, Chan and Coulson (1975)	35	Power-law	No	Yes	Tube with circular cross-section Constant heat flux at walls Approximate analytical solution Temperature profiles Experimental data (polymer solutions)
Galili, Rigbi and Takserman-Krozer (1975)	18	Power-law	Yes	Yes	Tube with circular cross-section (i) Isothermal walls (ii) Adiabatic walls Perturbation solution Temperature profiles

Table 2-1. (continued)

Investigator(s)	Ref.	Fluid	Viscous Dissipation	Temperature Dependent Viscosity	Comments
Winter (1975)	74	Power-law	Yes	Yes	Poiseuille flow-circular tube -plane slit -annular slit (i) Isothermal walls (ii) One isothermal, one adiabatic wall Finite difference solution Temperature profiles
Bassett and Welty (1975)	2				Experimental measurement of average Nusselt numbers (polymer solutions)
Sundaram and Nath (1976)	63	Power-law	Yes	No	Poiseuille flow-circular tube -parallel plates Constant heat flux at walls Approximate analytical solution Local Nusselt numbers
Astarita and Mashelkar (1977)	1				Review article (247 references)
Faghri and Welty (1977)	13	Power-law	No	No	Tube with circular cross-section Arbitrary circumferential wall heat flux Approximate analytical solution Temperature profiles and local Nusselt numbers

Table 2-1. (continued)

Investigator(s)	Ref.	Fluid	Viscous Dissipation	Temperature Dependent Viscosity	Comments
Winter (1977)	75				Review article (133 references)
Middleman (1977)	43				Discussion of heat and mass transfer to flowing polymer melts
Popovska and Wilkinson (1977)	53	Power-law	Yes	Yes	Tube with circular cross-section Isothermal walls Finite difference solution Temperature profiles and average Nusselt numbers Experimental data (polymer solutions)
Pearson (1977)	51	Power-law	Yes	Yes	Poiseuille flow-parallel plates -circular tube Isothermal walls Similarity solution No results given
Nunn and Fenner (1977)	46	Power-law	Yes	Yes	Tube with circular cross-section Adiabatic walls Finite difference solution Temperature profiles and bulk temperatures

CHAPTER 3

GENERAL MOMENTUM AND HEAT TRANSFER ANALYSIS

The problem of heat transfer to molten polymers flowing through narrow channels can be fully described in terms of the equations of conservation of mass, momentum and energy. To obtain solutions, we need the boundary conditions at the channel walls and constitutive relations which describe the stress and temperature behaviour of the melts. Solutions of the conservation equations in general form are very complicated even for Newtonian, constant property fluids. The introduction of constitutive equations describing polymer melt behaviour renders the system of equations extremely difficult even for very simple boundary conditions. The conservation equations must be simplified substantially to even make solution by numerical methods feasible. A usual simplification in polymer melt processing is referred to as the lubrication approximation (14).

In this chapter, the conservation equations, the constitutive relation and the method of solution are presented and discussed. The principal assumptions involved are numbered consecutively as they occur in the analysis. The boundary conditions will be covered in the subsequent chapters dealing with the individual flow cases.

3.1 Conservation Equations

In general tensorial form, the conservation equations are (6):

Mass: $$\frac{D\rho}{Dt} + \rho(\nabla \cdot \overline{v}) = 0 \qquad (3.1)$$

Momentum: $$\rho \frac{D\overline{v}}{Dt} = - \nabla p + \nabla \cdot \overline{\overline{\tau}} + \rho \overline{g} \qquad (3.2)$$

Energy: $$\rho C_p \frac{DT}{Dt} = - \nabla \cdot \overline{q} + \overline{\overline{\tau}} \cdot \nabla \overline{v} \qquad (3.3)$$

Assuming that:

(a) the melt is incompressible (constant density), the continuity equation for conservation of mass (3.1) reduces to:

$$\nabla \cdot \overline{v} = 0 \qquad (3.4)$$

The equation of conservation of momentum involves a balance between inertia, viscous, pressure and body forces. Because polymer melt flows are very slow flows with Re of the order of 10^{-4}, it may be assumed that:

(b) inertia effects are negligible in comparison with viscous and pressure forces.

Also assuming that:

(c) body forces (such as gravity) are negligible in comparison with viscous and pressure forces, and

(d) the flow is steady ($\frac{\partial}{\partial t} \equiv 0$),

the equation of conservation of momentum (3.2) reduces to:

$$- \nabla \cdot p + \nabla \cdot \overline{\overline{\tau}} = \overline{0} \qquad (3.5)$$

Turning to the equation of conservation of energy (3.3), the following assumptions are usually made:

(e) the thermal conductivity, k, is constant, and

(f) the specific heat at constant pressure, C_p, is constant.

The resulting energy equation is:

$$\rho C_p \, \overline{v} \cdot \nabla T = k\nabla^2 T + \overline{\overline{\tau}}:\nabla \overline{v} \tag{3.6}$$

Further simplifications to the conservation equations are usually introduced with the aid of the lubrication approximation (14) which is applicable for flows through narrow channels. Assuming that:

(g) the velocity components perpendicular to the direction of flow are negligible compared to the axial velocity component,

(h) the pressure is uniform perpendicular to the direction of flow,

(i) normal stresses are neglected,

(j) there is no slip at the walls,

(k) heat transfer by conduction in the direction of flow is negligible compared to both convection in the direction of flow and conduction perpendicular to the direction of flow,

the conservation equations (3.4, 3.5 and 3.6) reduce to the following, in Cartesian co-ordinates:

Mass: $$\frac{du}{dx} = 0 \tag{3.7}$$

Momentum: $$-\frac{dp}{dx} + \frac{d\tau_{yx}}{dy} = 0 \tag{3.8}$$

Energy: $$\rho C_p u \frac{\partial T}{\partial x} = k\frac{\partial^2 T}{\partial y^2} + \tau_{yx}\left(\frac{du}{dy}\right)^2 \tag{3.9}$$

For flow through a circular tube, the above equations must be expressed using cylindrical co-ordinates.

3.2 Constitutive Equation

Constitutive equations describe the stress and temperature behaviour of polymer melts. For polymer melts flowing through narrow channels, the power-law temperature-dependent constitutive equation has been used extensively in the literature. One way of expressing such an equation is (64):

$$\overline{\overline{\tau}} = \eta \, \overline{\overline{\Delta}} \tag{3.10}$$

where the shear viscosity, η, is given by

$$\eta = Ae^{-Bn(T-T_m)} \left| \sqrt{\frac{I_2}{2}} \right|^{n-1} \tag{3.11}$$

and A, B are empirical constants

n = power-law index

T_m = melting temperature of polymer

$\overline{\overline{\Delta}}$ = deformation rate tensor, in 2 dimensions

$$= \begin{matrix} 2\frac{\partial u}{\partial x} & \frac{\partial u}{\partial y} + \frac{\partial v}{\partial x} \\ \frac{\partial v}{\partial x} + \frac{\partial u}{\partial y} & 2\frac{\partial v}{\partial y} \end{matrix}$$

I_2 = second invariant of $\overline{\overline{\Delta}}$

$$= \Delta_{ij} \, \Delta_{ji}$$

$$= 4\left(\frac{\partial u}{\partial x}\right)^2 + 2\left(\frac{\partial u}{\partial y} + \frac{\partial v}{\partial x}\right)^2 + 4\left(\frac{\partial v}{\partial y}\right)^2$$

Using the continuity equation (3.7) and the assumption (g) that the velocity component, v, is negligible compared to the velocity component, u, Eqs. (3.10) and (3.11) reduce to the following:

$$\tau_{yx} = \eta \frac{du}{dy} \tag{3.12}$$

$$\eta = Ae^{-Bn(T-T_m)} \left|\frac{du}{dy}\right|^{n-1} \tag{3.13}$$

In using the above form of constitutive equation, it is assumed that the viscosity is independent of pressure. This is a good assumption for usual processing conditions.

Power-law constitutive equations, the above included, yield an infinite apparent viscosity at shear rates approaching zero, as is the case for flow at the centre-line of a tube. This problem can be overcome by choosing a minimum shear rate, below which the apparent viscosity is held constant. This is a good assumption because most polymer melts behave like Newtonian fluids at very low shear rates (usually less than 10^{-1}-10^{-2} sec^{-1}).

The type of constitutive equation described above has been applied quite successfully to polymer melts in steady shear flow. Earlier it was assumed that the effect of normal stresses on the flow is negligible. This assumption is valid for simple shear flow such as flow between long parallel plates and through long tubes. However, in flows through tapered channels, such as drag flow between converging plates, normal stresses have a small effect on the flow, but their importance in heat transfer is not known (43).

3.3 Method of Solution

Given a suitable constitutive equation and appropriate boundary conditions for velocity, pressure and temperature, the simplified conservations equations can be solved numerically. An iterative implicit finite difference method (21) has been used to obtain velocity and temperature profiles and a pressure distribution in each of the four flow cases. A brief description of the method will be given here. More detailed descriptions are located in the subsequent chapters dealing with the different types of flow.

A finite difference grid is superimposed on the flow field as illustrated in Fig. 3-1.

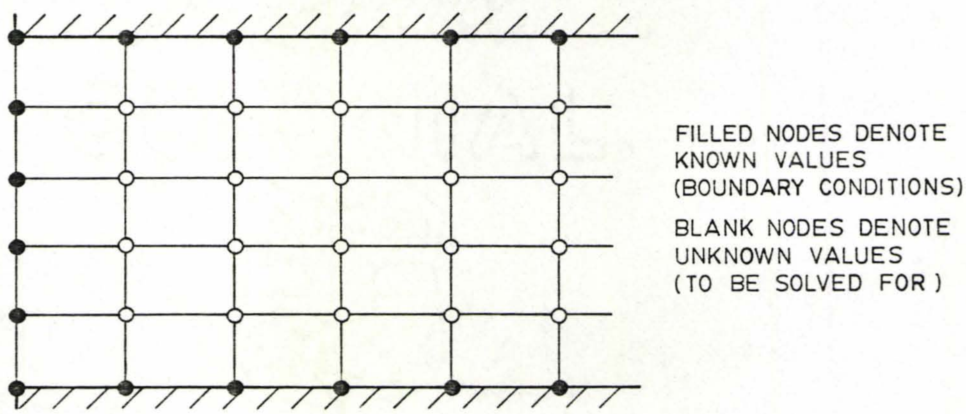

Fig. 3-1. Finite difference grid.

Values of velocity, pressure and temperature are calculated at the nodal points of the grid by replacing the derivatives in the conservation equations with the appropriate finite difference approximations, and then solving these difference equations at each node. This can be done explicitly or implicitly. In the explicit method, the difference equations are solved one node at a time for all the nodes in the grid. In the implicit method, two possibilities exist. The equations for an entire column of nodes can be solved simultaneously, in which case progress through the grid is made by "marching" downstream column by column. Alternatively, the equations at each node in the grid can be solved simultaneously. When the system of equations is parabolic (when boundary conditions are specified at three of the four boundaries of the flow field) the marching procedure is used. When the system of equations is elliptic (when boundary conditions are specified at all four boundaries) the equations for the entire grid must be solved simultaneously.

Looking at the conservation equations and keeping in mind the constitutive equations (3.12) and (3.13), we see that the momentum equation (3.8) contains a viscosity term which is a function of temperature and shear rate, and that the energy equation (3.9) contains a viscosity, velocity and velocity gradient. Since these equations are coupled by velocity and temperature, they cannot be solved independently. It is, however, possible to iterate to a solution by alternately solving the momentum and energy equations until the solutions converge. For example, in the "marching" procedure at a given column, the initial estimates of the velocity and temperature profiles along the column are obtained from the final profiles calculated in the preceding column. Once the new profiles have been calculated, they are compared with the estimated profiles. If the changes are greater than a specified tolerance, the profiles are recalculated until the desired error tolerance is achieved. The most recently calculated profiles are always used as profile estimates in the next iteration. When the desired error tolerance has been attained, the profiles at the next column downstream are calculated. Thus, the temperature and velocity profiles and the pressure distribution is calculated for the entire flow field.

3.4 Convergence, Stability and Step Size

Problems with convergence and stability arise from the substitution of finite difference approximations in the differential equations. By convergence, it is meant that the results of the finite difference method approach analytical values as the step sizes become infinitely small (21). By stability, it is meant that errors made at one stage of the calculations do not grow as the computations are continued, but instead damp out (21). These errors are due to round-off, the choice of a finite step size, and the use of a finite tolerance in the iteration procedure.

Convergence to the correct solution of the finite difference results can only be rigorously tested by comparison with an analytical solution. In simpler cases, stability criteria have been developed, such as for the solution of single linear partial differential equations (21). However, in our case, less rigorous techniques for testing convergence and stability must be used since no analytical solutions have been developed, and the equations to be solved are much more complex.

A good indication of the convergence and stability of the finite difference results is the negligible change in results obtained when the step sizes in the finite difference grid are decreased (10). In selecting step sizes, it should be remembered that by using smaller step sizes, the cost of computing increases. This increase can be significant when an iterative type of solution is used. There is also a lower limit of accuracy attainable by decreasing the step size, that being when round-off errors begin to dominate. Usually, however, such accuracy is not necessary in engineering design.

These general guidelines were followed in selecting the appropriate step sizes in the finite difference programs. The programs were run using several step sizes and step size ratios across and along the flow field. The step sizes used are given in the subsequent chapters. In each case, the results obtained are independent of step size within at least 3 significant digits.

CHAPTER 4

DRAG FLOW BETWEEN PARALLEL PLATES

4.1 Mathematical Formulation

The physical system for drag (or Couette) flow between semi-infinite parallel plates is illustrated in Fig. 4-1. The two plates are spaced apart by a distance, b. One plate is stationary and has a constant temperature, T_{w1}, and the other plate is moving with a constant velocity, u_{max}, and has a constant temperature, T_{w2}.

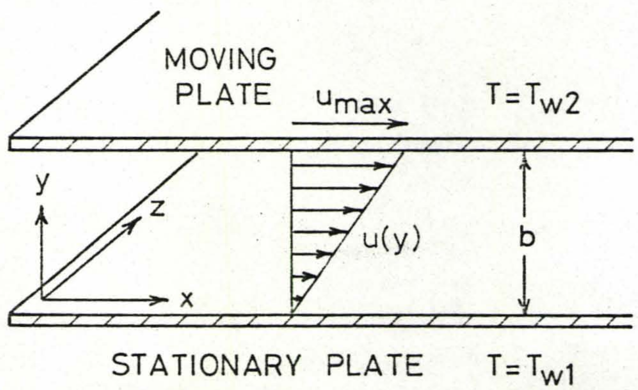

Fig. 4-1. Drag flow between parallel plates.

Flow Equations

The simplified conservation equations for drag flow between parallel plates are:

Momentum: $$\frac{d\tau_{yx}}{dy} = 0 \tag{4.1}$$

Energy: $$\rho C_p u \frac{\partial T}{\partial x} = k \frac{\partial^2 T}{\partial y^2} + \tau_{yx} \frac{du}{dy} \tag{4.2}$$

By substituting the constitutive relation, Eqs. (3.12) and (3.13), into the above equations, we obtain:

Momentum: $$\eta \frac{d^2u}{dy^2} + \frac{d\eta}{dy}\frac{du}{dy} = 0 \tag{4.3}$$

Energy: $$\rho C_p u \frac{\partial T}{\partial x} = k \frac{\partial^2 T}{\partial y^2} + \eta \left(\frac{du}{dy}\right)^2 \tag{4.4}$$

where $$\eta = Ae^{-Bn(T-T_m)} \left|\frac{du}{dy}\right|^{n-1}$$

The boundary conditions for the above equations are:

$$\begin{array}{llll} x = 0 & u = u_o(y) = u_{max}\cdot\frac{y}{b} & T = T_o & \\ y = 0 & u = 0 & T = T_{w1} & (4.5) \\ y = b & u = u_{max} & T = T_{w2} & \end{array}$$

A linear velocity profile, $u_o(y)$, and a constant temperature profile have been chosen at x = 0. However, other profiles can also be used.

Let $$U = \frac{u}{u_{max}}$$

$$\theta = \frac{T-T_{w1}}{T_o-T_{w1}}$$

$$X = \frac{kx}{\rho C_p u_{max} b^2} \tag{4.6}$$

$$Y = \frac{y}{b}$$

Substituting the above into Eqs. (4.3) and (4.4), we obtain in terms of dimensionless parameters:

Momentum: $$\eta\frac{d^2U}{dY^2} + \frac{d\eta}{dY}\frac{dU}{dY} = 0 \tag{4.7}$$

Energy: $$U\frac{\partial\theta}{\partial X} = \frac{\partial^2\theta}{\partial Y^2} + \beta\left(\frac{dU}{dY}\right)^2 \tag{4.8}$$

where $$\beta = \frac{\eta u_{max}^2}{k(T_o - T_{w1})}$$

$$\eta = Ae^{-Bn(T-T_m)}\left|\frac{dU}{dY}\cdot\frac{u_{max}}{b}\right|^{n-1}$$

The accompanying non-dimensional boundary conditions are:

$$\begin{array}{llll} X = 0 & U = U_o(Y) = Y & \theta = 1 & \\ Y = 0 & U = 0 & \theta = 0 & (4.9) \\ Y = 1 & U = 1 & \theta = \dfrac{T_{w2}-T_{w1}}{T_o-T_{w1}} & \end{array}$$

Finite Difference Equations

An implicit finite difference method is used to solve Eqs. (4.7) and (4.8) with the accompanying boundary conditions (4.9). The finite difference grid is illustrated in Fig. 4-2.

Momentum Equation

For the momentum equation, the following finite difference approximations are used:

$$\frac{dU}{dY} = \frac{U^n_{m+1} - U^n_{m-1}}{2\Delta Y} \tag{4.10}$$

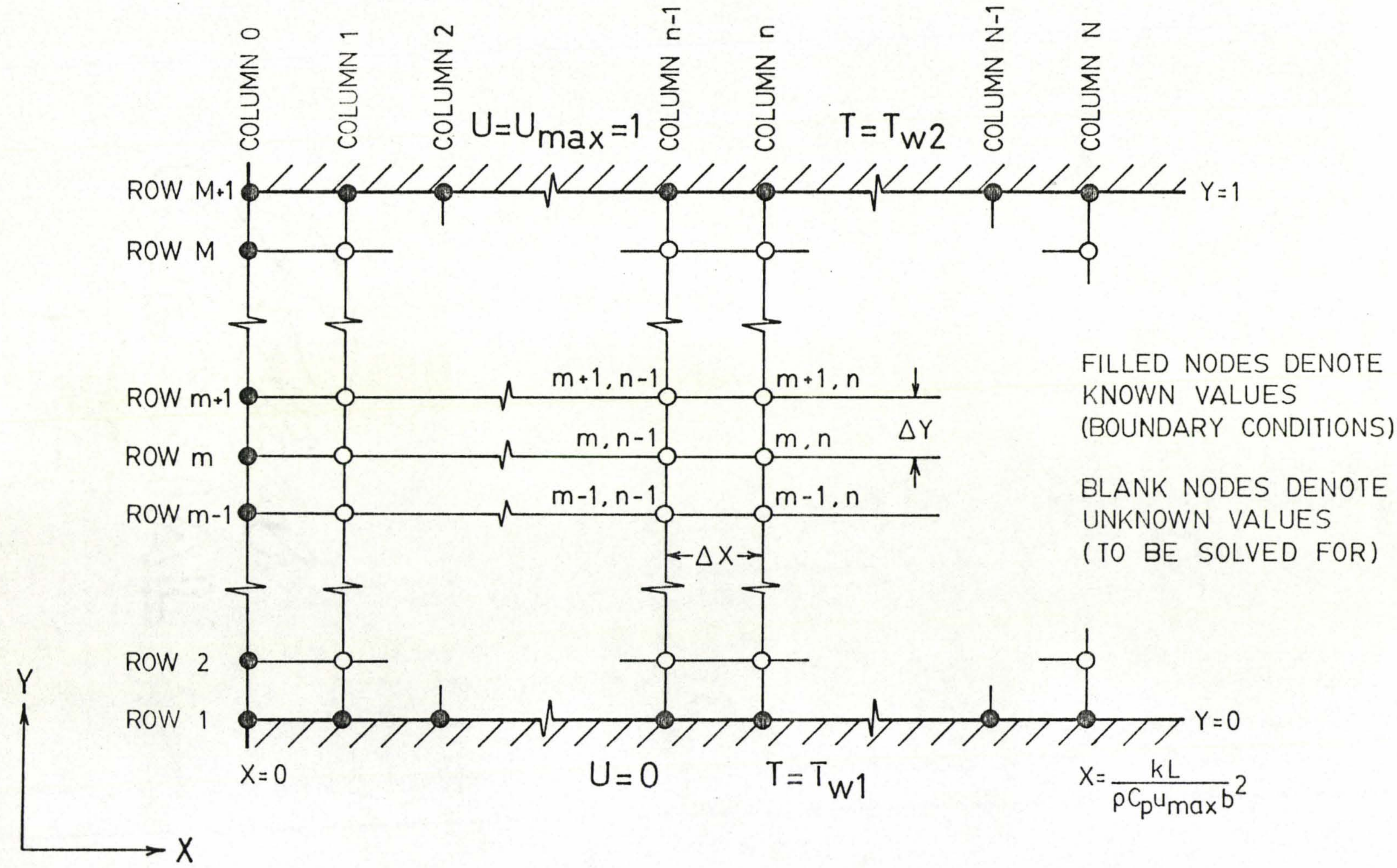

Fig. 4-2. Finite difference grid. Drag flow between parallel plates.

$$\frac{d^2U}{dY^2} = \frac{U^n_{m-1} - 2U^n_m + U^n_{m+1}}{(\Delta Y)^2} \tag{4.11}$$

Substituting Eqs. (4.10) and (4.11) into Eq. (4.7), we obtain for column n (details in App. A, Sec. 1.1):

$$A_m\, U^n_{m-1} + B_m\, U^n_m + C_m\, U^n_{m+1} = 0 \tag{4.12}$$

$$\left.\begin{aligned} A_m &= -\frac{\Delta Y}{2\eta^n_m}\left(\frac{d\eta}{dY}\right)^n_m + 1 \\ B_m &= -2 \\ C_m &= \frac{\Delta Y}{2\eta^n_m}\left(\frac{d\eta}{dY}\right)^n_m + 1 \end{aligned}\right\} \quad (m = 2, 3, \ldots, M)$$

where the three coefficients are as above.

Thus, for column n we have a tridiagonal system of M-1 equations with M-1 unknowns (U^n_2 to U^n_M). The equations can be written as follows:

$$\begin{aligned} & A_2\, \overset{\nearrow 0}{U^n_1} + B_2\, U^n_2 + C_2\, U^n_3 = 0 \\ & A_m\, U^n_{m-1} + B_m\, U^n_m + C_m\, U^n_{m+1} = 0 \qquad (m = 3, 4, \ldots, M\text{-}1) \\ & A_M\, U^n_{M-1} + B_M\, U^n_M + C_M\, \underset{\searrow 1}{U^n_{M+1}} = 0 \end{aligned} \tag{4.13}$$

or in matrix form:

$$\begin{bmatrix} B_2 & C_2 & & & & & & \underline{0} \\ A_3 & B_3 & C_3 & & & & & \\ & \ddots & \ddots & \ddots & & & & \\ & & A_m & B_m & C_m & & & \\ & & & \ddots & \ddots & \ddots & & \\ & & & & A_{M-1} & B_{M-1} & C_{M-1} \\ \underline{0} & & & & & A_M & B_M \end{bmatrix} \begin{bmatrix} U_2^n \\ U_3^n \\ \vdots \\ U_m^n \\ \vdots \\ U_{M-1}^n \\ U_M^n \end{bmatrix} = \begin{bmatrix} 0 \\ 0 \\ \vdots \\ 0 \\ \vdots \\ 0 \\ -C_M \end{bmatrix} = \begin{bmatrix} H_2 \\ H_3 \\ \vdots \\ H_m \\ \vdots \\ H_{M-1} \\ H_M \end{bmatrix} \tag{4.14}$$

This system of equations is solved for the velocity profile at column n by Gaussian elimination using Thomas' method (details in App. D, Sec. 1).

<u>Energy Equation</u>

For the energy equation, the following finite difference approximations are used:

$$\frac{\partial \theta}{\partial X} = \frac{\theta_m^n - \theta_m^{n-1}}{\Delta X} \tag{4.15}$$

$$\frac{\partial^2 \theta}{\partial Y^2} = \frac{\theta_{m-1}^n - 2\theta_{m-1}^n + \theta_{m+1}^n}{2(\Delta Y)^2} + \frac{\theta_{m-1}^{n-1} - 2\theta_m^{n-1} + \theta_{m+1}^{n-1}}{2(\Delta Y)^2} \tag{4.16}$$

Substituting Eqs. (4.15) and (4.16) into Eq. (4.8), we obtain for column n (details in App. A, Sec. 1.2):

$$A_m \theta_{m-1}^n + B_m \theta_m^n + C_m \theta_{m+1}^n = D_m + E_m + F_m + G_m = H_m \tag{4.17}$$

where

$$\left.\begin{aligned}
A_m &= -1 \\
B_m &= \frac{2(\Delta Y)^2}{\Delta X} \cdot U_m^n + 2 \\
C_m &= -1 \\
D_m &= \theta_{m-1}^{n-1} \\
E_m &= \left[\frac{2(\Delta Y)^2}{\Delta X} \cdot U_m^n - 2\right] \theta_m^{n-1} \\
F_m &= \theta_{m+1}^{n-1} \\
G_m &= 2(\Delta Y)^2 \, \beta_m^n \left(\frac{dU}{dY}\right)_m^2
\end{aligned}\right\} \qquad (m = 2, 3, \ldots, M)$$

Thus, for column n we have a tridiagonal system of M-1 equations and M-1 unknowns (θ_2^n to θ_M^n). The equations can be written as follows:

$$A_2 \, \overset{\nearrow 0}{\theta_1^n} + B_2 \, \theta_2^n + C_2 \, \theta_3^n = H_2$$

$$A_m \, \theta_{m-1}^n + B_m \, \theta_m^n + C_m \, \theta_{m+1}^n = H_m \qquad (m = 3, 4, \ldots, M\text{-}1) \qquad (4.18)$$

$$A_M \, \theta_{M-1}^n + B_M \, \theta_M^n + C_M \, \underbrace{\theta_{M+1}^n}_{\searrow \frac{T_{w2}-T_{w1}}{T_o-T_{w1}}} = H_M$$

$$\begin{bmatrix} B_2 & C_2 & & & & \underline{0} \\ A_3 & B_3 & C_3 & & & \\ & \ddots & \ddots & \ddots & & \\ & & A_m & B_m & C_m & \\ & & & \ddots & \ddots & \ddots \\ & & & A_{M-1} & B_{M-1} & C_{M-1} \\ \underline{0} & & & & A_M & B_M \end{bmatrix} \begin{bmatrix} \theta_2^n \\ \theta_3^n \\ \vdots \\ \theta_m^n \\ \vdots \\ \theta_{M-1}^n \\ \theta_M^n \end{bmatrix} = \begin{bmatrix} H_2 \\ H_3 \\ \vdots \\ H_m \\ \vdots \\ H_{M-1} \\ H_M - C_M \theta_{M+1}^n \end{bmatrix} \tag{4.19}$$

Again, this system of equations is solved for the temperature profile along column n by Gaussian elimination using Thomas' method (details in App. D, Sec. 1).

Bulk Temperature

The dimensionless flow-average (bulk) temperature is defined as follows:

$$\theta_{bulk} = \frac{\int_{Y=0}^{Y=1} \theta(X,Y)\, U(X,Y)\, dY}{\int_{Y=0}^{Y=1} U(X,Y)\, dY} \tag{4.20}$$

Equation (4.20) for column n is written in finite difference form, using Simpson's Rule, as follows:

$$\theta_{bulk}^n = \frac{\overset{\nearrow 0}{\theta_1^n}\, U_1^n + 4\theta_2^n\, U_2 + 2\theta_3^n\, U_3 + \ldots + 4\theta_M^n\, U_M^n + \theta_{M+1}^n\, U_{M+1}^n}{\underset{\searrow 0}{U_1^n} + 4U_2^n + 2U_3^n + \ldots + 4U_M^n + \underset{\searrow 1}{U_{M+1}^n}} \tag{4.21}$$

Local Nusselt Number

The local Nusselt number is calculated from the following definition which is derived in App. B:

$$Nu_x = \frac{hb}{k} = \frac{\left(\frac{dT}{dy}\right)_{wall} \cdot b}{T_{bulk} - T_{wall}} \tag{4.22}$$

In dimensionless form we have:

$$(Nu_x)_{Y=0} = \frac{\left(\frac{d\theta}{dY}\right)_{Y=0}}{\theta_{bulk}} \tag{4.23}$$

$$(Nu_x)_{Y=1} = \frac{-\left(\frac{d\theta}{dY}\right)_{Y=1}}{(\theta_{bulk} - \theta_{w2})} \tag{4.24}$$

The dimensionless temperature gradients at the walls are estimated for column n by the following finite difference approximations:

$$\left(\frac{d\theta}{dY}\right)^n_{Y=0} = \frac{1}{6\Delta Y}\left(-\cancelto{0}{11\theta^n_1} + 18\theta^n_2 - 9\theta^n_3 + 2\theta^n_4\right) \tag{4.25}$$

$$\left(\frac{d\theta}{dY}\right)^n_{Y=1} = \frac{1}{6\Delta Y}\left(-2\theta^n_{M-2} + 9\theta^n_{M-1} - 18\theta^n_M + 11\theta^n_{M+1}\right) \tag{4.26}$$

The above equations are derived in App. C, Sec. 1 and 5.

4.2 Computational Procedure

It was stated in Chap. 3, Sec. 3, that the momentum and energy equations are coupled by velocity and temperature, and therefore cannot be solved independently. However, the coupled equations can be solved iteratively at a given column on the finite difference grid by alternately solving the set of momentum equations (4.13) and the set of energy equations (4.18) until the solutions converge. The iterative "marching" procedure used to calculate the velocity and temperature profiles, the bulk temperature and the local Nusselt numbers at each column in the grid is now outlined.

Notation

$U1^n_m$ (m = 1, 2, ..., M+1) refers to the estimated velocity profile at column n.

$U2^n_m$ (m = 1, 2, ..., M+1) refers to the most recently calculated velocity profile at column n.

θ^{n-1}_m (m = 1, 2, ..., M+1) refers to the temperature profile at column n-1.

$\theta1^n_m$ (m = 1, 2, ..., M+1) refers to the estimated temperature profile at column n.

$\theta2^n_m$ (m = 1, 2, ..., M+1) refers to the most recently calculated temperature profile at column n.

Procedure

1. Assume values for the velocity and temperature profiles at the entrance of the channel (at column 0).

$$\left.\begin{aligned} U1^0_m &= Y \\ \theta^o_m &= 1 \end{aligned}\right\} \quad (m = 1, 2, \ldots, M+1)$$

2. Print the velocity and temperature profiles at column 0.

3. Set the estimates of the velocity and temperature profiles to be used in the first iteration of column 1 equal to the values of the respective profiles at column 0.

$$n = 1$$

$$U1_m^1 = U1_m^0 \qquad (m = 1, 2, \ldots, M+1)$$

$$\theta 1_1^1 = \theta 2_1^1 = 0, \; \theta 1_{M+1}^1 = \theta 2_{M+1}^1 = \frac{T_{w2}-T_{w1}}{T_o-T_{w1}}$$

$$\theta 1_m^1 = \theta_m^0 \qquad (m = 2, 3, \ldots, M)$$

4. To economize on computing time, increase ΔX by a factor of 10 after the final velocity and temperature profiles have been calculated at column n = NA, and again after they have been calculated at column n = NB (see program listing, App. F, Sec. 1).

   $\Delta X = 10\ \Delta X$ at column NA + 1, and again at column NB + 1

5. Using $U1_m^n$ and $\theta 1_m^n$ $(m = 1, 2, \ldots, M+1)$, calculate $(\frac{dU}{dY})_m^n$ and η_m^n $(m = 1, 2, \ldots, M+1)$ at column n.
6. Using $U1_m^n$, $(\frac{dU}{dY})_m^n$, θ_m^n and θ_m^{n-1} $(m = 1, 2,\ldots,M+1)$, solve the set of energy equations (4.19) by Gaussian elimination using Thomas' method (see App. D, Sec. 1) to obtain $\theta 2_m^n$ $(m = 2, 3, \ldots, M)$.
7. Using $U1_m^n$ and $\theta 2_m^n$ $(m = 1, 2, \ldots, M+1)$, calculate η_m^n and $(\frac{d\eta}{dY})_m^n$ $(m = 1, 2, \ldots, M+1)$ at column n.
8. Using η_m^n and $(\frac{d\eta}{dY})_m^n$ $(m = 1, 2, \ldots, M+1)$, solve the set of momentum equations (4.14) by Gaussian elimination using Thomas' method (see App. D, Sec. 1) to obtain $U2_m^n$ $(m = 2, 3, \ldots, M)$.
9. Compare $U1_m^n$, $U2_m^n$ and $\theta 1_m^n$, $\theta 2_m^n$ $(m = 1, 2, \ldots, M+1)$. If $|U2_m^n - U1_m^n| <$ tolerance and $|\theta 2_m^n - \theta 1_m^n| <$ tolerance for all m, then proceed to step 12. Otherwise, continue to step 10.
10. Set the estimates of the velocity and temperature profiles to be used in the next iteration at column n equal to the most recently calculated profiles.

$$\left.\begin{array}{l} U1_m^n = U2_m^n \\ \theta 1_m^n = \theta 2_m^n \end{array}\right\} \qquad (m = 1, 2, \ldots, M+1)$$

11. Repeat steps 5 through 9 until the desired error tolerances have been achieved.

12. Set the velocity and temperature profiles to be used in the first iteration at column n + 1 equal to the final values of the profiles calculated at column n. Also, retain the final temperature profile calculated at column n for use in calculating temperature profiles at column n + 1.

$$\left.\begin{aligned} U1_m^{n+1} &= U2_m^n \\ \theta 1_m^{n+1} &= \theta 2_m^n \\ \theta_m^n &= \theta 2_m^n \end{aligned}\right\} \quad (m = 1, 2, \ldots, M+1)$$

13. Repeat steps 4 through 12 to calculate the velocity and temperature profiles at the next column downstream in the channel (n = n+1).

The following steps are to be carried out at periodic intervals along the length of the channel:

14. Print the velocity and temperature profiles.

15. Calculate the bulk temperature using Simpson's Rule (see Eq. (4.21)).

16. Calculate the local Nusselt numbers at the walls (see Eqs. (4.23) and (4.24)).

17. Print the bulk temperature and the local Nusselt numbers.

Computations using the above algorithm have been carried out in McMaster's CDC 6400 computer. A sample program listing with results is located in App. F, Sec. 1.

4.3 Convergence, Stability and Step Size

It was stated in Chap. 3, Sec. 4, that a good indication of the convergence and stability of the finite difference results is the negligible change in results obtained when the step sizes in the finite difference grid are decreased. It should be noted here that special care must be taken in choosing step sizes when calculating local Nusselt numbers. Although the temperature profiles may appear to be sufficiently accurate, the local Nusselt numbers can still be incorrect. Local Nusselt numbers are calculated from temperature derivatives (see Eq. (4.22)). Since derivatives are very sensitive to step size changes, smaller step sizes must be used when calculating local Nusselt numbers, than when only calculating velocity and temperature profiles. The step sizes shown in Table 4-1 were used in the finite difference program. The results presented in the subsequent figures in this chapter are independent of step size within at least 3 significant digits.

Table 4-1. Step sizes for finite difference program. Drag flow between parallel plates.

Range of X	ΔX	ΔY
0 -0.1	0.0001	1/60
0.1-0.4	0.001	1/60

An additional test for convergence was carried out by first calculating analytically the fully-developed temperature profile, the limiting bulk temperature and the limiting local Nusselt number (at large X) for a Newtonian, constant viscosity fluid with viscous dissipation (see App. E, Sec. 1), and then comparing these with the corresponding finite difference results for the same fluid. The analytical and finite difference results were indistinguishable.

4.4 Results and Discussion

Solutions of the momentum and energy equations for drag flow between parallel plates are presented in Figs. 4-3 through 4-14. The following velocity and temperature boundary conditions have been used:

$$\begin{array}{lll} x = 0 & u = 60y \text{ cm/s} & T_o = 130\,^\circ\text{C} \\ y = 0 & u = 0 & T_{w1} = 160\,^\circ\text{C} \\ y = b = 0.25 \text{ cm} & u = u_{max} = 15 \text{ cm/s} & T_{w2} = 160\,^\circ\text{C} \end{array} \qquad (4.27)$$

In obtaining some of the results, different temperature boundary conditions were used for comparison. The following power-law temperature-dependent viscosity model and fluid properties representing a typical high-density polyethylene melt were used in the computations:

Viscosity: $$\eta = Ae^{-Bn(T-T_m)} \left|\frac{du}{dy}\right|^{n-1} \qquad (4.28)$$

where $A = 282\ 000 \text{ poise}\cdot\text{s}^{n-1}$

$= 28\ 200 \text{ Pa}\cdot\text{s}^n$

$B = 0.024 \text{ K}^{-1}$

$n = 0.453$

$T_m = 399.5 \text{ K}$

Density: $\rho = 794 \text{ kg/m}^3$

Specific Heat: $C_p = 0.6$ cal/(g·K)

$= 2.51$ kJ/(kg·K)

Thermal conductivity: $k = 6.1 \times 10^{-4}$ cal/(cm·s·K)

$= 0.255$ W/(m·K)

The temperature profiles, bulk temperature and local Nusselt numbers in Figs. 4-3 through 4-14 are shown as functions of the dimensionless axial distance, X. Because the bulk temperatures and local Nusselt numbers change the most near the entrance of the flow channel, they have been plotted semi-logarithmically. X on the abscissa of these plots ranges from 0.001 to 0.4. This corresponds to x ranging from 0.7 cm to 293 cm. At X = 0.4, the temperature profile has become fully developed. Beyond this point in the channel, the temperature profiles, bulk temperatures and local Nusselt numbers remain the same, and thus are known as the limiting or asymptotic values.

In Figs. 4-3 and 4-4, the temperature profiles for the power-law temperature-dependent viscosity model and for a power-law temperature-independent viscosity model are compared. Two different temperature boundary conditions have been considered: both the stationary and moving plates at 160°C in Fig. 4-3, and the stationary plate at 190°C and the moving plate at 130°C in Fig. 4-4. The temperature-independent viscosity model used is identical to the temperature-dependent viscosity model given in Eq. (4.28), except that T is held constant and equal to the average of the temperatures of the two plates (160°C in both cases). The temperatures in the temperature-dependent cases are in general lower than in the temperature-independent cases. Since the viscosity decreases with increasing

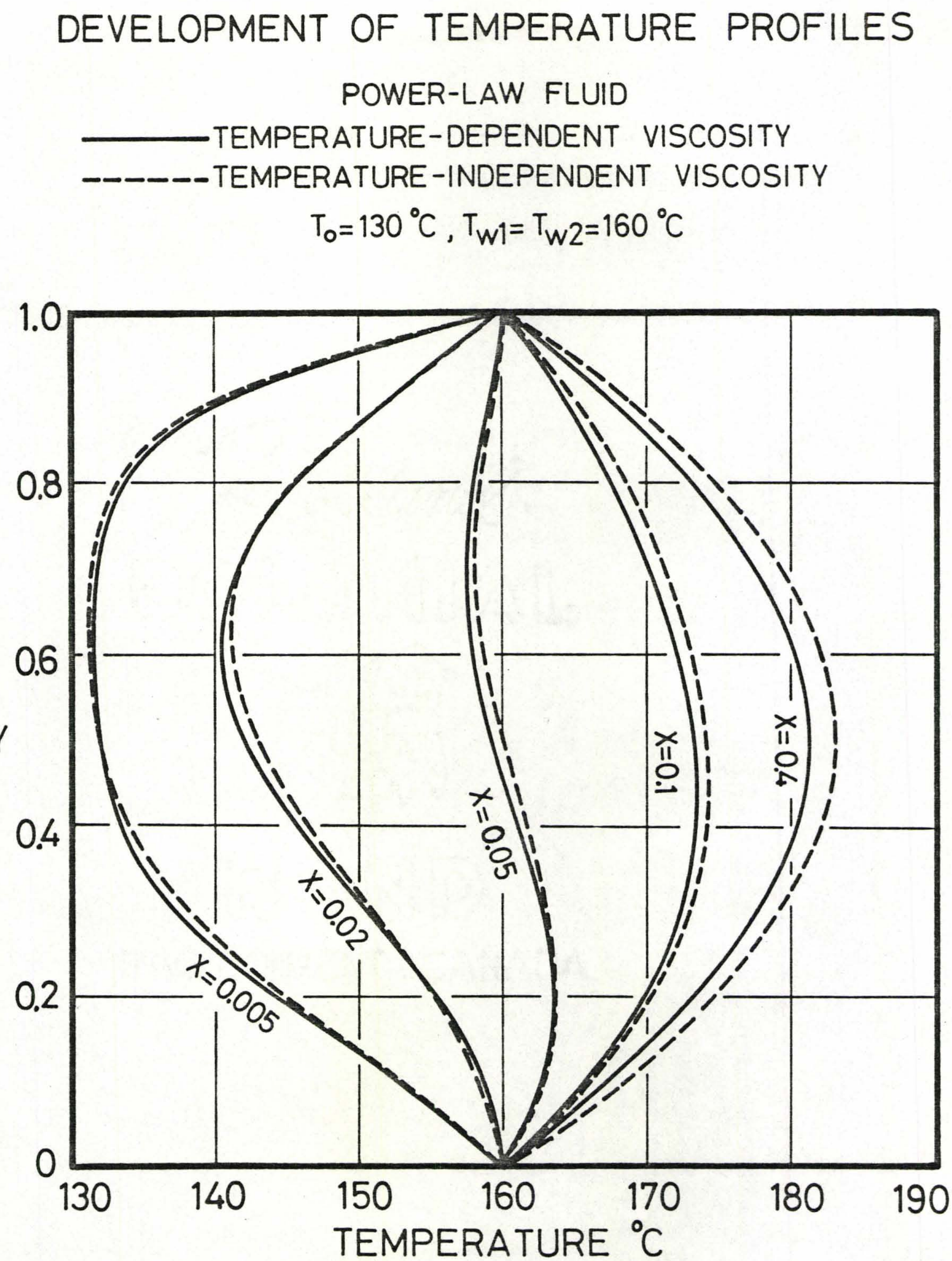

Fig. 4-3. Development of temperature profiles. Drag flow between parallel plates. Channel dimensions and flow properties given on pp. 45-46.

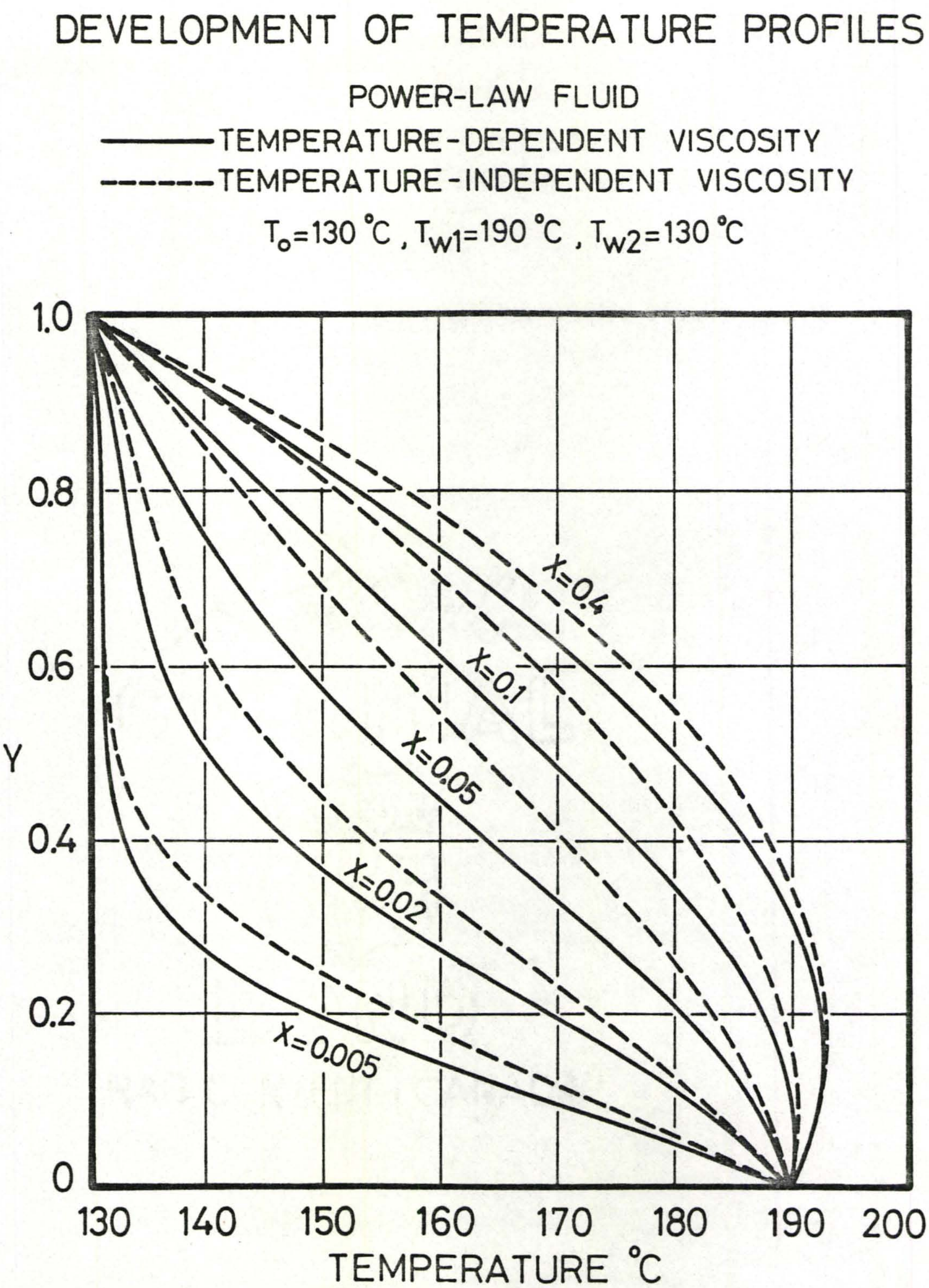

Fig. 4-4. Development of temperature profiles. Drag flow between parallel plates. Channel dimensions and fluid properties given on pp. 45-46.

temperature, the heat generated by viscous generation will be less for the fluid which has a higher temperature in the constitutive equation.

In Fig. 4-3, it is seen that the temperature profile is symmetric about the centre-line of flow only when it has become fully developed at $X = 0.4$. For $X < 0.4$, the temperatures near the moving plate are always lower than near the stationary plate. At a given distance along the channel, the fluid near the stationary plate has been heated more than the fluid near the moving plate. This also accounts for the bulging of the temperature profile near the stationary plate at $X = 0.02$ and 0.05.

Plots of the bulk temperatures along the length of the channel are presented in Figs. 4-5, 4-6 and 4-7 for the power-law temperature-dependent and temperature-independent viscosity models and for the Newtonian, constant viscosity model. In Fig. 4-5, the bulk temperatures are shown for power-law temperature-dependent viscosity fluids with different inlet temperatures. In each case, the limiting bulk temperature is the same (174°C). This is to be expected since the fully-developed velocity and temperature profiles are only influenced by the wall boundary conditions and by the viscosity and thermal conductivity of the fluid, but not by the inlet conditions of the fluid. Also shown in Fig. 4-5 is the effect of removing the viscous dissipation term from the energy equation. Without viscous dissipation, the limiting bulk temperature is equal to the wall temperature (160°C). The difference of 14°C is an indication of the importance of viscous dissipation in the drag flow of polymer melts between parallel plates. It will be seen in subsequent chapters, that for Poiseuille flow, the difference is even greater.

The rise in bulk temperature for the power-law temperature-dependent

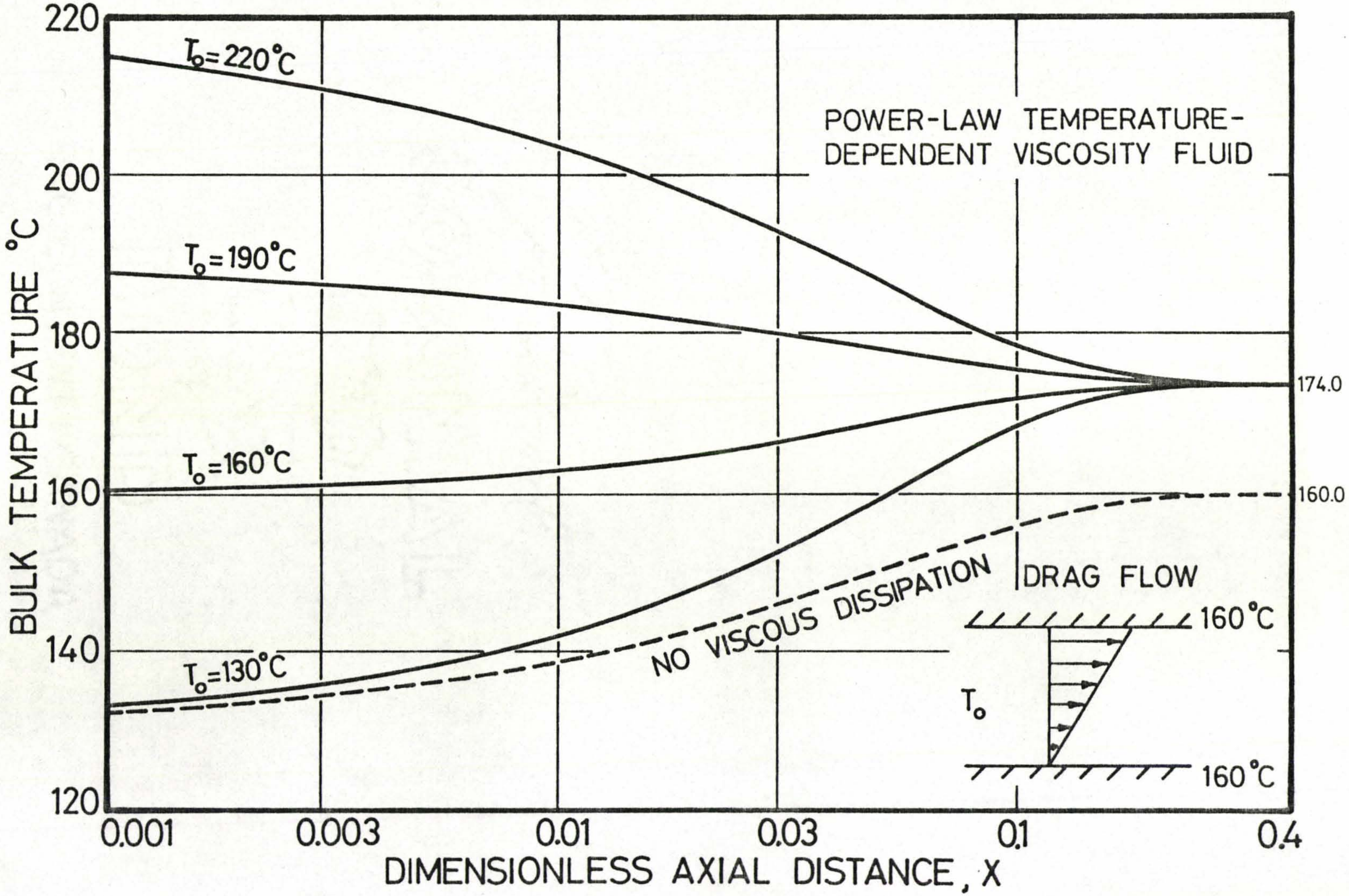

Fig. 4-5. Bulk temperature vs. X. Drag flow between parallel plates. Channel dimensions and fluid properties given on pp. 45-46.

and temperature-independent viscosity fluids is shown in Fig. 4-6 for the two temperature boundary conditions discussed earlier. In both cases, the limiting bulk temperature for the temperature-independent viscosity model is about 1°C higher than for the temperature-dependent viscosity model. In Fig. 4-7, the rise in bulk temperature is shown for the power-law temperature-dependent viscosity model and several Newtonian, constant viscosity models.

Plots of the local Nusselt numbers at both the stationary and moving plates are presented in Figs. 4-8 through 4-14 for the power-law temperature-dependent and temperature-independent viscosity models and the Newtonian, constant viscosity model. The local Nusselt numbers must be calculated at each wall separately because generally they are not the same for a given X. Since the local Nusselt number is a function of the temperature derivative (see Eq. (4.22)), it will be different as long as the temperature gradients at the walls are not the same. It can be seen that when both walls are at the same temperature, the local Nusselt numbers at both plates converge to one value when the temperature profile becomes fully developed.

In Figs. 4-8 and 4-9, the local Nusselt numbers for power-law temperature-dependent viscosity fluids with different inlet temperatures are shown for the stationary and moving plates respectively. In each case the limiting local Nusselt number at both walls is 5.63. Although not shown, the limiting Nusselt numbers for the case where viscous dissipation has been neglected are 3.63 and 5.85 at the stationary and moving walls respectively. It can be seen that when the fluid is heated by the channel walls (T_o = 130°C, T_{w1} = T_{w2} = 160°C), there is a region along the channel

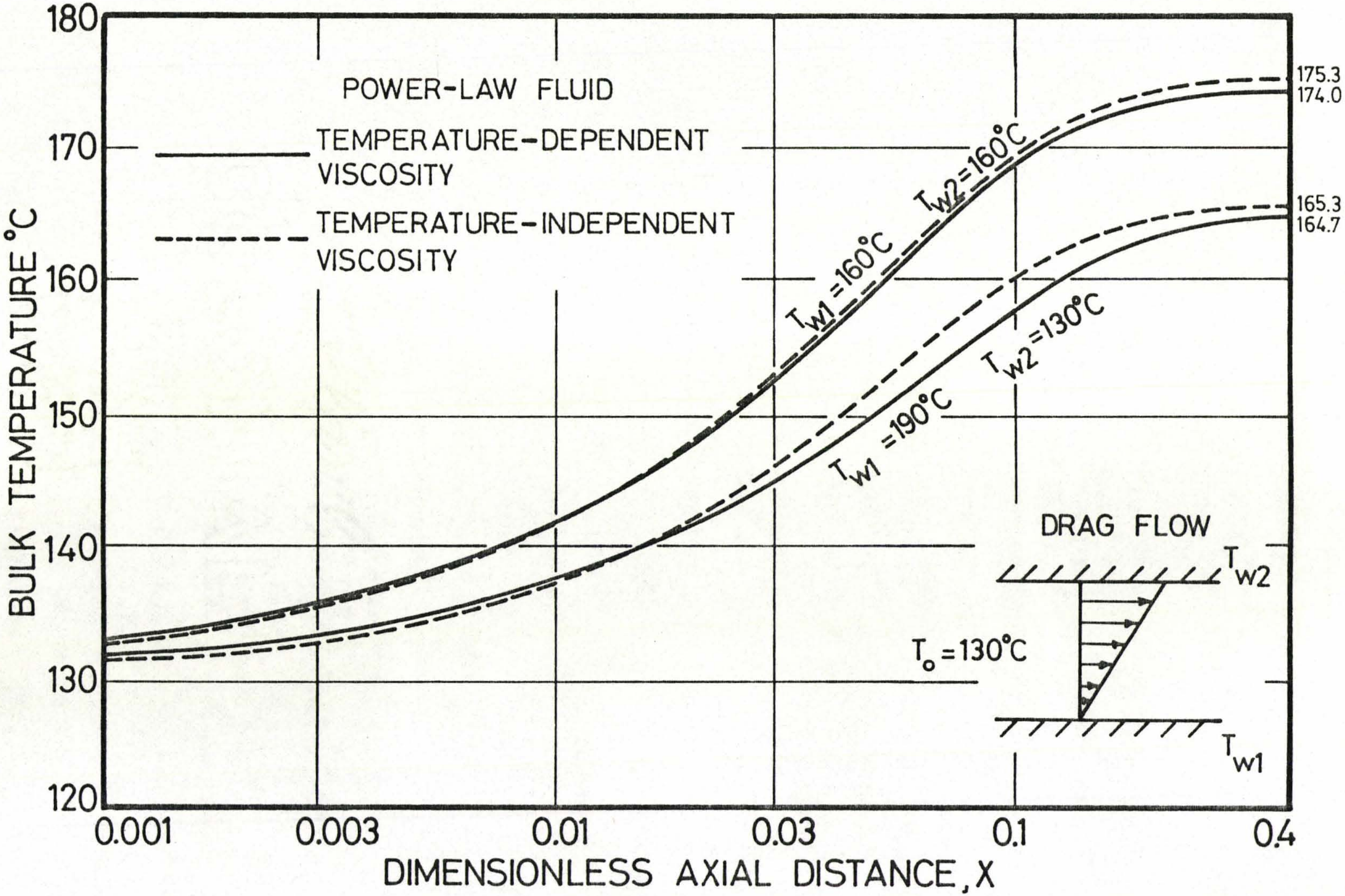

Fig. 4-6. Bulk temperature vs. X. Drag flow between parallel plates. Channel dimensions and fluid properties given on pp. 45-46.

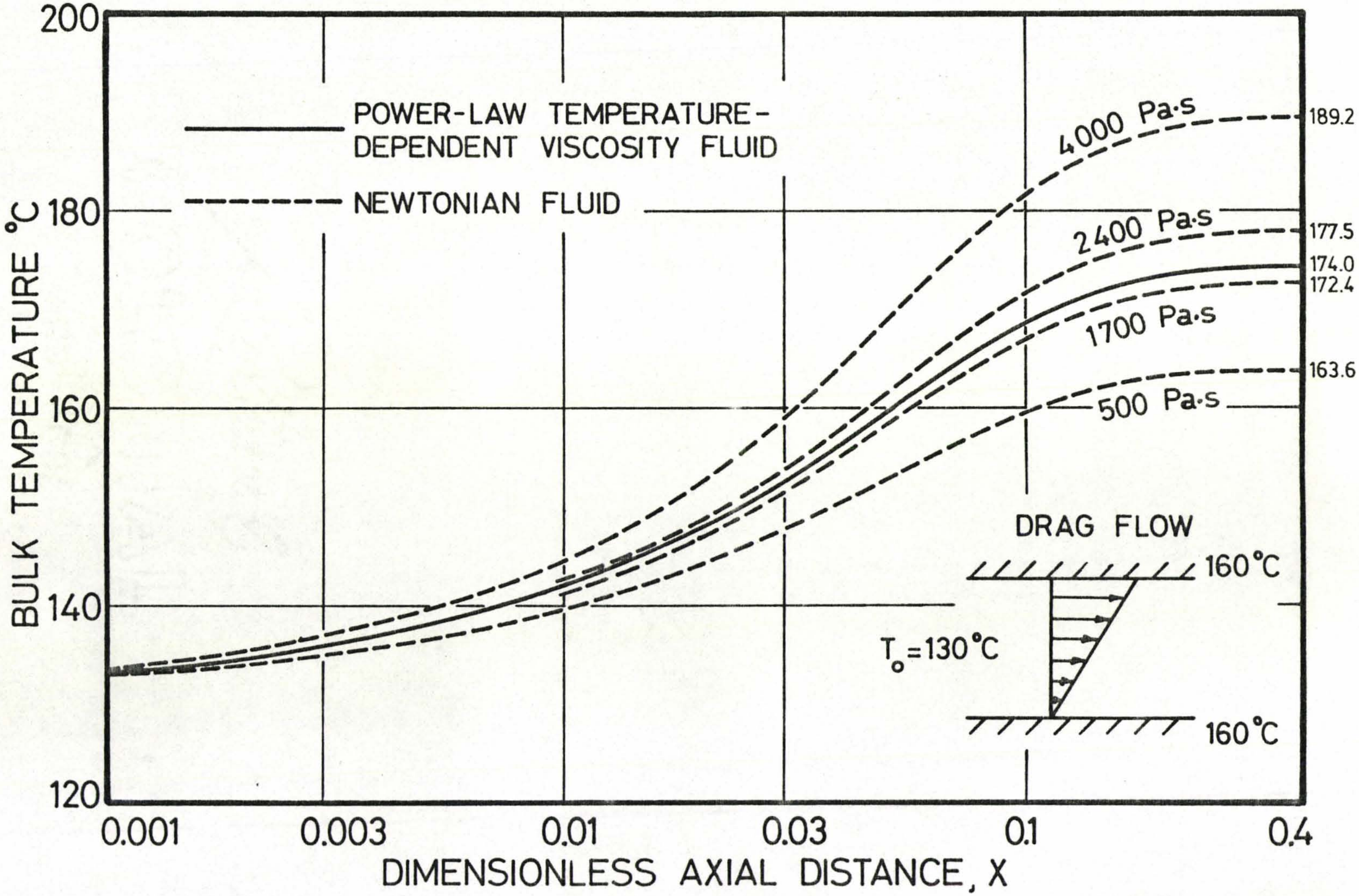

Fig. 4-7. Bulk temperature vs. X. Drag flow between parallel plates. Channel dimensions and fluid properties given on pp. 45-46.

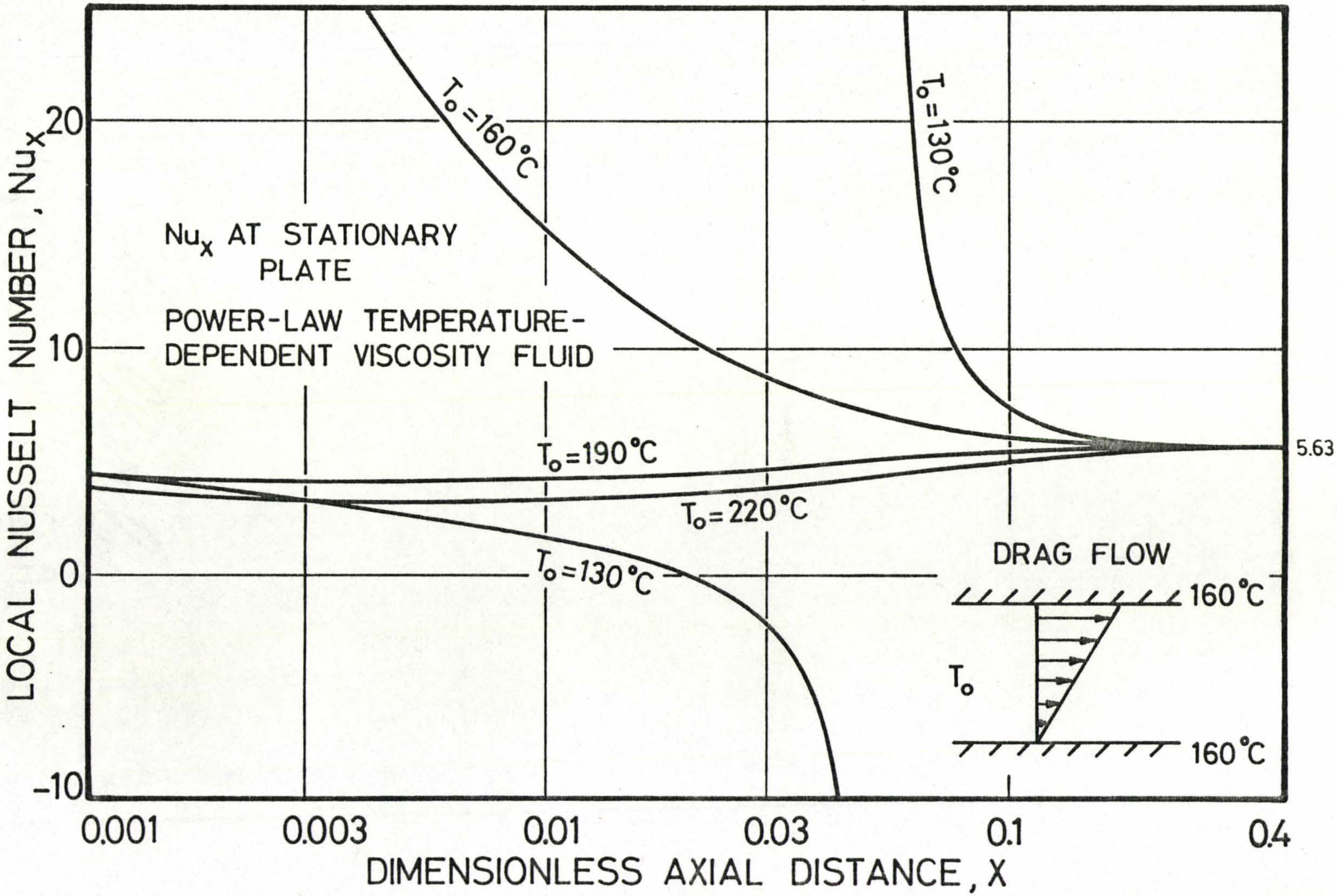

Fig. 4-8. Local Nusselt number vs. X. Drag flow between parallel plates. Channel dimensions and fluid properties given on pp. 45-46.

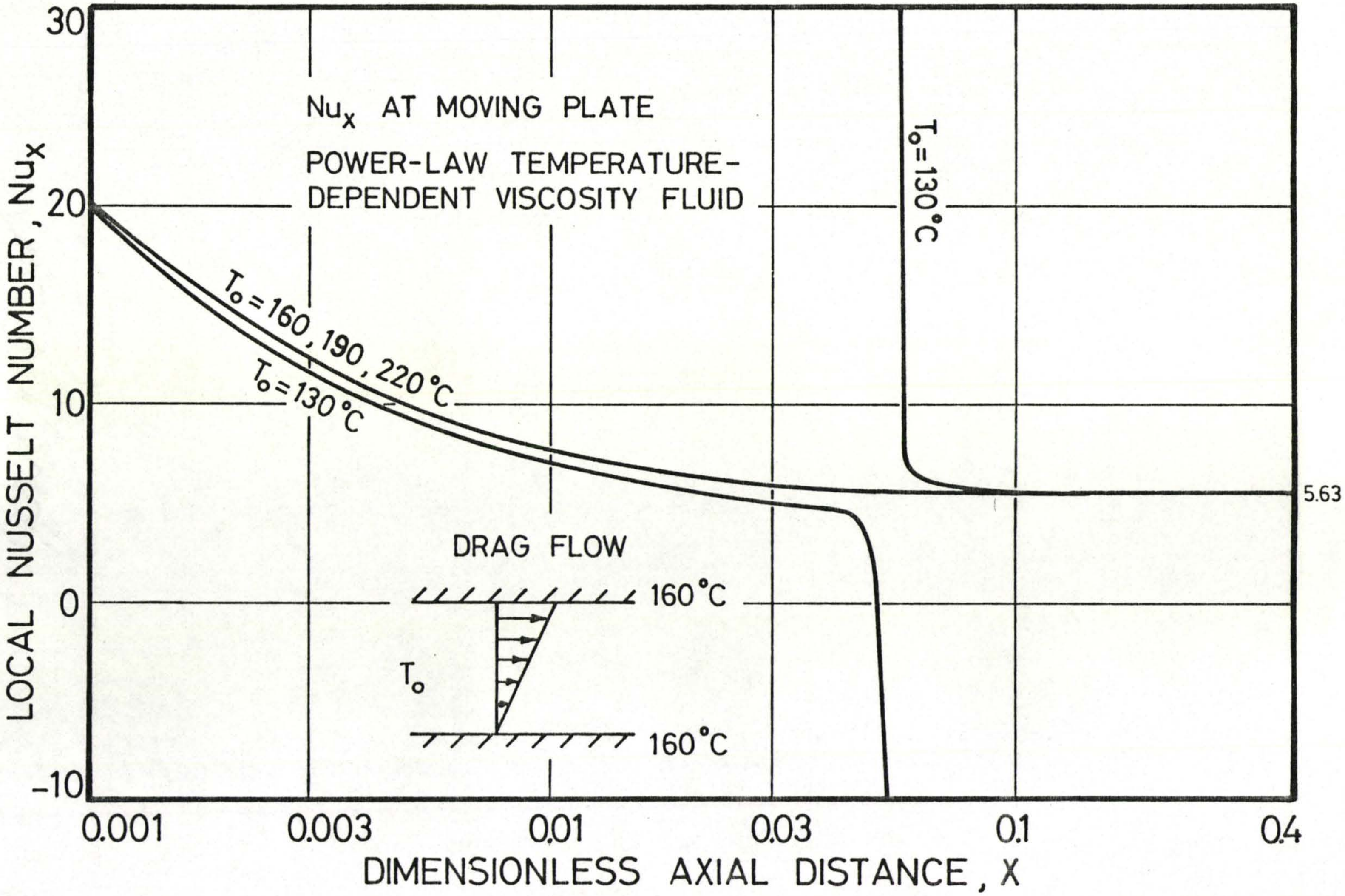

Fig. 4-9. Local Nusselt number vs. X. Drag flow between parallel plates. Channel dimensions and fluid properties given on pp. 45-46.

where the local Nusselt number is negative and a point where it is discontinuous. With the aid of Eq. (4.22), this behaviour is explained as follows for the stationary plate:

$$Nu_x = \frac{hb}{k} = \frac{(\frac{dT}{dy})_{wall} . b}{T_{bulk} - T_{wall}} \tag{4.21}$$

$X < 0.02$	$\frac{dT}{dy} < 0$	$T_b < T_w$	$Nu_x > 0$
$X \simeq 0.02$	$\frac{dT}{dy} = 0$	$T_b < T_w$	$Nu_x = 0$
$0.02 < X < 0.05$	$\frac{dT}{dy} > 0$	$T_b < T_w$	$Nu_x < 0$
$X \simeq 0.05$	$\frac{dT}{dy} > 0$	$T_b = T_w$	$Nu_x = \pm\infty$
$X > 0.05$	$\frac{dT}{dy} > 0$	$T_b > T_w$	$Nu_x > 0$

When the inlet temperature is higher than the wall temperature, the local Nusselt number is always positive.

The local Nusselt numbers for the power-law temperature-dependent and temperature-independent viscosity models are shown in Figs. 4-10, 4-11 and 4-12 for the two temperature boundary conditions discussed earlier. In Figs. 4-10 and 4-11, the local Nusselt numbers are shown for the case where both walls are at 160°C. There is very little difference between the temperature-dependent and temperature-independent viscosity models here. The limiting local Nusselt numbers for the two models are 5.63 and 6.00 respectively. The local Nusselt numbers for the case where the stationary plate is at 190°C and the moving plate is at 130°C are shown

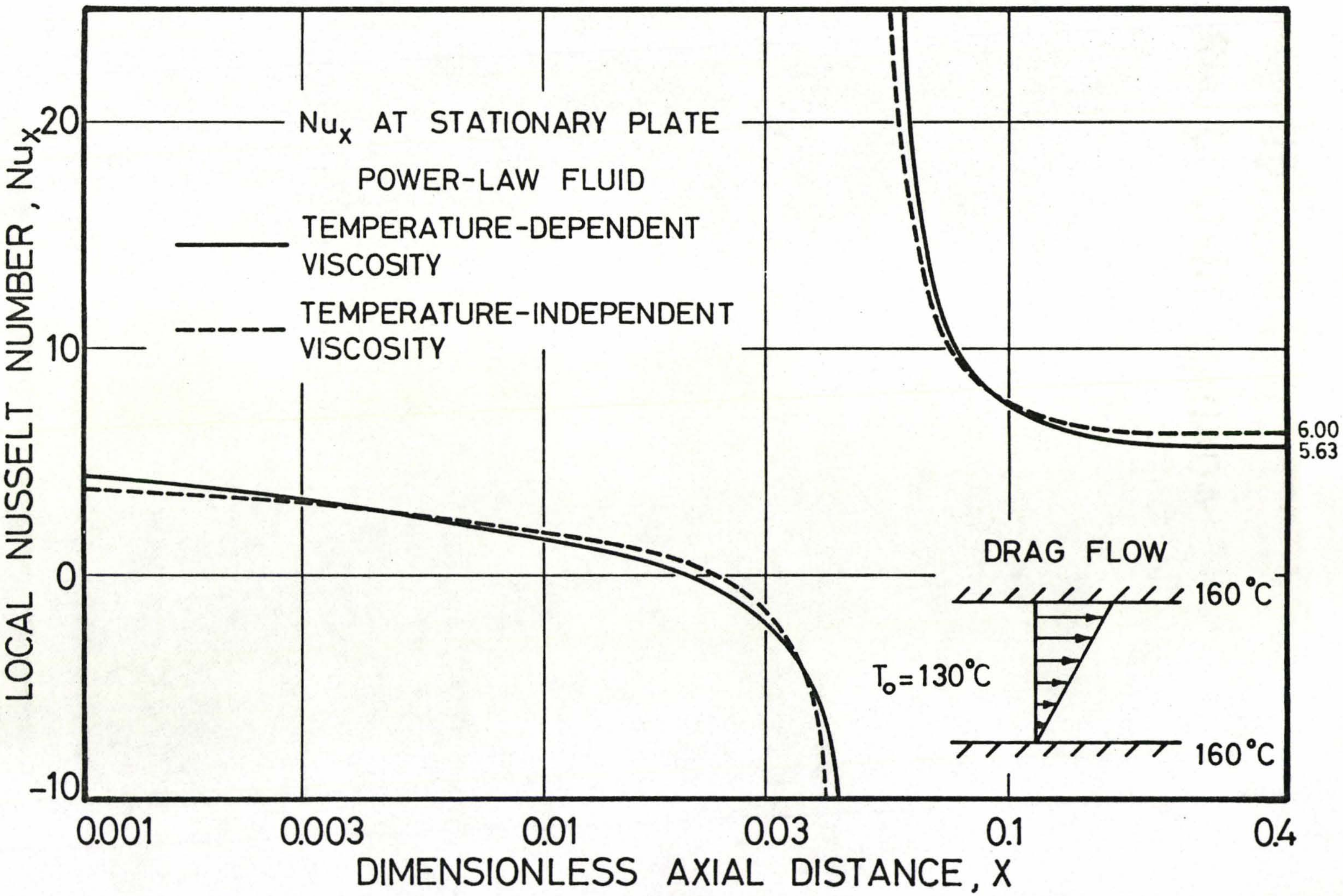

Fig. 4-10. Local Nusselt number vs. X. Drag flow between parallel plates. Channel dimensions and fluid properties given on pp. 45-46.

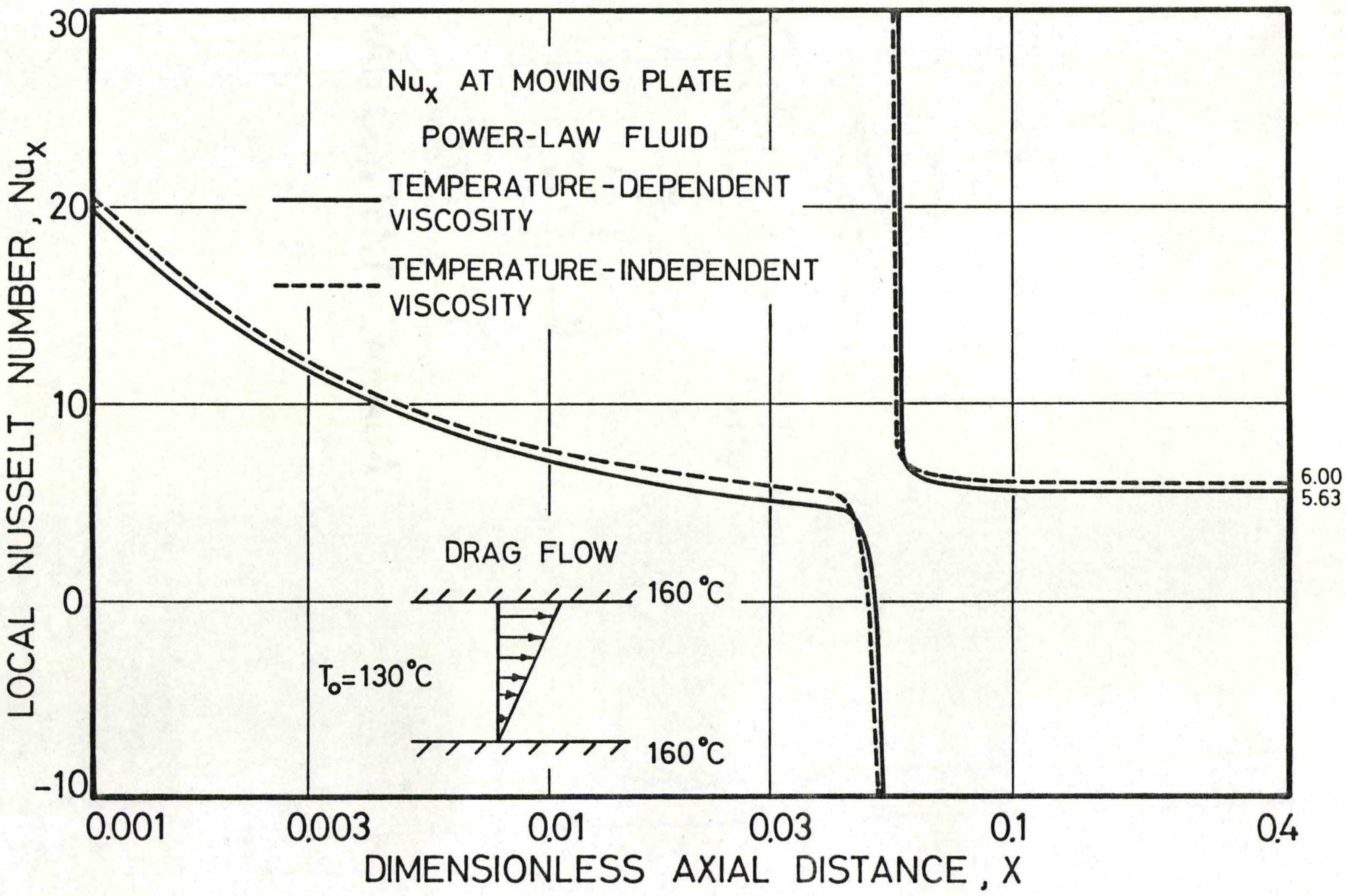

Fig. 4-11. Local Nusselt number vs. X. Drag flow between parallel plates. Channel dimensions and fluid properties given on pp. 45-46.

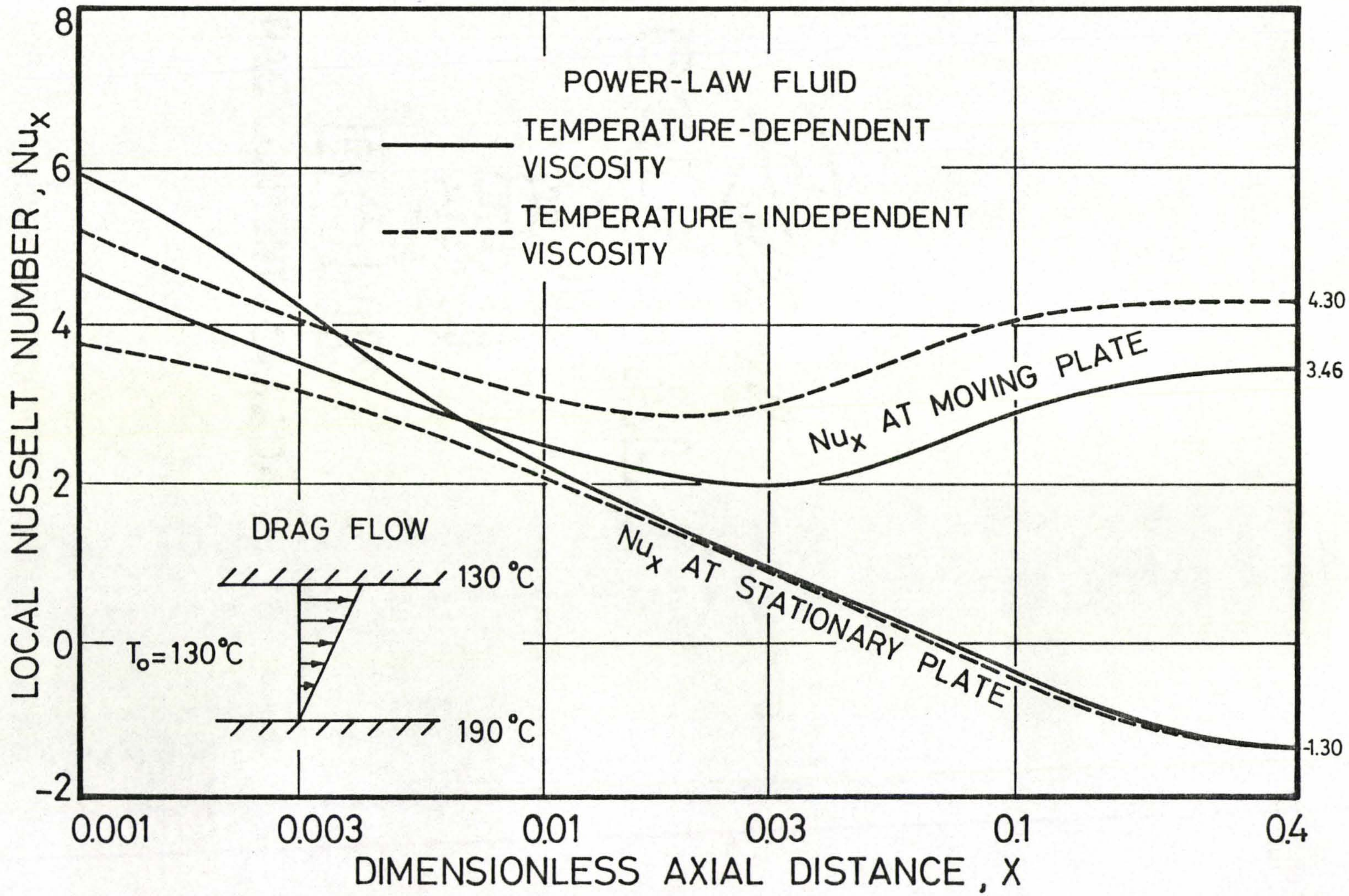

Fig. 4-12. Local Nusselt number vs. X. Drag flow between parallel plates. Channel dimensions and fluid properties given on pp. 45-46.

in Fig. 4-12. In Figs. 4-13 and 4-14, the local Nusselt numbers are presented for the power-law temperature-dependent viscosity model and several Newtonian, constant viscosity models.

The results for the power-law temperature-dependent viscosity model have been compared with the power-law temperature-independent viscosity model and the Newtonian, constant viscosity model results. Given an appropriate temperature for the temperature-independent model, or an appropriate viscosity for the Newtonian model, it can be seen that the temperature-dependent model results are adequately estimated by the use of either of the simpler models. The choice of temperature and viscosity was made by inspection. However, if we did not have any temperature-dependent model results to compare our more simplified model results with, then we would not have anything to base our choice of temperature of viscosity on. Furthermore, the given temperature or viscosity is usually suitable for one type of flow only. For example, in Fig. 4-7 it can be seen that the rise in bulk temperature for the temperature-dependent model is closely approximated by that of a Newtonian fluid with a viscosity of about 2000 Pa·s, while in Poiseuille flow between parallel plates (as described in Chap. 5), a Newtonian viscosity of 700 Pa·s is required (see Fig. 5-9).

4.5 Concluding Remarks

1. A computer program has been developed to analyze the heat transfer problem for the drag flow of polymer melts between parallel, constant temperature plates. Results have been presented for specified velocity and temperature boundary conditions, fluid properties and channel

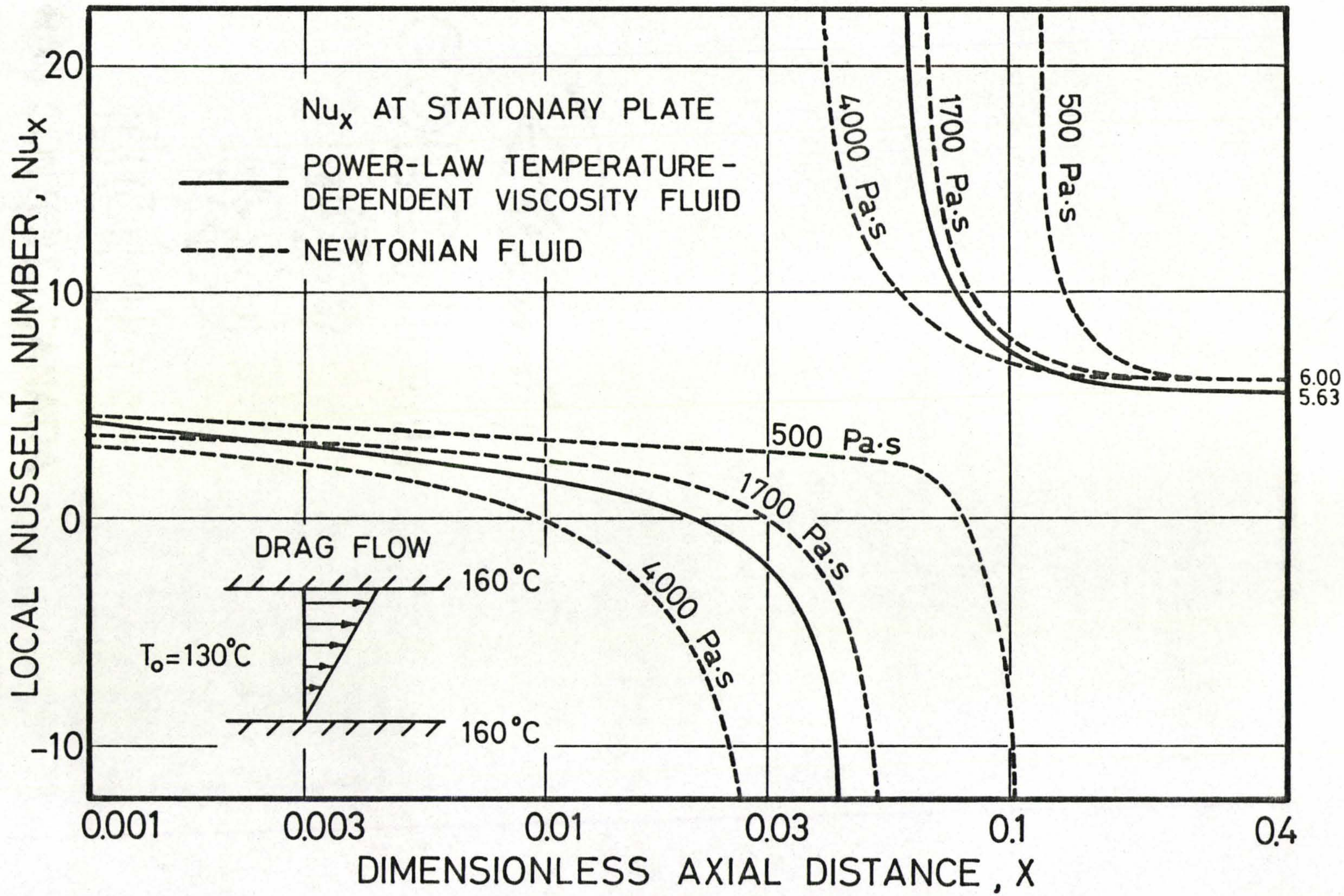

Fig. 4-13. Local Nusselt number vs. X. Drag flow between parallel plates. Channel dimensions and fluid properties given on pp. 45-46.

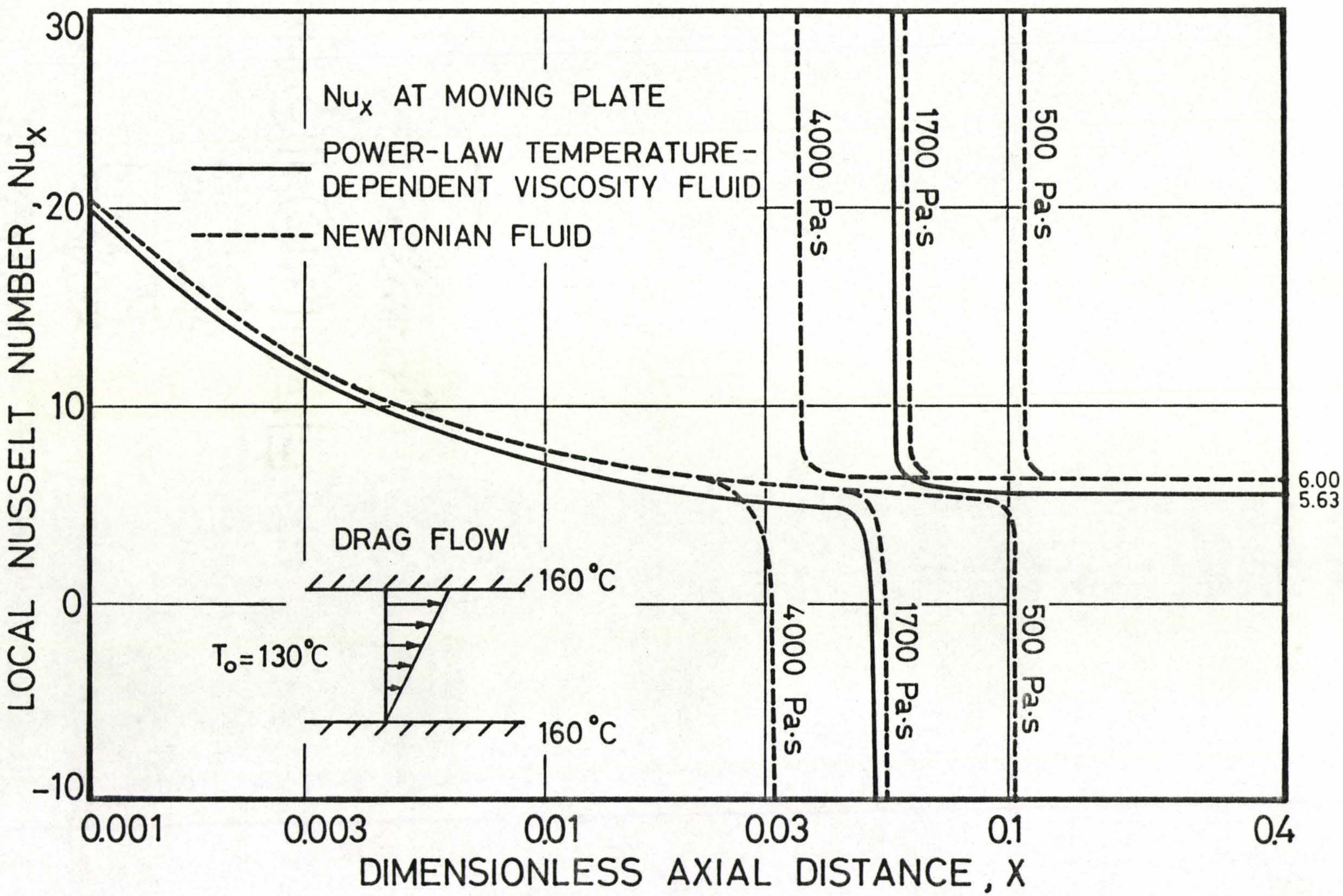

Fig. 4-14. Local Nusselt number vs. X. Drag flow between parallel plates. Channel dimensions and fluid properties given on pp. 45-46.

dimensions.

2. Care must be taken when choosing the proper step sizes to ensure that the local Nusselt numbers and not only the temperature profiles have converged.

3. It is very important to consider viscous dissipation in the drag flow of polymer melts between parallel plates. A rise of 14°C in the limiting bulk temperature due to viscous dissipation was obtained using the specified boundary conditions, fluid properties and channel dimensions given earlier in this chapter.

4. The results obtained using the power-law temperature-dependent viscosity model were compared with those using the simpler power-law temperature-independent viscosity model and the Newtonian, constant viscosity model. It was seen that the results obtained using the temperature-dependent model were in most cases adequately approximated by those of the two simpler models, provided that the choice of temperature or viscosity was correct. However, if there are no temperature-dependent model results available, then we have no basis with which to choose a temperature for the temperature-independent model, or a viscosity for the Newtonian, constant viscosity model.

CHAPTER 5

POISEUILLE FLOW BETWEEN PARALLEL PLATES

5.1 Mathematical Formulation

The physical system for Poiseuille (or pressure) flow between parallel plates is illustrated in Fig. 5-1. It consists of flow between two stationary semi-infinite parallel plates spaced apart by a distance, b. Each plate is at a constant temperature.

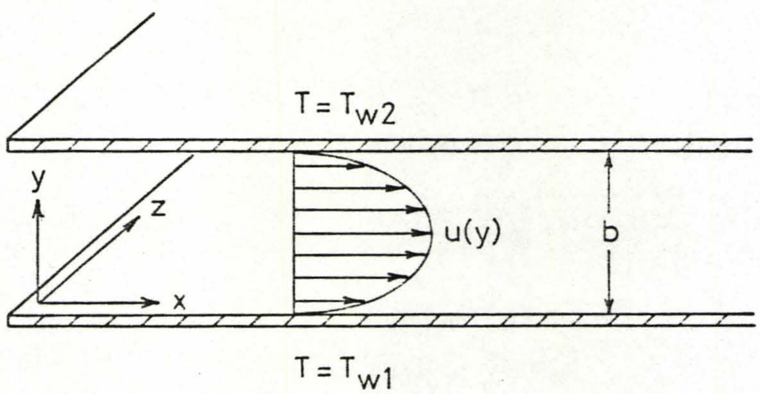

Fig. 5-1. Poiseuille flow between parallel plates.

Flow Equations

The simplified conservation equations for Poiseuille flow between parallel plates are:

Continuity (integral form):

$$\int_{y=0}^{y=b} u\,dy = u_{avg}.b \tag{5.1}$$

Momentum: $$-\frac{dp}{dx} + \frac{d\tau_{yx}}{dy} = 0 \tag{5.2}$$

Energy: $$\rho C_p u \frac{\partial T}{\partial x} = k \frac{\partial^2 T}{\partial y^2} + \tau_{yx} \frac{du}{dy} \tag{5.3}$$

Substituting the constitutive relation, Eqs. (3.12) and (3.13) into the above momentum and energy equations, we obtain:

Momentum: $$-\frac{dp}{dx} + \eta\frac{d^2u}{dy^2} + \frac{d\eta}{dy}\frac{du}{dy} = 0 \tag{5.4}$$

Energy: $$\rho C_p u \frac{\partial T}{\partial x} = k \frac{\partial^2 T}{\partial y^2} + \eta\left(\frac{du}{dy}\right)^2 \tag{5.5}$$

$$\text{where } \eta = Ae^{-Bn(T-T_m)} \left|\frac{du}{dy}\right|^{n-1}$$

The boundary conditions for the above equations are:

$$\begin{array}{llll} x = 0 & u = u_o(y) = u_{avg}\left(\frac{\nu+1}{\nu}\right)\left(1-\left|\frac{2y}{b} - 1\right|^{\nu}\right) & T=T_o & p=p_o \\ \multicolumn{4}{l}{\text{where } \nu = \frac{n+1}{n},\ n = \text{power-law index}} \\ y = 0 & u = 0 & T=T_{w1} & \\ y = b & u = 0 & T=T_{w2} & \end{array} \tag{5.6}$$

A $\frac{n+1}{n}$ degree parabolic velocity profile, $u_o(y)$, has been chosen at x=0. Since the hydrodynamic entrance length for the flow of polymer melts is very short[1], a fully-developed velocity profile can be assumed at the entrance of the channel. A constant temperature profile was used at $x = 0$.

$$\text{Let } U = \frac{u}{u_{avg}}$$

$$P = \frac{p-p_o}{\rho u^2_{avg}}$$

$$\theta = \frac{T-T_{w1}}{T_o-T_{w1}} \tag{5.7}$$

$$X = \frac{kx}{\rho C_p u_{avg} b^2}$$

$$Y = \frac{y}{b}$$

Substituting the above into Eqs. (5.1), (5.4) and (5.5), we obtain in terms of dimensionless parameters:

Continuity (integral form):

$$\int_{Y=0}^{Y=1} U dY = 1 \tag{5.8}$$

Momentum:

$$-\frac{k}{C_p}\frac{dP}{dX} + \eta\frac{d^2U}{dY^2} + \frac{d\eta}{dY}\frac{dU}{dY} = 0 \tag{5.9}$$

---

[1] $Re_D = \frac{\rho u D}{\eta} \simeq 10^{-4}$ for the flow of polymer melts. $\frac{x}{D} \simeq 0.05\ Re_D = 5 \times 10^{-6}$ where x is the hydrodynamic entrance length. When $D = 0.25$ cm, $x = 1.25 \times 10^{-6}$ cm.

Energy: $$U \frac{\partial \theta}{\partial X} = \frac{\partial^2 \theta}{\partial Y^2} + \beta \left(\frac{dU}{dY}\right)^2 \tag{5.10}$$

where $\beta = \dfrac{\eta u^2_{avg}}{k(T_o - T_{w1})}$

$$\eta = Ae^{-Bn(T-T_m)} \left| \frac{dU}{dY} \cdot \frac{u_{avg}}{b} \right|^{n-1}$$

The accompanying dimensionless boundary conditions are:

$$\begin{array}{llll} X = 0 & U = U_o(Y) = \left(\frac{\nu+1}{\nu}\right)(1 - |2Y - 1|^{\nu}) & \theta=1 & p=0 \\ Y = 0 & U = 0 & \theta=0 & \\ Y = 1 & U = 0 & \theta=0 & \end{array} \tag{5.11}$$

Finite Difference Equations

An implicit finite difference method is used to solve Eqs. (5.8), (5.9) and (5.10) with the accompanying boundary conditions (5.11). The finite difference grid is illustrated in Fig. 5-2.

Continuity Equation

Using Simpson's Rule, the integrated continuity equation is given in the following finite difference form:

$$\int_{Y=0}^{Y=1} U dY = \frac{\Delta Y}{3} (\cancelto{0}{U_1^n} + 4U_2^n + 2U_3^n + \ldots + 4U_M^n + \cancelto{0}{U_{M+1}^n}) \tag{5.12}$$

Substituting the above into Eq. (5.8), we obtain for column n:

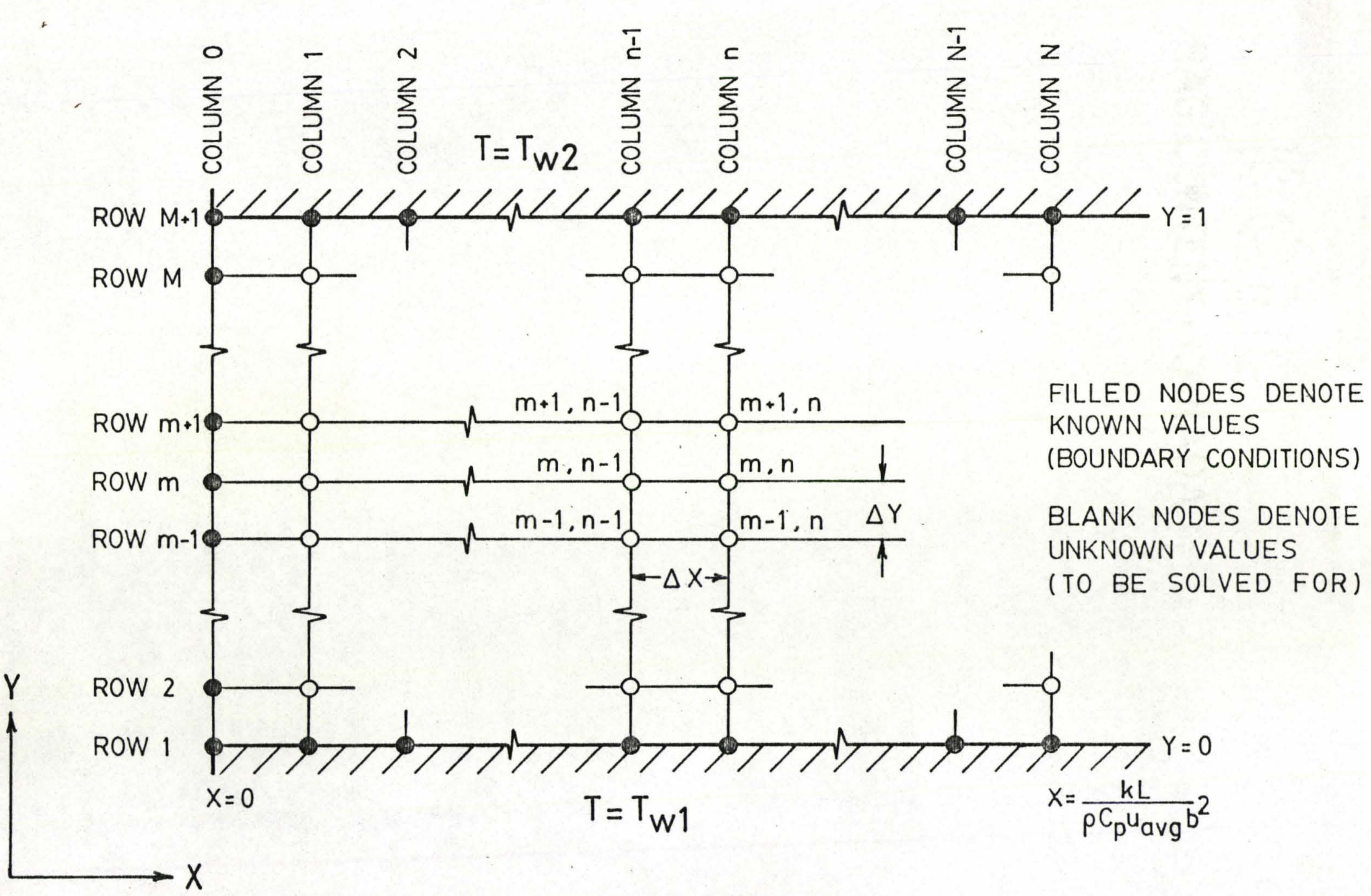

Fig. 5-2. Finite difference grid. Poiseuille flow between parallel plates.

$$4U_2^n + 2U_3^n + \ldots + 4U_M^n = \frac{3}{\Delta Y} = 3M \qquad (5.13)$$

Momentum Equation

For the momentum equation, the following finite difference approximations are used:

$$\frac{dP}{dX} = \frac{P^n - P^{n-1}}{\Delta X} \qquad (5.14)$$

$$\frac{dU}{dY} = \frac{U_{m+1}^n - U_{m-1}^n}{2\Delta Y} \qquad (5.15)$$

$$\frac{d^2U}{dY^2} = \frac{U_{m-1}^n - 2U_m^n + U_{m+1}^n}{(\Delta Y)^2} \qquad (5.16)$$

Substituting Eqs. (5.14), (5.15) and (5.16) into equation (5.9), we obtain for column n (details in App. A, Sec. 2.1):

$$A_m U_{m-1}^n + B_m U_m^n + C_m U_{m+1}^n + W_m P^n - W_m P^{n-1} = 0 \qquad (5.17)$$

$$\left.\begin{aligned} \text{where } A_m &= -\frac{\Delta Y}{2\eta_m^n}\left(\frac{d\eta}{dY}\right)_m^n + 1 \\ B_m &= -2 \\ C_m &= \frac{\Delta Y}{2\eta_m^n}\left(\frac{d\eta}{dY}\right)_m^n + 1 \\ W_m &= -\frac{k}{\eta_m^n C_p} \cdot \frac{(\Delta Y)^2}{\Delta X} \end{aligned}\right\} \quad (m = 2, 3, \ldots, M)$$

Combining Eqs. (5.13) and (5.17), we have for column n a modified tri-diagonal system of M equations and M unknowns (U_2^n to U_M^n and P^n). The equations can be written as follows:

$$A_2U_1^n + B_2U_2^n + C_2U_3^n + W_2P^n - W_2P^{n-1} = 0$$

$$A_mU_{m-1}^n + B_mU_m^n + C_mU_{m+1}^n + W_mP^n - W_mP^{n-1} = 0 \quad (m = 3, 4, \ldots, M-1)$$

$$A_MU_{M-1}^n + B_MU_M^n + C_MU_{M+1}^n + W_MP^n - W_MP^{n-1} = 0 \tag{5.18}$$

$$4U_2 + 2U_3 + \ldots + 4U_M = 3M$$

or in matrix form:

$$\begin{bmatrix} B_2 & C_2 & & & \underline{0} & & W_2 \\ A_3 & B_3 & C_3 & & & & W_3 \\ & \ddots & \ddots & \ddots & & & \vdots \\ & & A_m & B_m & C_m & & W_m \\ & & & \ddots & \ddots & \ddots & \vdots \\ & & & A_{M-1} & B_{M-1} & C_{M-1} & W_{M-1} \\ & \underline{0} & & & A_M & B_M & W_M \\ 4 & 2 & 4 & \ldots & 2 & 4 & 0 \end{bmatrix} \begin{bmatrix} U_2^n \\ U_3^n \\ \vdots \\ U_m^n \\ \vdots \\ U_{M-1}^n \\ U_M^n \\ P^n \end{bmatrix} = \begin{bmatrix} W_2P^{n-1} \\ W_3P^{n-1} \\ \vdots \\ W_mP^{n-1} \\ \vdots \\ W_{M-1}P^{n-1} \\ W_MP^{n-1} \\ 3M \end{bmatrix} \tag{5.19}$$

or

$$
\begin{bmatrix}
B_2 & C_2 & & & & \underline{0} & W_2 \\
A_3 & B_3 & C_3 & & & & W_3 \\
\ddots & \ddots & \ddots & & & & \vdots \\
 & A_m & B_m & C_m & & & W_m \\
 & & \ddots & \ddots & \ddots & & \vdots \\
 & & & A_{M-1} & B_{M-1} & C_{M-1} & W_{M-1} \\
 & \underline{0} & & & A_M & B_M & W_M \\
Z_2 & Z_3 & Z_4 & \cdots & Z_{M-1} & Z_M & Z_{M+1}
\end{bmatrix}
\begin{bmatrix}
U_2^n \\ U_3^n \\ \vdots \\ U_m^n \\ \vdots \\ U_{M-1} \\ U_M^n \\ P^n
\end{bmatrix}
=
\begin{bmatrix}
H_2 \\ H_3 \\ \vdots \\ H_m \\ \vdots \\ H_{M-1} \\ H_M \\ Z_{M+2}
\end{bmatrix}
\quad (5.20)
$$

This system of equations is solved for the velocity profile and pressure at column n by Gaussian elimination using the algorithm that is shown in App. D, Sec. 2.

Energy Equation

For the energy equation, the following finite difference approximations are used:

T(i-

$$\frac{\partial \theta}{\partial X} = \frac{\theta_m^n - \theta_m^{n-1}}{\Delta X} \quad (5.21)$$

$$\frac{\partial^2 \theta}{\partial Y^2} = \frac{\theta_{m-1}^n - 2\theta_m^n + \theta_{m+1}^n}{2(\Delta Y)^2} + \frac{\theta_{m-1}^{n-1} - 2\theta_m^{n-1} + \theta_{m+1}^{n-1}}{2(\Delta Y)^2} \quad (5.22)$$

Substituting Eqs. (5.21) and (5.22) into equation (5.10), we obtain for column n (details in App. A, Sec. 2.2):

$$A_m \theta_{m-1}^n + B_m \theta_m^n + C_m \theta_{m+1}^n = D_m + E_m + F_m + G_m = H_m \quad (5.23)$$

u(i,8)

$$
\left.
\begin{aligned}
\text{where } A_m &= -1 \\
B_m &= \frac{2(\Delta Y)^2}{\Delta X} \cdot U_m^n + 2 \\
C_m &= -1 \\
D_m &= \theta_{m-1}^{n-1} \\
E_m &= \left[\frac{2(\Delta Y)^2}{\Delta X} \cdot U_m^n + 2\right] \theta_m^{n-1} \\
F_m &= \theta_{m+1}^{n-1} \\
G_m &= 2(\Delta Y)^2 \; \beta_m^n \; \left(\frac{dU}{dY}\right)_m^2
\end{aligned}
\right\} \quad (m = 2, 3, \ldots, M)
$$

Thus for column n, we have a tridiagonal system of M-1 equations and M-1 unknowns (θ_2^n to θ_M^n). The equations can be written as follows:

$$A_2\overset{0}{\theta_1^n} + B_2\theta_2^n + C_2\theta_3^n = H_2$$

$$A_m\theta_{m-1}^n + B_m\theta_m^n + C_m\theta_{m+1}^n = H_m \qquad (m = 3, 4, \ldots, M\text{-}1) \qquad (5.24)$$

$$A_M\theta_{M-1}^n + B_M\theta_M^n + C_M\underset{\frac{T_{w2}-T_{w1}}{T_o-T_{w1}}}{\theta_{M+1}^n} = H_M$$

or in matrix form:

$$\begin{bmatrix} B_2 & C_2 & & & & & \underline{0} \\ A_3 & B_3 & C_3 & & & & \\ & \ddots & \ddots & \ddots & & & \\ & & A_m & B_m & C_m & & \\ & & & \ddots & \ddots & \ddots & \\ & & & & A_{M-1} & B_{M-1} & C_{M-1} \\ \underline{0} & & & & & A_M & B_M \end{bmatrix} \begin{bmatrix} \theta_2^n \\ \theta_3^n \\ \vdots \\ \theta_m^n \\ \vdots \\ \theta_{M-1}^n \\ \theta_M^n \end{bmatrix} = \begin{bmatrix} H_2 \\ H_3 \\ \vdots \\ H_m \\ \vdots \\ H_{M-1} \\ H_M - C_M \theta_{M+1}^n \end{bmatrix} \tag{5.25}$$

This system of equations is solved for the temperature profile along column n by Gaussian elimination using Thomas' method (details in App. D, Sec. 1).

Bulk Temperature

The dimensionless flow-average (bulk) temperature is calculated from the following definition:

$$\theta_{bulk} = \frac{\int_{Y=0}^{Y=1} \theta(X,Y)\ U(X,Y)\ dY}{\int_{Y=0}^{Y=1} U(X,Y)\ dY} \tag{5.26}$$

For column n, Eq. (5.26) is written in finite difference form using Simpson's Rule as follows:

$$\theta_{bulk}^n = \frac{\overset{0}{\overset{\nearrow}{\theta_1^n U_1^n}} + 4\theta_2^n U_2^n + 2\theta_3^n U_3^n + \ldots + 4\theta_M^n U_M^n + \overset{0}{\overset{\nearrow}{\theta_{M+1}^n U_{M+1}^n}}}{\underset{0}{\underset{\searrow}{U_1^n}} + 4U_2^n + 2U_3^n + \ldots + 4U_M^n + \underset{0}{\underset{\searrow}{U_{M+1}^n}}} \tag{5.27}$$

Local Nusselt Number

The local Nusselt number is calculated from the following definition which is derived in App. B:

$$Nu_x = \frac{hb}{k} = \frac{\left(\frac{dT}{dy}\right)_{wall} \cdot b}{(T_{bulk} - T_{wall})} \tag{5.28}$$

In dimensionless form, we have:

$$(Nu_x)_{Y=0} = \frac{\left(\frac{d\theta}{dY}\right)_{Y=0}}{\theta_{bulk}} \tag{5.29}$$

$$(Nu_x)_{Y=1} = \frac{-\left(\frac{d\theta}{dY}\right)_{Y=1}}{\theta_{bulk} - \theta_{w2}} \tag{5.30}$$

The dimensionless temperature gradients at the walls are estimated for column n by the following finite difference approximations:

$$\left(\frac{d\theta}{dY}\right)^n_{Y=0} = \frac{1}{6\Delta Y} (-11\overset{0}{\theta^n_1} + 18\theta^n_2 - 9\theta^n_3 + 2\theta^n_4) \tag{5.31}$$

$$\left(\frac{d\theta}{dY}\right)^n_{Y=1} = \frac{1}{6\Delta Y} (-2\theta^n_{M-2} + 9\theta^n_{M-1} - 18\theta^n_M + 11\theta^n_{M+1}) \tag{5.32}$$

The above equations are derived in App. C, Sec. 1 and 5.

5.2 Computational Procedure

It was stated in Chap. 3, Sec. 3, that the momentum and energy equations are coupled by velocity and temperature, and therefore cannot be solved independently. However, the coupled equations can be solved iteratively at a given column on the finite difference grid by alternately solving the set of continuity and momentum equations (5.18) and the set of energy equations (5.24) until the solutions converge. The iterative "marching" procedure used to calculate the velocity and temperature profiles, the pressure, the bulk temperature and the local Nusselt numbers at each column in the grid is now outlined.

Notation

$U1_m^n$ $(m = 1, 2, \ldots, M+1)$ refers to the estimated velocity profile at column n.

$U2_m^n$ $(m = 1, 2, \ldots, M+1)$ refers to the most recently calculated velocity profile at column n.

θ_m^{n-1} $(m = 1, 2, \ldots, M+1)$ refers to the temperature profile at column n-1.

$\theta 1_m^n$ $(m = 1, 2, \ldots, M+1)$ refers to the estimated temperature profile at column n.

$\theta 2_m^n$ $(m = 1, 2, \ldots, M+1)$ refers to the most recently calculated temperature profile at column n.

Procedure

1. Assume values for the velocity and temperature profiles and the pressure at the entrance of the channel (at column 0).

$$\left.\begin{aligned} U1_m^o &= \left(\frac{\nu+1}{\nu}\right)\left(1-|2Y - 1|^{\nu}\right) \\ \theta_m^o &= 1 \\ P^o &= 0 \end{aligned}\right\} \quad (m = 1, 2, \ldots, M+1)$$

2. Print the velocity and temperature profiles at column 0.

3. Set the estimates of the velocity and temperature profiles to be used in the first iteration at column 1 equal to the values of the respective profiles at column 0.

$$n = 1$$

$$U1_m^1 = U1_m^o \qquad (m = 1, 2, \ldots, M+1)$$

$$\theta 1_1^1 = \theta 2_1^1 = 0, \quad \theta 1_{M+1}^1 = \theta 2_{M+1}^1 = \frac{T_{w2}-T_{w1}}{T_o-T_{w1}}$$

$$\theta 1_m^1 = \theta_m^o \qquad (m = 2, 3, \ldots, M)$$

4. To economize on computing time, increase ΔX by a factor of 10 after the final velocity and temperature profiles have been calculated at column $n = NA$, and again after they have been calculated at column $n = NB$ (see program listing, App. F, Sec. 2).

$$\Delta X = 10\ \Delta X \text{ at column NA+1 and again at column NB+1}$$

5. Using $U1_m^n$ and $\theta 1_m^n$ $(m = 1, 2, \ldots, M+1)$, calculate $(\frac{dU}{dY})_m^n$ and η_m^n $(m = 1, 2, \ldots, M+1)$ at column n.

6. Using $U1_m^n$, $(\frac{dU}{dY})_m^n$, η_m^n and θ_m^{n-1} $(m = 1, 2, \ldots, M+1)$, solve the set of energy equations (5.25) by Gaussian elimination using Thomas' method (see App. D, Sec. 1) to obtain $\theta 2_m^n$ $(m = 2, 3, \ldots, M)$.

7. Using $U1_m^n$ and $\theta 2_m^n$ $(m = 1, 2, \ldots, M+1)$, calculate η_m^n and $(\frac{d\eta}{dY})_m^n$ $(m = 1, 2, \ldots, M+1)$ at column n.

8. Using P^{n-1}, η_m^n and $(\frac{d\eta}{dY})_m^n$ $(m = 1, 2, \ldots, M+1)$, solve the set of

continuity and momentum equations (5.19) by Gaussian elimination (see App. D, Sec. 2 for algorithm) to obtain $U2_m^n$ and P^n (m = 2, 3, ..., M).

9. Compare $U1_m^n$, $U2_m^n$ and $\theta1_m^n$, $\theta2_m^n$ (m = 1, 2, ..., M+1). If $|U2_m^n - U1_m^n|$ < tolerance and $|\theta2_m^n - \theta1_m^n|$ < tolerance for all m, then proceed to step 12. Otherwise, continue to step 10.

10. Set the estimates of the velocity and temperature profiles to be used in the next iteration at column n equal to the most recently calculated profiles.

$$\left.\begin{aligned} U1_m^n &= U2_m^n \\ \theta1_m^n &= \theta2_m^n \end{aligned}\right\} \qquad (m = 1, 2, \ldots, M+1)$$

11. Repeat steps 5 through 9 until the desired error tolerances have been achieved.

12. Set the estimates of the velocity and temperature profiles to be used in the first iteration at column n+1 equal to the final values of the profiles calculated at column n. Also, retain the final temperature profile calculated at column n for use in calculating temperature profiles at column n+1.

$$\left.\begin{aligned} U1_m^{n+1} &= U2_m^n \\ \theta1_m^{n+1} &= \theta2_m^n \\ \theta_m^n &= \theta2_m^n \end{aligned}\right\} \qquad (m = 1, 2, \ldots, M+1)$$

13. Repeat steps 4 through 12 to calculate the velocity and temperature

profiles at the next column downstream in the channel (n = n+1).

The following steps are to be carried out at periodic intervals along the length of the channel:

14. Print the velocity and temperature profiles and the pressure.

15. Calculate the bulk temperature using Simpson's Rule (see Eq. (5.27)).

16. Calculate the local Nusselt numbers at the walls (see Eqs. (5.29) and (5.30)).

17. Print the bulk temperature and the local Nusselt numbers.

Computations using the above algorithm have been carried out in McMaster's CDC 6400 computer. A sample program listing with results is located in App. F, Sec. 2.

5.3 Convergence, Stability and Step Size

It was stated in Chap. 3, Sec. 4, that a good indication of the convergence and stability of the finite difference results is the negligible change in results obtained when the step sizes in the finite difference grid are decreased. It should be noted that special care must be taken in choosing step sizes when calculating local Nusselt numbers. Although the temperature profiles may appear to be sufficiently accurate, the local Nusselt numbers can still be incorrect. Local Nusselt numbers are calculated from temperature derivatives (see Eq. (5.28)). Since derivatives are very sensitive to step size changes, smaller step sizes must be used when calculating local Nusselt numbers, than when only calculating velocity and temperature profiles. The step sizes shown in Table 5-1 were used in the finite difference program. The results presented in the subsequent figures are independent of step size within at least 3 significant digits.

Table 5-1. Step sizes for finite difference program Poiseuille flow between parallel plates.

Range of X	ΔX	ΔY
0 -0.1	0.0001	0.01
0.1-0.3	0.001	0.01
0.3-1.0	0.01	0.01

Two additional tests for the convergence of the finite difference results were carried out. In the first test, the dimensionless bulk temperatures and local Nusselt numbers were obtained for a Newtonian, constant viscosity fluid with no viscous dissipation, and compared with the results obtained by Vlachopoulos and Keung (70) by the explicit finite difference method. The results are compared in Table 5-2, and as can be seen, differ by very little. In the second test, the fully-developed temperature profile, the limiting bulk temperature and the limiting local Nusselt number (at large X) were calculated analytically for a Newtonian, constant viscosity fluid with viscous dissipation (see App. E, Sec. 2), and compared with the corresponding finite difference results for the same fluid. The analytical and finite difference results were indistinguishable.

Table 5-2. Comparison of dimensionless bulk temperatures and local Nusselt numbers. Newtonian fluid with no viscous dissipation.

	Present work		Vlachopoulos and Keung	
X	θ_{bulk}	Nu_x	θ_{bulk}	Nu_x
0.0075	0.892	5.36	0.89	5.35
0.01875	0.798	4.31	0.80	4.31
0.0375	0.690	3.89	0.69	3.89
0.075	0.520	3.77	0.52	3.77
0.150	0.293	3.77	0.29	3.77
0.225	0.167	3.77	0.18	3.77
0.300	0.095	3.77	0.09	3.77
0.375	0.054	3.77	0.05	3.77

5.4 Results and Discussion

Solutions of the continuity, momentum and energy equations for Poiseuille flow between parallel plates are presented in Figs. 5-3 through 5-13. The following velocity and temperature boundary conditions have been used:

$$
\begin{array}{lll}
x = 0 & u = u_{avg}\left(\frac{\nu+1}{\nu}\right)\left(1-\left|\frac{2y}{b} - 1\right|^{\nu}\right) & T_o=130°C \quad p_o=0 \\
\multicolumn{3}{l}{\text{where } u_{avg} = 15 \text{ cm/s}, \ \nu = \frac{n+1}{n}, \quad n = 0.453} \\
y = 0 & u = 0 & T_{w1}=160°C \\
y = b = 0.25 \text{ cm} & u = 0 & T_{w2}=160°C
\end{array}
\tag{5.33}
$$

In obtaining some of the results, different temperature boundary conditions were used for comparison. The following power-law temperature-dependent viscosity model and fluid properties representing a typical high-density polyethylene melt were used in the computations:

Viscosity: $$\eta = Ae^{-Bn(T-T_m)} \left|\frac{du}{dy}\right|^{n-1} \tag{5.34}$$

where $A = 282\ 000$ poise$\cdot s^{n-1}$

$= 28\ 200$ Pa$\cdot s^n$

$B = 0.024\ K^{-1}$

$n = 0.453$

$T_m = 399.5$ K

Density: $\rho = 794$ kg/m^3

Specific heat:

$C_p = 0.6$ cal/(g$\cdot$K)

$= 2.51$ kJ/(kg$\cdot$K)

Thermal conductivity:

$k = 6.1 \times 10^{-4}$ cal/(cm$\cdot$s$\cdot$K)

$= 0.255$ W/(m$\cdot$K)

The temperature profiles, bulk temperatures and local Nusselt numbers in Figs. 5-3 through 5-13 are shown as functions of the dimensionless axial distance, X. Because the bulk temperatures and local Nusselt numbers change the most near the entrance of the flow channel, they have been plotted semi-logarithmically. X on the abscissa of these plots ranges from 0.001 to 1.0. This corresponds to x ranging from 0.7 cm to 732 cm. At X = 1.0, the temperature profile has become fully developed. Beyond this point in the channel, the temperature profiles, bulk temperatures and local Nusselt numbers remain the same, and thus are known as the limiting or asymptotic values.

In Figs. 5-3 and 5-4, the temperature profiles for the power-law temperature-dependent viscosity model and for a power-law temperature-independent viscosity model are compared. Two different temperature boundary conditions have been considered: both plates at 160°C in Fig. 5-3, and one plate at 190°C and the other at 130°C in Fig. 5-4. The temperature-independent viscosity model used is identical to the temperature-dependent viscosity model given in Eq. (5.34), except that T is held constant and equal to the average of the temperatures of the two plates (160°C in both cases). In Fig. 5-4, it can be seen that near the cold wall (T=130°C) the temperature of the fluid is higher with the temperature-dependent model than with the temperature-independent model. The opposite is true near the hot wall (T=190°C). The reason for this is that the viscosity decreases with increasing temperature. Near the cold wall, the temperature in the constitutive equation of the temperature-dependent model is lower than that of the temperature-independent model. Therefore, the viscosity will be higher in the temperature-dependent case resulting in more heat generated by viscous dissipation. Near the hot wall, more heat is generated in the temperature-independent case. In

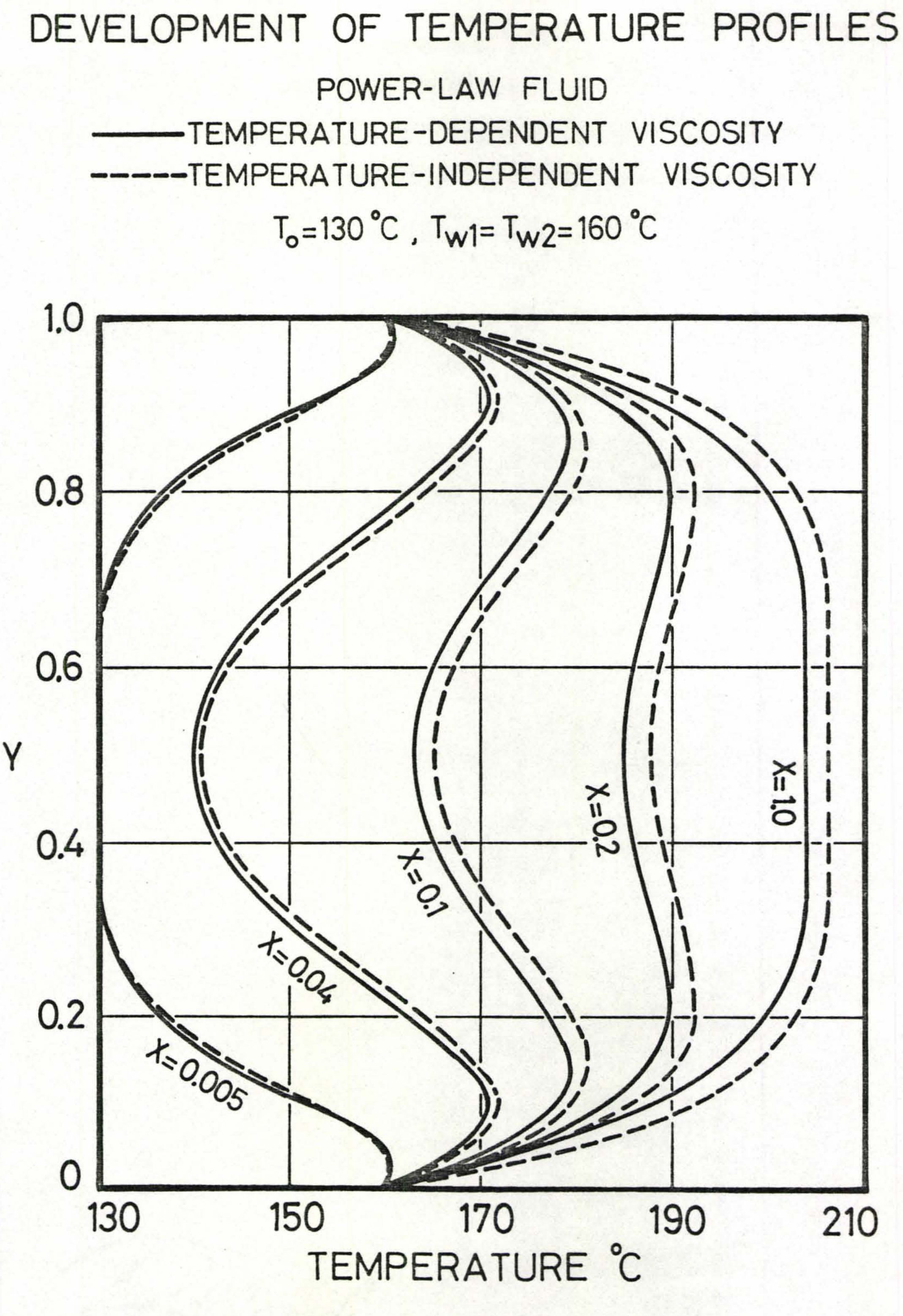

Fig. 5-3. Development of temperature profiles. Poiseuille flow between parallel plates. Channel dimensions and fluid properties given on pp. 80-81.

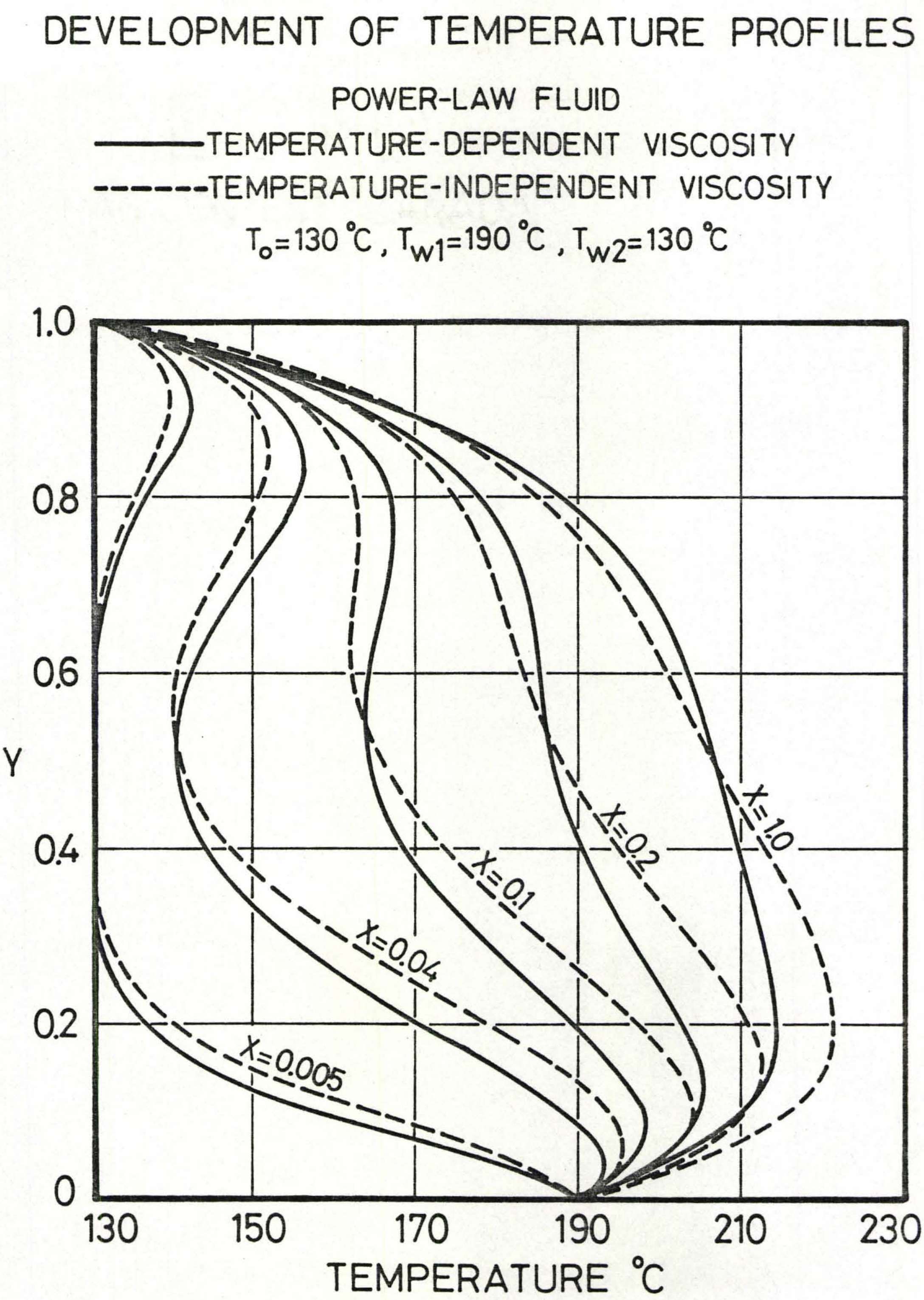

Fig. 5-4. Development of temperature profiles. Poiseuille flow between parallel plates. Channel dimensions and fluid properties given on pp. 80-81.

both Figs. 5-3 and 5-4, the bulges in the temperature profiles indicate that more heat is generated by viscous dissipation near the walls than near the centre-line of flow. This is due to the fact that the shear rates are highest near the channel walls.

Plots of the bulk temperatures along the length of the channel are presented in Figs. 5-5 through 5-9 for the power-law temperature-dependent and temperature-independent viscosity models and for the Newtonian, constant viscosity model. In Fig. 5-5, the bulk temperatures are shown for power-law temperature-dependent viscosity fluids with different inlet temperatures. In each case, the limiting bulk temperature is the same (201.2°C). This is to be expected since the fully-developed velocity and temperature profiles are only influenced by the wall boundary conditions and by the viscosity and the thermal conductivity of the fluid, but not by the inlet conditions of the fluid. Also shown in Fig. 5-5 is the effect of removing the viscous dissipation term from the energy equation. Without viscous dissipation, the limiting bulk temperature is equal to the wall temperature (160°C). The difference of 41.2°C is an indication of the importance of viscous dissipation in the Poiseuille flow of polymer melts between parallel plates.

The rise in bulk temperature of the power-law temperature-dependent viscosity fluid is shown in Fig. 5-6 for the two temperature boundary conditions discussed earlier. Even though the average of the wall temperatures is the same (160°C), the limiting bulk temperatures differ by 3°C. In Figs. 5-7 and 5-8, the bulk temperatures of the power-law temperature-dependent and temperature-independent viscosity fluids are compared

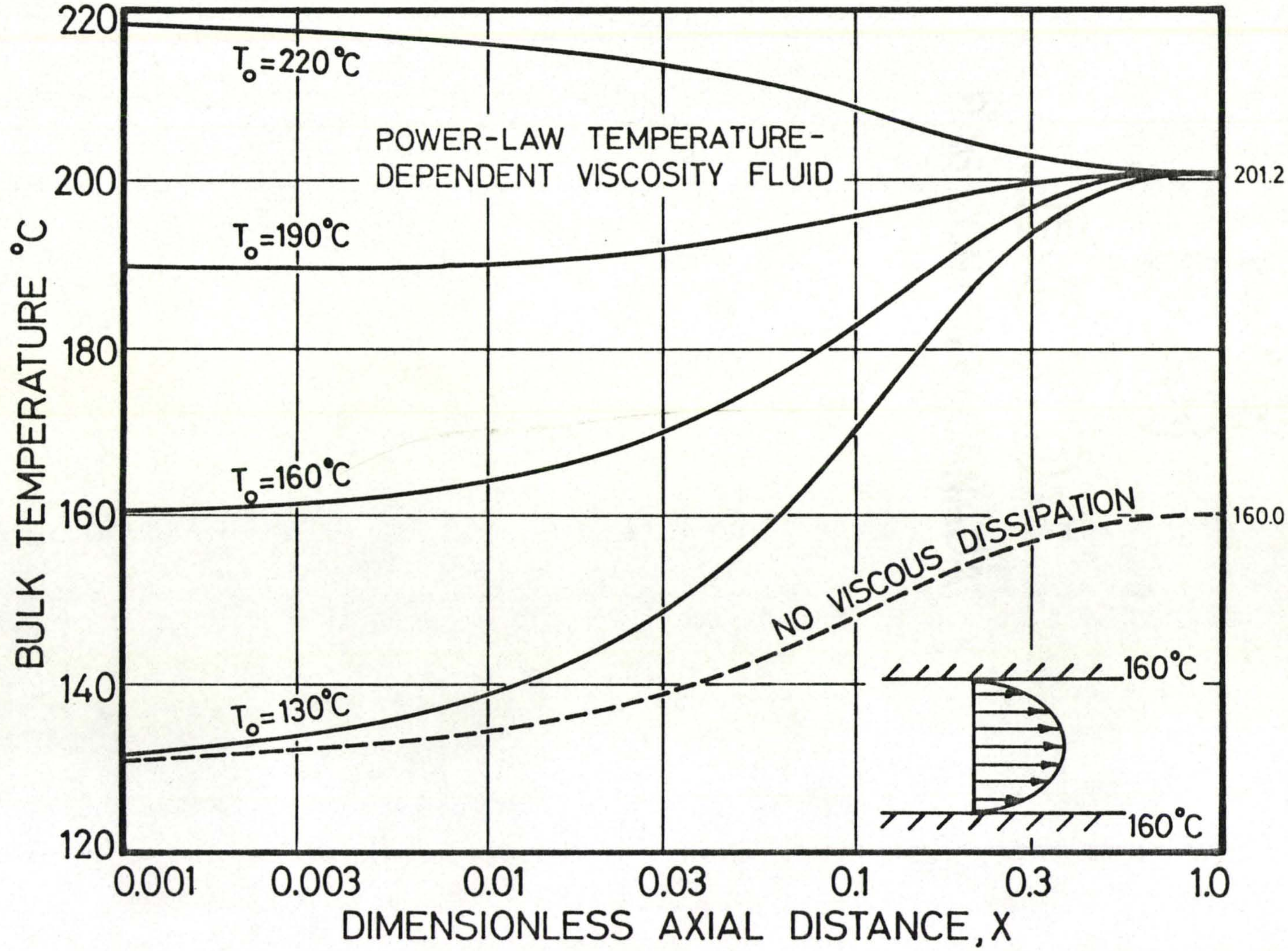

Fig. 5-5. Bulk temperature vs. X. Poiseuille flow between parallel plates. Channel dimensions and fluid properties given on pp. 80-81.

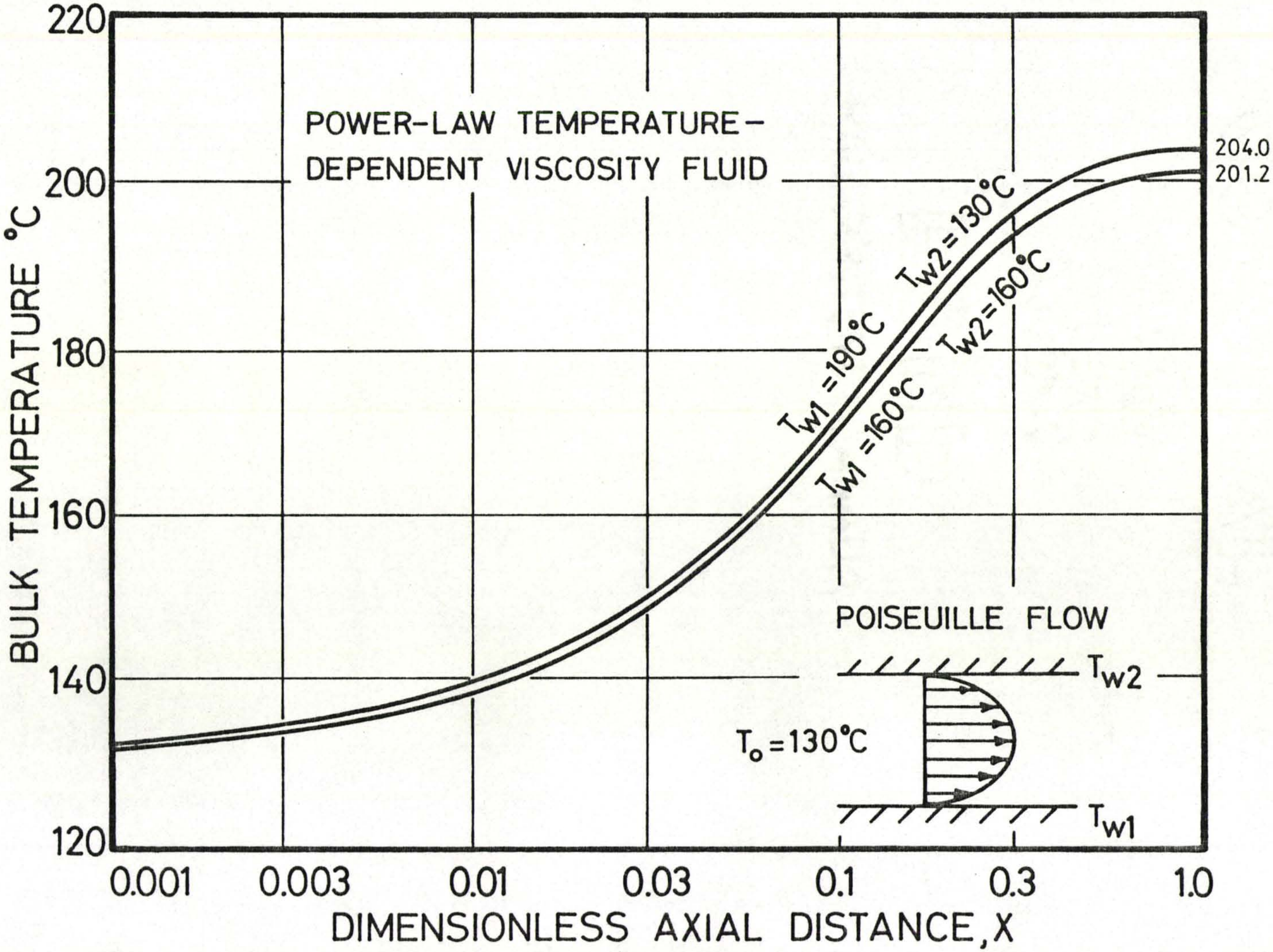

Fig. 5-6. Bulk temperature vs. X. Poiseuille flow between parallel plates. Channel dimensions and fluid properties given on pp. 80-81.

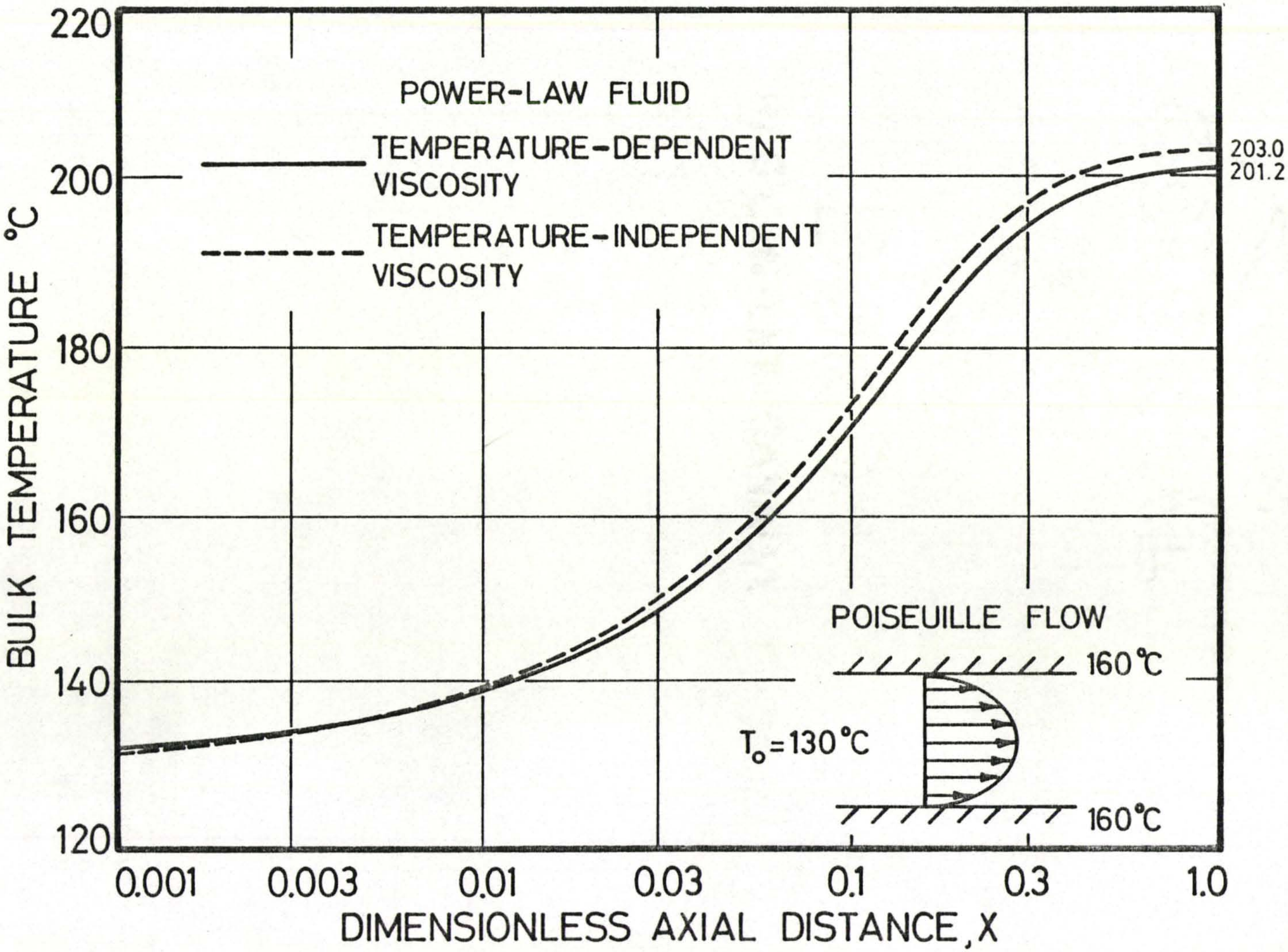

Fig. 5-7. Bulk temperature vs. X. Poiseuille flow between parallel plates. Channel dimensions and fluid properties given on pp. 80-81.

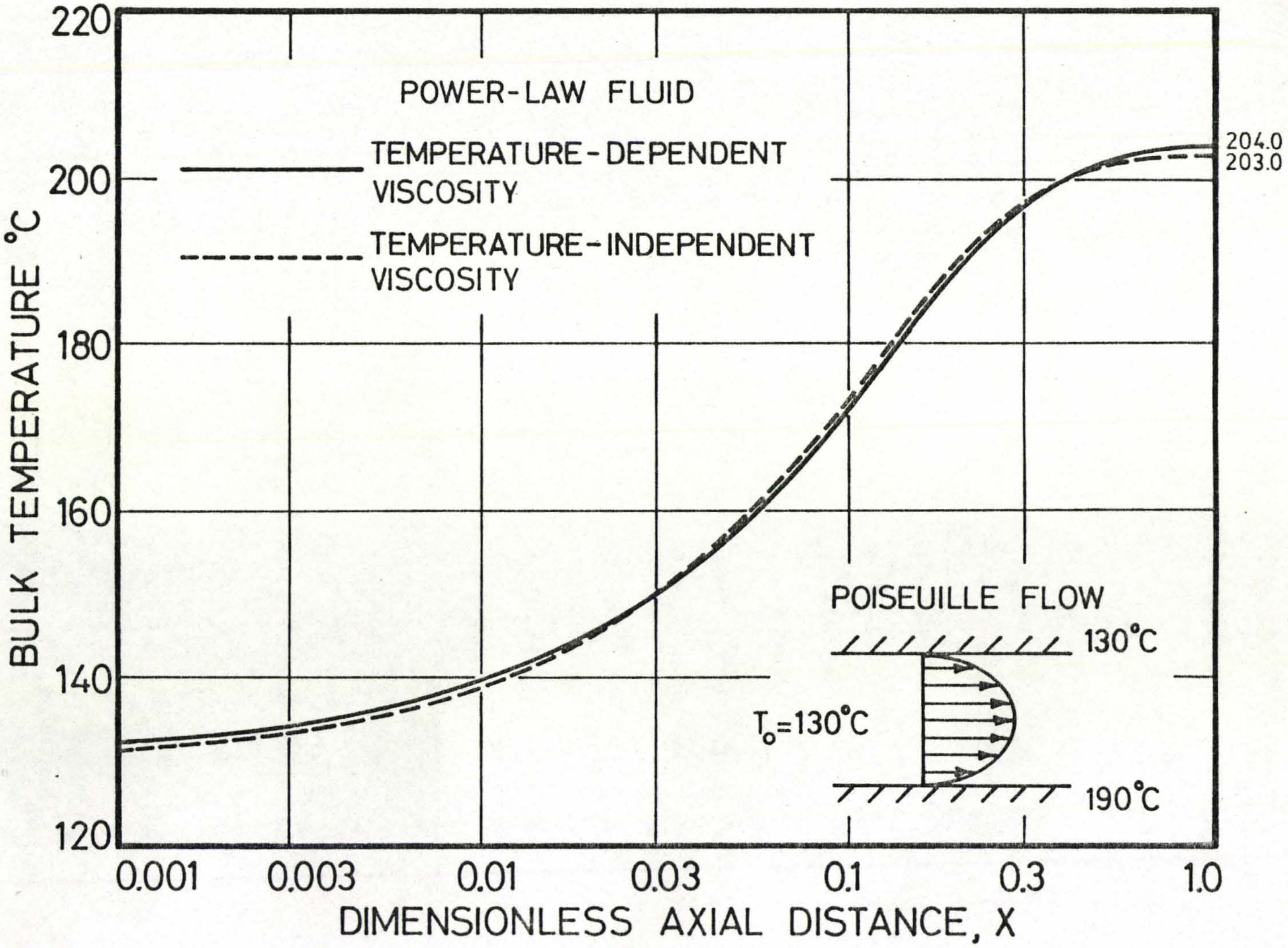

Fig. 5-8. Bulk temperature vs. X. Poiseuille flow between parallel plates. Channel dimensions and fluid properties given on pp. 80-81.

for the two temperature boundary conditions. Although the temperature profiles of the temperature-dependent and temperature-independent viscosity fluids differ substantially, especially when the two wall temperatures are different, the bulk temperatures differ much less. The rise in bulk temperature of the power-law temperature-dependent viscosity fluid is compared with several Newtonian, constant viscosity fluids in Fig. 5-9.

Plots of the local Nusselt number along the length of the channel are presented in Figs. 5-10 through 5-13 for the power-law temperature-dependent and temperature-independent viscosity models and the Newtonian, constant viscosity model. When the two wall temperatures are not the same, the local Nusselt number must be calculated at each wall separately. Since the local Nusselt number is a function of the temperature gradient at the wall (see Eq. (5.28)), it will be different at the two walls when the wall temperatures are different.

In Fig. 5-10, the local Nusselt numbers are shown for the power-law temperature-dependent viscosity fluids having different inlet temperatures. In each case, the limiting local Nusselt number is 8.95. Although not shown, the limiting local Nusselt number for the case where viscous dissipation has been neglected is 4.00. It can be seen that when the fluid is heated by the channel walls (T_o=130°C, T_{w1}=T_{w2}=160°C), there is a region along the channel where the local Nusselt number is negative, and a point where it is discontinuous. With the aid of Eq. (5.28), this behaviour is explained as follows:

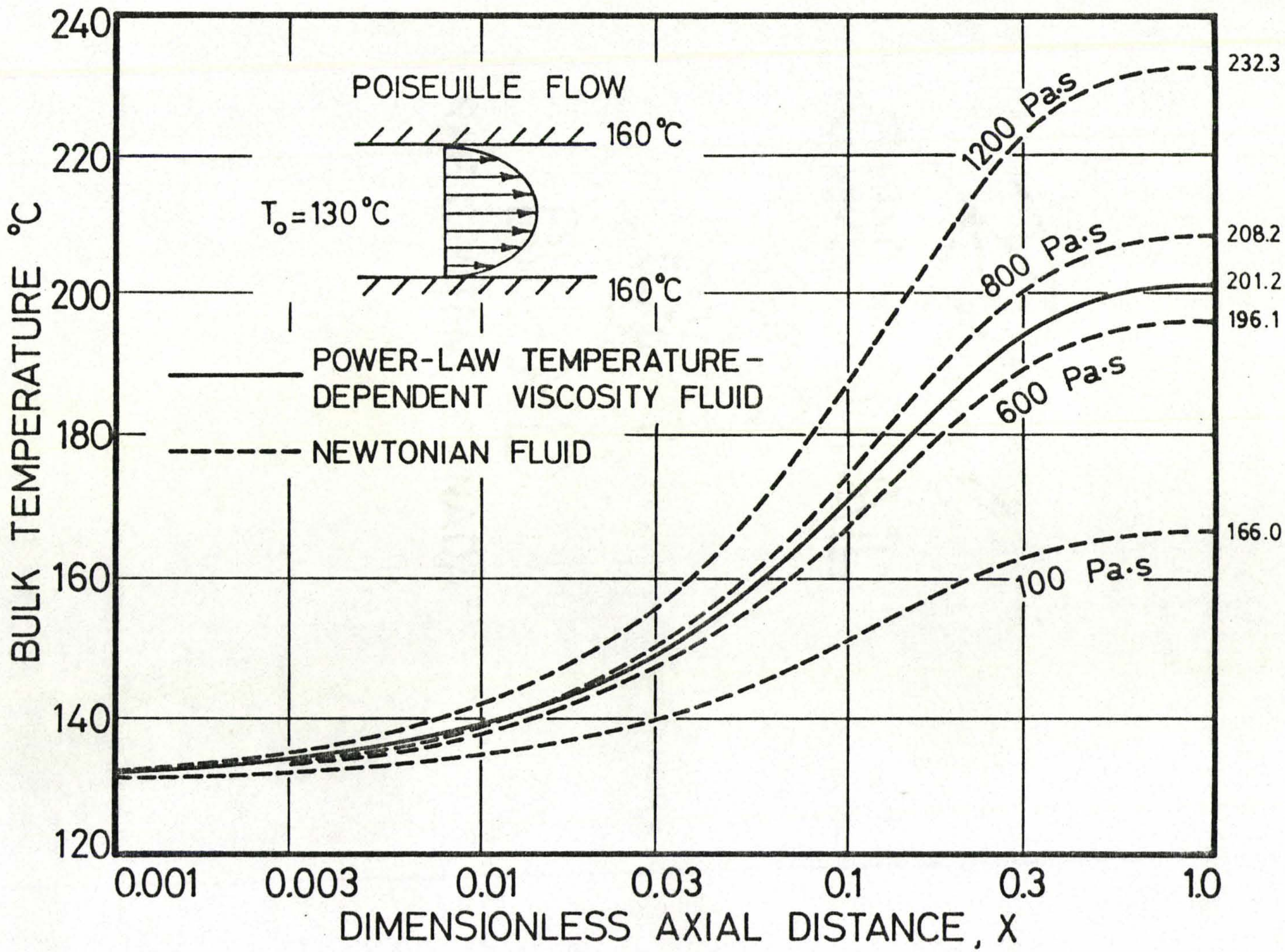

Fig. 5-9. Bulk temperature vs. X. Poiseuille flow between parallel plates. Channel dimensions and fluid properties given on pp. 80-81.

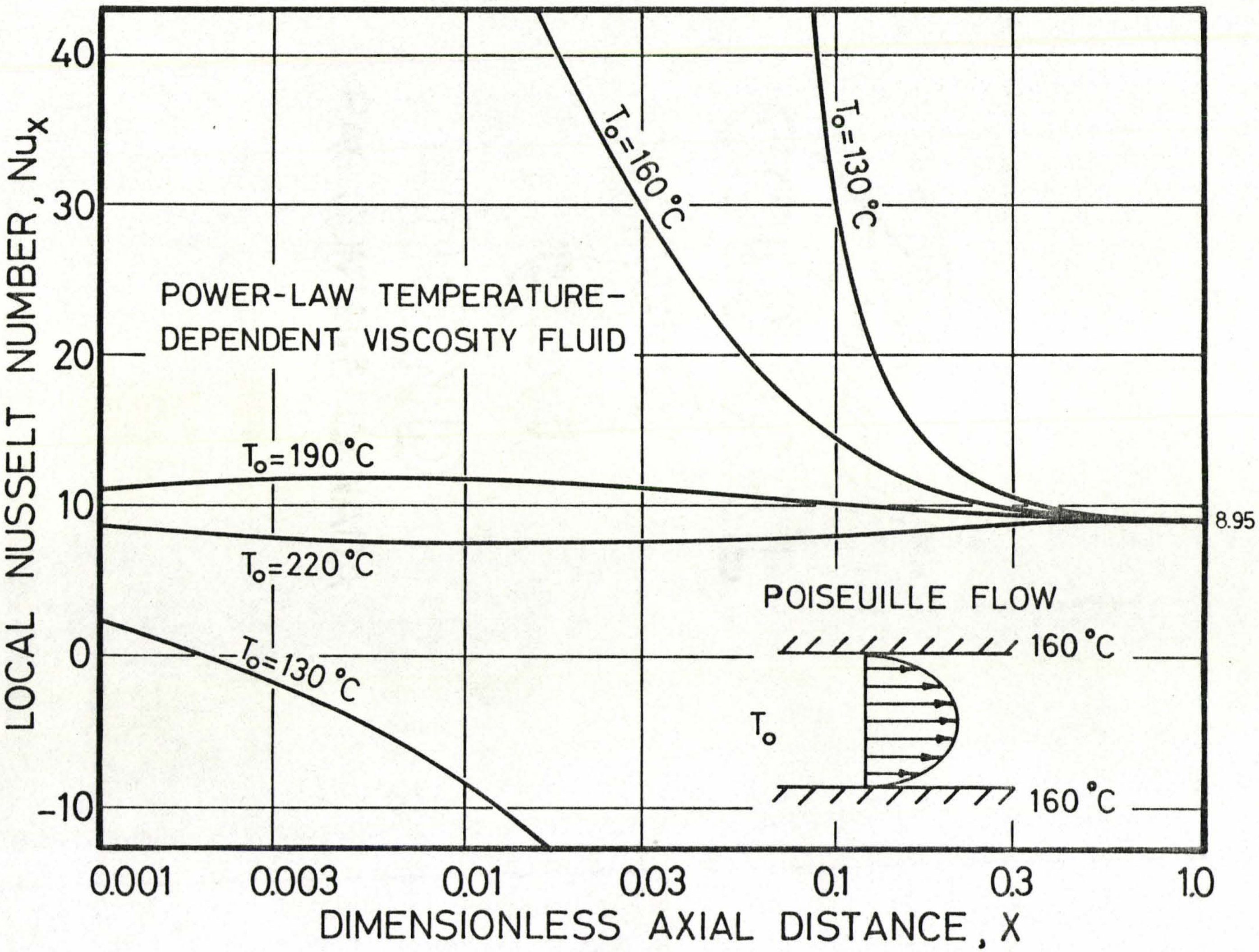

Fig. 5-10. Local Nusselt number vs. X. Poiseuille flow between parallel plates. Channel dimensions and fluid properties given on pp. 80-81.

$$Nu_x = \frac{hb}{k} = \frac{(\frac{dT}{dy})_{wall} \cdot b}{T_{bulk} - T_{wall}} \tag{5.28}$$

$X < 0.002$	$\frac{dT}{dy} < 0$	$T_b < T_w$	$Nu_x > 0$
$X \simeq 0.002$	$\frac{dT}{dy} = 0$	$T_b < T_w$	$Nu_x = 0$
$0.002 < X < 0.06$	$\frac{dT}{dy} > 0$	$T_b < T_w$	$Nu_x < 0$
$X \simeq 0.06$	$\frac{dT}{dy} > 0$	$T_b = T_w$	$Nu_x = \pm\infty$
$X > 0.06$	$\frac{dT}{dy} > 0$	$T_b > T_w$	$Nu_x > 0$

When the inlet temperature is higher than the wall temperature, the local Nusselt number is always positive.

The local Nusselt numbers for the power-law temperature-dependent and temperature-independent viscosity models are presented in Figs. 5-11 and 5-12 for the temperature boundary conditions discussed earlier. In Fig. 5-11, the local Nusselt numbers are shown for the case where both walls are at 160°C. The limiting local Nusselt numbers for the temperature-dependent and temperature-independent cases are 8.95 and 11.22 respectively. In Fig. 5-12, the local Nusselt numbers are shown for the case where one wall is at 190°C and the other is at 130°C. Here, the limiting local Nusselt numbers for the temperature-dependent and temperature-independent cases are 5.77 and 7.43 at the 190°C wall and 21.88 and 32.50 at the 130°C wall. In Fig. 5-13, the local Nusselt numbers are presented for the power-law temperature-dependent viscosity model and several Newtonian,

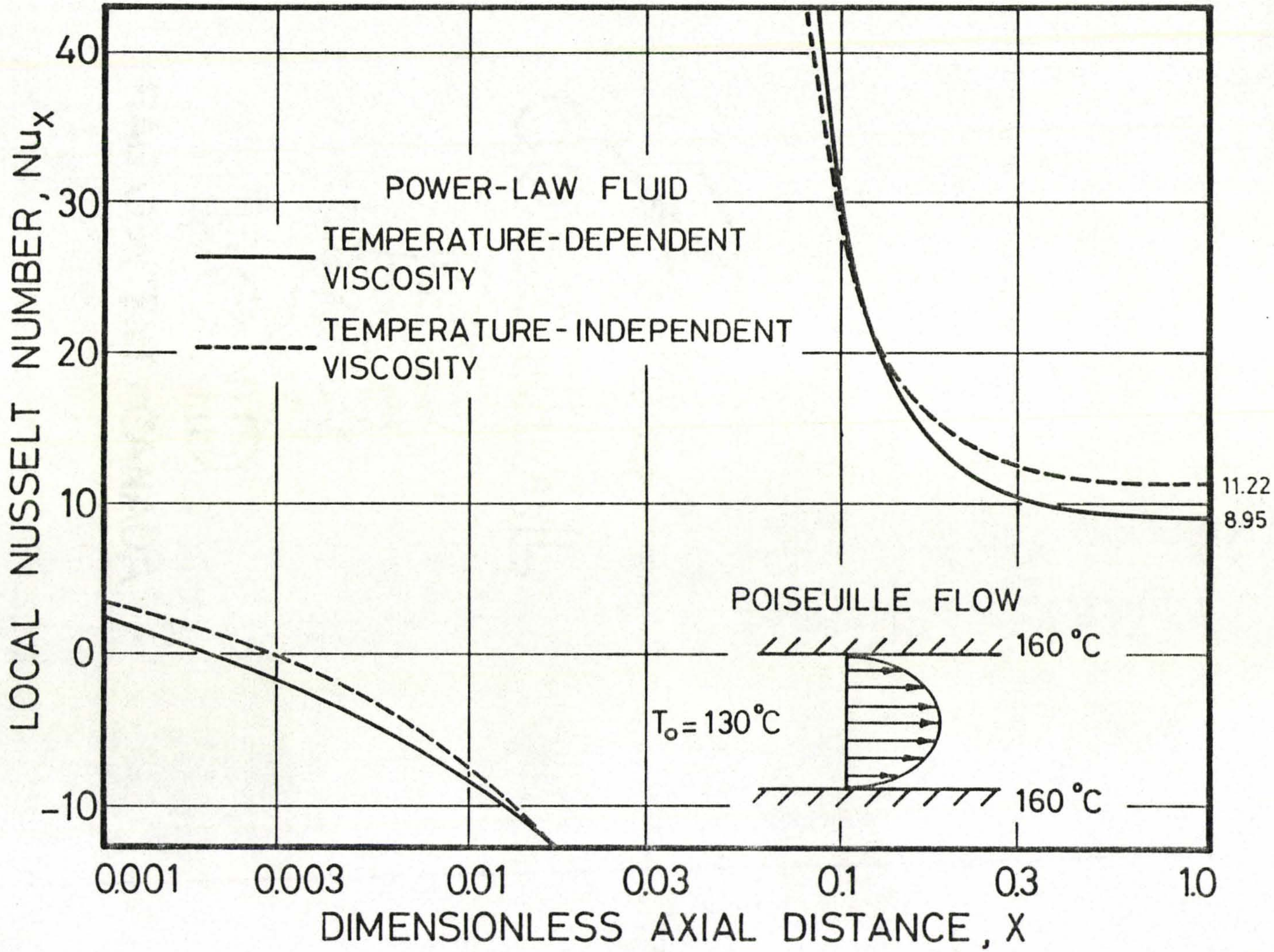

Fig. 5-11. Local Nusselt number vs. X. Poiseuille flow between parallel plates. Channel dimensions and fluid properties given on pp. 80-81.

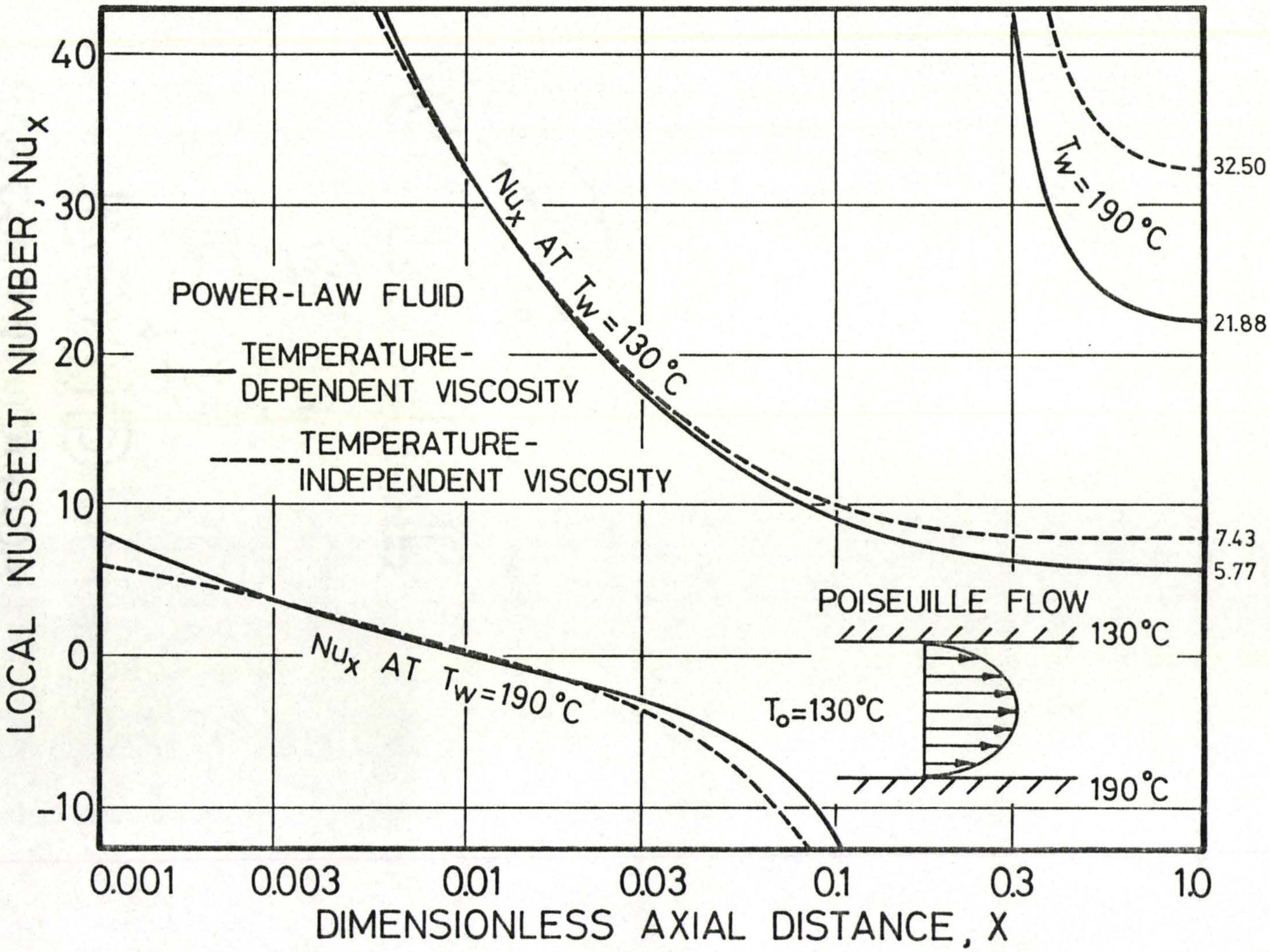

Fig. 5-12. Local Nusselt number vs. X. Poiseuille flow between parallel plates. Channel dimensions and fluid properties given on pp. 80-81.

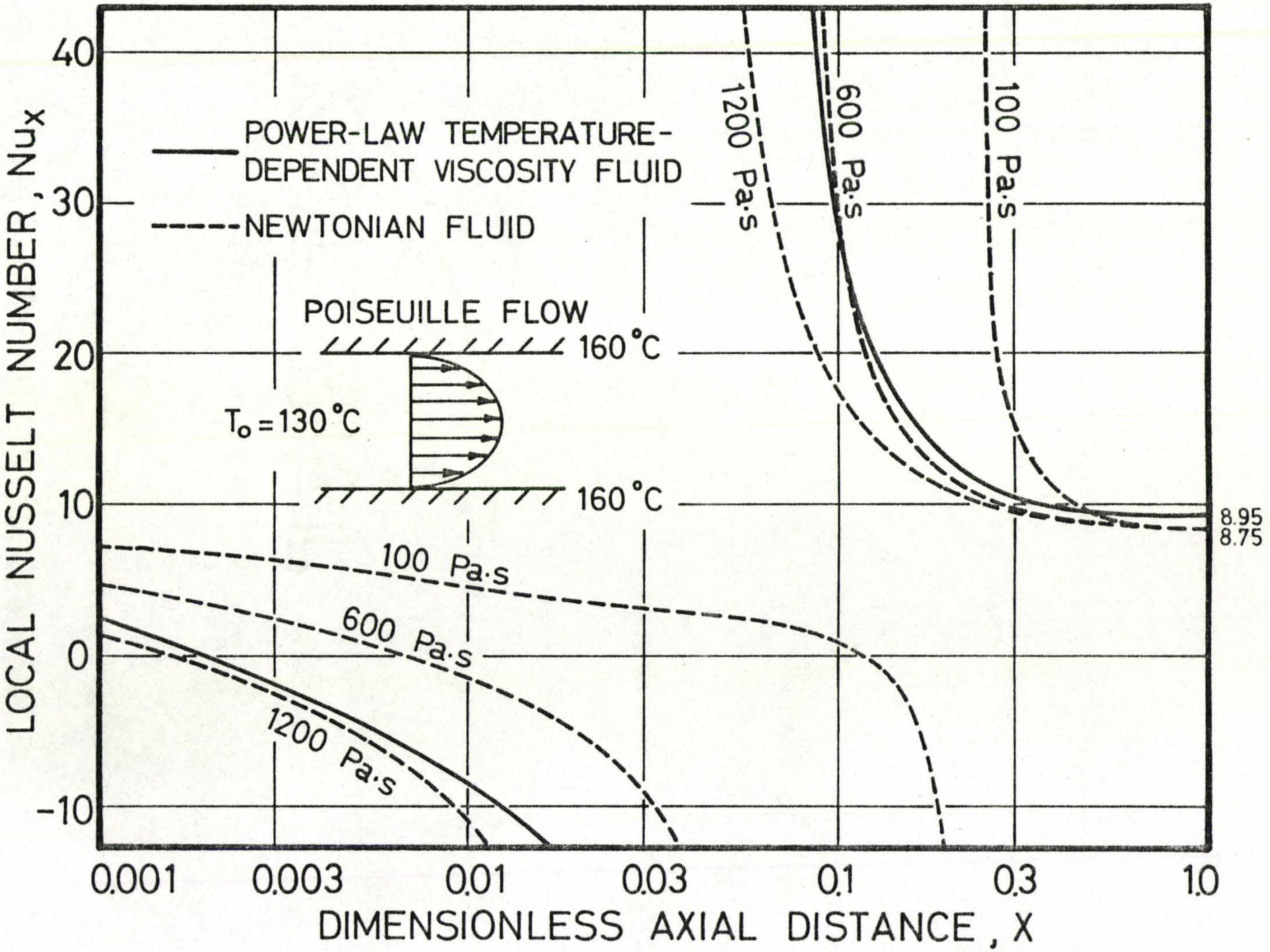

Fig. 5-13. Local Nusselt number vs. X. Poiseuille flow between parallel plates. Channel dimensions and fluid properties given on pp. 80-81.

constant viscosity models.

The results for the power-law temperature-dependent viscosity model have been compared with the power-law temperature-independent viscosity model and the Newtonian, constant viscosity model results. Given an appropriate temperature for the temperature-independent model, or an appropriate viscosity for the Newtonian model, it can be seen that the temperature-dependent model results are adequately estimated by the use of either of the simpler models. The choice of temperature and viscosity was made by inspection. However, if we did not have any temperature-dependent model results to compare our more simplified model results with, then we would not have anything to base our choice of temperature or viscosity on. Furthermore, the given temperature or viscosity is usually suitable for one type of flow only. For example, in Fig. 5-9 it can be seen that the rise in bulk temperature for the temperature-dependent model is closely approximated by that of a Newtonian fluid with a viscosity of about 700 Pa·s, while in drag flow between parallel plates, a Newtonian viscosity of 2000 Pa·s is required (see Fig.-4-7).

5.5 Concluding Remarks

1. A computer program has been developed to analyze the heat transfer problem for the Poiseuille flow of polymer melts between parallel, constant temperature plates. Results have been presented for specified velocity, pressure and temperature boundary conditions, fluid properties and channel dimensions.

2. Care must be taken when choosing the proper step sizes to ensure that the local Nusselt numbers and not only the temperature profiles have converged.

3. It is very important to consider viscous dissipation in the Poiseuille flow of polymer melts between parallel plates. A rise of 41.2°C in the limiting bulk temperature due to viscous dissipation was obtained using the specified boundary conditions, fluid properties and channel dimensions given earlier in this chapter.

4. The results obtained using the power-law temperature-dependent viscosity model were compared with those using the simpler power-law temperature-independent viscosity model and the Newtonian, constant viscosity model. It was seen that the results obtained using the temperature-dependent model were in most cases adequately approximated by either of the two simpler models, provided that a correct temperature or viscosity was chosen. However, if there are no temperature-dependent model results available, we have then no basis with which to choose a temperature for the temperature-independent model, or a viscosity for the Newtonian, constant viscosity model.

CHAPTER 6

POISEUILLE FLOW THROUGH A TUBE WITH CIRCULAR CROSS-SECTION

6.1 Mathematical Formulation

The physical system for Poiseuille (or pressure) flow through a tube with circular cross-section is illustrated in Fig. 6-1. It consists of flow through a tube with an inside radius, a, and constant temperature walls.

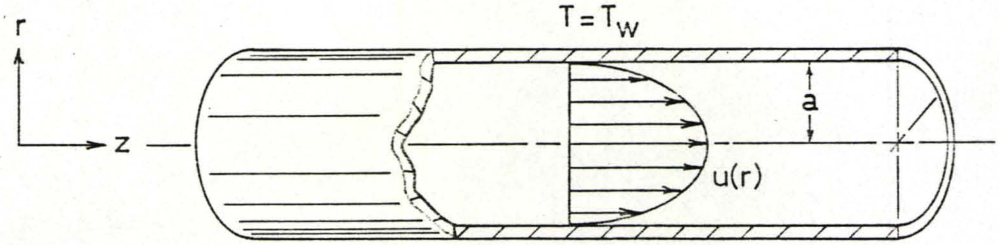

Fig. 6-1. Poiseuille flow through a tube with circular cross-section.

Flow Equations

The simplified conservation equations for Poiseuille flow through a circular tube are:

Continuity (integral form):

$$\int_{r=0}^{r=a} urdr = \frac{a^2}{2} \; u_{avg} \tag{6.1}$$

Momentum: $$-\frac{dp}{dz} + \frac{1}{r}\frac{d}{dr}(r\,\tau_{rz}) = 0 \tag{6.2}$$

or $$-\frac{dp}{dz} + \frac{1}{r}\,\tau_{rz} + \frac{d}{dr}\,\tau_{rz} = 0 \tag{6.3}$$

Energy: $$\rho C_p u\,\frac{\partial T}{\partial z} = \frac{k}{r}\frac{\partial}{\partial r}\left(r\,\frac{\partial T}{\partial r}\right) + \tau_{rz}\,\frac{du}{dr} \tag{6.4}$$

or $$\rho C_p u\,\frac{\partial T}{\partial z} = k\,\frac{\partial^2 T}{\partial r^2} + \frac{k}{r}\frac{\partial T}{\partial r} + \tau_{rz}\,\frac{du}{dr} \tag{6.5}$$

Substituting the constitutive relation, Eqs. (3.12) and (3.13) into the momentum and energy equations, we obtain:

Momentum: $$-\frac{dp}{dz} + \eta\,\frac{d^2u}{dr^2} + \left(\frac{\eta}{r} + \frac{d\eta}{dr}\right)\frac{du}{dr} = 0 \tag{6.6}$$

Energy: $$\rho C_p u\,\frac{\partial T}{\partial r} = k\,\frac{\partial^2 T}{\partial r^2} + \frac{k}{r}\frac{\partial T}{\partial r} + \eta\left(\frac{du}{dr}\right)^2 \tag{6.7}$$

where $\eta = Ae^{-Bn(T-T_m)} \left|\frac{du}{dr}\right|^{n-1}$

The boundary conditions for the above equations are

$z = 0 \qquad u = u_o(r) = u_{avg}\left[\frac{\nu+2}{\nu}\right]\left[1-\left(\frac{r}{a}\right)^{\nu}\right] \qquad T=T_o \qquad p=p_o$

where $\nu = \frac{n+1}{n}$, n = power-law index

$$r = 0 \qquad \frac{du}{dr} = 0 \qquad\qquad \frac{\partial T}{\partial r} = 0 \quad \text{(symmetry)} \tag{6.8}$$

$$r = a \qquad u = 0 \qquad\qquad T = T_w$$

A $\frac{n+1}{n}$ degree parabolic velocity profile, $u_o(r)$, has been chosen at $z = 0$. Since the entrance length for the flow of polymer melts is very short,[2] a fully-developed velocity profile can be assumed at the entrance of the tube. In addition, a constant temperature profile was used at $z = 0$.

Let

$$u = \frac{u}{u_{avg}}$$

$$P = \frac{p-p_o}{\rho u^2_{avg}}$$

$$\theta = \frac{T-T_w}{T_o-T_w} \tag{6.9}$$

$$z = \frac{kz}{\rho C_p u_{avg} a^2}$$

$$R = \frac{r}{a}$$

Substituting the above into Eqs. (6.1), (6.6) and (6.7), we obtain in terms of dimensionless parameters:

Continuity (integral form):

$$\int_{R=0}^{R=1} URdR = \frac{1}{2} \tag{6.10}$$

---

[2] $Re_D = \frac{\rho uD}{\eta} \simeq 10^{-4}$ for the flow of polymer melts. $\frac{z}{D} \simeq 0.05\ Re_D = 5 \times 10^{-6}$ where z is the entrance length. When D = 0.25 cm, z = 1.25×10^{-6} cm.

Momentum: $$-\frac{k}{C_p}\frac{dP}{dz} + \eta\frac{d^2U}{dR^2} + \left(\frac{\eta}{R} + \frac{d\eta}{dR}\right)\frac{dU}{dR} = 0 \tag{6.11}$$

Energy: $$U\frac{\partial\theta}{\partial z} = \frac{\partial^2\theta}{\partial R^2} + \frac{1}{R}\frac{\partial\theta}{\partial R} + \gamma\left(\frac{dU}{dR}\right)^2 \tag{6.12}$$

where $\gamma = \dfrac{\eta\, u_{avg}}{k(T_o-T_w)}$

$$\eta = Ae^{-Bn(T-T_m)}\left|\frac{dU}{dR}\cdot\frac{u_{avg}}{a}\right|^{n-1}$$

The accompanying dimensionless boundary conditions are:

$$\begin{array}{llll} Z = 0 & U = U_o(R) = \frac{\nu+2}{\nu}[1-R^{\nu}] & \theta = 1 & P = 0 \\ R = 0 & \frac{dU}{dR} = 0 & \frac{\partial\theta}{\partial R} = 0 & \\ R = 1 & U = 0 & \theta = 0 & \end{array} \tag{6.13}$$

In Eqs. (6.11) and (6.12), when R = 0 (at the centre of the tube), $\frac{1}{R}\frac{dU}{dR}$ and $\frac{1}{R}\frac{\partial\theta}{\partial R}$ are represented by the indeterminate form, $\frac{0}{0}$. By L'Hospital's Rule[3]:

$$\lim_{R\to 0}\left[\frac{1}{R}\frac{dU}{dR}\right] = \frac{d^2U}{dR^2} \tag{6.14}$$

$$\lim_{R\to 0}\left[\frac{1}{R}\frac{\partial\theta}{\partial R}\right] = \frac{\partial^2\theta}{\partial R^2} \tag{6.15}$$

---

[3]L'Hospital's Rule: If $\lim_{x\to a}\left[\frac{f(x)}{g(x)}\right] = \frac{0}{0}$, then $\lim_{x\to a}\left[\frac{f(x)}{g(x)}\right] = \lim_{x\to a}\left[\frac{f^I(x)}{g^I(x)}\right]$.

Thus, the momentum and energy equations become:

Momentum: $$-\frac{k}{C_p}\frac{dP}{dz} + \frac{d\eta}{dR}\cancelto{0}{\frac{dU}{dR}} + 2\eta\frac{d^2U}{dR^2} = 0 \qquad \text{for } R = 0 \qquad (6.16a)$$

$$-\frac{k}{C_p}\frac{dP}{dz} + \eta\frac{d^2U}{dR^2} + \left(\frac{\eta}{R} + \frac{d\eta}{dR}\right)\frac{dU}{dR} = 0 \qquad \text{for } R > 0 \qquad (6.16b)$$

Energy: $$U\frac{\partial\theta}{\partial z} = 2\frac{\partial^2\theta}{\partial R^2} + \gamma\cancelto{0}{\left(\frac{dU}{dR}\right)^2} \qquad \text{for } R = 0 \qquad (6.17a)$$

$$U\frac{\partial\theta}{\partial z} = \frac{\partial^2\theta}{\partial R^2} + \frac{1}{R}\frac{\partial\theta}{\partial R} + \gamma\left(\frac{dU}{dR}\right)^2 \qquad \text{for } R > 0 \qquad (6.17b)$$

Finite Difference Equations

An implicit finite difference method is used to solve Eqs. (6.10), (6.16a,b) and (6.17a,b) with the accompanying boundary conditions (6.13). The finite difference grid is illustrated in Fig. 6-2.

Continuity Equation

Using Simpson's Rule, the integrated continuity equation is given in the following finite difference form:

$$\int_{R=0}^{R=1} URdR = \frac{\Delta R}{3}\left(\cancelto{0}{U_1^nR_1} + 4U_2^nR_2 + 2U_3^nR_3 + \ldots + 4U_M^nR_M + \cancelto{0}{U_{M+1}^nR_{M+1}}\right) \qquad (6.18)$$

Substituting Eq. (6.18) into Eq. (6.10), we obtain for column n:

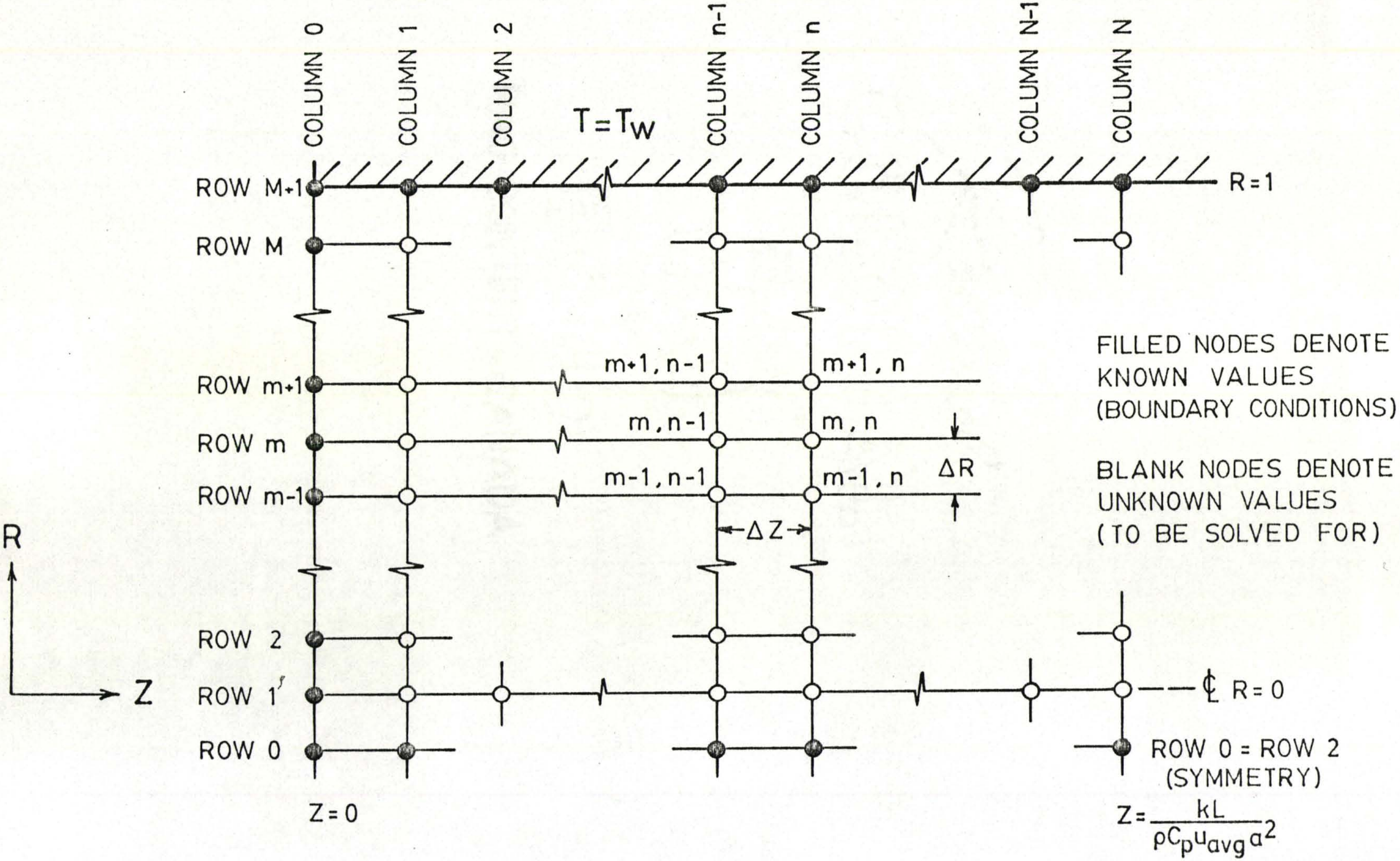

Fig. 6-2. Finite difference grid. Poiseuille flow through a tube with circular cross-section.

$$4U_2R_2 + 2U_3R_3 + \ldots + 4U_MR_M = \frac{3}{2\Delta R} = 1.5\ M \quad (6.19)$$

Momentum Equation

For the momentum equation, the following finite difference approximations are used:

$$\frac{dP}{dz} = \frac{P^n - P^{n-1}}{\Delta z} \quad (6.20)$$

$$\frac{dU}{dR} = \frac{U^n_{m+1} - U^n_{m-1}}{2\Delta R} \quad (6.21)$$

$$\frac{d^2U}{dR^2} = \frac{U^n_{m-1} - 2U^n_m + U^n_{m+1}}{(\Delta R)^2} \quad (6.22)$$

Substituting Eqs. (6.20), (6.21) and (6.22) into Eqs. (6.16a) and (6.16b), we obtain for column n (details in App. A, Sec. 3.1):

$$\underbrace{U^n_o}_{U^n_2 \text{ by symmetry}} - 2U^n_1 + U^n_2 + \frac{W_1}{2} P^n - \frac{W_1}{2} P^{n-1} = 0 \qquad \text{for } R = 0 \quad (6.23a)$$

$$A_m U^n_{m-1} + B_m U^n_m + C_m U^n_{m+1} + W_m P^n - W_m P^{n-1} = 0 \qquad \text{for } R > 0 \quad (6.23b)$$

$$\left.\begin{aligned} \text{where } A_m &= -\left[\frac{\Delta R}{2R_m} + \left(\frac{d\eta}{dR}\right)^n_m \frac{\Delta R}{\eta_m}\right] + 1 \\ B_m &= -2 \\ C_m &= \left[\frac{\Delta R}{2R_m} + \left(\frac{d\eta}{dR}\right)^n_m \frac{\Delta R}{\eta_m}\right] + 1 \end{aligned}\right\} \quad (m = 2, 3, \ldots, M)$$

$$W_m = -\frac{k}{\eta_m C_p}\frac{(\Delta R)^2}{\Delta z} \qquad (m = 1, 2, \ldots, M)$$

Combining Eqs. (6.19), (6.23a) and (6.23b), we have for column n a modified tridiagonal system of M+1 equations and M+1 unknowns (U_1 to U_M and P^n). The equations can be written as follows:

$$
\begin{aligned}
&-2U_1^n + 2U_2^n + \frac{W_1}{2}P^n - \frac{W_1}{2}P^{n-1} = 0 \\
&A_2U_1^n + B_2U_2^n + C_2U_3^n + W_2P^n - W_2P^{n-1} = 0 \\
&A_mU_{m-1}^n + B_mU_m^n + C_mU_{m+1}^n + W_mP^n - W_mP^{n-1} = 0 \quad (m = 3, 4, \ldots, M-1) \\
&4R_2U_2^n + 2R_3U_3^n + \ldots + 4R_MU_M^n = 1.5\ M
\end{aligned}
\tag{6.24}
$$

or in matrix form:

$$
\begin{bmatrix}
-2 & 2 & & & & \underline{0} & \frac{W_1}{2} \\
A_2 & B_2 & C_2 & & & & W_2 \\
 & \ddots & \ddots & \ddots & & & \vdots \\
 & & A_m & B_m & C_m & & W_m \\
 & & & \ddots & \ddots & \ddots & \vdots \\
 & & & A_{M-1} & B_{M-1} & C_{M-1} & W_{M-1} \\
 & \underline{0} & & & A_M & B_M & W_M \\
0 & 4R_2 & 2R_3 & \cdots & & 4R_M & 0
\end{bmatrix}
\begin{bmatrix}
U_1^n \\ U_2^n \\ \vdots \\ U_m^n \\ \vdots \\ U_{M-1}^n \\ U_M^n \\ P^n
\end{bmatrix}
=
\begin{bmatrix}
\frac{W_1}{2}P^{n-1} \\ W_2P^{n-1} \\ \vdots \\ W_mP^{n-1} \\ \vdots \\ W_{M-1}P^{n-1} \\ W_MP^{n-1} \\ 1.5\ M
\end{bmatrix}
\tag{6.25}
$$

or

$$\begin{bmatrix} B_1 & C_1 & & & & & \underline{0} & \frac{W_1}{2} \\ A_2 & B_2 & C_2 & & & & & W_2 \\ & \ddots & \ddots & \ddots & & & & \vdots \\ & & A_m & B_m & C_m & & & W_m \\ & & & \ddots & \ddots & \ddots & & \vdots \\ & & & & A_{M-1} & B_{M-1} & C_{M-1} & W_{M-1} \\ & \underline{0} & & & & A_M & B_M & W_M \\ X_1 & X_2 & \cdots & & & X_{M-1} & X_M & X_{M+1} \end{bmatrix} \begin{bmatrix} U_1^n \\ U_2^n \\ \vdots \\ U_m^n \\ \vdots \\ U_{M-1}^n \\ U_M^n \\ P^n \end{bmatrix} = \begin{bmatrix} H_1 \\ H_2 \\ \vdots \\ H_m \\ \vdots \\ H_{M-1} \\ H_M \\ X_{M+2} \end{bmatrix} \quad (6.26)$$

This system of equations is solved for the velocity profile and pressure at column n by Gaussian elimination using the algorithm that is shown in App. D, Sec. 2.

Energy Equation

For the energy equation, the following finite difference approximations are used:

$$\frac{\partial \theta}{\partial z} = \frac{\theta_m^n - \theta_m^{n-1}}{\Delta z} \quad (6.27)$$

$$\frac{\partial \theta}{\partial R} = \frac{\theta_{m+1}^n - \theta_{m-1}^n}{4\Delta R} + \frac{\theta_{m+1}^{n-1} - \theta_{m-1}^{n-1}}{4\Delta R} \quad (6.28)$$

$$\frac{\partial^2\theta}{\partial R^2} = \frac{\theta^n_{m-1} - 2\theta^n_m + \theta^n_{m+1}}{2(\Delta R)^2} + \frac{\theta^{n-1}_{m-1} - 2\theta^{n-1}_m + \theta^{n-1}_{m+1}}{2(\Delta R)^2} \qquad (6.29)$$

Substituting Eqs. (6.27), (6.28) and (6.29) into Eqs. (6.17a) and (6.17b), we obtain for column n (details in App. A, Sec. 3.2):

θ^n_2 by symmetry

$$A_1\theta^n_o + B_1\theta^n_1 + C_1\theta^n_2 = D_1 + E_1 + F_1 + G_1 = H_1 \qquad \text{for } R = 0 \qquad (6.30a)$$

where $A_1 = -1$

$$B_1 = \frac{(\Delta R)^2}{\Delta z} U^n_1 + 2$$

$$C_1 = -1$$

$$D_1 = \theta^{n-1}_o = \theta^{n-1}_2 \quad \text{by symmetry}$$

$$E_1 = \left[\frac{(\Delta R)^2}{\Delta z} U^n_1 - 2\right] \theta^{n-1}_1$$

$$F_1 = \theta^n_2$$

0

$$G_1 = 2(\Delta R)^2 \gamma^n_1 \left(\frac{dU}{dR}\right)^2 = 0$$

$$A_m\theta^n_{m-1} + B_m\theta^n_m + C_m\theta^n_{m+1} = D_m + E_m + F_m + G_m = H_m \qquad \text{for } R > 0 \qquad (6.30b)$$

where $A_m = \dfrac{\Delta R}{2R_m} - 1$

$$B_m = \frac{2(\Delta R)^2}{\Delta z} U^n_m + 2$$

$$\left.\begin{aligned}
C_m &= -\left(\frac{\Delta R}{2R_m} + 1\right) \\
D_m &= \left[-\frac{\Delta R}{2R_m} + 1\right] \theta_{m-1}^{n-1} \\
E_m &= \left[\frac{2(\Delta R)^2}{\Delta z} U_m^n - 2\right] \theta_m^{n-1} \\
F_m &= \left[\frac{\Delta R}{2R_m} + 1\right] \theta_{m+1}^{n-1} \\
G_m &= 2(\Delta R)^2 \, \gamma_m^n \left(\frac{dU}{dR}\right)_m^2
\end{aligned}\right\} \quad (m = 2, 3, \ldots, M)$$

Thus for column n, we have a tridiagonal system of M equations and M unknowns (θ_1^n to θ_M^n). The equations can be written as follows:

$$\begin{aligned}
&B_1\theta_1^n + 2C_1\theta_2^n = H_1 \\
&A_2\theta_1^n + B_2\theta_2^n + C_2\theta_3^n = H_2 \\
&A_m\theta_{m-1}^n + B_m\theta_m^n + C_m\theta_{m+1}^n = H_m \qquad (m = 3, 4, \ldots, M\text{-}1) \\
&A_M\theta_{M-1}^n + B_M\theta_M^n + \underbrace{\cancel{C_M\theta_{M+1}^n}}_{0} = H_M
\end{aligned} \tag{6.31}$$

or in matrix form:

$$\begin{bmatrix} B_1 & 2C_1 & & & & \underline{0} \\ A_2 & B_2 & C_3 & & & \\ & \ddots & \ddots & \ddots & & \\ & & A_m & B_m & C_m & \\ & & & \ddots & \ddots & \ddots \\ \underline{0} & & & A_{M-1} & B_{M-1} & C_{M-1} \\ & & & & A_M & B_M \end{bmatrix} \begin{bmatrix} \theta_1^n \\ \theta_2^n \\ \vdots \\ \theta_m^n \\ \vdots \\ \theta_{M-1}^n \\ \theta_M^n \end{bmatrix} = \begin{bmatrix} H_1 \\ H_2 \\ \vdots \\ H_m \\ \vdots \\ H_{M-1} \\ H_M \end{bmatrix} \tag{6.32}$$

This system of equations is solved for the temperature profile profile along column n by Gaussian elimination using Thomas' method (see App. D, Sec. 1).

Bulk Temperature

The dimensionless flow-average (bulk) temperature is calculated from the following definition:

$$\theta_{bulk} = \frac{\int_{R=0}^{R=1} \theta(Z,R)U(Z,R)RdR}{\int_{R=0}^{R=1} U(Z,R)RdR} \, . \tag{6.33}$$

For column n, Eq. (6.33) is written in finite difference form using Simpson's Rule as follows:

$$\theta^n_{bulk} = \frac{\theta^n_1 U^n_1 \overset{\nearrow 0}{R_1} + 4\theta^n_2 U^n_2 R_2 + 2\theta^n_3 U^n_3 R_3 + \ldots + 4\theta^n_M U^n_M R_M + \theta^n_{M+1} \overset{\nearrow 0}{U^n_{M+1}} R_{M+1}}{U^n_1 \underset{\searrow 0}{R_1} + 4U^n_2 R_2 + 2U^n_3 R_3 + \ldots + 4U^n_M R_M + \underset{\searrow 0}{U^n_{M+1}} R_{M+1}} \qquad (6.34)$$

Local Nusselt Number

The local Nusselt number is calculated from the following definition which is derived in App. B:

$$Nu_z = 2\,\frac{ha}{k} = \frac{-2\left(\frac{dT}{dr}\right)_{wall} \cdot a}{(T_{bulk} - T_{wall})} \qquad (6.35)$$

In dimensionless form, we have:

$$(Nu_z)_{R=1} = \frac{-2\left(\frac{d\theta}{dR}\right)_{R=1}}{\theta_{bulk}} \qquad (6.36)$$

The dimensionless gradient at the wall is estimated for column n by the following finite difference approximation:

$$\left(\frac{d\theta}{dR}\right)^n_{R=1} = \frac{1}{6\Delta R}\left(-2\theta^n_{M-2} + 9\theta^n_{M-1} - 18\theta^n_M + 11\theta^n_{M+1}\right) \qquad (6.37)$$

The above equation is derived in App. C, Sec. 5.

6.2 Computational Procedure

It was stated in Chap. 3, Sec. 3, that the momentum and energy equations are coupled by velocity and temperature, and therefore cannot be solved independently. However, the coupled equations can be solved iteratively at a given column on the finite difference grid by alternately solving the set of continuity and momentum equations (6.24) and the set of energy equations (6.31) until the solutions converge. The iterative procedure used to calculate the velocity and temperature profiles, the pressure, the bulk temperature and the local Nusselt number at each column in the grid is now outlined.

Notation

$U1_m^n$ (m = 1, 2, ..., M+1) refers to the estimated velocity profile at column n.

$U2_m^n$ (m = 1, 2, ..., M+1) refers to the most recently calculated velocity profile at column n.

θ_m^{n-1} (m = 1, 2, ..., M+1) refers to the temperature profile at column n-1.

$\theta 1_m^n$ (m = 1, 2, ..., M+1) refers to the estimated temperature profile at column n.

$\theta 2_m^n$ (m = 1, 2, ..., M+1) refers to the most recently calculated temperature profile at column n.

Procedure

1. Assume values for the velocity and temperature profiles and the pressure at the entrance of the tube (at column 0).

$$\left.\begin{aligned} U1_m^o &= \frac{\nu+2}{\nu}\,[1-R^\nu] \\ \theta_m^o &= 1 \\ P^o &= 0 \end{aligned}\right\} \quad (m = 1, 2, \ldots, M+1)$$

2. Print the velocity and temperature profiles at column 0.

3. Set the estimates of the velocity and temperature profiles to be used in the first iteration at column 1 equal to the values of the respective profiles at column 0.

$$n = 1$$

$$U1_m^1 = U1_m^o \qquad (m = 1, 2, \ldots, M+1)$$

$$\theta 1_{M+1}^1 = \theta 2_{M+1}^1 = 0$$

$$\theta 1_m^1 = \theta_m^o \qquad (m = 1, 2, \ldots, M)$$

4. To economize on computing time, increase ΔX by a factor of 10 after the final velocity and temperature profiles have been calculated at column n = NA, and again after they have been calculated at column n = NB (see program listing, App. F, Sec. 3).

$$\Delta Z = 10\ \Delta Z \text{ at column NA + 1, and again at column NB + 1}$$

5. Using $U1_m^n$ and $\theta 1_m^n$ $(m = 1, 2, \ldots, M+1)$, calculate $(\frac{dU}{dR})_m^n$ and η_m^n $(m = 1, 2, \ldots, M+1)$ at column n.

6. Using $U1_m^n$, $(\frac{dU}{dR})_m^n$, η_m^n and θ_m^{n-1} $(m = 1, 2, \ldots, M+1)$, solve the set of energy equations (6.32) by Gaussian elimination using Thomas' method (see App. D, Sec. 1) to obtain $\theta 2_m^n$ $(m = 1, 2, \ldots, M)$.

7. Using $U1_m^n$ and $\theta 2_m^n$ $(m = 1, 2, \ldots, M+1)$, calculate η_m^n and $(\frac{d\eta}{dR})_m^n$ $(m = 1, 2, \ldots, M+1)$ at column n.

8. Using P^{n-1}, η_m^n and $(\frac{d\eta}{dR})_m^n$ (m = 1, 2, ..., M+1), solve the set of continuity and momentum equations (6.25) by Gaussian elimination (see App. D, Sec. 2 for algorithm) to obtain $U2_m^n$ and P^n (m = 1, 2, ..., M).

9. Compare $U1_m^n$, $U2_m^n$ and $\theta 1_m^n$, $\theta 2_m^n$ (m = 1, 2, ..., M+1). If $|U2_m^n - U1_m^n|$ < tolerance and $|\theta 2_m^n - \theta 1_m^n|$ < tolerance for all m, then proceed to step 12. Otherwise, continue to step 10.

10. Set the estimates of the velocity and temperature profiles to be used in the next iteration at column n equal to the most recently calculated profiles.

$$\left.\begin{aligned} U1_m^n &= U2_m^n \\ \theta 1_m^n &= \theta 2_m^n \end{aligned}\right\} \quad (m = 1, 2, \ldots, M+1)$$

11. Repeat steps 5 through 9 until the desired error tolerances have been achieved.

12. Set the estimates of the velocity and temperature profiles to be used in the first iteration at column n+1 equal to the final values of the profiles calculated at column n. Also, retain the final temperature profile calculated at column n for use in calculating temperature profiles at column n+1.

$$\left.\begin{aligned} U1_m^{n+1} &= U2_m^n \\ \theta 1_m^{n+1} &= \theta 2_m^n \\ \theta_m^n &= \theta 2_m^n \end{aligned}\right\} \quad (m = 1, 2, \ldots, M+1)$$

13. Repeat steps 4 through 12 to calculate the velocity and temperature profiles at the next column downstream ($n = n+1$).

The following steps are to be carried out at periodic intervals along the length of the tube:

14. Print the velocity and temperature profiles and the pressure.

15. Calculate the bulk temperature using Simpson's Rule (see Eq. (6.34)).

16. Calculate the local Nusselt number at the tube wall (see Eq. (6.36)).

17. Print the bulk temperature and the local Nusselt number.

Computations using the above algorithm have been carried out in McMaster's CDC 6400 computer. A sample program listing with results is located in App. F, Sec. 3.

6.3 Convergence, Stability and Step Size

It was stated in Chap. 3, Sec. 3, that a good indication of the convergence and stability of the finite difference results is the negligible change in results obtained when the step sizes in the finite difference grid are decreased. It should be noted that special care must be taken in choosing step sizes when calculating local Nusselt numbers. Although the temperature profiles may appear to be sufficiently accurate, the local Nusselt numbers can still be incorrect. Local Nusselt numbers are calculated from temperature derivatives (see Eq. (6.35)). Since derivatives are very sensitive to step size changes, smaller step sizes must be used when calculating local Nusselt numbers, than when only calculating velocity and temperature profiles.

The step sizes shown in Table 6-1 were used in the finite difference program. The results presented in the subsequent figures are independent of step size within at least 3 significant digits.

Table 6-1. Step sizes for finite difference program. Poiseuille flow through a tube with circular cross-section.

Range of Z	ΔZ	ΔR
0 -0.4	0.0004	0.02
0.4 -0.12	0.004	0.02
0.12-4.0	0.04	0.02

Two additional tests for the convergence of the finite difference results were carried out. In the first test, the fully-developed temperature profile, the limiting bulk temperature and the limiting local Nusselt number (at large Z) were calculated analytically for a Newtonian, constant viscosity fluid with viscous dissipation (see App. E, Sec. 3), and compared with the corresponding finite difference results for the same fluid. In the second test, the limiting local Nusselt number was obtained for a Newtonian, constant viscosity fluid without viscous dissipation, and was compared with the analytical value of 3.66 (12). In both cases, the analytical and finite difference results were indistinguishable.

6.4 Results and Discussion

Solutions of the continuity, momentum and energy equations for

Poiseuille flow through a tube with circular cross-section are presented in Figs. 6-3 through 6-9. The following velocity, pressure and temperature boundary conditions have been used:

$$
\begin{array}{lll}
z = 0 & u = u_{avg}\left[\frac{\nu+2}{\nu}\right]\left[1-\left(\frac{r}{a}\right)^{\nu}\right] & T_o = 130°C \quad p_o = 0 \\
 & \text{where } u_{avg} = 15 \text{ cm/s},\ \nu = \frac{n+1}{n},\ n = 0.453 & \\
r = 0 & & \frac{\partial T}{\partial r} = 0 \\
r = a = 0.125 \text{ cm} & & T_w = 160°C
\end{array}
\qquad (6.38)
$$

Also, the following power-law temperature-dependent viscosity model and fluid properties representing a typical high-density polyethylene melt were used in the computations:

Viscosity: $$\eta = Ae^{-Bn(T-T_m)} \left|\frac{du}{dr}\right|^{n-1} \qquad (6.39)$$

where $A = 282\ 000 \quad \text{poise}\cdot s^{n-1}$

$= 28\ 200 \quad \text{Pa}\cdot s^{n}$

$B = 0.024\ K^{-1}$

$n = 0.453$

$T_m = 399.5\ K$

Density: $\rho = 794\ \text{kg/m}^3$

Specific heat:

$$C_p = 0.6 \text{ cal/(g·K)}$$

$$= 2.51 \text{ kJ/(kg·K)}$$

Thermal conductivity:

$$k = 6.1 \times 10^{-4} \text{ cal/(cm·s·K)}$$

$$= 0.255 \text{ W/(m·K)}$$

The temperature profiles, bulk temperatures and local Nusselt numbers in Figs. 6-3 through 6-9 are shown as functions of the dimensionless axial distance, Z. Because the bulk temperatures and local Nusselt numbers change the most near the entrance of the tube, they have been plotted semi-logarithmically in the figures. Z on the abscissa of these plots ranges from 0.004 to 4.0.[4] This corresponds to z ranging from 0.7 to 732 cm. At Z = 4.0, the temperature profile has become fully developed. Beyond this point in the tube, the temperature profiles, bulk temperatures and local Nusselt numbers remain the same, and thus are known as the limiting or asymptotic values.

---

[4] Z is four times as large as X for a given x = z due to their respective definitions:

$$Z = \frac{kz}{\rho C_p u_{avg} a^2} \quad \text{where } a = \text{radius of tube}$$

$$X = \frac{kx}{\rho C_p u_{avg} b^2} \quad \text{where } b = \text{distance between plates}$$

In Fig. 6-3, the temperature profiles for the power-law temperature-dependent viscosity model and for a power-law temperature-independent viscosity model are compared. The temperature-independent viscosity model used is identical to the temperature-dependent viscosity model given in Eq. (6.39), except that T is held constant and equal to the tube wall temperature (160°C). It can be seen that the temperature of the fluid obtained with the temperature-independent model is generally higher than is the case with the temperature-dependent model. However, the fully-developed temperature profiles for the two models are about the same. At intermediate values of Z, the temperature profiles bulge near the wall, indicating that more heat is generated by viscous dissipation here, than is generated near the centre-line of the tube. This is due to the fact that the shear rates are the highest near the tube walls.

Plots of the bulk temperatures along the length of the tube are presented in Figs. 6-4, 6-5 and 6-6 for the power-law temperature-dependent and temperature-independent viscosity models and for the Newtonian, constant viscosity model. In Fig. 6-4, the bulk temperatures are shown for power-law temperature-dependent viscosity fluids with different inlet temperatures. In each case, the limiting bulk temperature is the same (204.7°C). This is to be expected since the fully-developed velocity and temperature profiles are only influenced by the wall boundary conditions and by the viscosity and thermal conductivity of the fluid, but not by the inlet conditions of the fluid. Also shown in Fig. 6-4 is the effect of removing the viscous dissipation term from the energy equation. Without viscous dissipation,

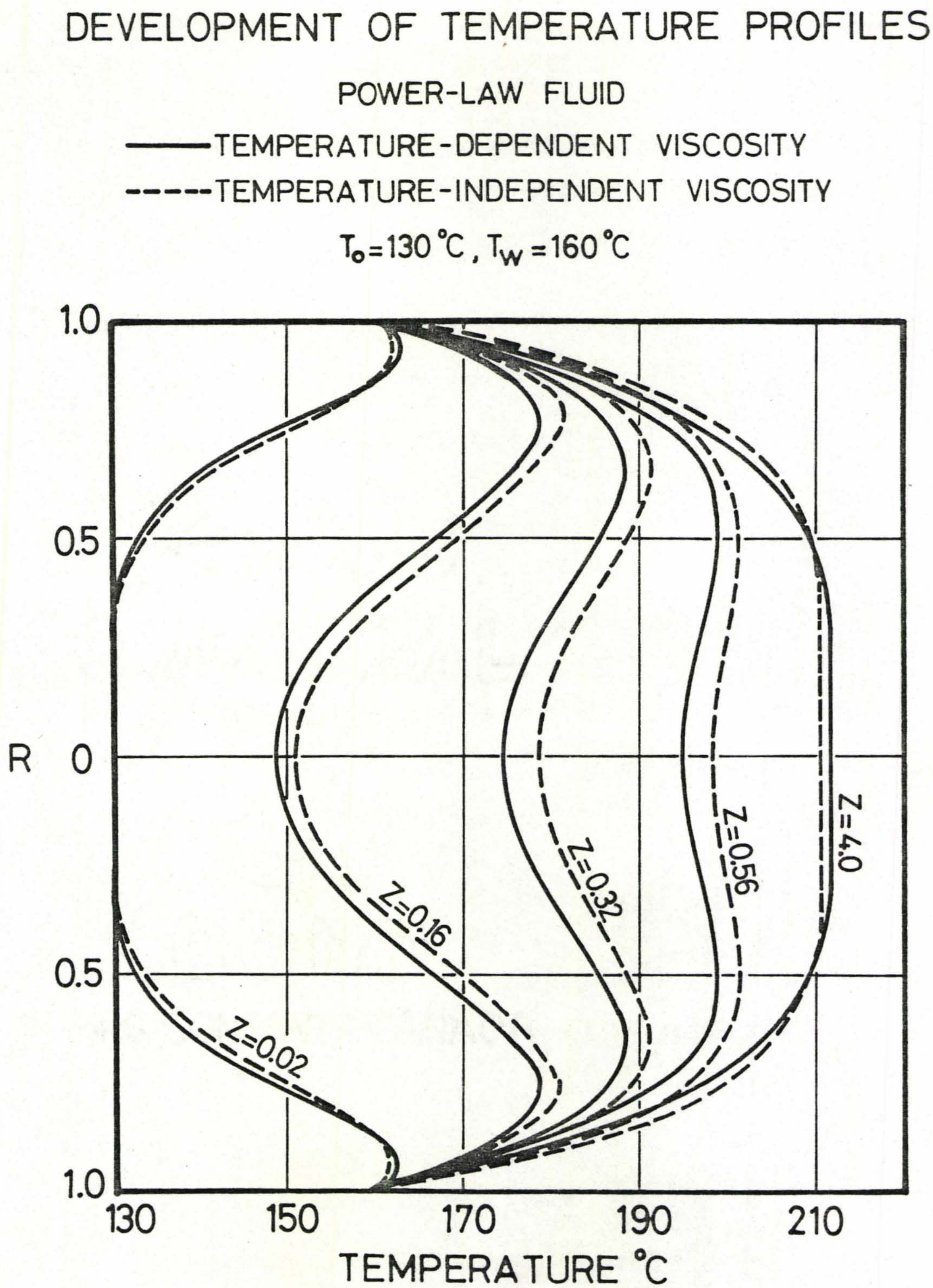

Fig. 6-3. Development of temperature profiles. Poiseuille flow through a tube with circular cross-section. Tube dimension and fluid properties given on pp. 117-118.

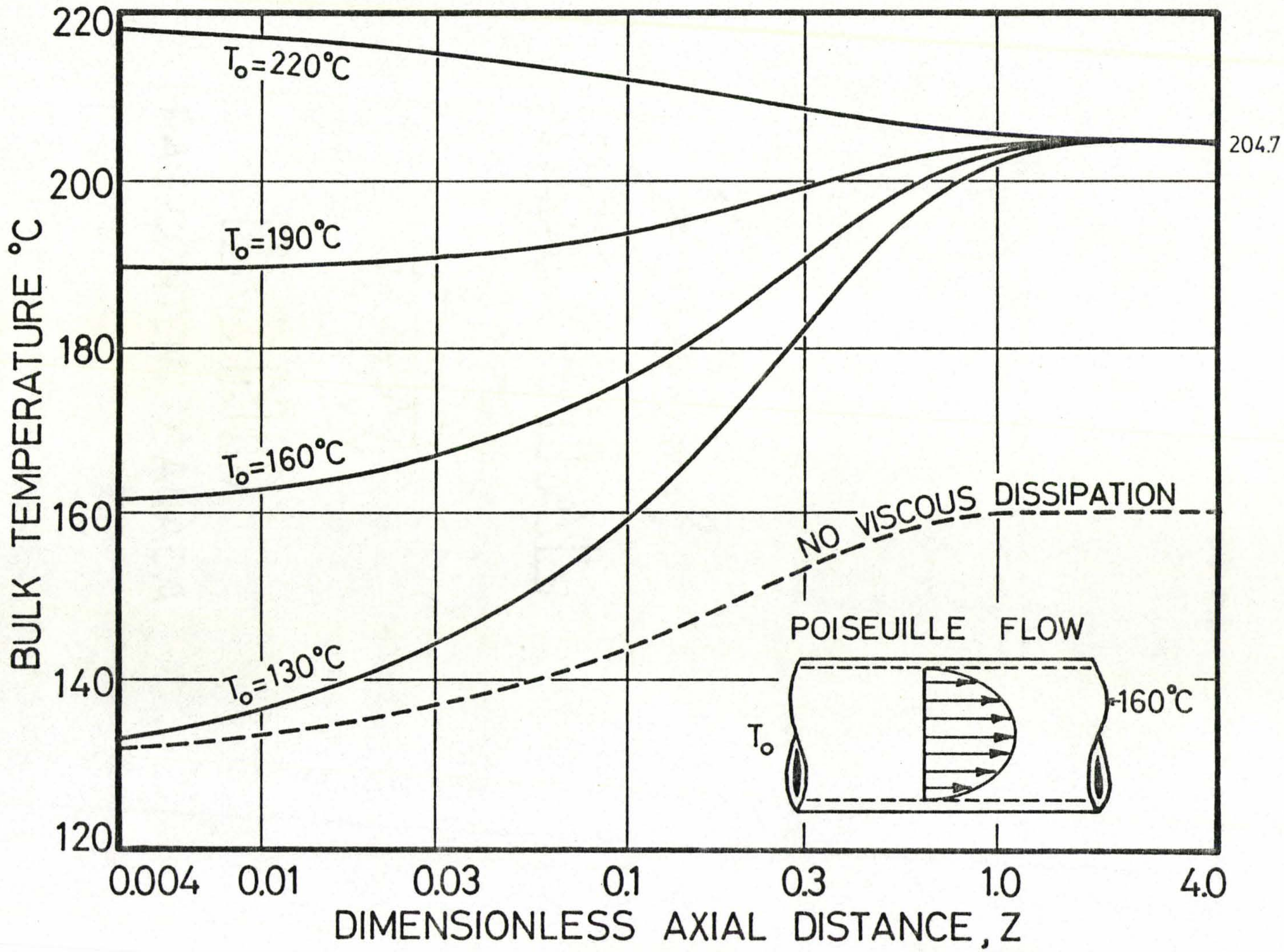

Fig. 6-4. Bulk temperature vs. Z. Poiseuille flow through a tube with circular cross-section. Tube dimension and fluid properties given on pp. 117-118.

the limiting bulk temperature is equal to the wall temperature (160°C). The difference of 44.7°C is an indication of the importance of viscous dissipation in the Poiseuille flow of polymer melts through a tube. The rise in bulk temperature for the power-law temperature-dependent viscosity model is compared with the temperature-independent model and several Newtonian, constant viscosity models in Figs. 6-5 and 6-6 respectively.

Plots of the local Nusselt number along the length of the tube are presented in Figs. 6-7, 6-8 and 6-9 for the power-law temperature-dependent and temperature-independent viscosity models and for the Newtonian, constant viscosity model. In Fig. 6-7, the local Nusselt numbers are shown for power-law temperature-dependent viscosity fluids having different inlet temperatures. In each case, the limiting local Nusselt number is 8.97. Although not shown the limiting local Nusselt number for the case where viscous dissipation has been neglected is 4.00. It can be seen that when the fluid is heated by the tube walls (T_o = 130°C, T_w = 160°C), there is a region along the tube where the local Nusselt number is negative, and a point where it is discontinuous. With the aid of Eq. (6.35), this behaviour is explained as follows:

$$Nu_z = 2\,\frac{ha}{k} = \frac{-\left(\frac{dT}{dr}\right)_{wall}\cdot 2a}{T_{bulk}-T_{wall}} \tag{6.35}$$

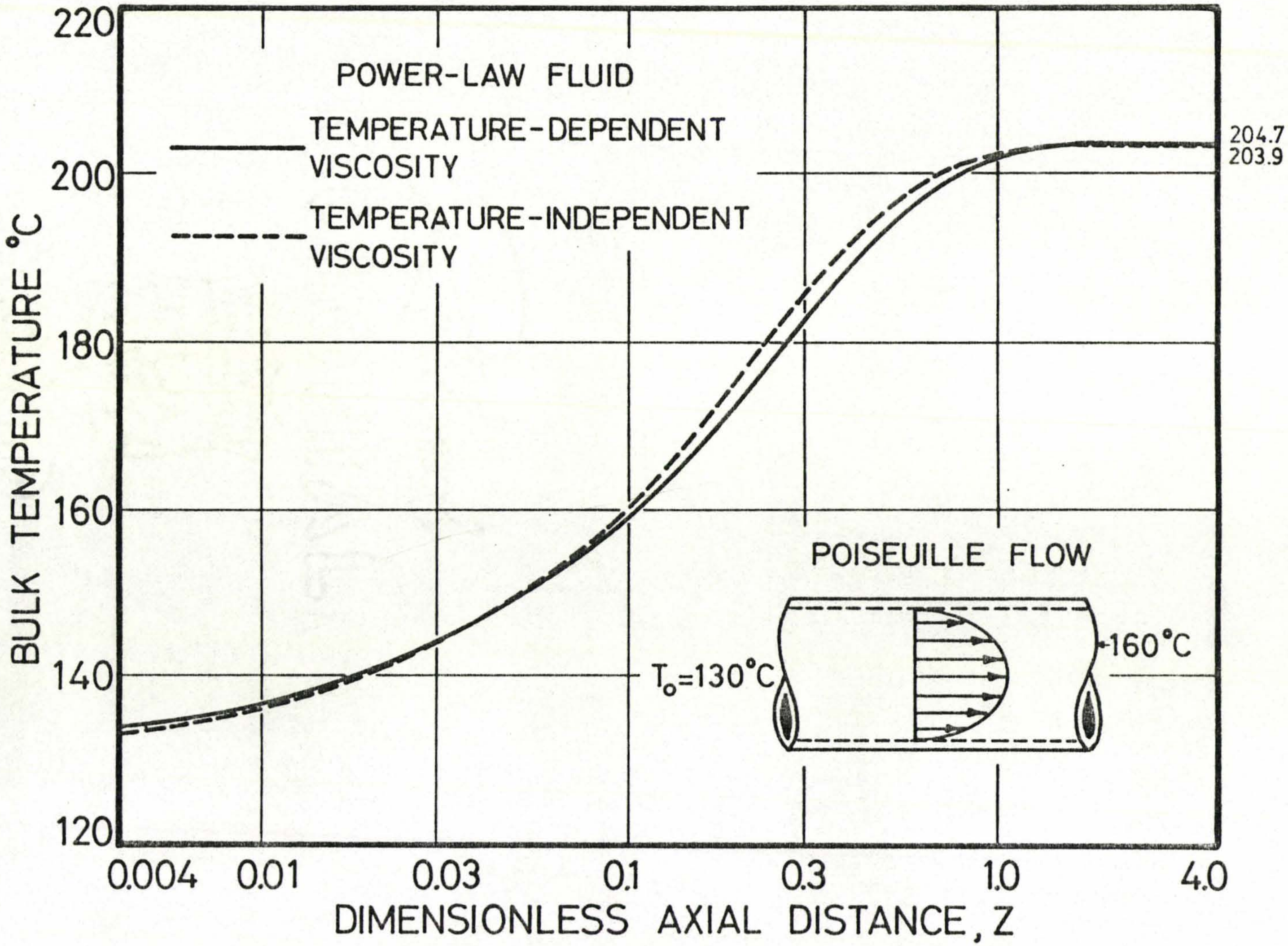

Fig. 6-5. Bulk temperature vs. Z. Poiseuille flow through a tube with circular cross-section. Tube dimension and fluid properties given on pp. 117-118.

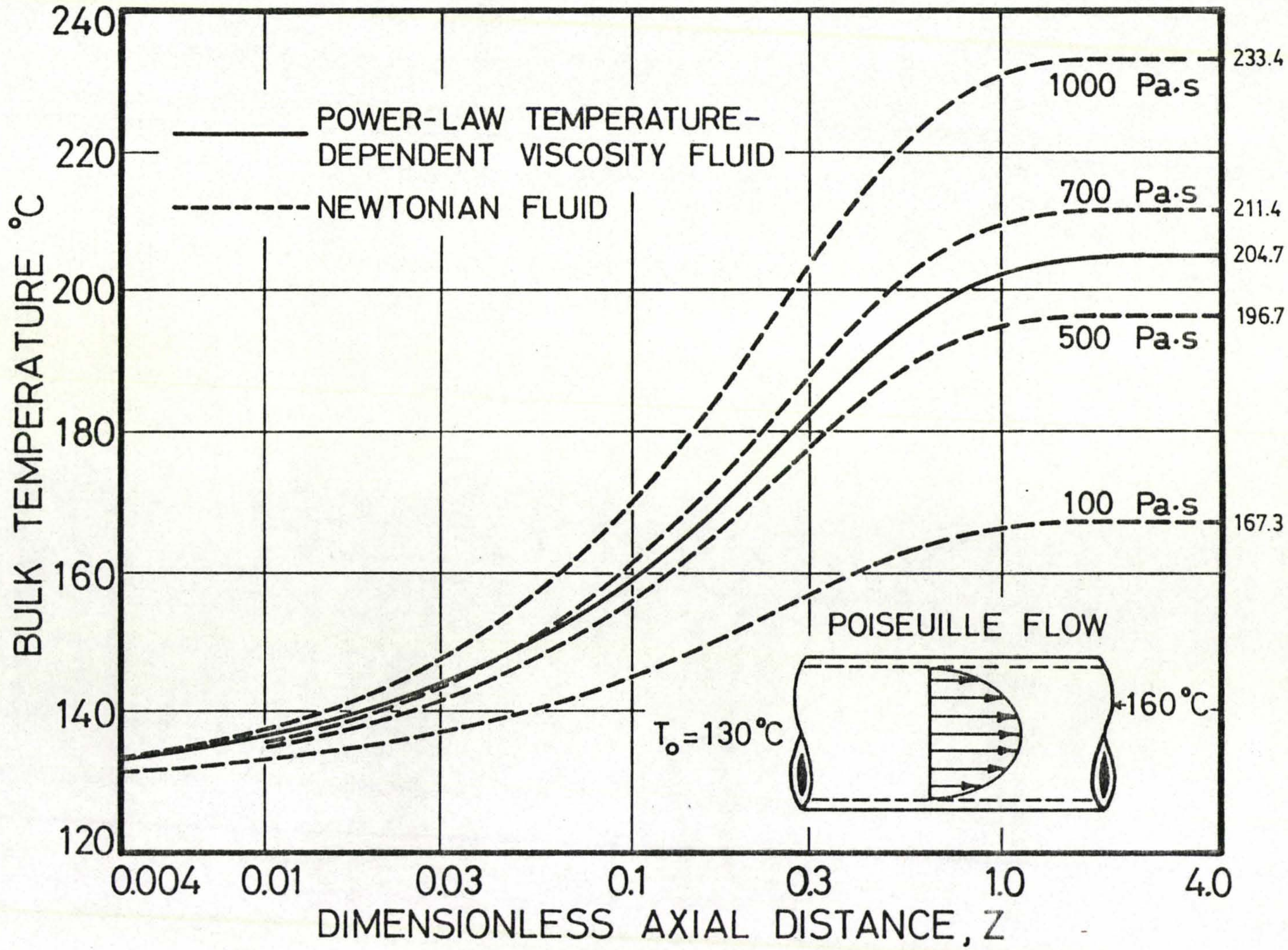

Fig. 6-6. Bulk temperature vs. Z. Poiseuille flow through a tube with circular cross-section. Tube dimension and fluid properties given on pp. 117-118.

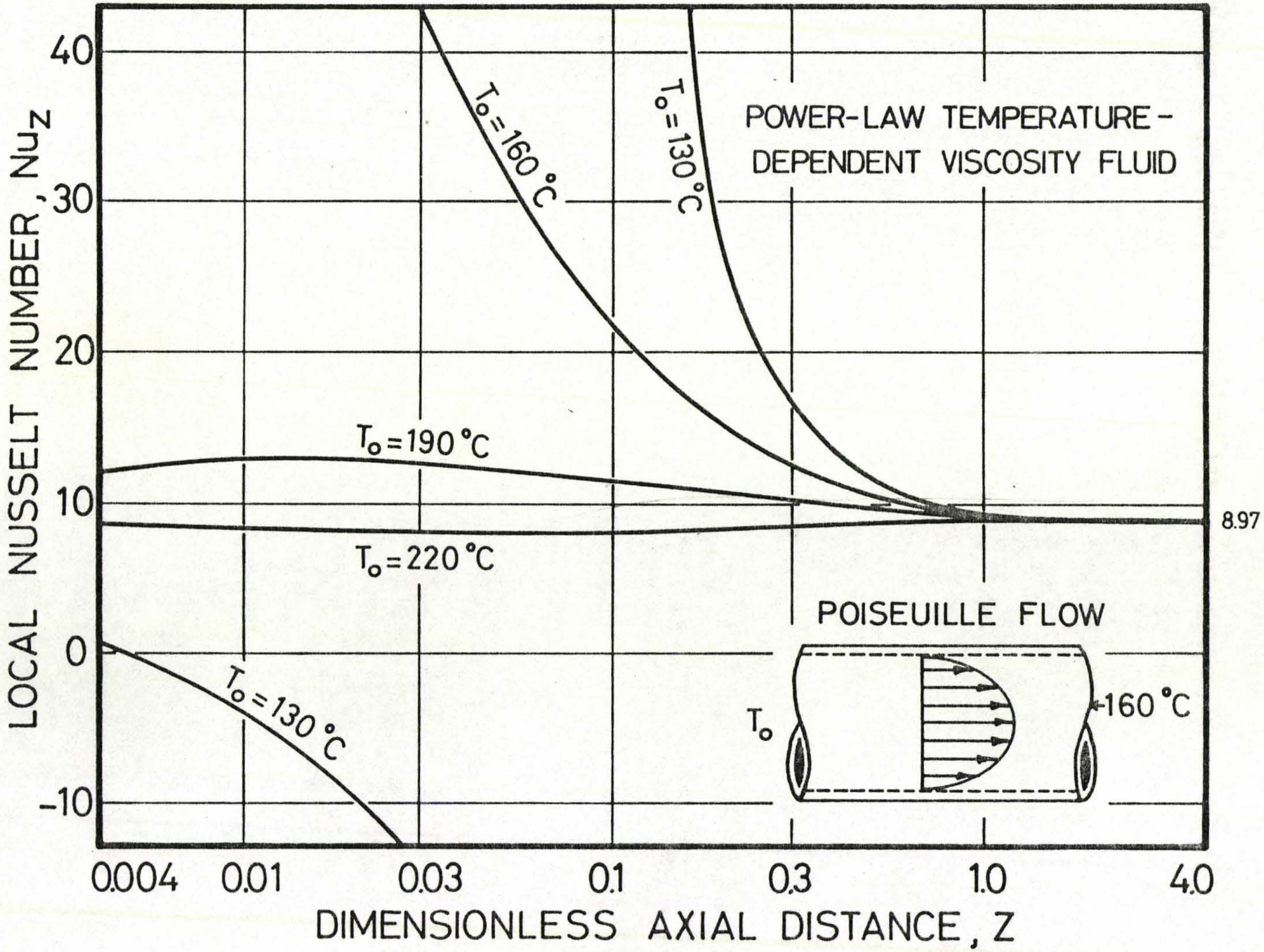

Fig. 6-7. Bulk temperature vs. Z. Poiseuille flow through a tube with circular cross-section. Tube dimension and fluid properties given on pp. 117-118.

$Z < 0.005$	$\frac{dT}{dr} < 0$	$T_b < T_w$	$Nu_z > 0$
$Z \simeq 0.005$	$\frac{dT}{dr} = 0$	$T_b < T_w$	$Nu_z = 0$
$0.005 < Z < 0.01$	$\frac{dT}{dr} > 0$	$T_b < T_w$	$Nu_z < 0$
$Z \simeq 0.01$	$\frac{dT}{dr} > 0$	$T_b = T_w$	$Nu_z = \pm\infty$
$Z > 0.01$	$\frac{dT}{dr} > 0$	$T_b > T_w$	$Nu_z > 0$

When the inlet temperature is higher than the tube wall temperature, the local Nusselt number is always positive.

The local Nusselt numbers for the power-law temperature-dependent and temperature-independent viscosity fluids are compared in Fig. 6-8. The limiting local Nusselt numbers are 8.97 and 12.09 respectively for the two fluids. In Fig. 6-9, the local Nusselt numbers are shown for the power-law temperature-dependent viscosity fluid and several Newtonian, constant viscosity fluids.

The results for the power-law temperature-dependent viscosity model have been compared with the power-law temperature-independent viscosity model and the Newtonian, constant viscosity model results. Given an appropriate temperature for the temperature-independent model, or an appropriate viscosity for the Newtonian model, it can be seen that the temperature-dependent model results are adequately estimated by the use of either of the simpler models. The choice of temperature and viscosity was made by inspection. However, if we did not have any temperature-dependent model

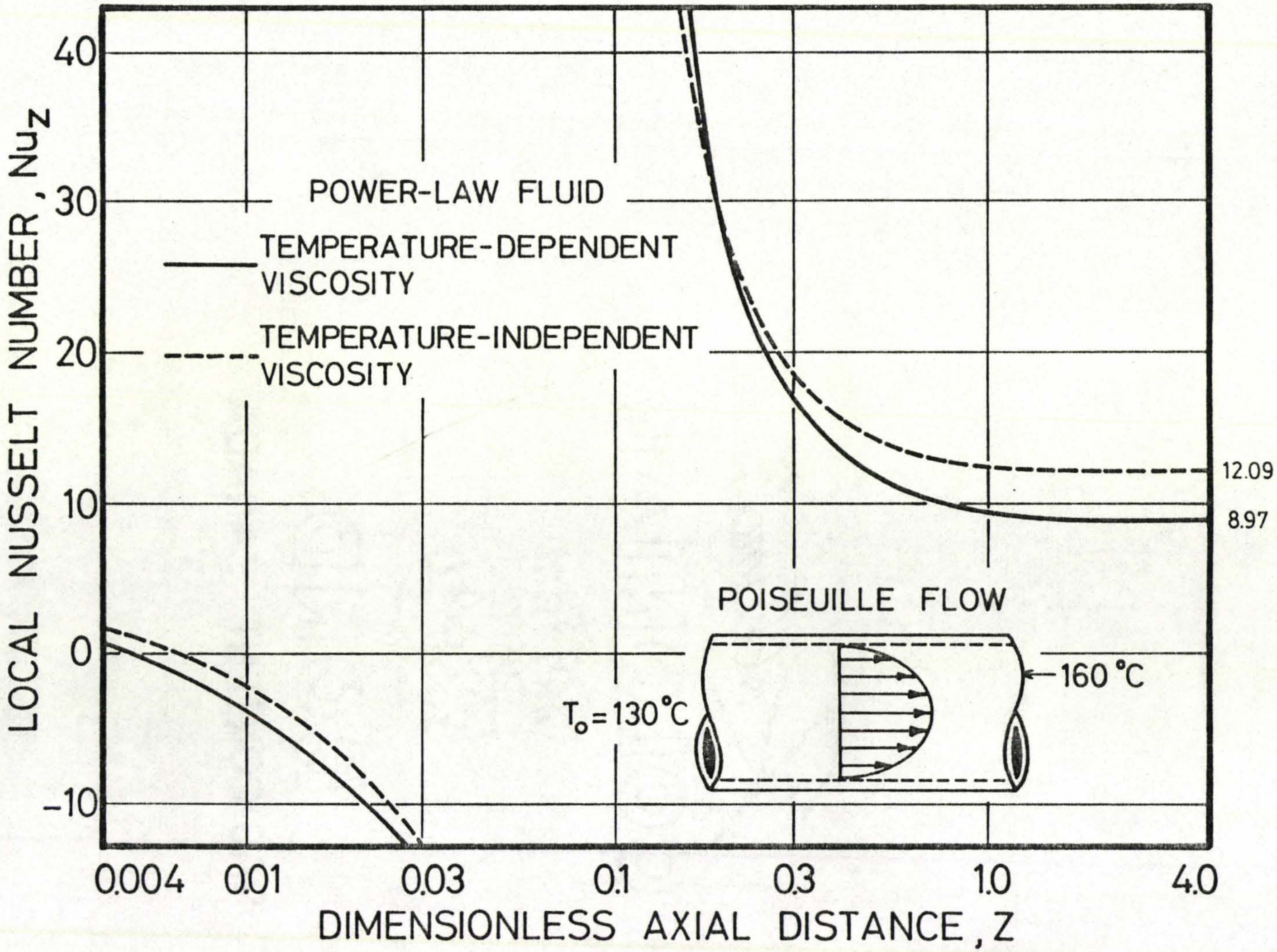

Fig. 6-8. Local Nusselt number vs. Z. Poiseuille flow through a tube with circular cross-section. Tube dimension and fluid properties given on pp. 117-118.

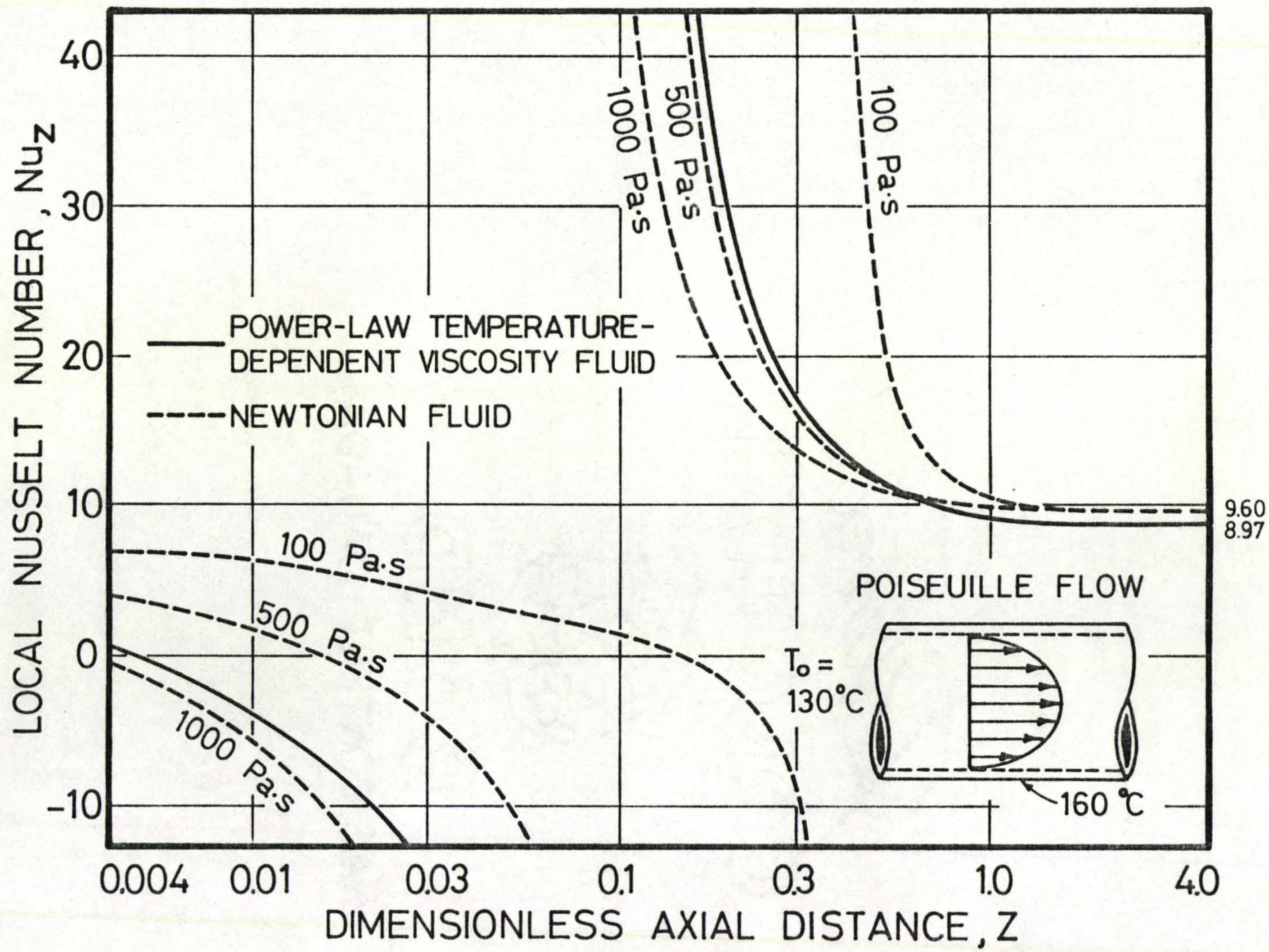

Fig. 6-9. Local Nusselt number vs. Z. Poiseuille flow through a tube with circular cross-section. Tube dimension and fluid properties given on pp. 117-118.

results to compare our more simplified model results with, then we would not have anything to base our choice of temperature or viscosity on. Furthermore, the given temperature or viscosity usually works for one type of flow only. For example, in Fig. 6-6 it can be seen that the rise in bulk temperature for the temperature-dependent model is closely approximated by a Newtonian fluid with a viscosity of about 600 Pa.s, while in Poiseuille flow between parallel plates, a viscosity of about 700 Pa.s is required (see Fig. 5-9).

6.5 Concluding Remarks

1. A computer program has been developed to analyze the heat transfer problem for the Poiseuille flow of polymer melts through a constant temperature tube with circular cross-section. Results have been presented for specified velocity, pressure and temperature boundary conditions, fluid properties and tube dimensions.

2. Care must be taken when choosing the proper step sizes in order to ensure that the local Nusselt numbers and not only the temperature profiles have converged.

3. It is very important to consider viscous dissipation in the flow of polymer melts through a tube. A rise of 44.7°C in the limiting bulk temperature due to viscous dissipation was obtained using the specified boundary conditions, fluid properties and channel dimensions given earlier in this chapter.

4. The results obtained using the power-law temperature-dependent

viscosity model were compared with those using the simpler power-law temperature-independent viscosity model and the Newtonian, constant viscosity model. It was seen that the results obtained using the temperature-dependent model were in most cases adequately approximated by either of the two simpler models, provided that a correct temperature or viscosity was chosen. However, if there are no temperature-dependent model results available, we have then no basis with which to choose a temperature for the temperature-independent model, or a viscosity for the Newtonian, constant viscosity model.

CHAPTER 7

DRAG FLOW BETWEEN CONVERGING PLATES

7.1 Mathematical Formulation

The physical system for drag (or Couette) flow between converging plates is illustrated in Fig. 7-1. The lower plate is moving with a constant velocity, u_{max}, and has a constant temperature, T_{w1}. The upper inclined plate is stationary and has a constant temperature, T_{w2}. The distance, b(x), between the plates is very small compared to the length, L, of the lower plate. Often this flow case is referred to as the slider-bearing problem (58).

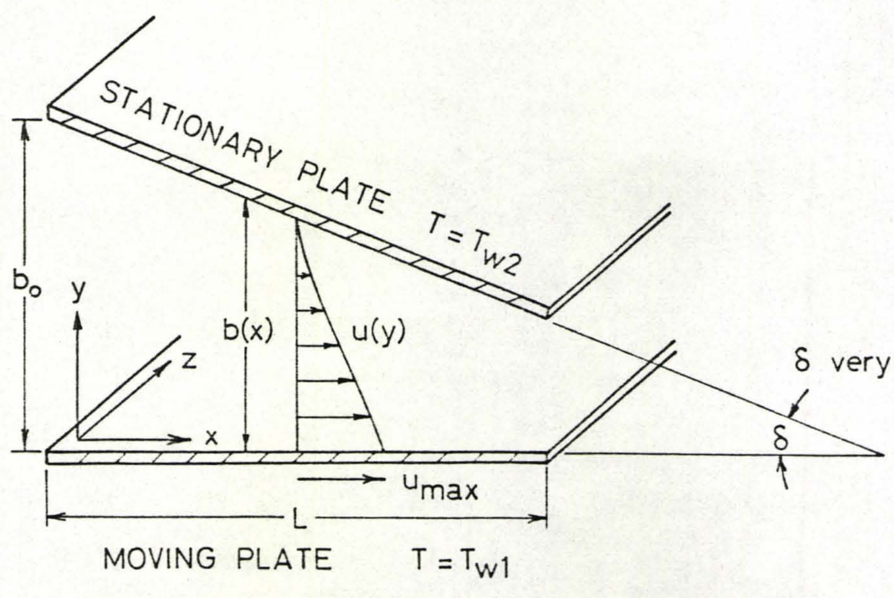

Fig. 7-1. Drag flow between converging plates

Flow Equations

The simplified conservation equations for drag flow between converging plates are:

Continuity (integral form):

$$\int_{y=0}^{y=b(x)} u\,dy = Q = u_{avg,o} \cdot b_o \tag{7.1}$$

Momentum:
$$-\frac{dp}{dx} + \frac{d}{dy}\tau_{yx} = 0 \tag{7.2}$$

Energy:
$$\rho C_p u \frac{\partial T}{\partial x} = k \frac{\partial^2 T}{\partial y^2} + \tau_{yx}\frac{du}{dy} \tag{7.3}$$

Substituting the constitutive relation, Eqs. (3.12) and (3.13) into the momentum and energy equations, we obtain:

Momentum:
$$-\frac{dp}{dx} + \frac{d\eta}{dy}\frac{du}{dy} + \eta\frac{d^2u}{dy^2} = 0 \tag{7.4}$$

Energy:
$$\rho C_p u \frac{\partial T}{\partial x} = k \frac{\partial^2 T}{\partial y^2} + \eta\left(\frac{du}{dy}\right)^2 \tag{7.5}$$

$$\text{where } \eta = Ae^{-Bn(T-T_m)}\left|\frac{du}{dy}\right|^{n-1}$$

The boundary conditions for the above equations are:

$$
\begin{array}{llll}
x = 0 & T = T_o & p = p_o & \\
x = L & p = p_o & & \\
y = 0 & u = u_{max} & T = T_{w1} & \\
y = b(x) & u = 0 & T = T_{w2} &
\end{array}
\tag{7.6}
$$

Let

$$
\begin{aligned}
U &= \frac{u}{u_{max}} \\
P &= \frac{p-p_o}{\rho u_{max}^2} \\
\theta &= \frac{T-T_{w1}}{T_o-T_{w1}} \\
X &= \frac{kx}{\rho C_p u_{max} b_o^2} \\
Y &= \frac{y}{b_o} \\
B(X) &= \frac{b(x)}{b_o}
\end{aligned}
\tag{7.7}
$$

Substituting the above into Eqs. (7.1), (7.4) and (7.5), we obtain in terms of dimensionless parameters:

Continuity (integral form):

$$\int_{Y=0}^{Y=B(X)} U dY = U_{avg,o} \tag{7.8}$$

Momentum:

$$-\frac{k}{C_p}\frac{dP}{dX} + \frac{d\eta}{dY}\frac{dU}{dY} + \eta\frac{d^2U}{dY^2} = 0 \tag{7.9}$$

Energy: $$U \frac{\partial\theta}{\partial X} = \frac{\partial^2\theta}{\partial Y^2} + \delta\left(\frac{dU}{dY}\right)^2 \tag{7.10}$$

$$\text{where } \delta = \frac{\eta\, u_{max}^2}{k(T_o - T_{w1})}$$

$$\eta = Ae^{-Bn(T-T_m)} \left| \frac{du}{dY} \cdot \frac{u_{max}}{b_o} \right|^{n-1}$$

The accompanying dimensionless boundary conditions are:

$$\begin{array}{lll} X = 0 & \theta = 1 & P = 0 \\ X = \dfrac{kL}{\rho C_p u_{max} b_o^2} & P = 0 & \\ Y = 0 & U = 1 & \theta = 0 \\ Y = B(X) & U = 0 & \theta = \dfrac{T_{w2} - T_{w1}}{T_o - T_{w1}} \end{array} \tag{7.11}$$

Finite Difference Equations

An implicit finite difference method is used to solve Eqs. (7.8), (7.9) and (7.10) with the accompanying boundary conditions (7.11).

Continuity and Momentum Equations

The continuity and momentum equations are solved simultaneously over the entire finite differences grid because velocity or pressure boundary conditions have been specified at each of the four boundaries in this problem. An 18-point grid, shown in Fig. 7-2, has been chosen

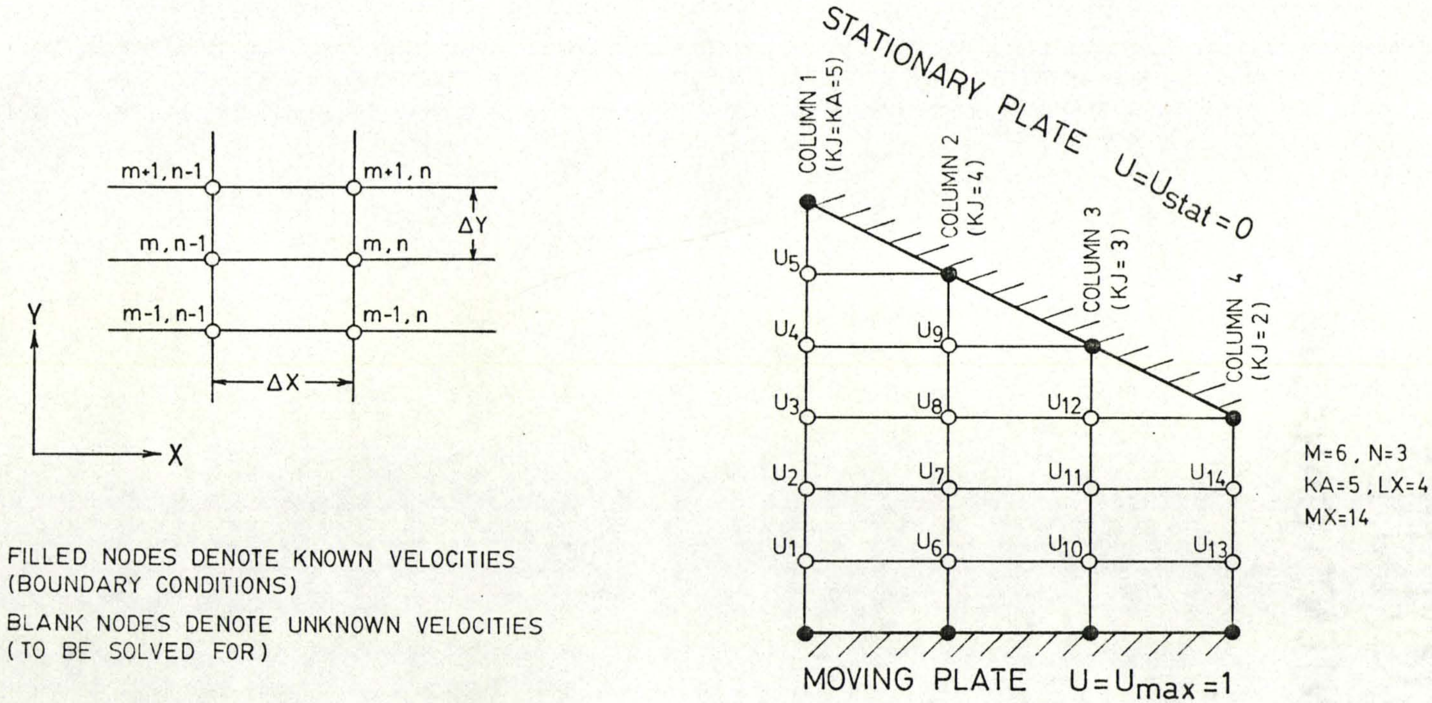

Fig. 7-2. Finite difference grid for continuity and momentum equations. Drag flow between converging plates.

to illustrate the method. Naturally, more points are used in the actual computations.

To represent the integrated continuity equation (7.8) in finite difference form, we use the trapezoidal rule:[5]

$$\int_{Y=0}^{Y=B(X)} U dY = \frac{\Delta Y}{2}\left(\cancelto{1}{U_{max}} + 2U_1 + \ldots + 2U_5 + \cancelto{0}{U_{stat}}\right) \quad \text{for column 1}$$

$$\vdots \tag{7.12}$$

$$= \frac{\Delta Y}{2}\left(\cancelto{1}{U_{max}} + 2U_{13} + 2U_{14} + \cancelto{0}{U_{stat}}\right) \quad \text{for column 4}$$

Substituting the above into Eq. (7.8), we obtain:

$$\begin{aligned}
&\text{column 1:} \quad 2U_1 + 2U_2 + \ldots + 2U_5 - 2M\cdot U_{avg,o} = -1 \quad \left(M=\frac{1}{\Delta Y}\right) \\
&\text{column 2:} \quad 2U_6 + 2U_7 + \ldots + 2U_9 - 2M\cdot U_{avg,o} = -1 \\
&\text{column 3:} \quad 2U_{10} + 2U_{11} + 2U_{12} - 2M\cdot U_{avg,o} = -1 \\
&\text{column 4:} \quad 2U_{13} + 2U_{14} - 2M\, U_{avg,o} = -1
\end{aligned} \tag{7.13}$$

Thus, we have 4 continuity equations and 15 unknowns (U_1 to U_{14} and $U_{avg,o}$).

For the momentum equation (7.9), the following finite difference approximations are used:

---

[5]Simpson's Rule cannot be used because the number of grid divisions at each column alternates between even and odd along the length of the flow channel.

$$\frac{dP}{dX} = \frac{P^{n+1} - P^n}{\Delta X} \tag{7.14}$$

$$\frac{dU}{dy} = \frac{U^n_{m+1} - U^n_{m-1}}{2\Delta Y} \tag{7.15}$$

$$\frac{d^2U}{dY^2} = \frac{U^n_{m-1} - 2U^n_m + U^n_{m+1}}{(\Delta Y)^2} \tag{7.16}$$

Substituting the above approximations into Eq. (7.9), we obtain the following for each node on the grid (details in App. A, Sec. 4.1):

$$A^n_m U^n_{m-1} + B^n_m U^n_m + C^n_m U^n_{m+1} + \phi^n_m P^n + \psi^n_m P^{n+1} = 0 \tag{7.17}$$

$$\left.\begin{aligned}
\text{where } A^n_m &= -\frac{\Delta Y}{2\eta^n_m}\left(\frac{d\eta}{dY}\right)^n_m + 1 \\
B^n_m &= -2 \\
C^n_m &= \frac{\Delta Y}{2\eta^n_m}\left(\frac{d\eta}{dY}\right)^n_m + 1 \\
\phi^n_m &= \frac{k}{\eta^n_m C_p}\,\frac{(\Delta Y)^2}{\Delta X} \\
\psi^n_m &= \frac{-k}{\eta^n_m C_p}\,\frac{(\Delta Y)^2}{\Delta X}
\end{aligned}\right\}
\quad
\begin{aligned}
m &= 1, 2, \ldots, KJ \\
n &= 1, 2, \ldots, N+1
\end{aligned}$$

Combining the 4 continuity equations (7.13) and the 14 momentum equations (7.17), we have for the entire grid, a modified tridiagonal system of 18 equations with 18 unknowns (U_1 to U_{14}, P^2, P^3, P^5 and $U_{avg,o}$). The equation can be written as follows:

$$\text{node 1:} \quad \cancel{A_1}\cancelto{1}{U_{max}} + B_1U_1 + C_1U_2 + \cancel{\phi_1}\cancelto{0}{P^1} + \psi_1P^2 = 0$$

$$\text{node 2:} \quad A_2U_1 + B_2U_2 + C_2U_3 + \cancel{\phi_2}\cancelto{0}{P^1} + \psi_2P^2 = 0$$

$$\vdots$$

$$\text{node 14:} \quad A_{14}U_{13} + B_{14}U_{14} + \cancel{C_{14}}\cancelto{0}{U_{stat}} + \cancel{\phi_{14}}\cancelto{0}{P^4} + \psi_{14}P^5 = 0 \qquad (7.18)$$

$$\text{column 1:} \quad 2U_1 + 2U_2 + \ldots + 2U_5 - 2M \cdot U_{avg,o} = -1$$

$$\vdots$$

$$\text{column 4:} \quad 2U_{13} + 2U_{14} - 2M \cdot U_{avg,o} = -1$$

or in matrix form:

$$\begin{bmatrix}
B_1 & C_1 & & & & & & & & & & & & & \psi_1 & 0 & 0 & 0 \\
A_2 & B_2 & C_2 & & & & & & & \underline{0} & & & & & \psi_2 & 0 & 0 & 0 \\
& \ddots & \ddots & \ddots & & & & & & & & & & & \vdots & \vdots & \vdots & \vdots \\
& & & A_5 & B_5 & 0 & & & & & & & & & \psi_5 & 0 & & \\
& & & & 0 & B_6 & C_6 & & & & & & & & \phi_6 & \psi_6 & & \\
& & & & & A_7 & B_7 & C_7 & & & & & & & & & & \\
& & & & & & \ddots & \ddots & \ddots & & & & & & \vdots & \vdots & & \\
& & & & & & & & & & & & & & \phi_9 & \psi_9 & & \\
& & & & & & & & & & & & & & 0 & \phi_{10} & \vdots & \\
& & & & & & & & & & & & & & & \phi_{11} & \vdots & \\
& & & & & & & & & & \ddots & \ddots & \ddots & & \vdots & \phi_{12} & 0 & \vdots \\
& & & \underline{0} & & & & & & & & A_{13} & B_{13} & C_{13} & 0 & 0 & \psi_{13} & 0 \\
& & & & & & & & & & & & A_{14} & B_{14} & 0 & 0 & \psi_{14} & 0 \\
2 & 2 & 2 & 2 & 2 & 0 & \ldots & & & & & & & & \vdots & \vdots & 0 & -2M \\
& & & \ldots & 0 & 2 & 2 & 2 & 2 & 0 & \ldots & & & & & & \vdots & -2M \\
& & & & & & & \ldots & 0 & 2 & 2 & 2 & 0 & 0 & & & & -2M \\
& & & & & & & & & & \ldots & 0 & 2 & 2 & & & & -2M
\end{bmatrix}
\begin{bmatrix}
U_1 \\ U_2 \\ \vdots \\ \\ \\ \\ \\ \\ \\ \\ \vdots \\ U_{13} \\ U_{14} \\ P^2 \\ P^3 \\ P^5 \\ U_{avg,o}
\end{bmatrix}
=
\begin{bmatrix}
-A_1 \\ 0 \\ \vdots \\ 0 \\ -A_6 \\ \\ \vdots \\ \\ \vdots \\ \\ 0 \\ -A_{13} \\ 0 \\ -1 \\ -1 \\ -1 \\ -1
\end{bmatrix} \qquad (7.19)$$

$$
\begin{bmatrix}
B_1 & C_1 & & & & & & & & & & & & & \psi_1 & 0 & 0 & 0 \\
A_2 & B_2 & C_2 & & & & & \underline{0} & & & & & & & \psi_2 & 0 & 0 & 0 \\
 & \ddots & \ddots & \ddots & & & & & & & & & & & \vdots & \vdots & \vdots & \vdots \\
 & & & & & & & & & & & & & & \psi_5 & 0 & & \\
 & & & & & & & & & & & & & & \phi_6 & \psi_6 & & \\
 & & & & & & & & & & & & & & \vdots & \vdots & & \\
 & & & & & & & & & & & & & & \phi_9 & \psi_9 & & \\
 & & & & & & & & & & & & & & 0 & \phi_{10} & \vdots & \\
 & & & & & & & & & & & & & & \vdots & \phi_{11} & \vdots & \\
 & & & & & & & & & & \ddots & \ddots & \ddots & & & \phi_{12} & 0 & \vdots \\
 & & & & \underline{0} & & & & & & & 0 & B_{13} & C_{13} & 0 & 0 & \psi_{13} & 0 \\
 & & & & & & & & & & & & A_{14} & B_{14} & 0 & 0 & \psi_{14} & 0 \\
Z_1 & Z_2 & Z_3 & Z_4 & Z_5 & 0 \cdots & & & & & & & & & & & & \\
 & & & \cdots 0 & & Z_6 & Z_7 & Z_8 & Z_9 & 0 \cdots & & & & & & & & \\
 & & & & & & \cdots 0 & & & Z_{10} & Z_{11} & Z_{12} & 0 & 0 & & \underline{\underline{W}} & & \\
 & & & & & & & & & & \cdots 0 & & Z_{13} & Z_{14} & & & &
\end{bmatrix}
\begin{bmatrix}
U_1 \\ U_2 \\ \vdots \\ \\ \\ \\ \\ \\ \\ \vdots \\ U_{13} \\ U_{14} \\ P^2 \\ P^3 \\ P^5 \\ U_{avg,o}
\end{bmatrix}
=
\begin{bmatrix}
E_1 \\ E_2 \\ \vdots \\ \\ \\ \\ \\ \\ \\ \vdots \\ E_{13} \\ E_{14} \\ W_{6,1} \\ \vdots \\ \\ W_{6,4}
\end{bmatrix}
\qquad (7.20)
$$

This system of equations is solved for the velocities at each grid point, the pressures at each column, and the average velocity at X = 0 by Gaussian elimination using the algorithm that is shown in App. D, Sec. 3.

Energy Equation

The energy equation is solved by the "marching" procedure, that is, one column at a time, and not like the continuity and momentum equations which were solved simultaneously for the entire grid. However, in order that the finite difference method can work properly for the energy equation, the grid used for the velocities and pressures must be subdivided along the X-axis, as illustrated in Fig. 7-3. Velocities at the intermediate points are calculated by linear-interpolation. For the energy equation (7.10), the following finite difference approximations are used:

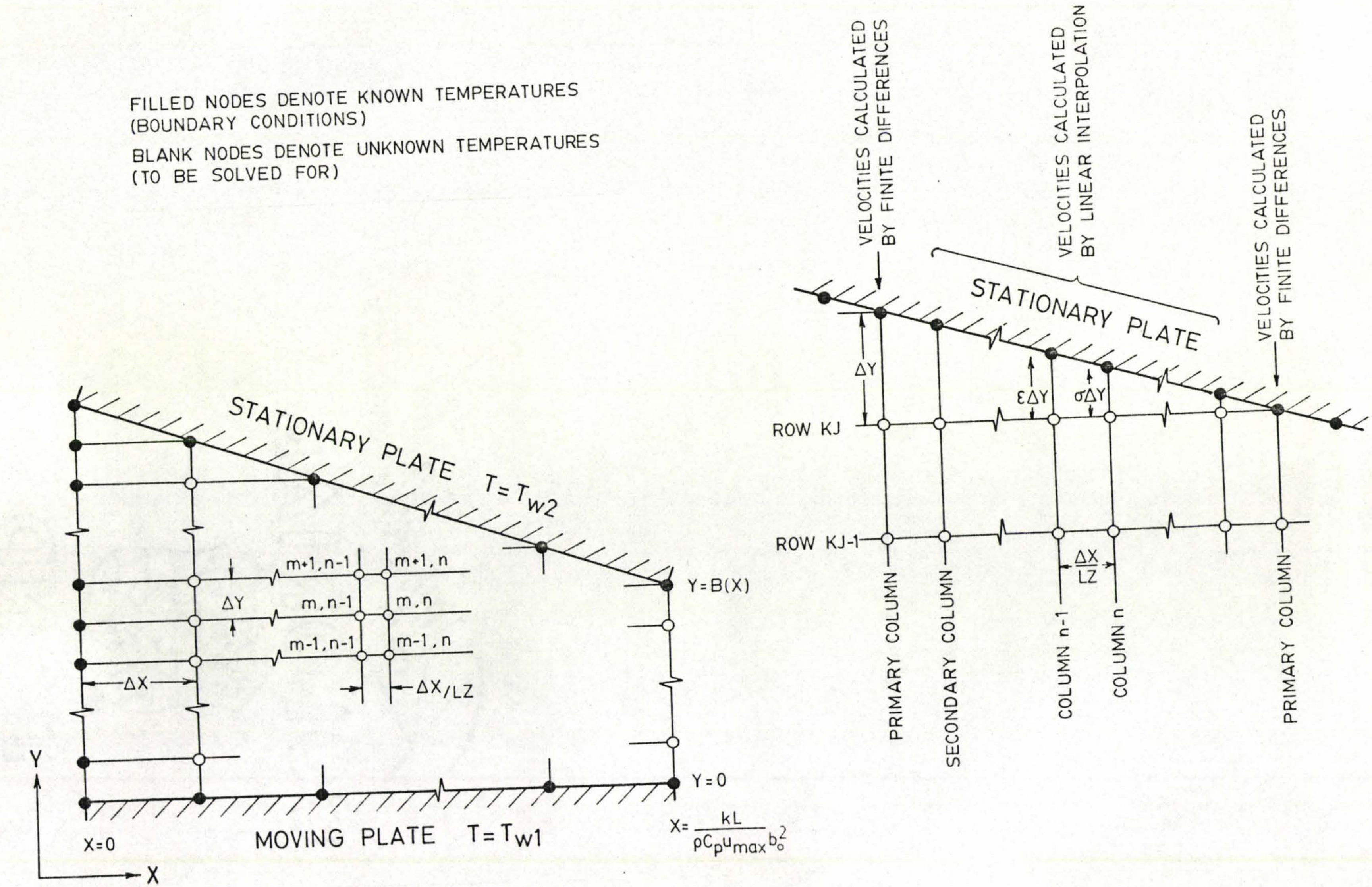

Fig. 7-3. Finite difference grid for energy equation. Drag flow between converging plates.

$$\frac{\partial\theta}{\partial X} = \frac{\theta_m^n - \theta_m^{n-1}}{\Delta X} \qquad (7.21)$$

$$\frac{\partial^2\theta}{\partial Y^2} = \frac{\theta_{m-1}^n - 2\theta_m^n + \theta_{m+1}^n}{2(\Delta Y)^2} + \frac{\theta_{m-1}^{n-1} - 2\theta_m^{n-1} + \theta_{m+1}^{n-1}}{2(\Delta Y)^2} \qquad (7.22)$$

Adjacent to the stationary, inclined wall, the second derivative is approximated as follows (see App. A, Sec. 4.2 for derivation):

$$\frac{\partial^2\theta}{\partial Y^2} = \frac{1}{(1+\sigma)(\Delta Y)^2}\left[\theta_{m-1}^n - \left(\frac{1}{\sigma} + 1\right)\theta_m^n + \frac{1}{\sigma}\,\theta_{m+1}^n\right]$$

$$+ \frac{1}{(1+\varepsilon)(\Delta Y)^2}\left[\theta_{m-1}^{n-1} - \left(\frac{1}{\varepsilon} + 1\right)\theta_m^{n-1} + \frac{1}{\varepsilon}\,\theta_{m+1}^{n-1}\right] \qquad (7.23)$$

where σ and ε are defined in Fig. 7-3.

Substituting the above approximations into Eq. (7.10), we obtain for column n (details in App. A, Sec. 4.2):

$$A_m\theta_{m-1}^n + B_m\theta_m^n + C_m\theta_{m+1}^n = D_m + E_m + F_m + G_m = H_m \qquad (7.24)$$

where $A_m = -1$

$$B_m = \frac{2(\Delta Y)^2}{\Delta X} \cdot U_m^n + 2$$

$$C_m = -1$$

$$D_m = \theta_{m-1}^{n-1}$$

$$\left.\begin{aligned}
E_m &= [\frac{2(\Delta Y)^2}{\Delta X} \cdot U_m^n - 2]\ \theta_m^{n-1} \\
F_m &= \theta_{m+1}^{n-1} \\
G_m &= 2(\Delta Y)^2\ \delta_m^n\ (\frac{dU}{dY})_m^2
\end{aligned}\right\} \quad m = 1, 2, \ldots, KJ-1$$

and

$$A_{KJ} = \frac{-1}{1+\sigma}$$

$$B_{KJ} = \frac{(\Delta Y)^2}{\Delta X}\ U_{KJ}^n + \frac{1}{\sigma}$$

$$C_{KJ} = \frac{-1}{\sigma+\sigma^2}$$

$$D_{KJ} = [\frac{1}{1+\varepsilon}]\ \theta_{KJ-1}^{n-1}$$

$$E_{KJ} = \left[\frac{(\Delta Y)^2}{\Delta X} \cdot U_{KJ}^n - \frac{1}{\varepsilon}\right] \theta_{KJ}^{n-1}$$

$$F_{KJ} = \left[\frac{1}{\varepsilon+\varepsilon^2}\right] \theta_{KJ+1}^{n-1}$$

$$G_{KJ} = (\Delta Y)^2\ \delta_{KJ}^n\ (\frac{dU}{dY})_{KJ}^2$$

Thus, for column n, we have a tridiagonal system of KJ equations with KJ unknowns (θ_1^n to θ_{KJ}^n). The equations can be written as follows:

$$\cancelto{0}{A_1 \theta_0^n} + B_1 \theta_1^n + C_1 \theta_2^n = H_1$$

$$A_m\theta^n_{m-1} + B_m\theta^n_m + C_m\theta^n_{m+1} = H_m \qquad (m = 2, 3, \ldots, KJ\text{-}1) \tag{7.25}$$

$$A_{KJ}\theta^n_{KJ-1} + B_{KJ}\theta^n_{KJ} + C_{KJ}\underset{\displaystyle\frac{T_{w2}-T_{w1}}{T_o-T_{w1}}}{\underset{\downarrow}{\theta^n_{KJ+1}}} = H_{KJ}$$

The above equations can be written in matrix form as follows:

$$\begin{bmatrix} B_1 & C_1 & & & & & \underline{0} \\ A_2 & B_2 & C_2 & & & & \\ & \ddots & \ddots & \ddots & & & \\ & & A_m & B_m & C_m & & \\ & & & \ddots & \ddots & \ddots & \\ & & & & A_{KJ-1} & B_{KJ-1} & C_{KJ-1} \\ \underline{0} & & & & & A_{KJ} & B_{KJ} \end{bmatrix} \begin{bmatrix} \theta^n_1 \\ \theta^n_2 \\ \vdots \\ \theta^n_m \\ \vdots \\ \theta^n_{KJ-1} \\ \theta^n_{KJ} \end{bmatrix} = \begin{bmatrix} H_1 \\ H_2 \\ \vdots \\ H_m \\ \vdots \\ H_{KJ-1} \\ H_{KJ} - C_{KJ}\theta^{n-1}_{KJ+1} \end{bmatrix} \tag{7.26}$$

This system of equations is solved for the temperature profile at column n by Gaussian elimination using Thomas' method (details in App. D, Sec. 1).

Bulk Temperature

The dimensionless flow-average (bulk) temperature is defined as follows:

$$\theta_{bulk} = \frac{\int_{Y=0}^{Y=B(X)} \theta(X,Y)U(X,Y)\,dY}{\int_{Y=0}^{Y=B(X)} U(X,Y)\,dY} \tag{7.27}$$

For column n, Eq. (7.27) is written in finite difference form using the trapezoidal rule as follows:

$$\theta_{bulk}^{n} = \frac{\overset{\nearrow 0}{\theta_o^n U_o^n} + 2\theta_1^n U_1^n + \ldots + 2\theta_{KJ}^n U_{KJ}^n + \overset{\nearrow 0}{\theta_{KJ+1}^n U_{KJ+1}^n}}{\underset{\searrow 1}{U_o^n} + 2U_1^n + \ldots + 2U_{KJ}^n + \underset{\searrow 0}{U_{KJ+1}^n}} \tag{7.28}$$

It should be noted that the above equation can be used only when all the points in column n are evenly spaced. In secondary columns, the step adjacent to the stationary inclined plate is smaller than the other steps. This will result in an error when Eq. (7.28) is used to calculate the bulk temperature.

Local Nusselt Number

The local Nusselt number is calculated from the following definition which is derived in App. B:

$$Nu_x = \frac{hb_o}{k} = \frac{(\frac{dT}{dy})_{wall} \cdot b_o}{(T_{bulk} - T_{wall})} \tag{7.29}$$

In dimensionless form, we have:

$$(Nu_x)_{Y=0} = \frac{(\frac{d\theta}{dY})_{Y=0}}{\theta_{bulk}} \tag{7.30}$$

$$(Nu_x)_{Y=B(X)} = \frac{-(\frac{d\theta}{dY})_{Y=B(X)}}{(\theta_{bulk} - \theta_{w2})} \tag{7.31}$$

The dimensionless temperature gradients at the walls at column n are estimated by the following finite difference approximations:

$$\left(\frac{d\theta}{dY}\right)_{Y=0} = \frac{1}{6\Delta Y}\left(-11\overset{0}{\theta_o^n} + 18\theta_1^n - 9\theta_2^n + 2\theta_3^n\right) \qquad (7.32)$$

$$\left(\frac{d\theta}{dY}\right)_{Y=B(X)} = \frac{1}{6\Delta Y}\left(-2\theta_{KJ-2}^n + 9\theta_{KJ-1}^n - 18\theta_{KJ}^n + 11\overset{\theta_{w2}}{\theta_{KJ+1}^n}\right) \qquad (7.33)$$

The above Eqs. (7.32) and (7.33) are derived in App. C, Sec. 1 and 5.

7.2 Computational Procedure

It was stated in Chap. 3, Sec. 3, that the momentum and energy equations are coupled by velocity and temperature, and therefore cannot be solved independently. However, the coupled equations can be solved iteratively at each node on the finite difference grid by alternately solving the set of continuity and momentum equations (7.18) and the set of energy equations (7.25) until the solutions converge. The velocity at each node and the pressure at each column are calculated simultaneously for the entire grid, while the temperatures at the nodes are calculated simultaneously one column at a time for all the columns in the grid. The iterative procedure used to calculate the velocity and temperature profiles, the pressure, the bulk temperature and the local Nusselt numbers at each column in the grid is now outlined.

Notation

$U1_m^n$ refers to the estimated velocity at node (m,n) on a primary column.

$U2_m^n$ refers to the most recently calculated velocity at node (m,n) on a primary column.

V_m^n refers to the velocity at node (m,n) on a secondary column (calculated by interpolation from values of U2).

$\theta 1_m^n$ refers to the estimated temperature at node (m,n) on a primary column.

$\theta 2_m^n$ refers to the most recently calculated temperature at node (m,n) on a primary column.

θP_m^{n-1} (m = 1, 2, ..., KJ) refers to the temperature profile at column n-1 (primary or secondary).

θQ_m^n (m = 1, 2, ..., KJ) refers to the temperature calculated at column n (primary or secondary). When θQ_m^n (m = 1, 2, ..., KJ) is calculated at a primary column, then $\theta 2_m^n$ is set equal to θQ_m^n for each node in the column.

Procedure

1. Assume values for the velocity and temperature at each node on the grid.

$$\left.\begin{array}{l} U1_m^n = \dfrac{Y(X)}{B(X)} \\[2ex] \theta 1_m^n = 1 \end{array}\right\} \quad \begin{array}{l} m = 1, 2, \ldots, KJ \\[2ex] n = 1, 2, \ldots, N+1 \end{array}$$

2. Using $U1_m^n$ and $\theta 1_m^n$ (m = 1, 2, ..., KJ and n = 1, 2, ..., N+1) calculate η_m^n and $(\frac{d\eta}{dY})_m^n$ at each node on the grid.

3. Using η_m^n and $(\frac{d\eta}{dY})_m^n$ (m = 1, 2, ..., KJ and n = 1, 2, ..., N+1), solve the set of continuity and momentum equations (7.19) by Gaussian elimination (see App. D, Sec. 3 for algorithm) to obtain $U2_m^n$ and P^n (m = 1, 2, ..., KJ and n = 1, 2, ..., N+1).

4. Assume a temperature profile at the entrance of the channel.

$$\theta P_m^o = 1 \qquad\qquad (m = 1, 2, \ldots, KJ)$$

Perform steps 5 through 11 at each primary column n on the grid (n = 1, 2, ..., N).

5. Divide the primary step from column n to n+1 into LZ secondary steps.

Perform steps 6 through 9 at each secondary column ℓ (ℓ = 1, 2, ..., LZ-1).

6. Calculate V_m^ℓ and θQ_m^ℓ (m = 1, 2, ..., KJ) at column ℓ by linear interpolation from values of $U2_m^n$, $U2_m^{n+1}$ and $\theta 1_m^n$, $\theta 1_m^{n+1}$ (m = 1, 2, ..., KJ).

7. Using V_m^ℓ and θQ_m^ℓ (m = 1, 2, ..., KJ), calculate $(\frac{dV}{dY})_m^\ell$ and η_m^ℓ (m = 1, 2, ..., KJ) at column ℓ.

8. Using V_m^ℓ, $(\frac{dV}{dY})_m^\ell$, η_m^ℓ and $\theta P_m^{\ell-1}$ (m = 1, 2, ..., KJ), solve the set of energy equations (7.26) by Gaussian elimination using Thomas' method (see App. D, Sec. 1) to obtain θQ_m^ℓ (m = 1, 2, ..., KJ).

9. Retain the temperature profile calculated at column ℓ for use in calculating the temperature profile at column ℓ+1, and then proceed to column ℓ+1.

$$\theta P_m^{\ell} = \theta Q_m^{\ell} \qquad (m = 1, 2, \ldots, KJ)$$

$$\ell = \ell + 1$$

When a primary column has been reached (when ℓ = LZ), the following steps are carried out:

10. Repeat steps 7 through 9, replacing V_m^{ℓ} and θQ_m^{ℓ} (m = 1, 2, ..., KJ) by $U2_m^{n+1}$ and $\theta 1_m^{n+1}$ (m = 1, 2, ..., KJ).

11. Retain the temperature profile calculated at column LZ as a temperature profile for primary column n+1 and also for use in calculating the temperature profile at secondary column 1 in the next primary step.

$$\left.\begin{aligned} \theta 2_m^{n+1} &= \theta Q_m^{LZ} \\ \theta P_m^{o} &= \theta Q_m^{LZ} \end{aligned}\right\} \quad (m = 1, 2, \ldots, KJ)$$

When the temperature profiles at all the primary columns (n = 2, 3, ..., N+1) have been calculated, the following steps are carried out:

12. Compare $U1_m^n$, $U2_m^n$ and $\theta 1_m^n$, $\theta 2_m^n$ (m = 1, 2, ..., KJ and n = 1, 2, ..., N+1). If $|U2_m^n - U1_m^n| <$ tolerance and $|\theta 2_m^n - \theta 1_m^n| <$ tolerance for all m and n, then proceed to step 15. Otherwise continue to step 13.

13. Set the estimates of the velocities and temperatures at each node in the grid equal to the most recently calculated values.

$$\left.\begin{aligned} U1_m^n &= U2_m^n \\ \theta 1_m^n &= \theta 2_m^n \end{aligned}\right\} \quad \begin{aligned} m &= 1, 2, \ldots, KJ \\ n &= 1, 2, \ldots, N+1 \end{aligned}$$

14. Repeat steps 2 through 12 until the desired error tolerances have been achieved.

15. Print the final velocity and temperature profiles and the pressure at the primary columns.

16. Calculate the bulk temperature at each primary column using the trapezoidal rule (see Eq. (7.28)).

17. Calculate the local Nusselt numbers at the walls of the channel (see Eqs. (7.30) and (7.31)).

18. Print the bulk temperatures and local Nusselt numbers.

Computations using the above algorithm have been carried out in McMaster's CDC 6400 computer. A sample program listing with results is located in App. F, Sec. 4.

7.3 Convergence, Stability and Step Size

It was stated in Chap. 3, Sec. 4, that a good indication of the convergence and stability of the finite difference results is the negligible change in results obtained when the step sizes in the finite difference grid are decreased. This was the main criterion used in deciding which step sizes should be used in the finite difference program. However, when the velocity profiles and pressure distribution are calculated, the number of nodes in the finite difference grid that can be used is limited by the memory capacity of the computer. When solving the energy equation, it is necessary to divide each primary step in the X-direction into 100 secondary steps to ensure that the temperature profiles and local Nusselt numbers converge. This is especially important in the calculation of the local Nusselt numbers because they are calculated from temperature derivatives (see Eq. (7.29)), and derivatives are very sensitive to step size changes. The following step sizes were used in the finite difference program:

Continuity and momentum equations:

$$\Delta X = 0.0546$$

$$\Delta Y = 0.02$$

Energy Equation:

$$\Delta X = 0.000546$$

$$\Delta Y = 0.02$$

The results presented in the subsequent figures are independent of step size within at least 2 significant digits.

An additional test for convergence was carried out by calculating the pressure distribution for a Newtonian, constant viscosity fluid using an analytical expression given by Schlichting (58), and comparing this with the corresponding finite difference results for the same fluid (for details, see App, Sec. 4). A difference of 4% between the analytical and finite difference results was primarily due to the use of a coarse finite difference network.

7.4 Results and Discussion

Solutions of the continuity, momentum and energy equations for drag flow between converging plates are presented in Figs. 7-4 through 7-17. The following velocity, pressure and temperature boundary conditions have been used:

$$\begin{array}{llll} x = 0 & b_o = 0.025 \text{ cm} & T_o = 130°C & p_o = 0 \\ x = L = 10 \text{ cm} & b_L = 0.0125 \text{ cm} & p_L = 0 & \\ y = 0 & u = u_{max} = 15 \text{ cm/s} & T_{w1} = 160°C & \\ y = b(x) & u = 0 & T_{w2} = 160°C & \end{array} \tag{7.34}$$

In obtaining some of the results, different temperature boundary conditions were used for comparison. The following power-law temperature-dependent viscosity model and fluid properties representing a typical high-density polyethylene melt were used in the computations:

Viscosity:

$$\eta = Ae^{-Bn(T-T_m)} \left|\frac{du}{dy}\right|^{n-1} \tag{7.35}$$

where $A = 282\ 000 \quad \text{poise}\cdot s^{n-1}$

$= 28\ 200 \quad Pa\cdot s^n$

$B = 0.024\ K^{-1}$

$n = 0.453$

$$T_m = 399.5 \text{ K}$$

Density: $\rho = 794 \text{ kg/m}^3$

Specific heat:

$$C_p = 2.51 \text{ kJ/(kg}\cdot\text{K)}$$

Thermal conductivity:

$$k = 6.1 \times 10^{-4} \text{ cal/(cm}\cdot\text{s}\cdot\text{K)}$$

$$= 0.255 \text{ W/(m}\cdot\text{K)}$$

The velocity and temperature profiles, pressure distributions, bulk temperatures and local Nusselt numbers in Figs. 7-4 through 7-17 are shown as functions of the dimensionless axial distance, X. Because the bulk temperatures and local Nusselt numbers change the most near the entrance of the flow channel, they have been plotted semi-logarithmically. X on the abscissa of these plots ranges from 0.0055 to 1.366. This corresponds to x ranging from 0.04 cm to 10 cm.

In Fig. 7-4, the velocity profiles are shown for the power-law temperature-dependent viscosity model. Near the entrance of the channel, the profiles are characteristic of drag flow, but near the exit, they resemble more those of Poiseuille flow. The reason for the transition is the rise in pressure in the channel as seen in Fig. 7-5. The pressure distributions for the power-law temperature-dependent viscosity model and several Newtonian, constant viscosity models are presented in Fig. 7-5. In the case of the power-law fluid, the maximum pressure of about 50 MPa

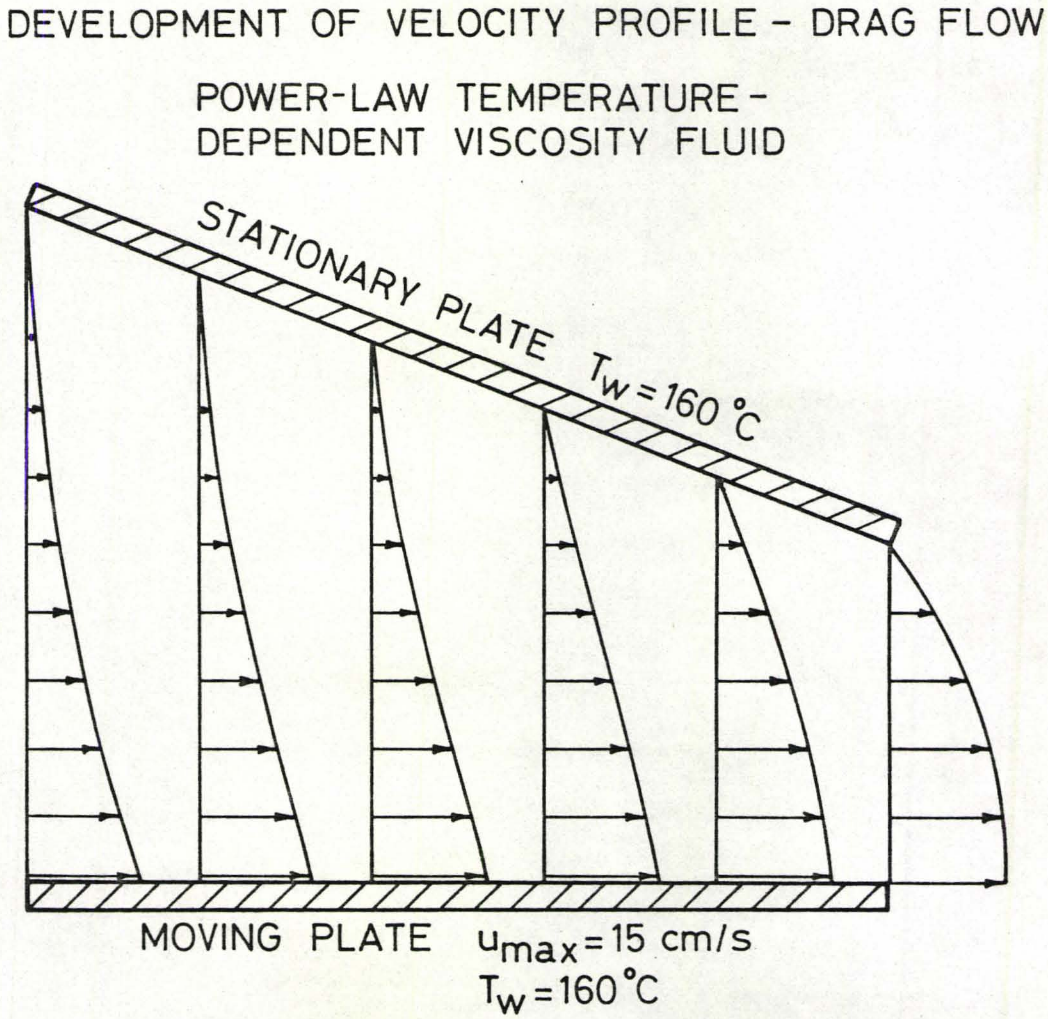

Fig. 7-4. Development of velocity profile. Drag flow between converging plates. Channel dimensions and fluid properties given on pp. 151-152.

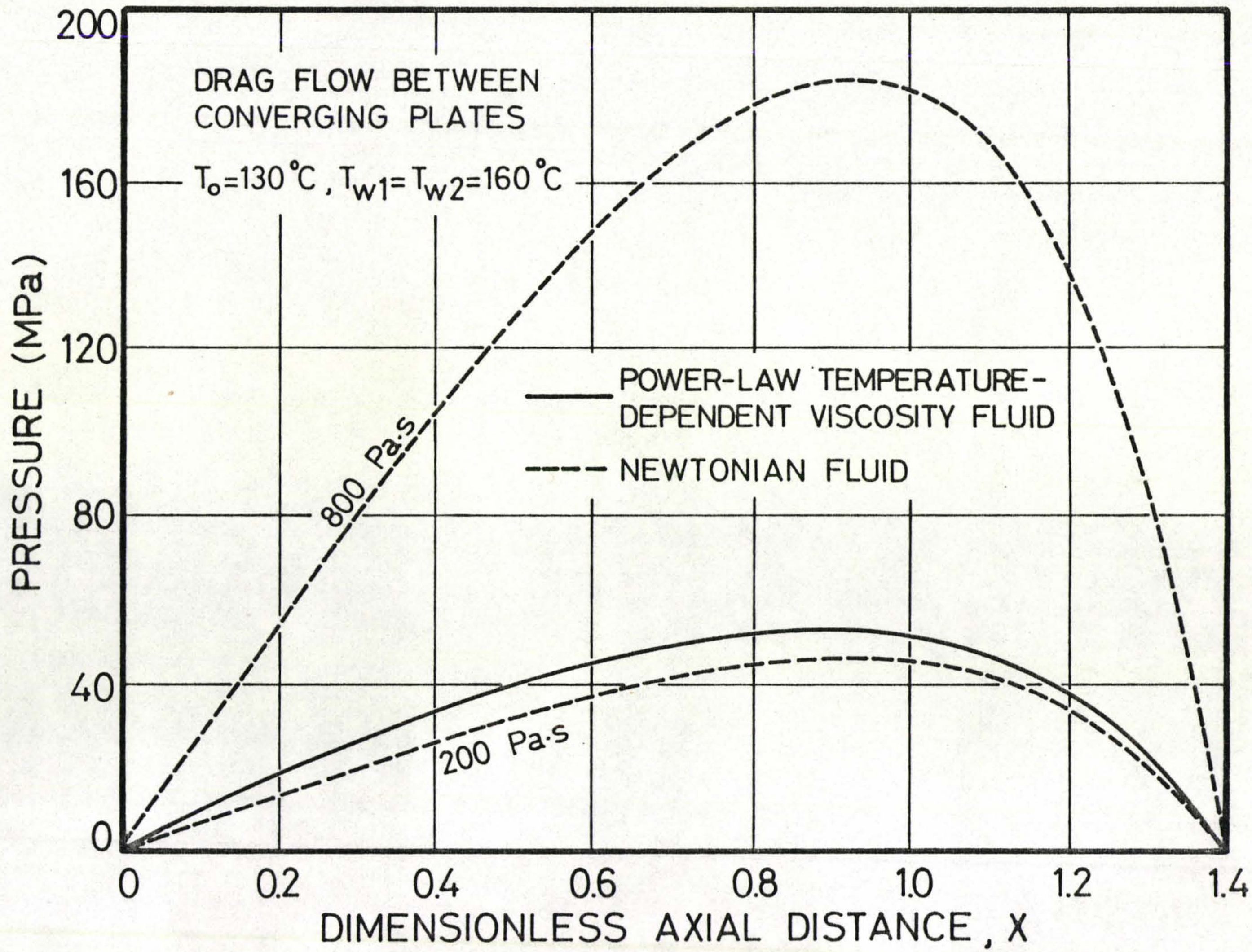

Fig. 7-5. Pressure distributions. Drag flow between converging plates. Channel dimensions and fluid properties given on pp. 151-152.

is approximately equal to the pressure build-up inside the barrel of an extruder. The pressure distributions for the Newtonian fluids are shown for comparison.

In Fig. 7-6, the temperature profiles for the power-law temperature-dependent viscosity model and for a power-law temperature-independent viscosity model are shown. The temperature-independent viscosity model used is identical to the temperature-dependent viscosity model given in Eq. (7.35), except that T is held constant and equal to the average of the temperatures of the two plates (160°C). Near the entrance of the channel, the temperatures in the temperature-dependent case are higher than in the temperature-independent case. However, farther downstream, the opposite is true. The reason for this is that as the temperature in the constitutive equation increases, the viscosity decreases. Near the channel entrance, the temperature in the constitutive equation of the temperature-dependent fluid is lower than that of the temperature-independent fluid. Therefore, the viscosity will be higher in the temperature-dependent case resulting in more heat generated by viscous dissipation. Farther downstream, more heat is generated by viscous dissipation in the temperature-independent case. Also, it is seen that after a maximum in temperature rise has been reached, the temperature decreases with decreasing gap between the plates. This is to be expected since the temperature of the fluid will approach the wall temperature as the gap becomes smaller and smaller.

Plots of the bulk temperatures along the length of the channel are

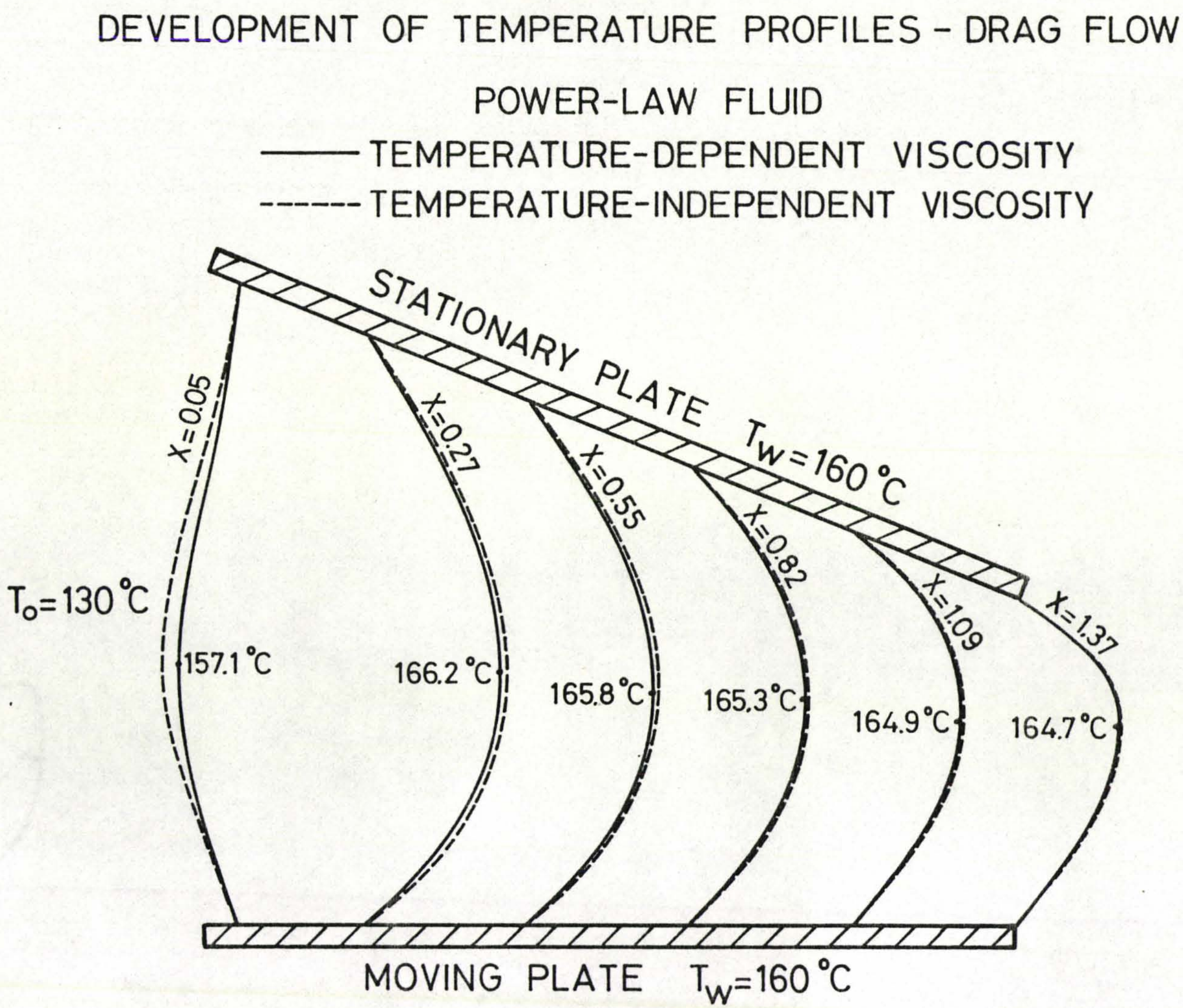

Fig. 7-6. Development of temperature profiles. Drag flow between converging plates. Channel dimensions and fluid properties given on pp. 151-152.

presented in Figs. 7-7 through 7-10 for the power-law temperature-dependent and temperature-independent viscosity model and the Newtonian, constant viscosity model. In Fig. 7-7, the bulk temperatures are shown for power-law temperature-dependent viscosity fluids with different inlet temperatures. In each case, the bulk temperature at X = 0.2 is the same (164.2°C). This is to be expected since the temperature profiles at large X are not influenced by the inlet temperature of the fluid. At the exit of the channel, the bulk temperature is 162.9°C. Also shown in Fig. 7-7 is the effect of removing the viscous dissipation term from the energy equation. Without viscous dissipation, the bulk temperature at large X is equal to the wall temperature (160°C). The difference of 4°C is an indication of the importance of viscous dissipation in the drag flow of polymer melts between converging plates. If a wider gap or higher plate velocity were used, the temperature rise due to viscous dissipation would be much more significant.

The rise in bulk temperature for the power-law temperature-dependent and temperature-independent viscosity fluids is shown in Fig. 7-8 for two temperature boundary conditions: both stationary and moving plate at 160°C, and the stationary plate at 130°C and the moving plate at 190°C. When both walls are at 160°C, the difference between the two models is almost negligible. However, when the stationary wall is at 130°C and the moving wall is at 190°C, the difference between the two models is quite significant. Here the bulk temperatures differ between 1.5° and 5°C at a given X. In Fig. 7-9 the rise in bulk temperature for

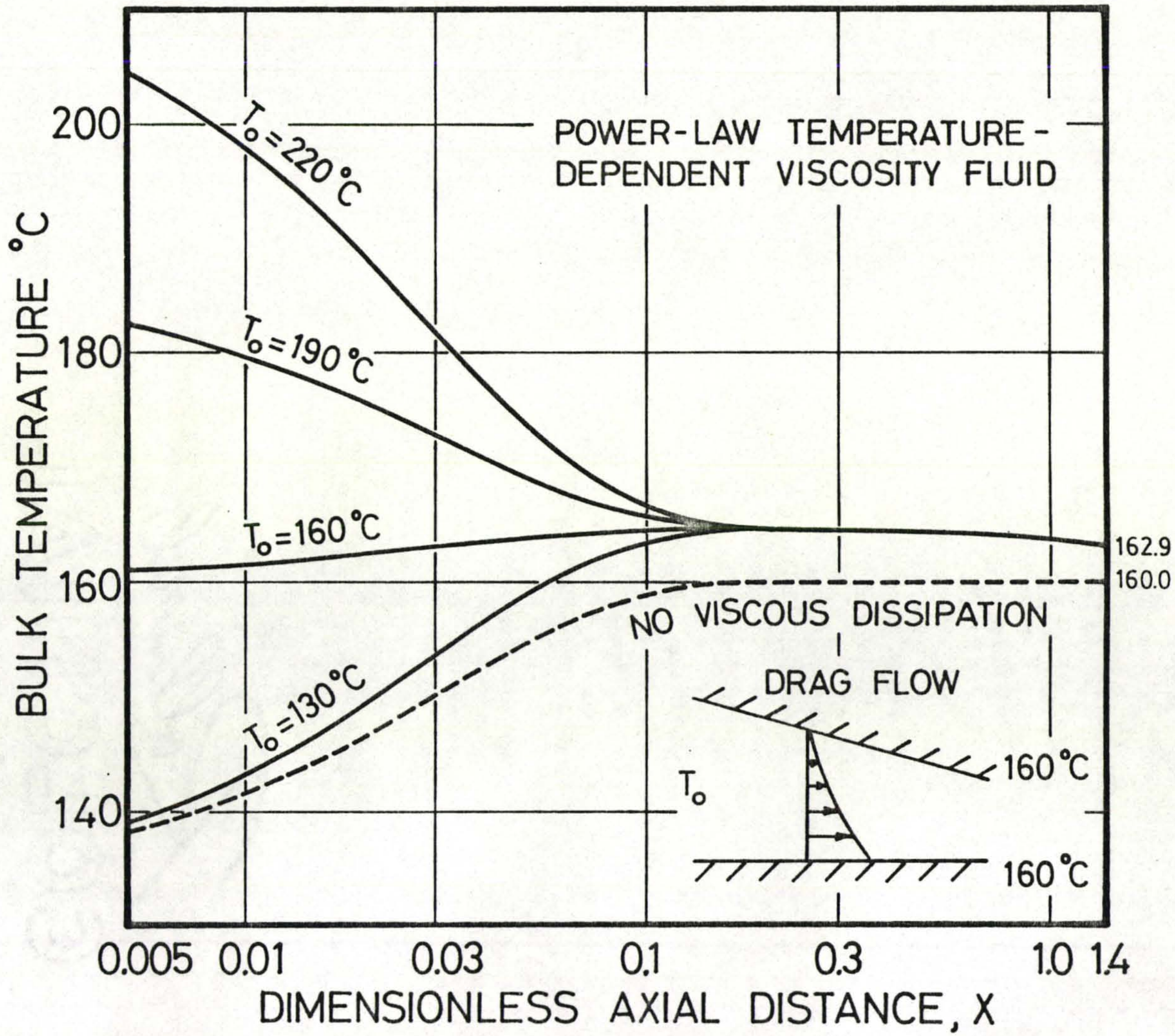

Fig. 7-7. Bulk temperature vs. X. Drag flow between converging plates. Channel dimensions and fluid properties given on pp. 151-152

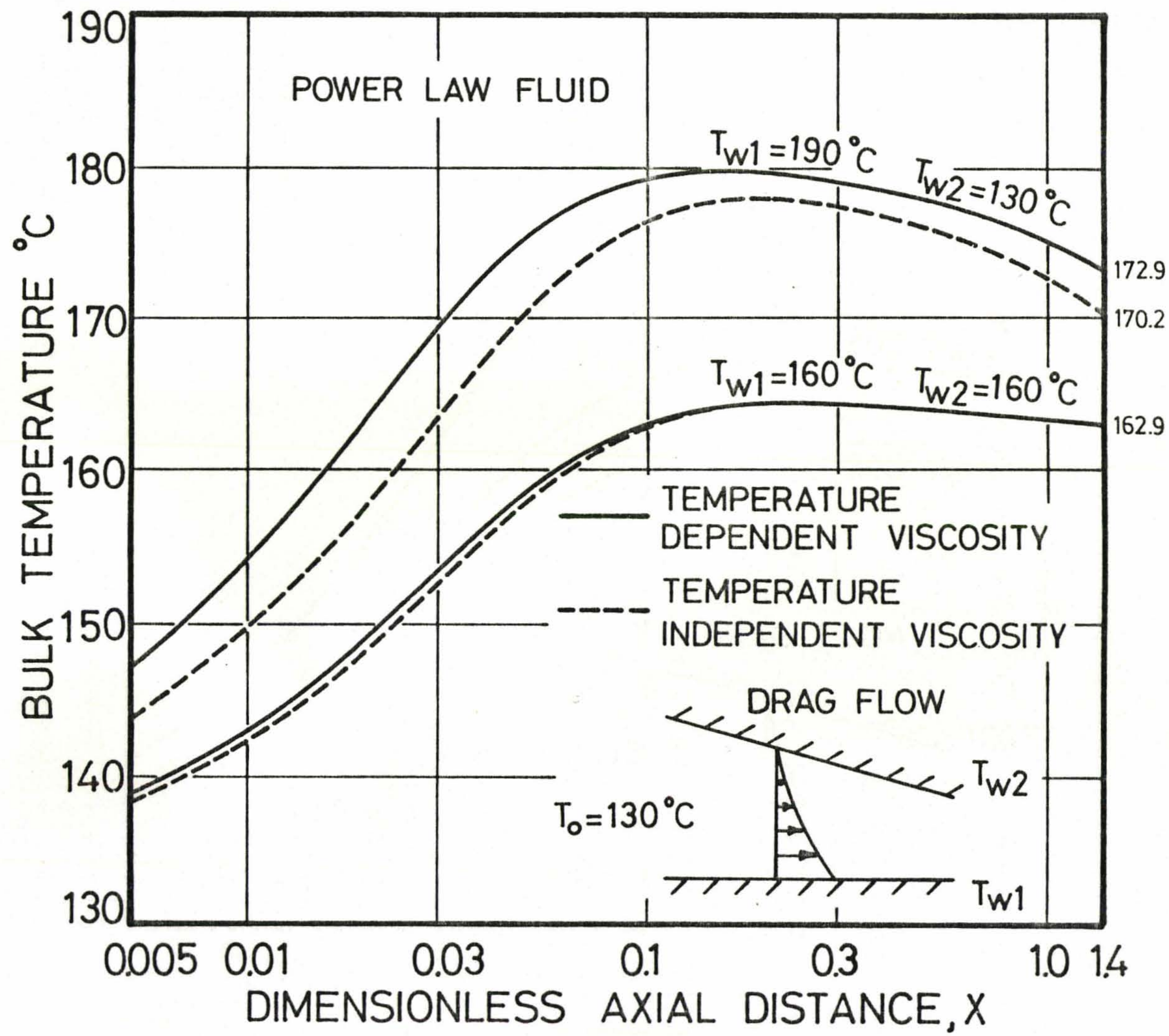

Fig. 7-8. Bulk temperature vs. X. Drag flow between converging plates. Channel dimensions and fluid properties given on pp. 151-152.

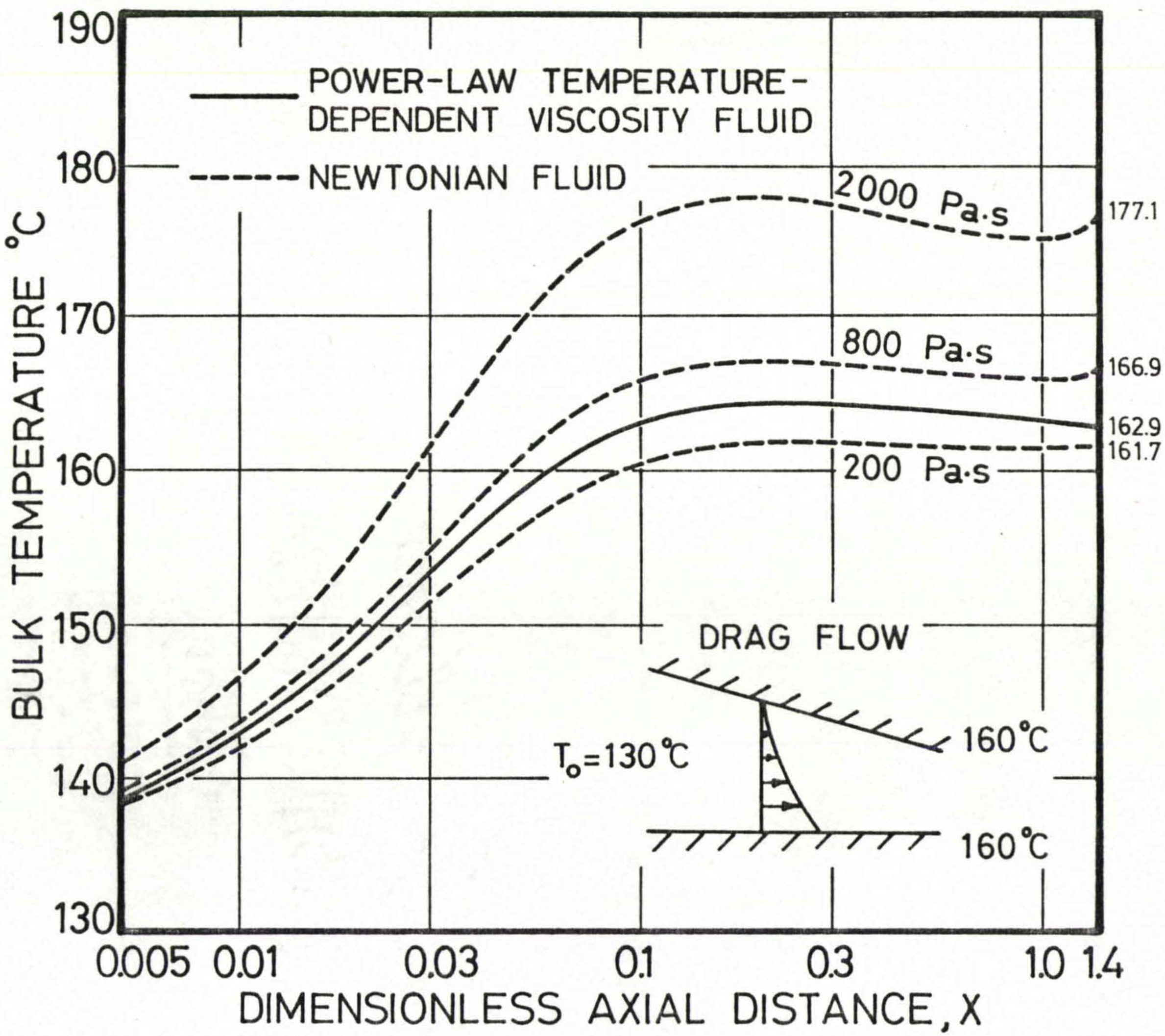

Fig. 7-9. Bulk temperature vs. X. Drag flow between converging plates. Channel dimensions and fluid properties given on pp. 151-152.

the power-law temperature-dependent viscosity fluid and several Newtonian, constant viscosity fluids is compared. In Fig. 7-10, the rise in bulk temperature for the power-law temperature-dependent viscosity fluid is compared for drag flow between parallel and converging plates. The distance between the parallel plates is 0.025 cm, the same as the inlet gap of the converging plates. The temperature rise between the converging plates is faster, but at $X \geq 0.2$, the difference between the two cases is quite small.

Plots of the local Nusselt numbers at both the stationary and moving plates are presented in Figs. 7-11 through 7-17 for the power-law temperature-dependent and temperature-independent viscosity models and the Newtonian, constant viscosity model. The local Nusselt numbers are shown for both plates because in general they are not the same for a given X. Since the local Nusselt number is a function of the temperature derivative (see Eq. (7.29)), it will be different as long as the temperature gradients at the walls are not the same.

In Fig. 7-11 and 7-12, the local Nusselt numbers for power-law temperature-dependent viscosity fluids with different inlet temperatures are shown for the moving and stationary (inclined) plates respectively. It can be seen that when the fluid is heated by the channel walls (T_o = 130°C, $T_{w1} = T_{w2}$ = 160°C), there is a region along the channel where the local Nusselt number is negative and a point where it is discontinuous. With the aid of Eq. (7.29), this behaviour is explained as follows for the moving plate:

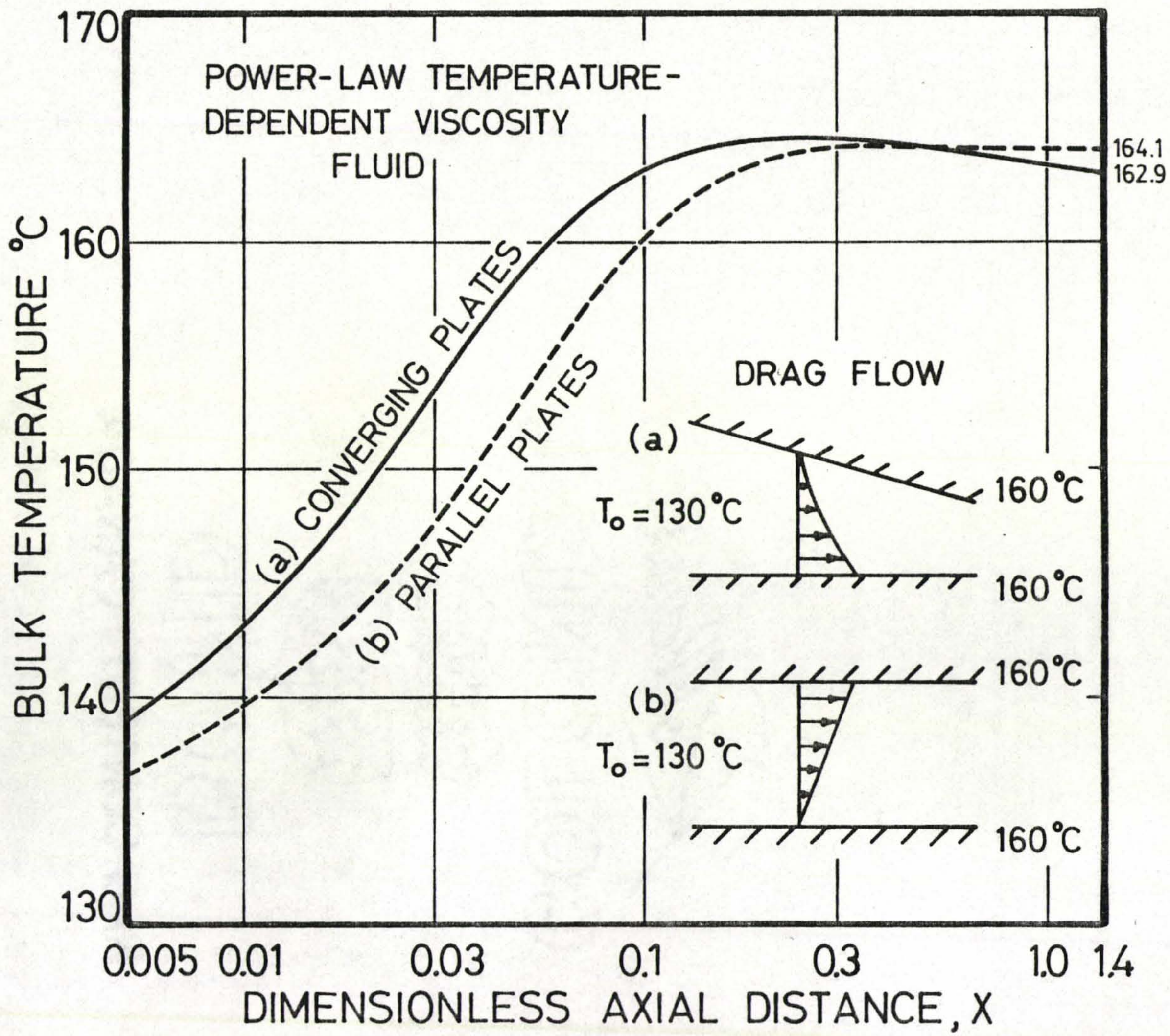

Fig. 7-10. Bulk temperature vs. X. Drag flow between (a) converging and (b) parallel plates. Gap at channel entrance is 0.025 cm in both cases. Fluid properties given on pp. 151-152.

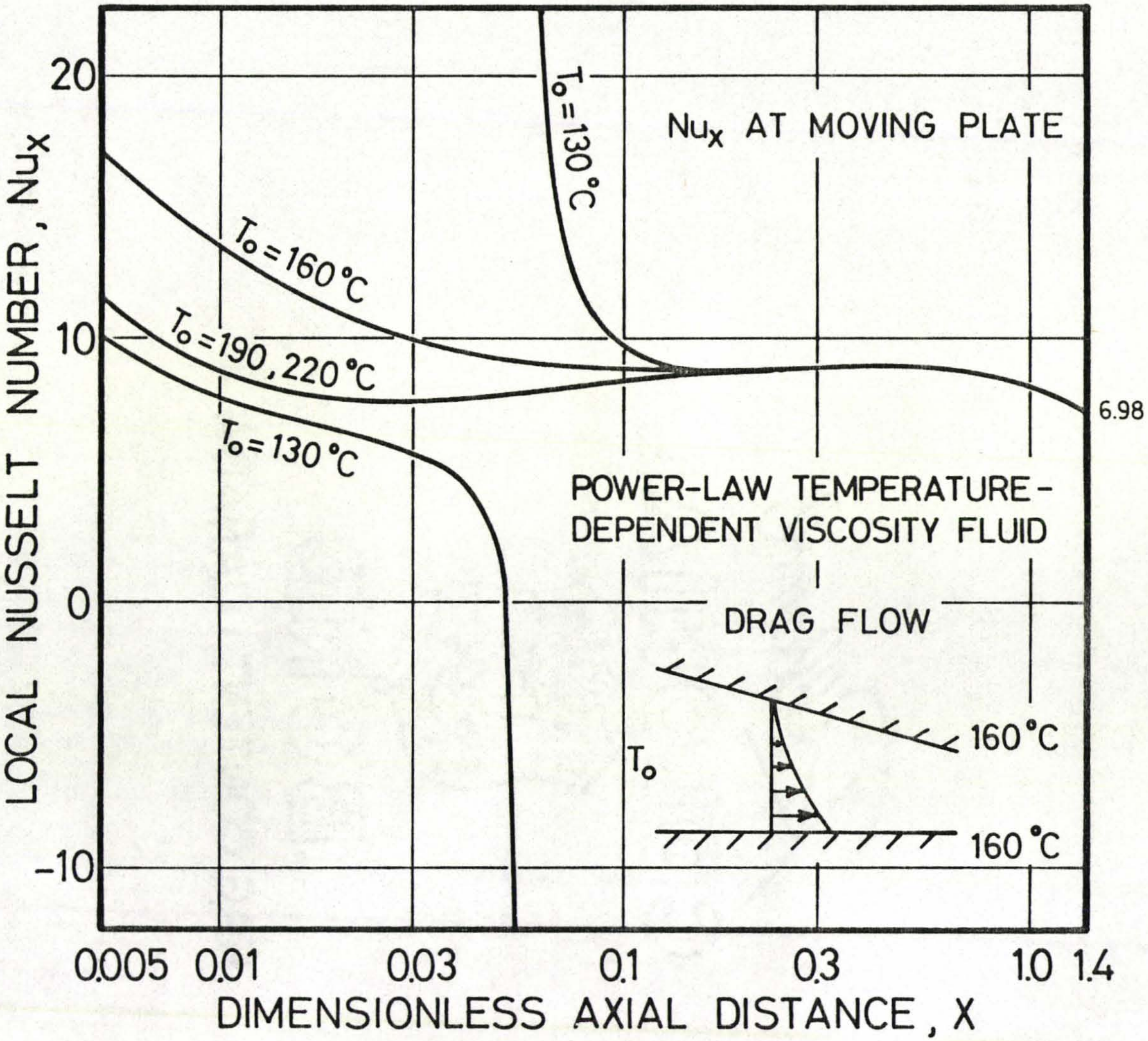

Fig. 7-11. Local Nusselt number vs. X. Drag flow between converging plates.
Channel dimensions and fluid properties given on pp. 151-152.

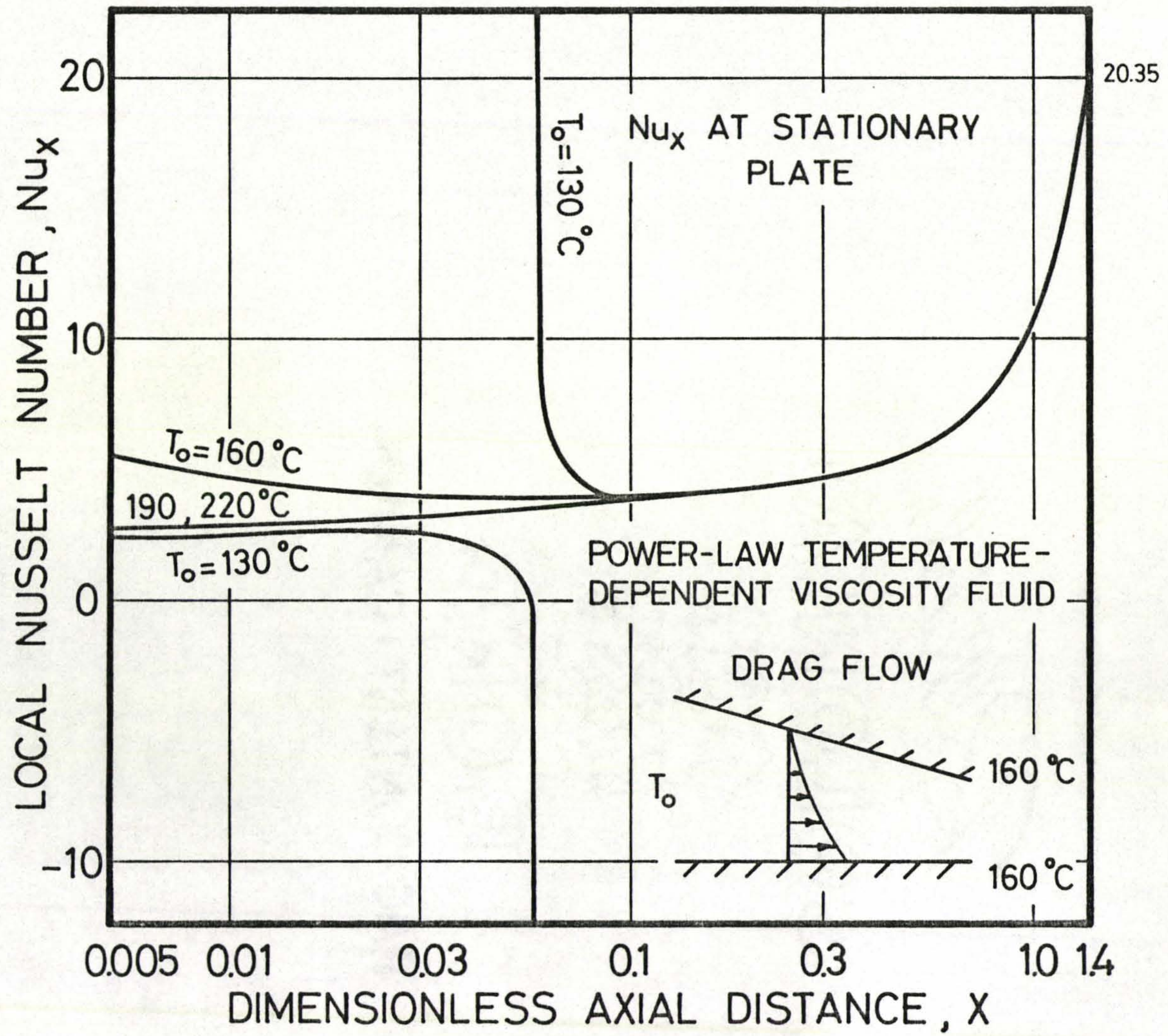

Fig. 7-12. Local Nusselt number vs. X. Drag flow between converging plates. Channel dimensions and fluid properties given in pp. 151-152.

$$Nu_x = \frac{hb_o}{k} = \frac{(\frac{dT}{dy})_{wall} \cdot b_o}{T_{bulk} - T_{wall}} \tag{7.29}$$

$X < 0.05$	$\frac{dT}{dy} < 0$	$T_b < T_w$	$Nu_x > 0$
$X \simeq 0.05$	$\frac{dT}{dy} = 0$	$T_b < T_w$	$Nu_x = 0$
$0.05 < X < 0.06$	$\frac{dT}{dy} > 0$	$T_b < T_w$	$Nu_x < 0$
$X \simeq 0.06$	$\frac{dT}{dy} > 0$	$T_b = T_w$	$Nu_x = \pm\infty$
$X > 0.06$	$\frac{dT}{dy} > 0$	$T_b > T_w$	$Nu_x > 0$

For the cases where the inlet temperature is higher than the wall temperature, the local Nusselt number is always positive.

The local Nusselt numbers for the power-law temperature-dependent and temperature-independent viscosity models are shown in Figs. 7-13, 7-14 and 7-15 for the two temperature boundary conditions discussed earlier. In all of the cases, it can be seen that there is very little difference between the local Nusselt numbers obtained by using either model. In Figs. 7-16 and 7-17, the local Nusselt numbers are shown for the power-law temperature-dependent viscosity model and several Newtonian, constant viscosity models.

The results for the power-law temperature-dependent viscosity model have been compared with the power-law temperature-independent viscosity model and the Newtonian, constant viscosity model results. Given an appropriate temperature for the temperature- independent model,

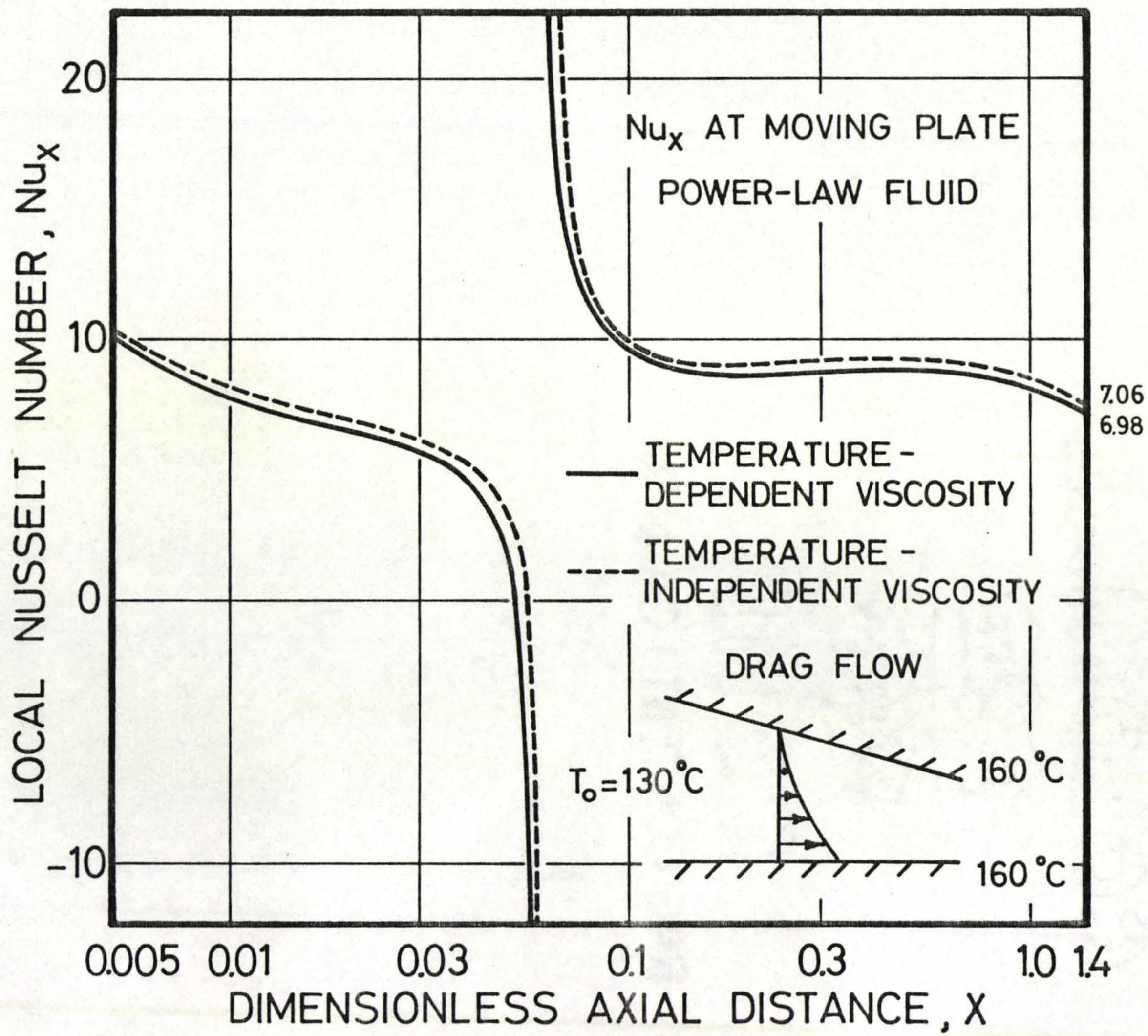

Fig. 7-13. Local Nusselt number vs. X. Drag flow between converging plates. Channel dimensions and fluid properties given on pp. 151-152.

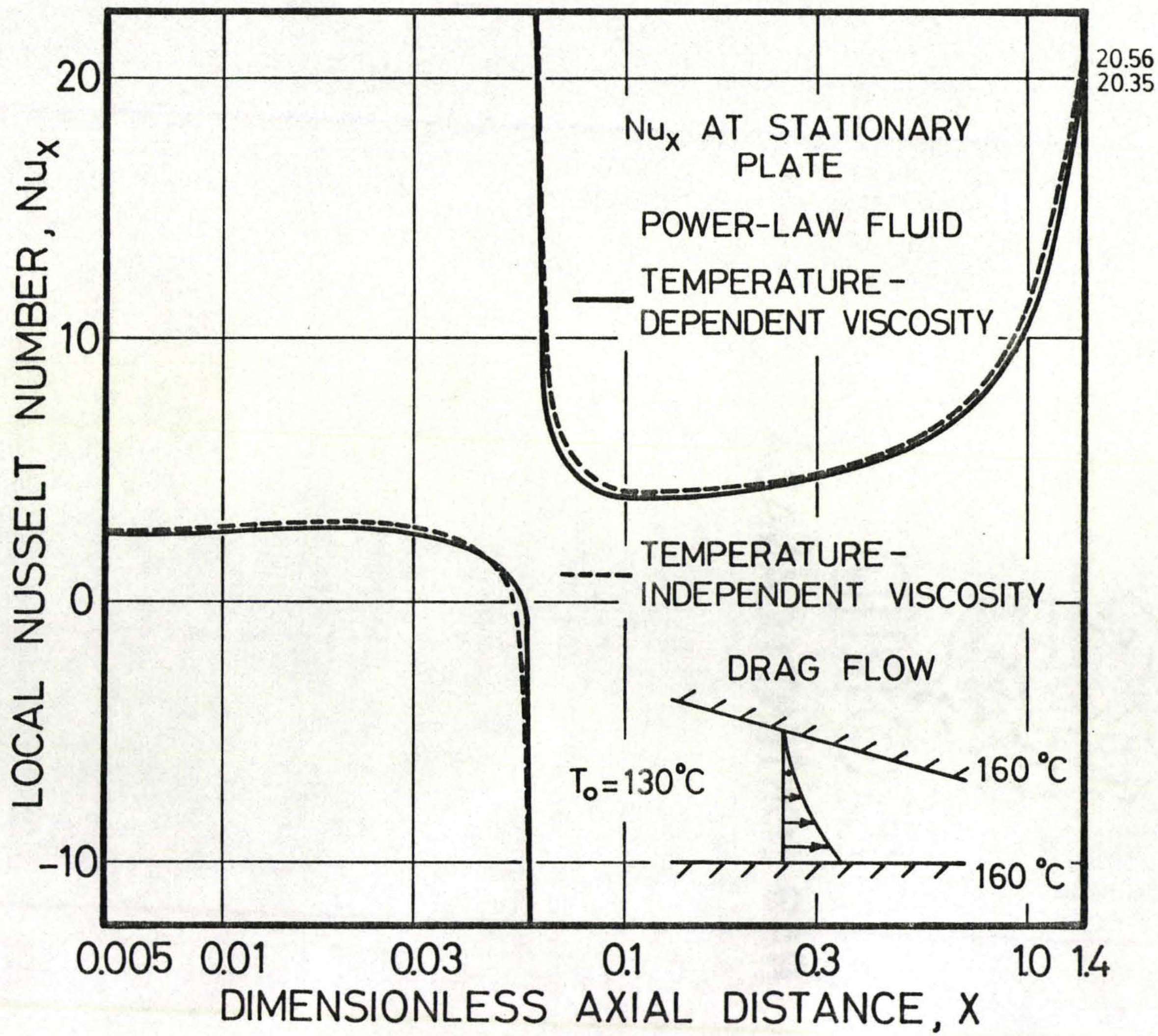

Fig. 7-14. Local Nusselt number vs. X. Drag flow between converging plates. Channel dimensions and fluid properties given on pp. 151-152.

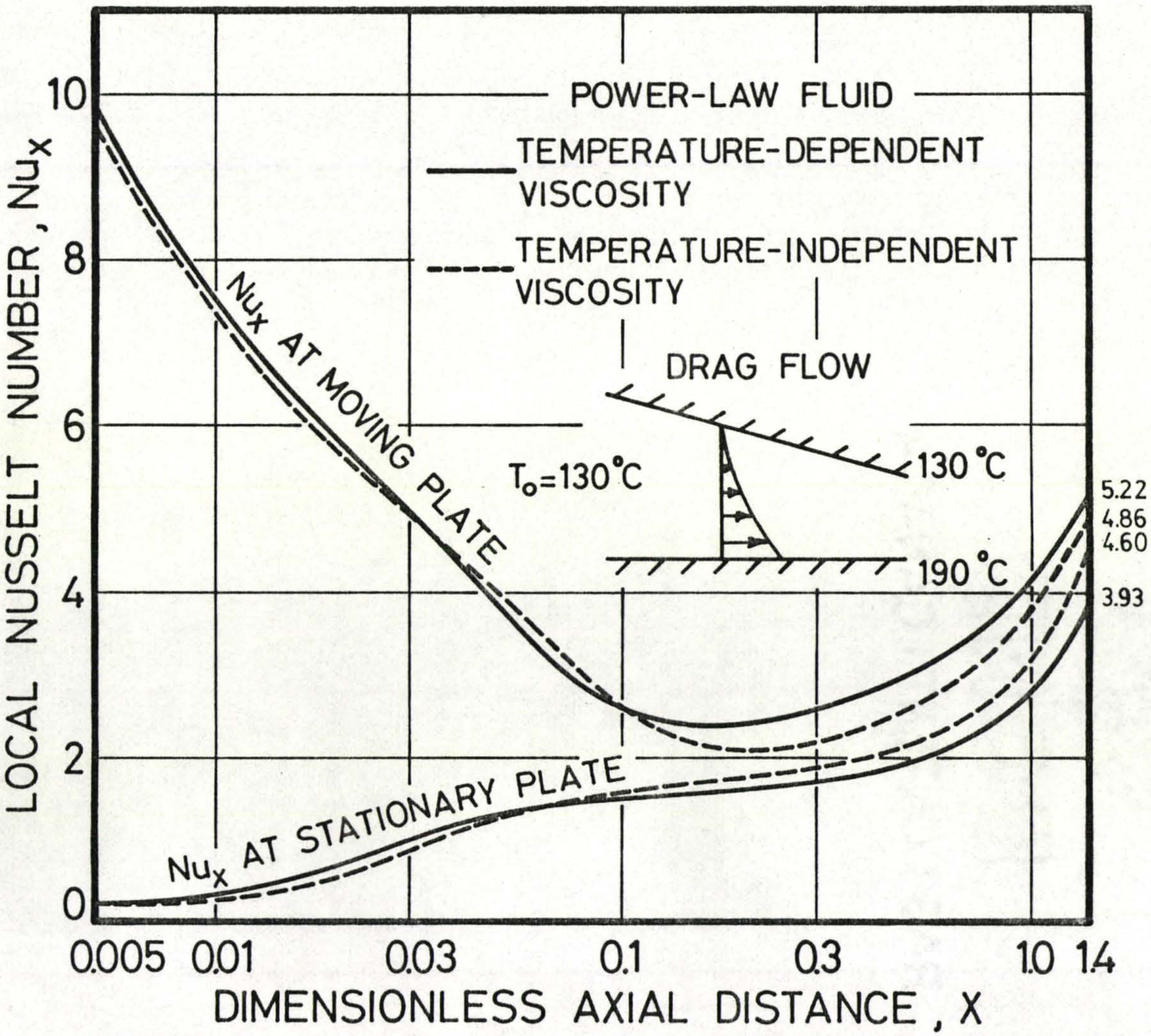

Fig. 7-15. Local Nusselt number vs. X. Drag flow between converging plates. Channel dimensions and fluid properties given on pp. 151-152.

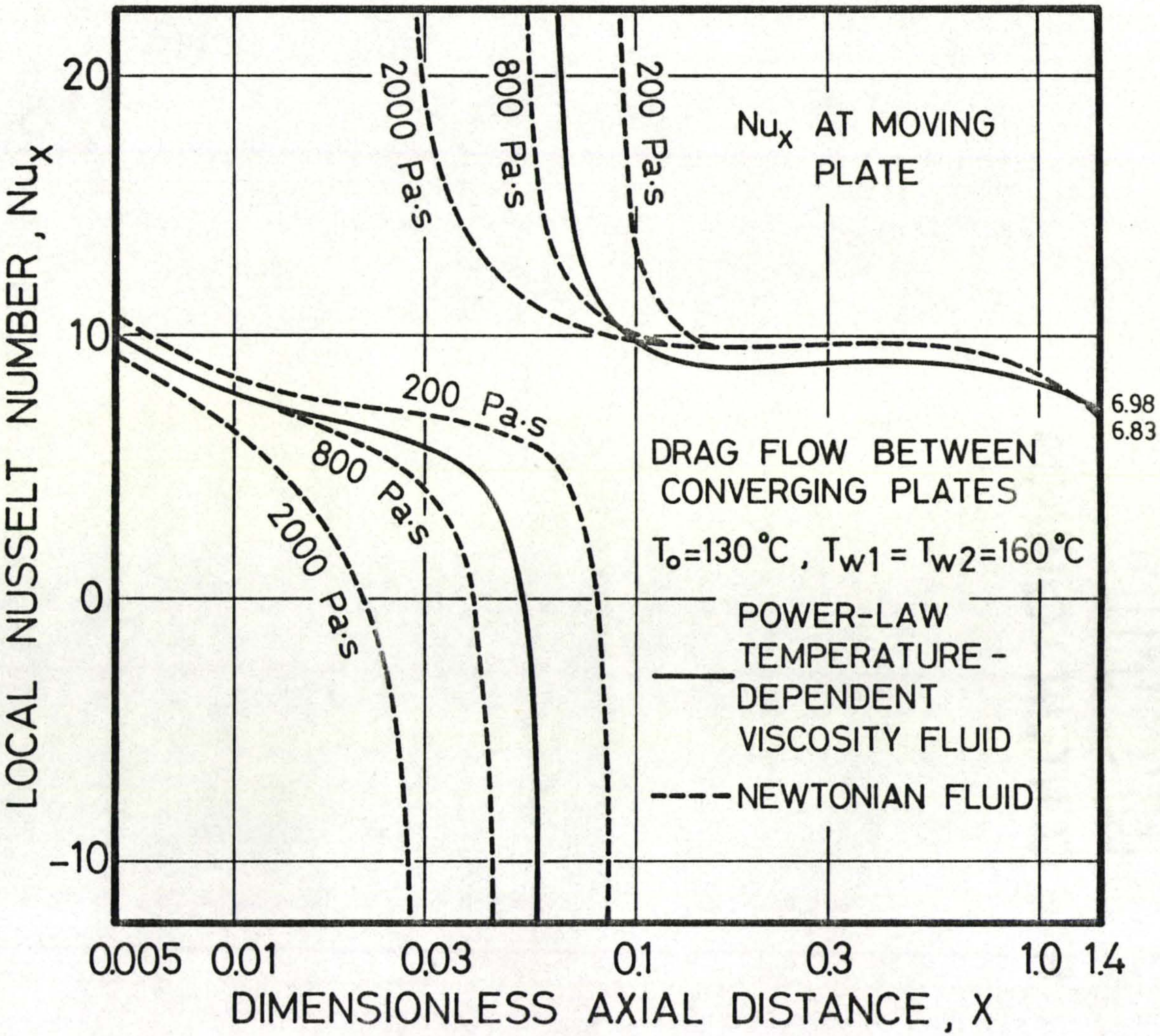

Fig. 7-16. Local Nusselt number vs. X. Drag flow between converging plates. Channel dimensions and fluid properties given on pp. 151-152.

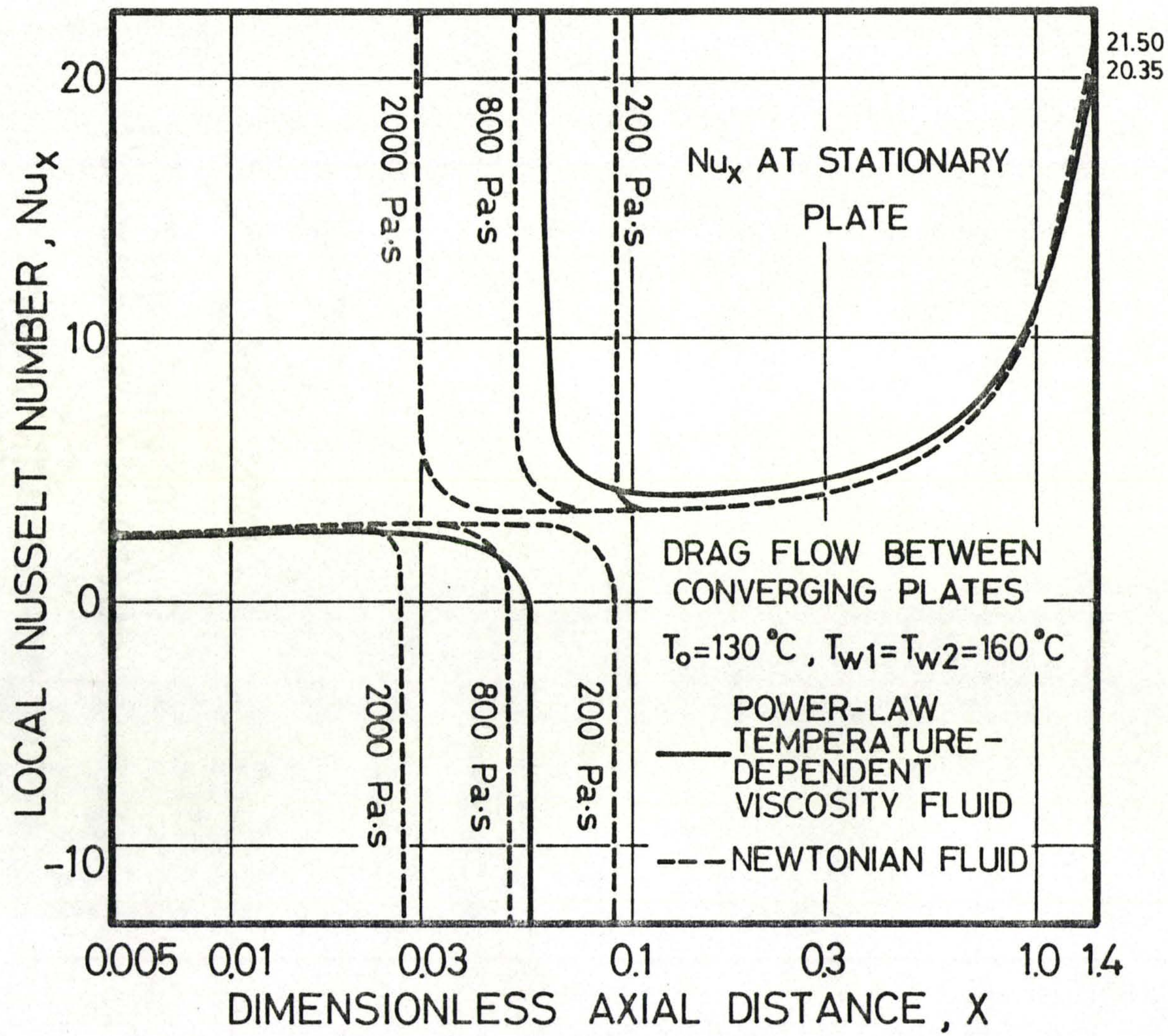

Fig. 7-17. Local Nusselt number vs. X. Drag flow between converging plates. Channel dimensions and fluid properties given on pp. 151-152.

or an appropriate viscosity for the Newtonian model, it can be seen that the temperature-dependent model results are adequately estimated by the use of either of the simpler models. The choice of temperature and viscosity was made by inspection. However, if we did not have any temperature-dependent model results to compare our more simplified model results with, then we would not have anything to base our choice of temperature or viscosity on. Furthermore, the given temperature or viscosity is usually suitable for one type of flow only. For example, in Fig. 7-9 it can be seen that the rise in bulk temperature for the temperature-dependent model is closely approximated by that of a Newtonian fluid with a viscosity of about 500 Pa·s while in drag flow between parallel plates (as described in Chap. 4), a Newtonian viscosity of 2000 Pa·s is required (see Fig. 4-7).

7.5 Concluding Remarks

1. A computer program has been developed to analyze the heat transfer problem for the drag flow of a polymer melt between converging constant temperature plates. Results have been presented for specified velocity, pressure and temperature boundary conditions, fluid properties and channel dimensions.

2. Care must be taken when choosing the proper step sizes to ensure that the local Nusselt numbers and not only the temperature profiles have converged.

3. It is very important to consider viscous dissipation in the drag flow of polymer melts between converging plates. A rise of 4°C in the bulk temperature at large X due to viscous dissipation was obtained using the specified boundary conditions, fluid properties and channel dimensions given earlier in this chapter. If a wider gap or higher plate velocity was used, the temperature rise due to viscous dissipation would be much greater.

4. The results obtained using the power-law temperature-dependent viscosity model were compared with those using the simpler power-law temperature-independent viscosity model and the Newtonian, constant viscosity model. It was seen that the results obtained using the temperature-dependent model were in most cases adequately approximated by those of the two simpler models, provided that the choice of temperature or viscosity was correct. However, if there are no temperature-dependent model results available, then we have no basis with which to choose a temperature for the temperature-independent model, or a viscosity for the Newtonian constant viscosity model.

CHAPTER 8

CONCLUSIONS AND RECOMMENDATIONS

Finite difference programs have been developed to solve the heat transfer problem for polymer melts flowing through narrow channels and tubes with constant temperature walls. Four types of flow were studied:

(i) drag flow between parallel plates,

(ii) Poiseuille flow between parallel plates,

(iii) Poiseuille flow through a tube with circular cross-section, and

(iv) drag flow between converging plates.

Results have been presented for typical velocity, pressure and temperature boundary conditions, fluid properties and channel dimensions encountered in polymer extrusion. It should be stressed that these results are not general in the sense that they are not applicable to other boundary conditions, fluid properties (in particular, viscosity) and channel dimensions. They do, however, show trends that would be expected when using a different set of conditions. To obtain results for a given type of flow and a given set of conditions, the corresponding finite difference program must be run specifically for these conditions. In all of the programs, a power-law temperature-dependent viscosity model representing a typical high-density polyethylene melt was used. It is possible, however, to use any constitutive equation in the programs.

In all of the flow cases, the results obtained using the power-law temperature-dependent viscosity model were compared with those obtained using the power-law temperature-independent viscosity model and the Newtonian, constant viscosity model. It was seen that given the proper choice of temperature or viscosity, the temperature-dependent viscosity model results could be adequately estimated by using either of the simpler models. If we had no power-law temperature-dependent viscosity model results with which to compare the results obtained using the simpler models, then we would have no basis with which to choose an appropriate temperature or viscosity. It may be possible to develop general guidelines on the choice of appropriate temperatures and viscosities when certain flow types, boundary conditions or shear rates are encountered. In any case, the best approach to solving a given flow problem is the use of a finite difference program that has been developed for temperature-dependent viscosities.

In the flow of polymer melts, it can be seen from the results presented that extremely long channel lengths are required to obtain fully-developed thermal conditions. The channels encountered in polymer processing (for example, extrusion dies) are much shorter (42, 46), and consequently the flows leaving these channels are far from being thermally fully developed. If fully-developed conditions were assumed in the channel (to simplify heat transfer calculations), serious errors would be obtained in the resulting calculations. The finite difference programs that have been developed, however, provide accurate heat transfer results for the thermally developing region of flow in the channels.

The discussion up to now has centred around the flow of polymer melts through channels with constant temperature walls. The finite difference programs can, however, be easily adapted to solve the problem of flow through channels with varying wall temperatures or with known heat flux at the walls (for example, adiabatic walls when the heat flux equals zero). Generally in polymer processing, the wall temperatures can be readily measured, and for this reason, the constant wall temperature case has been considered here.

In polymer extruders, the polymer granules are melted and then pumped through a die. As a future area of study, it is suggested that the finite difference programs be modified to take into account melting of the polymer at one of the boundaries of the flow field.

REFERENCES

1. Astarita, G. and Mashelkar, R.A.: "Heat and Mass Transfer in Non-Newtonian Fluids", Chem. Eng. (London), No. 317, 100 (1977).

2. Bassett, C.E. and Welty, J.R.: "Non-Newtonian Heat Transfer in the Thermal Entrance Region of Uniformly Heated, Horizontal Pipes", AIChE J., 21, 699 (1975).

3. Bergen, J.T. (E.C. Bernhardt, ed.): Processing of Thermoplastic Materials, p. 405. Van Nostrand Reinhold (1959).

4. Bird, R.B.: "Viscous Heat Effects in Extrusion of Molten Plastics", Soc. Plast. Eng. J., 11, 35 (1955).

5. Bird, R.B.: "Zur Theorie des Wärmeübergangs an nicht-Newtonsche Flüssigkeiten bei laminarer Rohrströmung", Chem.-Ing.-Tech., 31, 569 (1959).

6. Bird, R.B., Stewart, W.E. and Lightfoot, E.N.: Transport Phenomena, J. Wiley (1960).

7. Brinkman, H.C.: "Heat Effects in Capillary Flow I", Appl. Sci. Res., A2, 120 (1951).

8. Christiansen, E.B. and Craig, S.E. Jr.: "Heat Transfer to Pseudoplastic Fluids in Laminar Flow", AIChE J., 8, 154 (1962).

9. Christiansen, E.B., Jensen, G.E. and Tao, F-S.: "Laminar Flow Heat Transfer", AIChE J., 12, 1196 (1966).

10. Churchill, S.W.: "Choosing between Theory and Experiment", Chem. Eng. Prog., 66, No. 7, 86 (1970).

11. Cox, H.W. and Macosko, C.W.: "Viscous Dissipation in Die Flows", AIChE J., 20, 785 (1974).

12. Eckert, E.R.G. and Drake, R.M. Jr.: Analysis of Heat and Mass Transfer. McGraw-Hill (1972).

13. Faghri, M. and Welty, J.R.: "Analysis of Heat Transfer for Laminar Power-Law Pseudoplastic Fluids in a Tube with an Arbitrary Circumferential Wall Heat Flux", AIChE J., 23, 288 (1977).

14. Fenner, R.T.: "Developments in the Analysis of Steady Screw Extrusion of Polymers", Polymer, 18, 617 (1977).

15. Foraboschi, F.P. and Di Federico, I.: "Heat Transfer in Laminar Flow of Non-Newtonian Heat-Generating Fluids", Int. J. Heat Mass Transfer, 7, 315 (1964).

16. Forrest, G. and Wilkinson, W.L.: "Laminar Heat Transfer to Power Law Fluids in Tubes with Constant Wall Temperature", Trans. Inst. Chem. Eng., 51, 331 (1973).

17. Forsyth, T.H. and Murphy, N.F.: "Temperature Profiles of Molten Flowing Polymers in a Heat Exchanger", AIChE J., 15, 758 (1969).

18. Galili, N., Rigbi, Z. and Takserman-Krozer, R.: "Heat and Pressure Effects in Viscous Flow through a Pipe. Part II. Analytical Solution for Non-Newtonian Flow", Rheol. Acta, 14, 816 (1975).

19. Gavis, J. and Laurence, R.L.: "Viscous Heating of a Power-Law Liquid in Plane Flow", Ind. Eng. Chem. Fundam., 7, 525 (1968).

20. Gee, R.E. and Lyon, J.B.: "Non-isothermal Flow of Viscous Non-Newtonian Fluids", Ind. Eng. Chem., 49, 956 (1957).

21. Gerald, C.F.: Applied Numerical Analysis. Addison-Wesley (1970).

22. Gill, W.N.: "Heat Transfer in Laminar Power-Law Flows with Energy Sources", AIChE J., 8, 137 (1962).

23. Gill, W.N.: "The Thermal Entrance Region in Laminar Power-Law Flows", Appl. Sci. Res., A11, 10 (1963).

24. Graetz, L.: "Über die Warmeleitungs fahigkeit von Flussigkeiten", Ann. Phys., 25, 337 (1885).

25. Griskey, R.G. and Wiehe, I.A.: "Heat Transfer to Molten Flowing Polymers", AIChE J., 12, 308 (1966).

26. Griskey, R.G., Choi, M.H. and Siskovic, N.: "Heat Transfer to Flowing Thermally Softened Polymers", Polym. Eng. Sci., 13, 287 (1973).

27. Huebner, K.H.: "Application of Finite Element Methods to Thermohydrodynamic Lubrication", Int. J. Numerical Methods Eng., 8, 139 (1974).

28. Kim, H.T. and Collins, E.A.: "Temperature Profiles for Polymer Melts in Tube Flow. Part II. Conduction and Shear Heating Corrections", Polym. Eng. Sci., 11, 83 (1971).

29. Koyama, K., Kanamaru, K. and Wada, E.: "Temperature Distribution in Laminar Flow through a Circular Tube", Int. Chem. Eng., 12, 541 (1972).

30. Lapidus, L.: Digital Computation for Chemical Engineers. McGraw-Hill (1962).

31. Larocque, J.: Pseudoplastic Entry Flow in Straight and Convergent Channels. M.Eng. Thesis, McMaster University, (1973).

32. Lévêque, J., Ann. Mines, 13, 201 (1928).

33. Lyche, B.C. and Bird, R.B.: "The Graetz-Nusselt Problem for a Power-Law Non-Newtonian Fluid", Chem. Eng. Sci., 6, 35 (1956).

34. Mahalingam, R., Tilton, L.O. and Coulson, J.M.: "Heat Transfer in Laminar Flow of Non-Newtonian Fluids", Chem. Eng. Sci., 30, 921 (1975).

35. Mahalingam, R., Chan, S.F. and Coulson, J.M.: "Laminar Pseudoplastic Flow Heat Transfer with Prescribed Wall Heat Flux", Chem. Eng. J., 9, 161 (1975).

36. Martin, B.: "Some Analytical Solutions for Viscometric Flows of Power-Law Fluids with Heat Generation and Temperature Dependent Viscosity", Int. J. Non-Linear Mechanics, 2, 285 (1967).

37. Matsuhisa, S. and Bird, R.B.: "Analytical and Numerical Solutions for Laminar Flow of the Non-Newtonian Ellis Fluid", AIChE J., 11, 588 (1965).

38. McKillop, A.A.: "Heat Transfer for Laminar Flow of Non-Newtonian Fluids in Entrance Region of a Tube", Int. J. Heat Mass Transfer, 7, 853 (1964).

39. Metzner, A.B., Vaughn, R.D. and Houghton, G.L.: "Heat Transfer to Non-Newtonian Fluids", AIChE J., 3, 92 (1957).

40. Metzner, A.B. and Gluck, D.F.: "Heat Transfer to Non-Newtonian Fluids under Laminar-Flow Conditions", Chem. Eng. Sci., 12, 185 (1960).

41. Metzner, A.B.: "Heat Transfer in Non-Newtonian Fluids", Adv. Heat Transfer, 2, 357 (1965).

42. Michaeli, W. and Menges, G.: "Effects on Flow in Sheet Dies", Soc. Plast. Eng. 34th ANTEC, 22, 186, Atlantic City, N.J. (April 1976).

43. Middleman, S.: Fundamentals of Polymer Processing. McGraw-Hill (1977).

44. Mitsuishi, N. and Miyatake, O.: "Heat Transfer with Non-Newtonian Laminar Flow in a Tube Having a Constant Wall Heat Flux", Int. Chem. Eng., 9, 352 (1969).

45. Morrette, R.A. and Gogos, C.G.: "Viscous Dissipation in Capillary Flow of Rigid PVC and PVC Degradation", Polym. Eng. Sci., 8, 272 (1968).

46. Nunn, R.E. and Fenner, R.T.: "Flow and Heat Transfer in the Nozzle of an Injection Molding Machine", Polym. Eng. Sci., 17, 811 (1977).

47. Nusselt, W.: Z. Ver. Dtsch. Ing., 54, 1154 (1910).

48. Oliver, D.R. and Jenson, V.G.: "Heat Transfer to Pseudoplastic Fluids in Laminar Flow in Horizontal Tubes", Chem. Eng. Sci., 19, 115 (1964).

49. Payvar, P.: "Asymptotic Nusselt Numbers for Dissipative Non-Newtonian Flow through Ducts", Appl. Sci. Res., 27, 297 (1973).

50. Pearson, J.R.A.: "Heat-Transfer Effects in Flowing Polymers", Prog. Heat Mass Transfer, 5, 73 (1972).

51. Pearson, J.R.A.: "Variable-Viscosity Flows in Channels with High Heat Generation", J. Fluid Mech., 83, 191 (1977).

52. Pigford, R.L.: "Non-isothermal Flow and Heat Transfer Inside Vertical Tubes", Chem. Eng. Prog. Symp. Ser., 51, No. 17, 79 (1955).

53. Popovska, F. and Wilkinson, W.L.: "Laminar Heat Transfer to Newtonian and Non-Newtonian Fluids in Tubes", Chem. Eng. Sci., 32, 1155 (1977).

54. Porter, J.E.: "Heat Transfer at Low Reynolds Number (Highly Viscous Liquids in Laminar Flow)", Trans. Inst. Chem. Eng., 49, 1 (1971).

55. Prins, J.A., Mulder, J. and Schenk, J.: "Heat Transfer in Laminar Flow between Parallel Plates", Appl. Sci. Res., A2, 431 (1951).

56. Saltuk, I., Siskovic, N. and Griskey, R.G.: "Energy Transport to Molten Flowing Polymer Systems. Part I. Analysis of Data and Development of Temperature Profiles with Axial Length", Polym. Eng. Sci., 12, 402 (1972).

57. Schenk, J. and Van Laar, J.: "Heat Transfer in Non-Newtonian Laminar Flow in Tubes", Appl. Sci. Res., A7, 449 (1958).

58. Schlichting, H. (J. Kestin, trans.): Boundary Layer Theory (6th ed.). McGraw-Hill (1968).

59. Šesták, J. and Charles, M.E.: "Limiting Values of the Nusselt Number for Heat Transfer to the Pipeline Flow of Non-Newtonian Fluids with Arbitrary Internal Heat Generation", Chem. Eng. Prog. Symp. Ser., 64, No. 82, 212 (1968).

60. Smorodinskii, E.L. and Froishteter, G.B." "Analytical Solution of the Problem of the Laminar Heat Transfer of Non-linearly Viscoplastic Fluids Taking Account of the Dissipation of Kinetic Energy", Teor. Osn. Khim. Tekhnol., 5, 542 (1971).

61. Suckow, W.H., Hrycak, P. and Griskey, R.G.: "Heat Transfer to Polymer Solutions and Melts Flowing between Parallel Plates", Polym. Eng. Sci., 11, 401 (1971).

62. Sukanek, P.C.: "Poiseuille Flow of a Power-Law Fluid with Viscous Heating", Chem. Eng. Sci., 26, 1775 (1971).

63. Sundaram, K.M. and Nath, G.: "Heat Transfer to Power-Law Fluids in Thermal Entrance Region with Viscous Dissipation for Constant Heat Flux Conditions", Proc. Indian Acad. Sci., 83A, 50 (1976).

64. Tadmor, Z. and Klein, I.: Engineering Principles of Plasticating Extrusion. Van Nostrand Reinhold (1970).

65. Tien, C.: "The Extension of Couette Flow Solution to Non-Newtonian Fluid", Can. J. Chem. Eng., 39, 45 (1961).

66. Tien, C.: "Laminar Heat Transfer of Power-Law Non-Newtonian Fluid - The Extension of Graetz-Nusselt Problem", Can. J. Chem. Eng., 40, 130 (1962).

67. Toor, H.L.: "Heat Generation and Conduction in the Flow of a Viscous Compressible Liquid", Trans. Soc. Rheol., 1, 177 (1957).

68. Toor, H.L.: "Heat Transfer in Forced Convection with Internal Heat Generation", AIChE J., 4, 319 (1958).

69. Turian, R.M.: "Viscous Heating in the Cone-and-Plate Viscometer. Part III. Non-Newtonian Fluids with Temperature-Dependent Viscosity and Thermal Conductivity", Chem. Eng. Sci., 20, 771 (1965).

70. Vlachopoulos, J. and Keung, C.K.J.: "Heat Transfer to a Power-Law Fluid Flowing between Parallel Plates", AIChE J., 18, 1272 (1972).

71. Vlachopoulos, J., Larocque, J. and Ho, J.S-J.: "Numerical Studies of Non-Newtonian Fluid Flow and Heat Transfer", Symposium-Heat Transfer in Polymer Processing, Paper 5. University of Bradford (1974).

72. Whiteman, I.R. and Drake, W.B.: "Heat Transfer to Flow in a Round Tube with Arbitrary Velocity Distribution", Trans. ASME, 80, 728 (1958).

73. Winter, H.H.: "Wärmedissipation in Polymerschmelzen bei ebener Schleppströmung, thermischer Anfahrvorgang und Gleichgewichtszustand", Rheol. Acta., 11, 216 (1972).

74. Winter, H.H.: "Temperature Fields in Extruder Dies with Circular, Annular, or Slit Cross-Section", Polym. Eng. Sci., 15, 84 (1975).

75. Winter, H.H.: "Viscous Dissipation in Shear Flows of Molten Polymers", Adv. Heat Transfer, 13, 205 (1977).

APPENDIX A

DERIVATION OF FINITE DIFFERENCE EQUATIONS

The finite difference equations used in Chaps. 4, 5, 6 and 7 are derived in detail in this appendix.

A.1 Drag Flow Between Parallel Plates

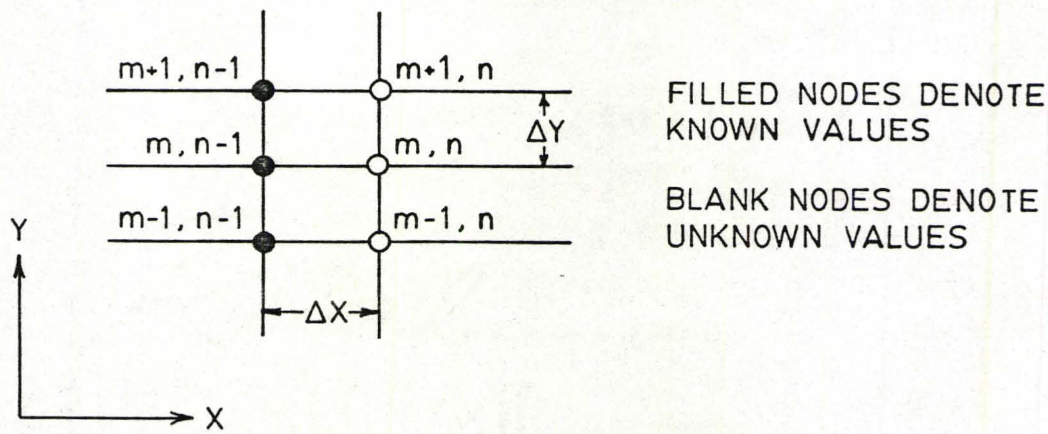

Fig. A-1. Finite difference grid. Drag flow between parallel plates.

Momentum Equation

$$\eta \frac{d^2U}{dY^2} + \frac{d\eta}{dY}\frac{dU}{dY} = 0 \tag{A.1}$$

Let $$\frac{dU}{dY} = \frac{U^n_{m+1} - U^n_{m-1}}{2\Delta Y} \qquad \text{(A.2)}$$

$$\frac{d^2U}{dY^2} = \frac{U^n_{m-1} - 2U^n_m - U^n_{m+1}}{(\Delta Y)^2} \qquad \text{(A.3)}$$

Substitute Eqs. (A.2) and (A.3) into Eq. (A.1):

$$\eta^n_m \left[\frac{U^n_{m-1} - 2U^n_m + U^n_{m+1}}{(\Delta Y)^2}\right] + \left(\frac{d\eta}{dY}\right)^n_m \frac{U^n_{m+1} - U^n_{m-1}}{2\Delta Y} = 0 \qquad \text{(A.4)}$$

Rearranging, we obtain:

$$U^n_{m-1} - 2U^n_m + U^n_{m+1} + \frac{\Delta Y}{2\eta^n_m} \left(\frac{d\eta}{dY}\right)^n_m [U^n_{m+1} - U^n_{m-1}] = 0 \qquad \text{(A.5)}$$

Let $$\alpha^n_m = \frac{\Delta Y}{2\eta^n_m} \left(\frac{d\eta}{dY}\right)^n_m$$

Thus, Eq. (A.5) becomes:

$$(-\alpha^n_m + 1)\, U^n_{m-1} - 2U^n_m + (\alpha^n_m + 1)\, U^n_{m+1} = 0 \qquad \text{(A.6)}$$

Energy Equation

$$U \frac{\partial\theta}{\partial X} = \frac{\partial^2\theta}{\partial Y^2} + \beta \left(\frac{dU}{dY}\right)^2 \qquad \text{(A.7)}$$

where $$\beta = \frac{\eta\, u^2_{max}}{k(T_o - T_{w1})}$$

Let $$\frac{\partial\theta}{\partial X} = \frac{\theta^n_m - \theta^{n-1}_m}{\Delta X} \qquad \text{(A.8)}$$

$$\frac{\partial^2\theta}{\partial Y^2} = \left[\frac{\theta^n_{m-1} - 2\theta^n_m + \theta^n_{m+1}}{2(\Delta Y)^2}\right] + \left[\frac{\theta^n_{m-1} - 2\theta^{n-1}_m + \theta^{n-1}_{m+1}}{2(\Delta Y)^2}\right] \tag{A.9}$$

Substitute Eqs. (A.8) and (A.9) into Eqs. (A.7):

$$U^n_m\left[\frac{\theta^n_m - \theta^{n-1}_m}{\Delta X}\right] = \left[\frac{\theta^n_{m-1} - 2\theta^n_m + \theta^n_{m+1}}{2(\Delta Y)^2}\right] + \left[\frac{\theta^{n-1}_{m-1} - 2\theta^{n-1}_m + \theta^{n-1}_{m+1}}{2(\Delta Y)^2}\right] + \beta^n_m\left(\frac{dU}{dY}\right)^2 \tag{A.10}$$

Rearranging, we obtain:

$$\frac{2(\Delta Y)^2}{\Delta X}\cdot U^n_m\,[\theta^n_m - \theta^{n-1}_m] = \theta^n_{m-1} - 2\theta^n_m + \theta^n_{m+1} + \theta^{n-1}_{m-1} + \theta^{n-1}_m + \theta^{n-1}_{m+1} + 2(\Delta Y)^2\,\beta^n_m\left(\frac{dU}{dY}\right)^2 \tag{A.11}$$

Let $\alpha^n_m = \frac{2(\Delta Y)^2}{\Delta X}\ U^n_m$

Thus, Eqs. (A.12) becomes:

$$-\theta^n_{m-1} + (\alpha^n_m + 2)\ \theta^n_m - \theta^n_{m+1} = \theta^{n-1}_{m-1} + (\alpha^n_m - 2)\ \theta^{n-1}_m + \theta^{n-1}_{m+1} + 2(\Delta Y)^2\,\beta^n_m\left(\frac{dU}{dY}\right)^2 \tag{A.12}$$

A.2 Poiseuille Flow Between Parallel Plates

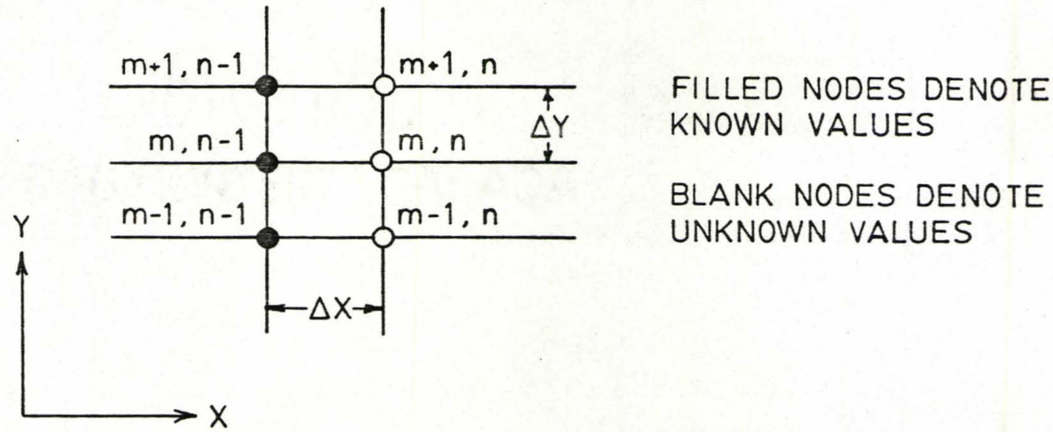

Fig. A-2. Finite difference grid. Poiseuille flow between parallel plates.

Momentum Equation

$$\frac{-k}{C_p}\frac{dP}{dX} + \eta\frac{d^2U}{dY^2} + \frac{d\eta}{dY}\frac{dU}{dY} = 0 \tag{A.13}$$

Let

$$\frac{dP}{dX} = \frac{P^n - P^{n-1}}{\Delta X} \tag{A.14}$$

$$\frac{dU}{dY} = \frac{U^n_{m+1} - U^n_{m-1}}{2\Delta Y} \tag{A.15}$$

$$\frac{d^2U}{dY^2} = \frac{U^n_{m-1} - 2U^n_m + U^n_{m+1}}{(\Delta Y)^2} \tag{A.16}$$

Substitute Eqs. (A.14), (A.15) and (A.16) into Eq. (A.13):

$$\frac{-k}{C_p}\left[\frac{P^n - P^{n-1}}{\Delta X}\right] + \eta_m^n \left[\frac{U_{m-1}^n - 2U_m^n + U_{m+1}^n}{(\Delta Y)^2}\right] + (\frac{d\eta}{dY})_m^n$$

$$\cdot \left[\frac{U_{m+1}^n - U_{m-1}^n}{2\Delta Y}\right] = 0 \qquad (A.17)$$

Rearranging, we obtain:

$$\frac{-k}{\eta_m^n\ C_p}\frac{(\Delta Y)^2}{\Delta X}[P^n - P^{n-1}] + U_{m-1}^n - 2U_m^n + U_{m+1}^n + \frac{\Delta Y}{2\eta_m^n}(\frac{d\eta}{dY})_m^n$$

$$\cdot [U_{m+1}^n - U_{m-1}^n] = 0 \qquad (A.18)$$

Let $\alpha_m^n = \frac{\Delta Y}{2\eta_m^n}(\frac{d\eta}{dY})_m^n$

$\beta_m^n = \frac{k}{\eta_m^n\ C_p}\frac{(\Delta Y)^2}{\Delta X}$

Thus, Eq. (A.18) becomes:

$$(-\alpha_m^n + 1)\ U_{m-1}^n - 2U_m^n + (\alpha_m^n + 1)\ U_{m+1}^n - \beta_m^n\ P^n + \beta_m^n\ P^{n-1} = 0 \qquad (A.19)$$

<u>Energy Equation</u>

$$U\frac{\partial\theta}{\partial X} = \frac{\partial^2\theta}{\partial Y^2} + \beta(\frac{dU}{dY})^2 \qquad (A.20)$$

where $\beta = \frac{\eta\ u_{avg}^2}{k(T_o - T_{w1})}$

Let $$\frac{\partial\theta}{\partial X} = \frac{\theta_m^n - \theta_{m-1}^n}{\Delta X} \tag{A.21}$$

$$\frac{\partial^2\theta}{\partial Y^2} = \frac{\theta_{m-1}^n - 2\theta_m^n + \theta_{m+1}^n}{2(\Delta Y)^2} + \frac{\theta_{m-1}^{n-1} - 2\theta_m^{n-1} + \theta_{m+1}^{n-1}}{2(\Delta Y)^2} \tag{A.22}$$

Substitute Eqs. (A.21) and (A.22) into Eq. (A.20):

$$U_m^n \left[\frac{\theta_m^n - \theta_m^{n-1}}{\Delta X}\right] = \frac{\theta_{m-1}^n - 2\theta_m^n + \theta_{m+1}^n}{2(\Delta Y)^2} + \frac{\theta_{m-1}^{n-1} - 2\theta_m^{n-1} + \theta_{m+1}^{n-1}}{2(\Delta Y)^2}$$

$$+ \beta_m^n \left(\frac{dU}{dY}\right)^2 \tag{A.23}$$

Rearranging, we obtain:

$$\frac{2(\Delta Y)^2}{\Delta X} \cdot U_m^n \left[\theta_m^n - \theta_m^{n-1}\right] = \theta_{m-1}^n - 2\theta_m^n + \theta_{m+1}^n + \theta_{m-1}^{n-1} - 2\theta_m^{n-1}$$

$$+ \theta_{m+1}^{n-1} + 2(\Delta Y)^2 \beta_m^n \left(\frac{dU}{dY}\right)^2 \tag{A.24}$$

Let $$\alpha_m^n = \frac{2(\Delta Y)^2}{\Delta X} U_m^n$$

Thus, Eq. (A.24) becomes:

$$-\theta_{m-1}^n + (\alpha_m^n + 2)\,\theta_m^n - \theta_{m+1}^n = \theta_{m-1}^{n-1} + (\alpha_m^n - 2)\,\theta_m^{n-1} + \theta_{m+1}^{n-1}$$

$$+ 2(\Delta Y)^2 \beta_m^n \left(\frac{dU}{dY}\right)^2 \tag{A.25}$$

A.3 Poiseuille Flow Through a Tube with Circular Cross-Section

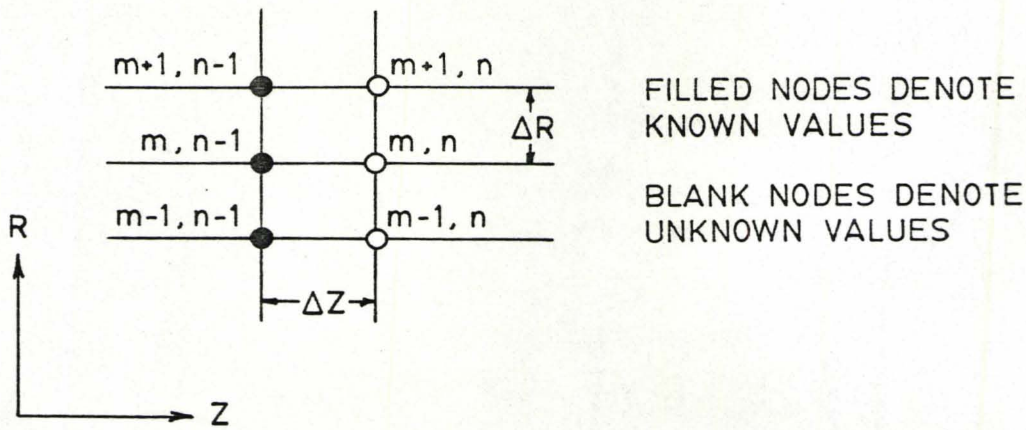

Fig. A-3. Finite difference grid. Poiseuille flow through a tube with circular cross-section.

Momentum Equation

For $R = 0$,

$$\frac{-k}{C_p}\,\frac{dP}{dz} + 2\eta\,\frac{d^2U}{dR^2} + \overset{\text{o by symmetry}}{\cancel{\frac{d\eta}{dR}\,\frac{dU}{dR}}} = 0 \tag{A.26a}$$

For $R > 0$,

$$\frac{-k}{C_p}\,\frac{dP}{dZ} + \eta\,\frac{d^2U}{dR^2} + \left[\frac{\eta}{R} + \frac{d\eta}{dR}\right]\frac{dU}{dR} = 0 \tag{A.26b}$$

Let

$$\frac{dP}{dZ} = \frac{P^n - P^{n-1}}{\Delta Z} \tag{A.27}$$

$$\frac{dU}{dR} = \frac{U^n_{m+1} - U^n_{m-1}}{2\Delta R} \tag{A.28}$$

$$\frac{d^2U}{dR^2} = \frac{U_{m-1}^n - 2U_m^n + U_{m+1}^n}{(\Delta R)^2} \tag{A.29}$$

Substitute Eqs. (A.27), (A.28) and (A.29) into Eqs. (A.26a) and (A.26b):

For R = 0,

$$\frac{-k}{C_p}\left[\frac{P^n - P^{n-1}}{\Delta Z}\right] + 2\,\eta_1^n\left[\frac{U_o^n - 2U_1^n + U_2^n}{(\Delta R)^2}\right] = 0 \tag{A.30a}$$

For R > 0,

$$\frac{-k}{C_p}\left[\frac{P^n - P^{n-1}}{\Delta Z}\right] + \eta_m^n\left[\frac{U_{m-1}^n - 2U_m^n + U_{m+1}^n}{(\Delta R)^2}\right] + \left[\frac{\eta}{R} + \frac{d\eta}{dR}\right]_m^n \cdot \left[\frac{U_{m+1}^n - U_{m-1}^n}{2\Delta R}\right] = 0 \tag{A.30b}$$

Rearranging, we obtain:

For R = 0,

$$\frac{-k}{2\,\eta_1^n\,C_p}\,\frac{(\Delta R)^2}{\Delta Z}\,[P^n - P^{n-1}] + \overbrace{U_o^n}^{U_2^n \text{ by symmetry}} - 2U_1^n + U_2^n = 0 \tag{A.31a}$$

For R > 0,

$$\frac{-k}{\eta_m^n\,C_p}\,\frac{(\Delta R)^2}{\Delta Z}\,[P^n - P^{n-1}] + U_{m-1}^n - 2U_m^n + U_{m+1}^n + \frac{\Delta R}{2\eta_m^n} \cdot \left[\frac{\eta}{R} + \frac{d\eta}{dR}\right]_m^n\,[U_{m+1}^n - U_{m-1}^n] = 0 \tag{A.31b}$$

Let

$$\alpha_m^n = \frac{\Delta R}{2\eta_m^n}\left[\frac{\eta}{R} + \frac{d\eta}{dR}\right]_m^n$$

$$\beta_m^n = \frac{-k}{\eta_m^n\,C_p}\,\frac{(\Delta R)^2}{\Delta Z}$$

Thus, Eqs. (A.31a) and (A.31b) become:

For R = 0, $$-2U_1 + 2U_2^n - \beta_1^n P^n + \beta_1^n P^{n-1} = 0 \qquad \text{(A.32a)}$$

For R > 0, $$(-\alpha_m^n + 1)\, U_{m-1}^n - 2U_m^n + (\alpha_m^n + 1)\, U_{m+1}^n - \beta_m^n P^n + \beta_m^n P^{n-1} = 0 \qquad \text{(A.32b)}$$

A.3.2 Energy Equation

o by symmetry

For R = 0, $$U \frac{\partial\theta}{\partial Z} = 2 \frac{\partial^2\theta}{\partial R^2} + \gamma \left(\frac{dU}{dR}\right)^2 \qquad \text{(A.33a)}$$

For R > 0, $$U \frac{\partial\theta}{\partial Z} = \frac{\partial^2\theta}{\partial R^2} + \frac{1}{R}\frac{\partial\theta}{\partial R} + \gamma \left(\frac{dU}{dR}\right)^2 \qquad \text{(A.33b)}$$

where $$\gamma = \frac{\eta\, u_{avg}^2}{k(T_o - T_w)}$$

Let $$\frac{\partial\theta}{\partial z} = \frac{\theta_m^n - \theta_m^{n-1}}{\Delta Z} \qquad \text{(A.34)}$$

$$\frac{\partial\theta}{\partial R} = \frac{\theta_{m+1}^n - \theta_{m-1}^n}{4\Delta R} + \frac{\theta_{m+1}^{n-1} - \theta_{m-1}^{n-1}}{4\Delta R} \qquad \text{(A.35)}$$

$$\frac{\partial^2\theta}{\partial R^2} = \frac{\theta_{m-1}^n - 2\theta_m^n + \theta_{m+1}^n}{2(\Delta R)^2} + \frac{\theta_{m-1}^{n-1} - 2\theta_m^{n-1} + \theta_{m+1}^{n-1}}{2(\Delta R)^2} \qquad \text{(A.36)}$$

Substitute Eqs. (A.34), (A.35) and (A.36) into Eqs. (A.33a) and (A.33b):

$$\text{For } R = 0, \quad U_1^n \left[\frac{\theta_1^n - \theta_1^{n-1}}{\Delta Z} \right] = \frac{\theta_o^n - 2\theta_1^n + \theta_2^n}{(\Delta R)^2} + \frac{\theta_o^{n-1} - 2\theta_1^{n-1} + \theta_2^{n-1}}{(\Delta R)^2} \qquad \text{(A.37a)}$$

$$\text{For } R > 0, \quad U_m^n \left[\frac{\theta_m^n - \theta_m^{n-1}}{\Delta Z} \right] = \frac{\theta_{m-1}^n - 2\theta_m^n + \theta_{m+1}^n}{2(\Delta R)^2} + \frac{\theta_{m-1}^{n-1} - 2\theta_m^{n-1} + \theta_{m+1}^{n-1}}{2(\Delta R)^2}$$

$$+ \frac{1}{R_m} \left[\frac{\theta_{m+1}^n - \theta_{m-1}^n}{4\Delta R} + \frac{\theta_{m+1}^{n-1} - \theta_{m-1}^{n-1}}{4\Delta R} \right]$$

$$+ \gamma_m^n \left(\frac{dU}{dR}\right)^2 \qquad \text{(A.37b)}$$

Rearranging, we obtain:

θ_2^n by symmetry θ_2^{n-1}

$$\text{For } R = 0, \quad \frac{(\Delta R)^2}{\Delta Z} U_1^n [\theta_1^n - \theta_1^{n-1}] = \cancel{\theta_o^n} - 2\theta_1^n + \theta_2^n + \cancel{\theta_o^{n-1}} - 2\theta_1^{n-1}$$

$$+ \theta_2^{n-1} \qquad \text{(A.38a)}$$

$$\text{For } R > 0, \quad \frac{2(\Delta R)^2}{\Delta Z} U_m^n [\theta_m^n - \theta_m^{n-1}] = \theta_{m-1}^n - 2\theta_m^n + \theta_{m+1}^n + \theta_{m-1}^{n-1} - 2\theta_m^{n-1}$$

$$+ \theta_{m+1}^{n-1} + \frac{\Delta R}{2R_m} [\theta_{m+1}^n - \theta_{m-1}^n + \theta_{m+1}^{n-1}$$

$$- \theta_{m-1}^{n-1}] + 2(\Delta R)^2 \gamma_m^n \left(\frac{dU}{dR}\right)^2 \qquad \text{(A.38b)}$$

Let $\quad \alpha_m^n = \dfrac{2(\Delta R)^2}{\Delta Z} U_m^n$

$\beta_m^n = \dfrac{\Delta R}{2R_m}$

Thus, Eqs. (A.38a) and (A.38b) become:

$$\text{For } R = 0, \quad \left(\frac{\alpha_1^n}{2} + 2\right) \theta_1^n - 2\theta_2^n = \left(\frac{\alpha_1^n}{2} - 2\right) \theta_1^{n-1} - 2\theta_2^{n-1} \tag{A.39a}$$

$$\text{For } R > 0, \quad (\beta_m^n - 1)\, \theta_{m-1}^n + (\alpha_m^n + 2)\, \theta_m^n - (\beta_m^n + 1)\, \theta_{m+1}^n$$

$$= (-\beta_m^n + 1)\, \theta_{m-1}^{n-1} + (\alpha_m^n - 2)\, \theta_m^{n-1} + (\beta_m^n + 1)\, \theta_{m+1}^{n-1}$$

$$+ 2(\Delta R)^2\, \gamma_m^n \left(\frac{dU}{dR}\right)^2 \tag{A.39b}$$

A.4 Drag Flow Between Converging Plates

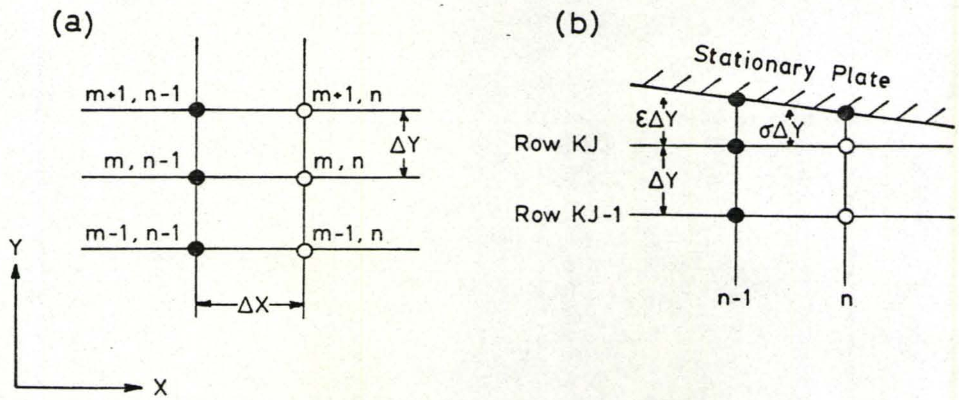

Fig. A-4. Finite difference grid. Drag flow between converging plates.
(a) Primary or secondary grid lines (in Y-direction),
(b) Secondary grid lines (in Y-direction) adjacent to inclined stationary plate.

A.4.1 Momentum Equation

$$\frac{-k}{C_p}\frac{dP}{dX} + \eta\,\frac{d^2U}{dY^2} + \frac{d\eta}{dY}\frac{dU}{dY} = 0 \qquad (A.40)$$

Let
$$\frac{dP}{dX} = \frac{P^{n+1} - P^n}{\Delta X} \qquad (A.41)$$

$$\frac{dU}{dY} = \frac{U^n_{m+1} - U^n_{m-1}}{2\Delta Y} \qquad (A.42)$$

$$\frac{d^2U}{dY^2} = \frac{U^n_{m-1} - 2U^n_m + U^n_{m+1}}{(\Delta Y)^2} \qquad (A.43)$$

Substitute Eqs. (A.41), (A.42) and (A.43) into Eqs. (A.40):

$$\frac{-k}{C_p}\left[\frac{P^{n+1} - P^n}{\Delta X}\right] + \eta^n_m\left[\frac{U^n_{m-1} - 2U^n_m + U^n_{m+1}}{(\Delta Y)^2}\right] + \left(\frac{d\eta}{dY}\right)^n_m$$

$$\cdot\left[\frac{U^n_{m+1} - U^n_{m-1}}{2\Delta Y}\right] = 0 \qquad (A.44)$$

Rearranging, we obtain:

$$\frac{-k}{\eta^n_m\, C_p}\,\frac{(\Delta Y)^2}{\Delta X}\,[P^{n+1} - P^n] + U^n_{m-1} - 2U^n_m + U^n_{m+1} + \frac{\Delta Y}{2\eta^n_m}\left(\frac{d\eta}{dY}\right)^n_m$$

$$\cdot\,[U^n_{m+1} - U^n_{m-1}] = 0 \qquad (A.45)$$

Let
$$\alpha^n_m = \frac{k}{\eta^n_m\, C_p}\,\frac{(\Delta Y)^2}{\Delta X}$$

$$\beta^n_m = \frac{\Delta Y}{2\eta^n_m}\left(\frac{d\eta}{dY}\right)^n_m$$

Thus, Eq. (A.45) becomes:

$$(-\beta_m^n + 1)\ U_{m-1}^n - 2U_m^n + (\beta_m^n + 1)\ U_{m+1}^n - \alpha_m^n\ P^{n+1} + \alpha_m^n\ P^n = 0 \tag{A.46}$$

A.4.2. Energy Equation

$$U\ \frac{\partial\theta}{\partial X} = \frac{\partial^2\theta}{\partial Y^2} + \delta\left(\frac{dU}{dY}\right)^2 \tag{A.47}$$

where $\delta = \dfrac{\eta\ u_{max}^2}{k(T_o - T_{w1})}$

Let
$$\frac{\partial\theta}{\partial X} = \frac{\theta_m^n - \theta_m^{n-1}}{\Delta X} \tag{A.48}$$

For rows n < KJ,

$$\frac{\partial^2\theta}{\partial Y^2} = \frac{\theta_{m-1}^n - 2\theta_m^n + \theta_{m+1}^n}{2(\Delta Y)^2} + \frac{\theta_{m-1}^{n-1} - 2\theta_m^{n-1} + \theta_{m+1}^{n-1}}{2(\Delta Y)^2} \tag{A.49}$$

Substitute Eqs. (A.48) and (A.49) into Eq. (A.47):

For rows n < KJ,

$$U_m^n\left[\frac{\theta_m^n - \theta_m^{n-1}}{\Delta X}\right] = \frac{\theta_{m-1}^n - 2\theta_m^n + \theta_{m+1}^n}{2(\Delta Y)^2} + \frac{\theta_{m-1}^{n-1} - 2\theta_m^{n-1} + \theta_{m+1}^{n-1}}{2(\Delta Y)^2} + \delta_m^n\left(\frac{dU}{dY}\right)^2 \tag{A.50}$$

Rearranging, we obtain:

$$\frac{2(\Delta Y)^2}{\Delta X} U_m^n [\theta_m^n - \theta_m^{n-1}] = \theta_{m-1}^n - 2\theta_m^n + \theta_{m+1}^n + \theta_{m-1}^{n-1} - 2\theta_m^{n-1}$$

$$+ \theta_{m+1}^{n-1} + 2(\Delta Y)^2 \delta_m^n \left(\frac{dU}{dY}\right)^2 \qquad \text{(A.51)}$$

Let $\gamma_m^n = \frac{2(\Delta Y)^2}{\Delta X} U_m^n$

Thus, Eq. (A.51) becomes:

For rows $n < KJ$,

$$-\theta_{m-1}^n + (\alpha_m^n + 2)\, \theta_m^n - \theta_{m+1}^n = \theta_{m-1}^{n-1} + (\alpha_m^n - 2)\, \theta_m^{n-1} + \theta_{m+1}^{n-1}$$

$$+ 2(\Delta Y)^2 \delta_m^n \left(\frac{dU}{dY}\right)^2 \qquad \text{(A.52)}$$

For row KJ,

$$\frac{\partial^2\theta}{\partial Y^2} = \frac{1}{2} \left[\frac{\dfrac{\theta_{KJ+1}^n - \theta_{KJ}^n}{\sigma\Delta Y} - \dfrac{\theta_{KJ}^n - \theta_{KJ-1}^n}{\Delta Y}}{\frac{1}{2}(\Delta Y + \sigma\Delta Y)}\right] +$$

$$\frac{1}{2} \left[\frac{\dfrac{\theta_{KJ+1}^{n-1} - \theta_{KJ}^{n-1}}{\varepsilon\Delta Y} - \dfrac{\theta_{KJ}^{n-1} - \theta_{KJ-1}^{n-1}}{\Delta Y}}{\frac{1}{2}(\Delta Y + \varepsilon\Delta Y)}\right] \qquad \text{(continued)}$$

$$= \frac{1}{(\Delta Y)^2(1+\sigma)} [\theta^n_{KJ-1} - (\frac{1}{\sigma} + 1) \theta^n_{KJ} + \frac{1}{\sigma} \theta^n_{KJ+1}]$$

$$+ \frac{1}{(\Delta Y)^2(1+\varepsilon)} [\theta^{n-1}_{KJ-1} - (\frac{1}{\varepsilon} + 1) \theta^{n-1}_{KJ} + \frac{1}{\varepsilon} \theta^{n-1}_{KJ+1}]$$

$$= \frac{1}{(\Delta Y)^2} \left[\frac{1}{1+\sigma} \theta^n_{KJ-1} - \frac{1}{\sigma} \theta^n_{KJ} + \frac{1}{\sigma+\sigma^2} \theta^n_{KJ+1} + \frac{1}{1+\varepsilon} \theta^{n-1}_{KJ-1}\right.$$

$$\left. - \frac{1}{\varepsilon} \theta^{n-1}_{KJ} + \frac{1}{\varepsilon+\varepsilon^2} \theta^{n-1}_{KJ+1}\right] \qquad (A.53)$$

Substitute Eqs. (A.48) and (A.53) into Eq. (A.47):

For row KJ,

$$U^n_{KJ} \left[\frac{\theta^n_{KJ} - \theta^{n-1}_{KJ}}{\Delta X}\right] = \frac{1}{(\Delta Y)^2} \left[\frac{1}{1+\sigma} \theta^n_{KJ-1} - \frac{1}{\sigma} \theta^n_{KJ} + \frac{1}{\sigma+\sigma^2} \theta^n_{KJ+1}\right.$$

$$\left. + \frac{1}{1+\varepsilon} \theta^{n-1}_{KJ-1} - \frac{1}{\varepsilon} \theta^{n-1}_{KJ} + \frac{1}{\varepsilon+\varepsilon^2} \theta^{n-1}_{KJ+1}\right]$$

$$+ \delta^n_m (\frac{dU}{dY})^2 \qquad (A.54)$$

Rearranging, we obtain:

$$\frac{(\Delta Y)^2}{\Delta X} U^n_{KJ} [\theta^n_{KJ} - \theta^{n-1}_{KJ}] = \frac{1}{1+\sigma} \theta^n_{KJ-1} - \frac{1}{\sigma} \theta^n_{KJ} + \frac{1}{\sigma+\sigma^2} \theta^n_{KJ+1}$$

$$+ \frac{1}{1+\varepsilon} \theta^{n-1}_{KJ-1} - \frac{1}{\varepsilon} \theta^{n-1}_{KJ} + \frac{1}{\varepsilon+\varepsilon^2} \theta^{n-1}_{KJ+1}$$

$$+ (\Delta Y)^2 \delta^{n}_{KJ} (\frac{dU}{dY})^2 \tag{A.55}$$

Since $\gamma^n_m = \frac{2(\Delta Y)^2}{\Delta X} U^n_m$,

then Eq. (A.55) becomes:

For row KJ,

$$\frac{-1}{1+\sigma} \theta^{n}_{KJ-1} + (\frac{\gamma^n_m}{2} + \frac{1}{\sigma}) \theta^{n}_{KJ} - \frac{1}{\sigma+\sigma^2} \theta^{n}_{KJ+1} = \frac{1}{1+\varepsilon} \theta^{n-1}_{KJ-1}$$

$$+ (\frac{\gamma^n_m}{2} - \frac{1}{\varepsilon}) \theta^{n-1}_{KJ} + \frac{1}{\varepsilon+\varepsilon^2} \theta^{n-1}_{KJ+1} + (\Delta Y)^2 \gamma^{n}_{KJ} (\frac{dU}{dY})^2 \tag{A.56}$$

APPENDIX B

THE LOCAL NUSSELT NUMBER

B.1 Derivation of the local Nusselt number

The local Nusselt number is calculated from the following definition:

$$Nu_x = \frac{hb}{k} \tag{B.1}$$

$$q = h(T_{wall} - T_{bulk}) = \mp k \left(\frac{dT}{dy}\right)_{wall} \tag{B.2}$$

where q = heat flux to fluid per unit area of wall

$$h = \pm \frac{k\left(\frac{dT}{dy}\right)_{wall}}{T_{bulk} - T_{wall}} \tag{B.3}$$

Substituting Eq. (B.3) into Eq. (B.1), we obtain:

$$Nu_x = \pm \frac{\left(\frac{dT}{dy}\right)_{wall} \cdot b}{T_{bulk} - T_{wall}} \tag{B.4}$$

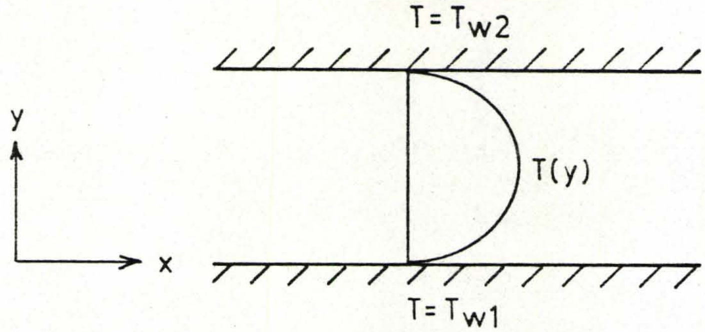

Fig. B-1. Temperature profile for flow between two parallel plates.

It can be seen in Fig. B-1 that at wall 1, $\frac{dT}{dy} > 0$ and $T_{bulk} > T_{w1}$, and at wall 2, $\frac{dT}{dy} < 0$ and $T_{bulk} > T_{w2}$. To keep the sign of the local Nusselt number at both walls consistent, Eq. (B.4) is written as follows:

For wall 1: $$(Nu_x)_{wall\ 1} = \frac{(\frac{dT}{dY})_{wall\ 1} \cdot b}{T_{bulk} - T_{w1}} \qquad (B.5)$$

For wall 2: $$(Nu_x)_{wall\ 2} = - \frac{(\frac{dT}{dy})_{wall\ 2} \cdot b}{T_{bulk} - T_{w2}} \qquad (B.6)$$

In dimensionless form we have:

$$(Nu_x)_{wall\ 1} = \frac{(\frac{d\theta}{dY})_{wall\ 1}}{\theta_{bulk}} \qquad (B.7)$$

$$(Nu_x)_{wall\ 2} = - \frac{(\frac{d\theta}{dY})_{wall\ 2}}{\theta_{bulk} - \theta_{w}2} \qquad (B.8)$$

B.2 Calculation of local heat transfer coefficients from plots of local Nusselt numbers

Given the local Nusselt number and bulk temperature, the local heat transfer coefficient and the heat flux to the fluid can be calculated using Eqs. (B.1) and (B.2). From Fig. 4-12, the local Nusselt numbers for drag flow between parallel plates (T_o = 130°C, T_{w1} = 190°C, T_{w2} = 130°C, $\bar{b}$ = 0.25 cm, k = 0.255 W/(m·K)) at X = 0.002 are 4.92 and 3.89 at the stationary and moving walls respectively. The bulk temperature at X = 0.002 is 132.5°C (from Fig. 4-6). Using Eqs. (B.1) and (B.2), we obtain the following:

$$h \text{ (at stationary wall)} = \frac{(4.92)(0.255\ \text{W/(m·K)})}{0.0025\ \text{m}} = 501.84\ \text{W/(m}^2\text{·K)}$$

$$h \text{ (at moving wall)} = \frac{(3.89)(0.255\ \text{W/(m·K)})}{0.0025\ \text{m}} = 396.78\ \text{W/(m}^2\text{·K)}$$

$$q \text{ (at stationary wall)} = (501.84)(190°\text{C}-132.5°\text{C}) = 28\ 855.8\ \text{W/m}^2$$

$$q \text{ (at moving wall)} = (396.78)(130°\text{C}-132.5°\text{C}) = -991.95\ \text{W/m}^2$$

It can be seen from the above calculations that the fluid at X = 0.002 is heated at the stationary plate, but at the moving plate it is being cooled. This is verified in Fig. 4-4 where the temperature profiles for this case are shown.

APPENDIX C

FINITE DIFFERENCE APPROXIMATIONS OF DERIVATIVES

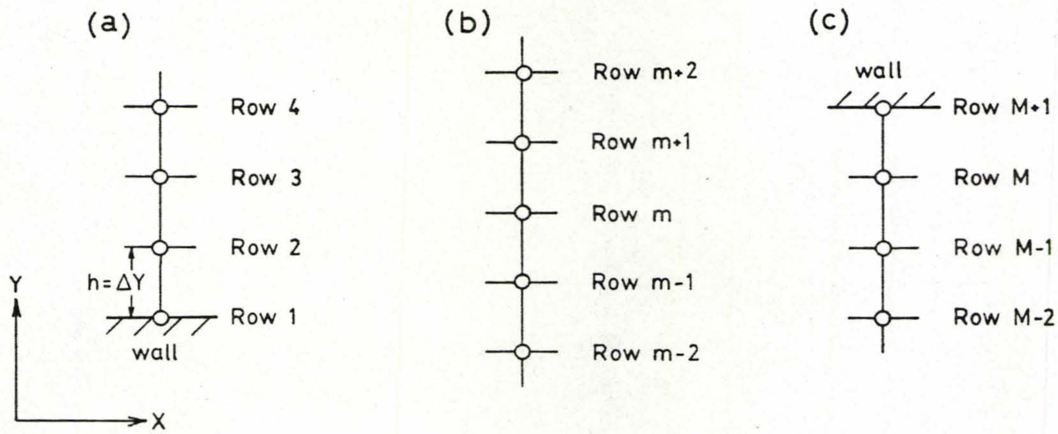

Fig. C-1. Finite difference grids for derivative estimation.

In this appendix, the finite difference approximations of first-order derivatives are derived for several nodes on the finite difference grid shown in Fig. C-1. Two-, three-, four-, and five-point formulae are derived using the following Taylor's series expansion about the point, a:

$$F(a+h) = F(a) + \frac{hF^{I}(a)}{1!} + \frac{h^2F^{II}(a)}{2!} + \frac{h^3F^{III}(a)}{3!} + \frac{h^4F^{IV}(a)}{4!} + \ldots$$

$$= F(a) + hF^{I}(a) + \frac{h^2F^{II}(a)}{2} + \frac{h^3F^{III}(a)}{6} + \frac{h^4F^{IV}(a)}{24} + \ldots \qquad (C.1)$$

C.1 Derivative at Node 1 (see Fig. C-1(a))

2-Point Formula

From Eq. (C.1), we obtain:

$$F(2) = F(1) + (\Delta Y)F^{I}(1) \qquad (C.2)$$

or

$$\boxed{F^{I}(1) = \frac{F(2) - F(1)}{\Delta Y}} \qquad (C.3)$$

3-Point Formula

From Eq. (C.1), we obtain the following:

$$F(3) = F(1) + 2(\Delta Y)F'(1) + \frac{4}{2}(\Delta Y)^2F^{II}(1) \qquad (C.4)$$

$$F(2) = F(1) + (\Delta Y)F^{I}(1) + \frac{1}{2}(\Delta Y)^2F^{II}(1) \qquad (C.5)$$

Add Eq. (C.4) and -4x Eq. (C.5) to eliminate $F^{II}(1)$:

$$F(3) - 4F(2) = -3F(1) - 2(\Delta Y)F^{I}(1) \qquad (C.6)$$

or

$$\boxed{F^{I}(1) = \frac{-3F(1) + 4F(2) - F(3)}{2\Delta Y}} \qquad (C.7)$$

4-Point Formula

From Eq. (C.1), we obtain the following:

$$F(4) = F(1) + 3(\Delta Y)F^{I}(1) + \frac{9}{2}(\Delta Y)^{2}F^{II}(1) + \frac{27}{6}(\Delta Y)^{3}F^{III}(1) \qquad (C.8)$$

$$F(3) = F(1) + 2(\Delta Y)F^{I}(1) + \frac{4}{2}(\Delta Y)^{2}F^{II}(1) + \frac{8}{6}(\Delta Y)^{3}F^{III}(1) \qquad (C.9)$$

$$F(2) = F(1) + 2(\Delta Y)F^{I}(1) + \frac{1}{2}(\Delta Y)^{2}F^{II}(1) + \frac{1}{6}(\Delta Y)^{3}F^{III}(1) \qquad (C.10)$$

Add -2x Eq. (C.8), 9x Eq. (C.9) and -18x Eq. (C.10) to eliminate $F^{II}(1)$ and $F^{III}(1)$:

$$-2F(4) + 9F(3) - 18F(2) = -11F(1) - 6(\Delta Y)F^{I}(1) \qquad (C.11)$$

or

$$\boxed{F^{I}(1) = \frac{-11F(1) + 18F(2) - 9F(3) + 2F(4)}{6\Delta Y}} \qquad (C.12)$$

C.2 Derivative at Node 2 (see Fig. C-1(a))

3-Point Formula

From Eq. (C.1), we obtain the following:

$$F(3) = F(2) + (\Delta Y)F^{I}(2) + \frac{1}{2}(\Delta Y)^{2}F^{II}(2) \qquad (C.13)$$

$$F(1) = F(2) - (\Delta Y)F^{I}(2) + \frac{1}{2}(\Delta Y)^{2}F^{II}(2) \qquad (C.14)$$

Add Eq. (C.13) and -1x Eq. (C.14) to eliminate $F^{II}(2)$:

$$F(3) - F(1) = 2(\Delta Y)F^{I}(2) \tag{C.15}$$

or

$$\boxed{F^{I}(2) = \frac{F(3) - F(1)}{2\Delta Y}} \tag{C.16}$$

4-Point Formula

From Eq. (C.1), we obtain the following:

$$F(4) = F(2) + 2(\Delta Y)F^{I}(2) + \frac{4}{2}(\Delta Y)^2F^{II}(2) + \frac{8}{6}(\Delta Y)^3F^{III}(2) \tag{C.17}$$

$$F(3) = F(2) + (\Delta Y)F^{I}(2) + \frac{1}{2}(\Delta Y)^2F^{II}(2) + \frac{1}{6}(\Delta Y)^3F^{III}(2) \tag{C.18}$$

$$F(1) = F(2) - (\Delta Y)F^{I}(2) + \frac{1}{2}(\Delta Y)^2F^{II}(2) - \frac{1}{6}(\Delta Y)^3F^{III}(2) \tag{C.19}$$

Add Eq. (C.17), -6x Eq. (C.18) and 2x Eq. (C.19) to eliminate $F^{II}(2)$ and $F^{III}(2)$:

$$F(4) - 6F(3) + 2F(1) = -3F(2) - 6(\Delta Y)F^{I}(2) \tag{C.20}$$

or

$$\boxed{F^{I}(2) = \frac{-F(4) + 6F(3) - 3F(2) - 2F(1)}{6\Delta Y}} \tag{C.21}$$

C.3 Derivative at Node m (see Fig. C-1(b))

3-Point Formula

From Eq. (C.1), we obtain the following:

$$F(m+1) = F(m) + (\Delta Y)F^{I}(m) + \frac{1}{2}(\Delta Y)^{2}F^{II}(m) \tag{C.22}$$

$$F(m-1) = F(m) - (\Delta Y)F^{I}(m) + \frac{1}{2}(\Delta Y)^{2}F^{II}(m) \tag{C.23}$$

Add Eq. (C.22) and -1x Eq. (C.23) to eliminate $F^{II}(m)$:

$$F(m+1) - F(m-1) = 2(\Delta Y)F^{I}(m) \tag{C.24}$$

or

$$\boxed{F^{I}(m) = \frac{F(m+1) - F(m-1)}{2\Delta Y}} \tag{C.25}$$

5-Point Formula

From Eq. (C.1), we obtain

$$F(m+2) = F(m) + 2(\Delta Y)F^{I}(m) + \frac{4}{2}(\Delta Y)^{2}F^{II}(m) + \frac{8}{6}(\Delta Y)^{3}F^{III}(m) + \frac{16}{24}(\Delta Y)^{4}F^{IV}(m) \tag{C.26}$$

$$F(m+1) = F(m) + (\Delta Y)F^{I}(m) + \frac{1}{2}(\Delta Y)^{2}F^{II}(m) + \frac{1}{6}(\Delta Y)^{3}F^{III}(m) + \frac{1}{24}(\Delta Y)^{4}F^{IV}(m) \tag{C.27}$$

$$F(m-1) = F(m) - (\Delta Y)F^{I}(m) + \frac{1}{2}(\Delta Y)^{2}F^{II}(m) - \frac{1}{6}(\Delta Y)^{3}F^{III}(m) + \frac{1}{24}(\Delta Y)^{4}F^{IV}(m) \tag{C.28}$$

$$F(m-2) = F(m) - 2(\Delta Y)F^{I}(m) + \frac{4}{2}(\Delta Y)^{2}F^{II}(m) - \frac{8}{6}(\Delta Y)^{3}F^{III}(m) + \frac{16}{24}(\Delta Y)^{4}F^{IV}(m) \tag{C.29}$$

Add -1x Eq. (C.26), 8x Eq. (C.27), -8x Eq. (C.28) and Eq. (C.29) to eliminate $F^{II}(m)$, $F^{III}(m)$ and $F^{IV}(m)$:

$$-F(m+2) + 8F(m+1) - 8F(m-1) + F(m-2) = 12(\Delta Y)F^{I}(m) \tag{C.30}$$

or

$$\boxed{F^{I}(m) = \frac{-F(m+2) + 8F(m+1) - 8F(m-1) + F(m-2)}{12\Delta Y}} \tag{C.31}$$

C.4 Derivative at Node M (see Fig. C-1(c))

3-Point Formula

From Eq. (C.1), we obtain the following:

$$F(M+1) = F(M) + (\Delta Y)F^{I}(M) + \frac{1}{2}(\Delta Y)^{2}F^{II}(M) \tag{C.32}$$

$$F(M-1) = F(M) - (\Delta Y)F^{I}(M) + \frac{1}{2}(\Delta Y)^{2}F^{II}(M) \tag{C.33}$$

Add -1x Eq. (C.32) and Eq. (C.33) to eliminate $F^{II}(M)$:

$$-F(M+1) + F(M-1) = -2(\Delta Y)F^{I}(M) \tag{C.34}$$

or

$$\boxed{F^{I}(M) = \frac{F(M+1) - F(M-1)}{2\Delta Y}} \tag{C.35}$$

4-Point Formula

From Eq. (C.1), we obtain the following:

$$F(M+1) = F(M) + (\Delta Y)F^{I}(M) + \frac{1}{2}(\Delta Y)^{2}F^{II}(M) + \frac{1}{6}(\Delta Y)^{3}F^{III}(M) \tag{C.36}$$

$$F(M-1) = F(M) - (\Delta Y)F^{I}(M) + \frac{1}{2}(\Delta Y)^{2}F^{II}(M) - \frac{1}{6}(\Delta Y)^{3}F^{III}(M) \tag{C.37}$$

$$F(M-2) = F(M) - 2(\Delta Y)F^{I}(M) + \frac{4}{2}(\Delta Y)^{2}F^{II}(M) - \frac{8}{6}(\Delta Y)^{3}F^{III}(M) \tag{C.28}$$

Add 2x Eq. (C.26), -6x Eq. (C.37) and Eq. (C.38) to eliminate $F^{II}(M)$ and $F^{III}(M)$:

$$2F(M+1) - 6F(M-1) + F(M-2) = -3F(M) + 6(\Delta Y)F^{I}(M) \tag{C.39}$$

or

$$\boxed{F^{I}(M) = \frac{2F(M+1) + 3F(M) - 6F(M-1) + F(M-2)}{6\Delta Y}} \tag{C.40}$$

C.5 Derivative at Node M+1 (see Fig. C-1(c))

2-Point Derivative

From Eq. (C.1), we obtain:

$$F(M) = F(M+1) - (\Delta Y)F^{I}(M+1) \tag{C.41}$$

or

$$\boxed{F^{I}(M+1) = \frac{F(M+1) - F(M)}{\Delta Y}} \tag{C.42}$$

3-Point Derivative

From Eq. (C.1), we obtain the following:

$$F(M) = F(M+1) - (\Delta Y)F^{I}(M+1) + \frac{1}{2}(\Delta Y)^{2}F^{II}(M+1) \tag{C.43}$$

$$F(M-1) = F(M+1) - 2(\Delta Y)F^{I}(M+1) + \frac{4}{2}(\Delta Y)^{2}F^{II}(M+1) \tag{C.44}$$

Add -4x Eq. (C.43) and Eq. (C.44) to eliminate $F^{II}(M+1)$:

$$-4F(M) + F(M-1) = -3F(M+1) + 2(\Delta Y)F^{I}(M+1) \tag{C.45}$$

or

$$\boxed{F^{I}(M+1) = \frac{3F(M+1) - 4F(M) + F(M-1)}{2\Delta Y}} \tag{C.46}$$

4-Point Derivative

From Eq. (C.1), we obtain the following:

$$F(M) = F(M+1) - (\Delta Y)F^{I}(M+1) + \frac{1}{2}(\Delta Y)^{2}F^{II}(M+1)$$
$$- \frac{1}{6}(\Delta Y)^{3}F^{III}(M+1) \tag{C.47}$$

$$F(M-1) = F(M+1) - 2(\Delta Y)F^{I}(M+1) + \frac{4}{2}(\Delta Y)^{2}F^{II}(M+1)$$
$$- \frac{8}{6}(\Delta Y)^{3}F^{III}(M+1) \quad (C.48)$$

$$F(M-2) = F(M+1) - 3(\Delta Y)F^{I}(M+1) + \frac{9}{2}(\Delta Y)^{2}F^{II}(M+1)$$
$$- \frac{27}{6}(\Delta Y)^{3}F^{III}(M+1) \quad (C.49)$$

Add -18x Eq. (C.47), 9x Eq. (C.48) and -2x Eq. (C.49) to eliminate $F^{II}(M+1)$ and $F^{III}(M+1)$:

$$-18F(M) + 9F(M-1) - 2F(M-2) = -11F(M+1) + 6(\Delta Y)F^{I}(M+1) \quad (C.50)$$

or

$$\boxed{F^{I}(M+1) = \frac{11F(M+1) - 18F(M) + 9F(M-1) - 2F(M-2)}{6\Delta Y}} \quad (C.51)$$

The accuracy of the above formulae is checked in Table C-1 for the following function:

$$F(y) = 1 - y^{\frac{n+1}{n}} \quad ; \quad 0 \le y \le 1 \quad (C.52)$$

where $n = 0.453$

True derivative:

$$F^{I}(y) = -\left(\frac{n+1}{n}\right) y^{\frac{1}{n}} \quad (C.53)$$

Table C-1. Estimates of $F^I(y)$ using finite difference formulae.

$M = 40,\ \Delta Y = \frac{1}{40}$.

	Node 1	Node 2	Node 3	Node 40	Node 41
2-point derivative	-3.1199				-0.0003
3-point derivative	-3.2057	-3.0340	-2.8650	-0.0013	0.0007
4-point derivative	-3.2075	-3.0332		-0.0009	0.0001
5-point derivative			-2.8641		
True derivative	-3.2075	-3.0332	-2.8641	-0.0009	0

From the above table, it is seen that $F^I(y)$ is accurate within 4 decimal places when either the 4- or 5-point formula is used.

APPENDIX D

ALGORITHMS FOR SOLVING SIMULTANEOUS EQUATIONS BY GAUSSIAN ELIMINATION

To solve a general system of n simultaneous equations with n unknowns by Gaussian elimination on the computer, about n(n+1) memory locations are required (one for each coefficient in the equations). Thus, the number of equations that can be solved simultaneously is limited by the storage capacity of the computer memory. In the tri-diagonal and modified tridiagonal systems of equations encountered in Chaps. 4, 5, 6 and 7, most of the coefficients in the equations are zeros. It would be more beneficial to solve these systems of equations by using algorithms such as Thomas' method (30) which do not require the storage of the zero elements. These algorithms are simpler and much faster than the more general methods because the zeros are not stored. More equations, therefore, can be solved simultaneously using these algorithms. Three algorithms used to solve the tridiagonal and modified tridiagonal systems of equations encountered in Chaps. 4, 5, 6 and 7 are now outlined.

D.1 Thomas' Method

Thomas' method (30) is used to solve a tridiagonal system of equations, such as the one given by matrix equation (D.1).

$$
\begin{bmatrix}
B_1 & C_1 & & & & & \underline{0} \\
A_2 & B_2 & C_2 & & & & \\
 & \ddots & \ddots & \ddots & & & \\
 & & A_m & B_m & C_m & & \\
 & & & \ddots & \ddots & \ddots & \\
 & & & & A_{M-1} & B_{M-1} & C_{M-1} \\
\underline{0} & & & & & A_M & B_M
\end{bmatrix}
\begin{bmatrix} X_1 \\ X_2 \\ \vdots \\ X_m \\ \vdots \\ X_{M-1} \\ X_M \end{bmatrix}
=
\begin{bmatrix} H_1 \\ H_2 \\ \vdots \\ H_m \\ \vdots \\ H_{M-1} \\ H_M \end{bmatrix}
\qquad (D.1)
$$

To solve matrix equation (D.1) by Thomas' method, the following steps are performed:

1. Set $S_1 = B_1$

$$T_1 = \frac{H_1}{S_1}$$

2. Set

$$
\left.
\begin{aligned}
Q_{i-1} &= \frac{C_{i-1}}{S_{i-1}} \\
S_i &= B_i - A_i \cdot Q_{i-1} \\
T_i &= \frac{H_i - A_i \cdot T_{i-1}}{S_i}
\end{aligned}
\right\} \quad (i = 2, 3, \ldots, M)
$$

Thus, matrix equation (D.1) becomes:

$$
\begin{bmatrix}
1 & Q_1 & & & \underline{0} \\
 & 1 & Q_2 & & \\
 & & \ddots & \ddots & \\
 & & & 1 & Q_{M-1} \\
\underline{0} & & & & 1
\end{bmatrix}
\begin{bmatrix} X_1 \\ X_2 \\ \vdots \\ X_{M-1} \\ X_M \end{bmatrix}
=
\begin{bmatrix} T_1 \\ T_2 \\ \vdots \\ T_{M-1} \\ T_M \end{bmatrix}
\qquad (D.2)
$$

3. Set $X_M = T_M$

4. Set $X_i = T_i - Q_i \cdot X_{i+1}$ $(i = M-1, M-2, \ldots, 2, 1)$

Thus, matrix equation (D.1) is solved for X_i $(i = 1, 2, \ldots, M)$.

D.2 Gaussian Elimination to Solve Continuity and Momentum Equations in Chaps. 5 and 6

An algorithm has been developed (31) to solve the following modified tridiagonal system of equations:

$$\begin{bmatrix} B_1 & C_1 & & & & W_1 \\ A_2 & B_2 & C_2 & & \underline{0} & W_2 \\ & \ddots & \ddots & \ddots & & \vdots \\ & & A_{M-1} & B_{M-1} & C_{M-1} & W_{M-1} \\ & \underline{0} & & A_M & B_M & W_M \\ Z_1 & Z_2 & \cdots & Z_{M-1} & Z_M & Z_{M+1} \end{bmatrix} \begin{bmatrix} U_1 \\ U_2 \\ \vdots \\ U_{M-1} \\ U_M \\ P \end{bmatrix} = \begin{bmatrix} H_1 \\ H_2 \\ \vdots \\ H_{M-1} \\ H_M \\ Z_{M+2} \end{bmatrix} \qquad (D.3)$$

To solve matrix equation (D.3), the following steps are performed:

1. Set $B_1' = B_1$

$W_1' = W_1$

$H_1' = H_1$

2. Set

$$\left.\begin{aligned}
SS_i &= \frac{-A_i}{B'_{i-1}} \\
B'_i &= B_i + C_{i-1} \cdot SS_i \\
W'_i &= W_i + W'_{i-1} \cdot SS_i \\
H'_i &= H_i + H'_{i-1} \cdot SS_i
\end{aligned}\right\} \quad (i = 2, 3, \ldots, M)$$

Thus, matrix equation (D.3) becomes:

$$\begin{bmatrix}
B'_1 & C_1 & & & & W'_1 \\
 & B'_2 & C_2 & & & W'_2 \\
 & & \ddots & \ddots & & \vdots \\
 & & & B'_{M-1} & C_{M-1} & W'_{M-1} \\
 & & & & B'_M & W'_M \\
Z_1 & Z_2 & \cdots & Z_{M-1} & Z_M & Z_{M+1}
\end{bmatrix}
\begin{bmatrix} U_1 \\ U_2 \\ \vdots \\ U_{M-1} \\ U_M \\ P \end{bmatrix}
=
\begin{bmatrix} H'_1 \\ H'_2 \\ \vdots \\ H'_{M-1} \\ H'_M \\ Z_{M+2} \end{bmatrix}
\qquad (D.4)$$

3. Set

$$B^*_M = B'_M$$

$$W^*_M = W'_M$$

$$H^*_M = H'_M$$

4. Set

$$SS_i = \frac{-C_i}{B^*_{i+1}}$$

$$\left.\begin{aligned} B_i^* &= B_i' \\ W_i^* &= W_i' + W_{i+1}^* \cdot SS_i \\ H_i^* &= H_i' + H_{i+1}^* \cdot SS_i \end{aligned}\right\} \quad (i = M\text{-}1,\ M\text{-}2,\ \ldots,\ 2,\ 1)$$

Thus, matrix equation (D.4) becomes:

$$\begin{bmatrix} B_1^* & & & \underline{0} & W_1^* \\ & B_2^* & & & W_2^* \\ & & \ddots & & \vdots \\ & & B_{M-1}^* & & W_{M-1}^* \\ \underline{0} & & & B_M^* & W_M^* \\ Z_1 & Z_2 \ldots & Z_{M-1} & Z_M & Z_{M+1} \end{bmatrix} \begin{bmatrix} U_1 \\ U_2 \\ \vdots \\ U_{M-1} \\ U_M \\ P \end{bmatrix} = \begin{bmatrix} H_1^* \\ H_2^* \\ \vdots \\ H_{M-1}^* \\ H_M^* \\ Z_{M+2} \end{bmatrix} \tag{D.5}$$

5. Set $Z_{M+1}^* = Z_{M+1}$

$$Z_{M+2}^* = Z_{M+2}$$

6. Set

$$\left.\begin{aligned} SS_i &= \frac{-Z_i}{B_i^*} \\ Z_{M+1}^* &= Z_{M+1}^* + W_i^* \cdot SS_i \\ Z_{M+2}^* &= Z_{M+2}^* + H_i^* \cdot SS_i \end{aligned}\right\} \quad (i = 1,\ 2,\ \ldots,\ M)$$

Thus, matrix equation (D.5) becomes:

$$\begin{bmatrix} B_1^* & & & & \underline{0} & W_1^* \\ & B_2^* & & & & W_2^* \\ & & \ddots & & & \vdots \\ & & & B_{M-1}^* & & W_{M-1}^* \\ & & & & B_M^* & W_M^* \\ & \underline{0} & & & & Z_{M+1}^* \end{bmatrix} \begin{bmatrix} U_1 \\ U_2 \\ \vdots \\ U_{M-1} \\ U_M \\ P \end{bmatrix} = \begin{bmatrix} H_1^* \\ H_2^* \\ \vdots \\ H_{M-1}^* \\ H_M^* \\ Z_{M+2}^* \end{bmatrix} \tag{D.6}$$

7. Set $\quad P = \dfrac{Z_{M+2}^*}{Z_{M+1}^*}$

8. Set $\quad U_i = \dfrac{H_i^* - W_i^* \cdot P}{B_i^*} \qquad (i = 1, 2, \ldots, M)$

Thus, matrix equation (D.3) is solved for U_i $(i = 1, 2, \ldots, M)$ and P.

D.3 Gaussian Elimination to Solve Continuity and Momentum Equations in Chap. 7

An algorithm has been developed to solve the following modified tridiagonal system of equations:

$$\begin{bmatrix}
B_1 & C_1 & & & & & & \underline{0} & & & \psi_1 & 0 & 0 & 0 \\
A_2 & B_2 & C_2 & & & & & & & & \vdots & \vdots & 0 & 0 \\
 & \ddots & \ddots & \ddots & & & & & & & & & \vdots & \vdots \\
 & & A_5 & B_5 & 0 & & & & & & \psi_5 & 0 & & \\
 & & & 0 & B_6 & C_6 & & & & & \phi_6 & \psi_6 & & \\
 & & & & A_7 & B_7 & C_7 & & & & \vdots & \vdots & & \\
 & & & & & \ddots & \ddots & \ddots & & & \phi_9 & \psi_9 & & \\
 & & & & & & & & & & 0 & \phi_{10} & & \\
 & & & & & & & & & & \vdots & \phi_{11} & \vdots & \vdots \\
 & & & & & & & \ddots & \ddots & \ddots & & \phi_{12} & 0 & \vdots \\
 & & \underline{0} & & & & & & A_{13} & B_{13} & C_{13} & 0 & 0 & \psi_{13} \;\; 0 \\
 & & & & & & & & & A_{14} & B_{14} & 0 & 0 & \psi_{14} \;\; 0 \\
Z_1 & Z_2 & Z_3 & Z_4 & Z_5 & 0 \ldots & & & & & & & & \\
 & & \ldots 0 & Z_6 & Z_7 & Z_8 & Z_9 & 0 \ldots & & & & \underline{\underline{W}} & & \\
 & & & & \ldots 0 & Z_{10} & Z_{11} & Z_{12} & 0 & 0 & & & & \\
 & & & & & & \ldots 0 & Z_{13} & Z_{14} & & & & &
\end{bmatrix}
\begin{bmatrix} U_1 \\ U_2 \\ \vdots \\ \\ \vdots \\ U_{13} \\ U_{14} \\ P^2 \\ P^3 \\ P^5 \\ U_{avg,o} \end{bmatrix}
=
\begin{bmatrix} E_1 \\ E_2 \\ \vdots \\ \\ \vdots \\ E_{13} \\ E_{14} \\ W_{6,1} \\ W_{6,2} \\ W_{6,3} \\ W_{6,4} \end{bmatrix} \tag{D.7}$$

where
$$\underline{\underline{W}} = \begin{bmatrix} W_{2,1} & W_{3,1} & W_{4,1} & W_{5,1} \\ W_{2,2} & W_{3,2} & W_{4,2} & W_{5,2} \\ W_{2,3} & W_{3,3} & W_{4,3} & W_{5,3} \\ W_{2,4} & W_{3,4} & W_{4,4} & W_{5,4} \end{bmatrix}$$

To solve matrix equation (D.7), the following steps are performed:

1. Set $B_1' = B_1$

$$\phi_1' = \phi_1 = 0$$

$$\psi_1' = \psi_1$$

$$E_1' = E_1$$

2. Set

$$\left.\begin{aligned} SS_i &= \frac{-A_i}{B'_{i-1}} \\ B'_i &= B_i + C_{i-1} \cdot SS_i \\ \phi'_i &= \phi_i + \phi_{i-1} \cdot SS_i \\ \psi'_i &= \psi_i + \psi_{i-1} \cdot SS_i \\ E'_i &= E_i + E_{i-1} \cdot SS_i \end{aligned}\right\} \quad (i = 2, 3, \ldots, 14)$$

3. Set

$$B^*_{14} = B'_{14}$$

$$\phi^*_{14} = \phi'_{14} = 0$$

$$\psi^*_{14} = \psi^*_{14} = 0$$

$$E^*_{14} = E'_{14}$$

4. Set

$$\left.\begin{aligned} SS_i &= \frac{-C_i}{B^*_{i+1}} \\ \phi^*_i &= \phi'_i + \phi^*_{i+1} \cdot SS_i \\ \psi^*_i &= \psi'_i + \psi^*_{i+1} \cdot SS_i \\ E^*_i &= E'_i + E^*_{i+1} \cdot SS_i \end{aligned}\right\} \quad (i = 13, 12, \ldots, 2, 1)$$

Thus, the matrix equation (C.7) becomes:

$$
\left[\begin{array}{lcccc}
B_1^* \qquad\qquad\qquad\qquad \underline{0} & \psi_1^* & 0 & 0 & 0 \\
\quad B_2^* & \vdots & \vdots & \vdots & \vdots \\
\qquad \ddots & \psi_5^* & 0 & & \\
 & \phi_6^* & \psi_6^* & & \\
 & \vdots & \vdots & & \\
 & \phi_9^* & \psi_9^* & \vdots & \\
 & 0 & \phi_{10}^* & & \\
 & \vdots & & 0 & \\
\qquad \underline{0} \qquad\qquad \ddots & & \phi_{12}^* & 0 & \vdots \\
\qquad\qquad\qquad\qquad\qquad B_{13}^* & 0 & 0 & \psi_{13}^* & 0 \\
\qquad\qquad\qquad\qquad\qquad\quad B_{14}^* & 0 & 0 & \psi_{14}^* & 0 \\
Z_1 \;\; Z_2 \;\; Z_3 \;\; Z_4 \;\; Z_5 \;\; 0 \cdots & & & & \\
\qquad \cdots 0 \;\; Z_6 \;\; Z_7 \;\; Z_8 \;\; Z_9 \;\; 0 \cdots & & \underline{\underline{W}} & & \\
\qquad\qquad \cdots 0 \;\; Z_{10} \;\; Z_{11} \;\; Z_{12} \;\; 0 \;\; 0 & & & & \\
\qquad\qquad\qquad \cdots 0 \;\; Z_{13} \;\; Z_{14} & & & &
\end{array}\right]
\left[\begin{array}{l}
U_1 \\ U_2 \\ \vdots \\ \\ \\ \\ \\ \\ \vdots \\ U_{13} \\ U_{14} \\ P^2 \\ P^3 \\ P^5 \\ U_{avg,o}
\end{array}\right]
=
\left[\begin{array}{l}
E_1^* \\ E_2^* \\ \vdots \\ \\ \\ \\ \\ \\ \vdots \\ E_{13}^* \\ E_{14}^* \\ W_{6,1} \\ W_{6,2} \\ W_{6,3} \\ W_{6,4}
\end{array}\right]
\qquad (D.8)
$$

5. Set $\qquad W_{i,j}^* = W_{i,j}$

6. Eliminate Z_k ($k = 1, 2, \ldots, 14$) from matrix equation (D.8).

$$
\left.\begin{array}{l}
SS_k = \dfrac{-Z_k}{B_k^*} \\[2ex]
W_{i,i}^* = W_{i,i}^* + \phi_k^* \cdot SS_i \\[2ex]
W_{i+1,i}^* = W_{i+1,i} + \psi_k^* \cdot SS_k \\[2ex]
W_{6,i}^* + W_{6,i}^* + E_k^* \cdot SS_i
\end{array}\right\}
\quad
\begin{array}{l}
(k = 1, 2, \ldots, 12) \\
\;i = 1, 2, \text{ or } 3 \\
\quad \equiv \text{ row in which } Z_k \text{ is} \\
\quad\;\; \text{located}
\end{array}
$$

$$\left.\begin{aligned} SS_k &= \frac{-z_k}{B_k^*} \\[2ex] W_{4,4}^* &= W_{4,4}^* + \psi_k^* \cdot SS_k \\[2ex] W_{6,4}^* &= W_{6,4}^* + E_k^* \cdot SS_k \end{aligned}\right\} \qquad (k = 13,\ 14)$$

Thus, matrix equation (C.8) becomes:

$$\begin{bmatrix}
B_1^* & & & & & & \psi_1^* & 0 & 0 & 0 \\
& B_2^* & & & \underline{0} & & \vdots & \vdots & 0 & 0 \\
& & \ddots & & & & \psi_3^* & 0 & \vdots & \vdots \\
& & & & & & \phi_6^* & \psi_6^* & & \\
& & & & & & \vdots & \vdots & & \\
& & & & & & \phi_9^* & \psi_9^* & & \\
& & & & & & 0 & \phi_{10}^* & & \\
& & & & & & & & \vdots & \\
& & & \ddots & & & \vdots & \phi_{12}^* & 0 & \vdots \\
& & & & B_{13}^* & & & 0 & \psi_{13}^* & 0 \\
& & & & & B_{14}^* & 0 & 0 & \psi_{14}^* & 0 \\
& & \underline{0} & & & & \multicolumn{4}{c}{\boxed{\quad \underline{\underline{W}}^* \quad}}
\end{bmatrix}
\begin{bmatrix} U_1 \\ U_2 \\ \vdots \\ \\ \\ \\ \\ \\ \vdots \\ U_{13} \\ U_{14} \\ P^2 \\ P^3 \\ P^5 \\ U_{avg,o} \end{bmatrix}
=
\begin{bmatrix} E_1^* \\ E_2^* \\ \vdots \\ \\ \\ \\ \\ \\ \vdots \\ E_{13}^* \\ E_{14}^* \\ W_{6,1}^* \\ \vdots \\ \\ W_{6,4}^* \end{bmatrix} \qquad (D.9)$$

7. Solve matrix equation (D.10) to obtain P^2, P^3, P^5 and $U_{avg,o}$.

$$\begin{bmatrix} \\ \underline{\underline{W}}^* \\ \\ \end{bmatrix} \begin{bmatrix} P^2 \\ P^3 \\ P^5 \\ U_{avg,o} \end{bmatrix} = \begin{bmatrix} W_{6,1}^* \\ \vdots \\ \\ W_{6,4}^* \end{bmatrix} \qquad (D.10)$$

8. Set

$$U_k = \frac{E_k^* - \psi_k^* P^2}{B_k^*} \qquad (k = 1, 2, \ldots, 5)$$

$$= \frac{E_k^* - \phi_k^* P^2 - \psi_k^* P^3}{B_k^*} \qquad (k = 6, 7, \ldots, 9)$$

$$= \frac{E_k^* - \phi_k^* P^3}{B_k^*} \qquad (k = 10, 11, 12)$$

$$= \frac{E_k^* - \psi_k^* P^5}{B_k^*} \qquad (k = 13, 14)$$

Thus, matrix equation (D.7) is solved for U_k $(k = 1, 2, \ldots, 14)$, P^2, P^3, P^5 and $U_{avg,o}$.

APPENDIX E

HEAT TRANSFER CALCULATIONS FOR A NEWTONIAN, CONSTANT VISCOSITY FLUID

The fully developed velocity and temperature profiles, the limiting bulk temperatures and local Nusselt numbers for a Newtonian, constant velocity fluid flowing between parallel plates or through a circular tube are calculated in this appendix. The analytical expressions given by Schlichting (58) for the velocity profiles and pressure distribution of a Newtonian fluid flowing between converging plates are also presented. The analytical and finite difference results are compared.

E.1 Drag Flow Between Parallel Plates

Momentum Equation

$$\eta \frac{d^2u}{dy^2} = 0 \tag{E.1}$$

$$\begin{aligned} y &= 0 & u &= 0 \\ y &= b = 0.25 \text{ cm} & u &= 15 \text{ cm/s} \end{aligned} \tag{E.2}$$

The velocity profile for a Newtonian fluid is obtained by integrating Eq. (E.1) and using the accompanying boundary conditions (E.2).

Velocity profile:

$$\boxed{u(y) = 60y} \qquad (E.3)$$

where $u [=]$ cm/s

$y [=]$ cm

Energy Equation

$$k \frac{d^2T}{dy^2} + \eta\left(\frac{du}{dy}\right)^2 = 0 \qquad (E.4)$$

$$\begin{aligned} y &= 0 & T &= T_w = 160°C \\ y &= b = 0.25 \text{ cm} & T &= T_w = 160°C \end{aligned} \qquad (E.5)$$

The fully developed temperature profile for a Newtonian fluid is obtained by integrating Eq. (E.4) and using the accompanying boundary conditions (E.5).

Fully developed temperature profile:

$$\boxed{T(y) = -0.18 \frac{\eta}{k} y^2 + 0.045 \frac{\eta}{k} y + 160} \qquad (E.6)$$

where $T [=]$ °C

$\eta [=]$ Pa.s

$k [=]$ W/(m.K)

$y [=]$ cm

When η = 2000 Pa.s and k = 0.255 W/(m.K), T = T_{max} = 182.1°C at the centre-line of flow.

Bulk Temperature

$$T_{bulk} = \frac{\int_o^b T(y)u(y)dy}{\int_o^b u(y)dy} \qquad (E.7)$$

By substituting Eqs. (E.3) and (E.6) into the above equation, the following expression for the limiting bulk temperature of a Newtonian fluid is obtained:

Limiting bulk temperature:

$$\boxed{T_{bulk} = -0.09 \frac{\eta}{k} b^2 + 0.03 \frac{\eta}{k} b + 160} \qquad (E.8)$$

When η = 2000 Pa.s and k = 0.255 W/(m.K), T_{bulk} = 174.71°C

Local Nusselt Number

$$Nu_x = \frac{(\frac{dT}{dy})_{wall} \cdot b}{T_{bulk} - T_{wall}} \qquad (E.9)$$

By substituting Eqs. (E.6) and (E.8) into the above equation, the following expression is obtained for the local Nusselt number for a Newtonian fluid:

Limiting local Nusselt number:

$$\boxed{Nu_x = 6.00} \tag{E.10}$$

E.2 Poiseuille Flow Between Parallel Plates

Momentum Equation

$$-\frac{dp}{dx} + \eta \frac{d^2u}{dy^2} = 0 \tag{E.11}$$

$$\begin{aligned} y &= 0 & u &= 1.5\ u_{avg} = 22.5\ \text{cm/s} \\ y &= \pm a = \pm 0.125\ \text{cm} & u &= 0 \end{aligned} \tag{E.12}$$

By integrating Eq. (E.11) and using the accompanying boundary conditions (E.12), the following velocity profile is obtained for a Newtonian fluid:

Velocity profile:

$$\boxed{u(y) = 1.5\ u_{avg}\ [1 - (\frac{y}{a})^2]} \tag{E.13}$$

where u, u_{avg} [=] cm/s

y, a [=] cm

Energy Equation

$$k \frac{d^2T}{dy^2} + \eta(\frac{du}{dy})^2 = 0 \tag{E.14}$$

$$y = \pm a = \pm 0.125 \text{ cm} \qquad T = T_w = 160°C \tag{E.15}$$

The fully developed temperature profile for a Newtonian fluid is obtained by integrating Eq. (E.14) and using the accompanying boundary conditions (E.15).

Fully developed temperature profile:

$$\boxed{T(y) = A[1 - (\frac{y}{a})^4] + 160} \tag{E.16}$$

where $A = 7.5 \times 10^{-4}\, u_{avg}^2 \, \frac{\eta}{k}$

u_{avg} [=] cm/s

η [=] Pa.s

k [=] W/(m.K)

T [=] °C

When u_{avg} = 15 cm/s, η = 700 Pa.s and k = 0.255 W/(m.K), $T = T_{max}$ = 206.3°C at the centre-line of the flow channel.

Bulk Temperature

$$T_{bulk} = \frac{\int_{-a}^{a} T(y)u(y)dy}{\int_{-a}^{a} u(y)dy} \tag{E.17}$$

By substituting Eqs. (E.13) and (E.16) into the above equation, the following expression for the limiting bulk temperature of a Newtonian fluid is obtained:

Limiting bulk temperature:

$$\boxed{T_{bulk} = \frac{32A}{35} + 160} \tag{E.18}$$

When u_{avg} = 15 cm/s, η = 700 Pa.s and k = 0.255 W/(m.K), T_{bulk} = 202.3°C

Local Nusselt Number

$$Nu_x = \frac{(\frac{dT}{dy})_{wall} \cdot 2a}{T_{bulk} - T_{wall}} \tag{E.19}$$

By substituting Eqs. (E.16) and (E.18) into the above equation, the following expression for the limiting local Nusselt number for a Newtonian fluid is obtained:

Limiting local Nusselt number:

$$\boxed{Nu_x = 8.75} \tag{E.20}$$

E.3 Poiseuille Flow Through a Tube with Circular Cross-section

Momentum Equation

$$- \frac{dp}{dz} + \frac{\eta}{r} \frac{d}{dr} (r \frac{du}{dr}) = 0 \qquad \text{(E.21)}$$

$$\begin{aligned} r &= 0 & u &= 2u_{avg} = 30 \text{ cm/s} \\ r &= a = 0.125 \text{ cm} & u &= 0 \end{aligned} \qquad \text{(E.22)}$$

By integrating Eq. (E.21) and using the accompanying boundary conditions (E.22), the following belocity profile is obtained for a Newtonian fluid:

Velocity profile:

$$\boxed{u(r) = 2u_{avg} [1 - (\frac{r}{a})^2]} \qquad \text{(E.23)}$$

where u, u_{avg} [=] cm/s

r, a [=] cm

Energy Equation

$$\frac{k}{r} \frac{d}{dr} (r \frac{dT}{dr}) + \eta (\frac{du}{dr})^2 = 0 \qquad \text{(E.24)}$$

$$r = a \qquad T = T_w = 160°C \qquad \text{(E.25)}$$

The fully developed temperature profile for a Newtonian fluid is obtained by integrating Eq. (E.24) and using the accompanying boundary condition (E.25).

Fully developed temperature profile:

$$T(r) = A[1 - (\frac{r}{a})^4] + 160 \tag{E.26}$$

where $A = 10^{-4} u_{avg}^2 \frac{\eta}{k}$

T [=] °C

u_{avg} [=] cm/s

η [=] Pa.s

k [=] W/(m.K)

When u_{avg} = 15 cm/s, η = 600 Pa.s and k = 0.255 W/(m.K), $T = T_{max}$ = 212.9°C at the centre-line of the tube.

Bulk Temperature

$$T_{bulk} = \frac{\int_o^a T(r)u(r)rdr}{\int_o^a u(r)rdr} \tag{E.27}$$

By substituting Eqs. (E.23) and (E.26) into the above equation, the following expression for the limiting bulk temperature of a Newtonian fluid is obtained:

Limiting bulk temperature:

$$\boxed{T_{bulk} = \frac{5A}{6} + 160} \tag{E.28}$$

When u_{avg} = 15 cm/s, η = 600 Pa.s and k = 0.255 W/(m.K), T_{bulk} = 204.1°C.

<u>Local Nusselt Number</u>

$$Nu_z = \frac{-(\frac{dT}{dr})_{wall} \cdot 2a}{T_{bulk} - T_{wall}} \tag{E.29}$$

By substituting Eqs. (E.26) and (E.28) into the above equation, the following expression is obtained for the limiting local Nusselt number for a Newtonian fluid:

Limiting local Nusselt number:

$$\boxed{Nu_z = 9.60} \tag{E.30}$$

E.4 Drag Flow Between Converging Plates

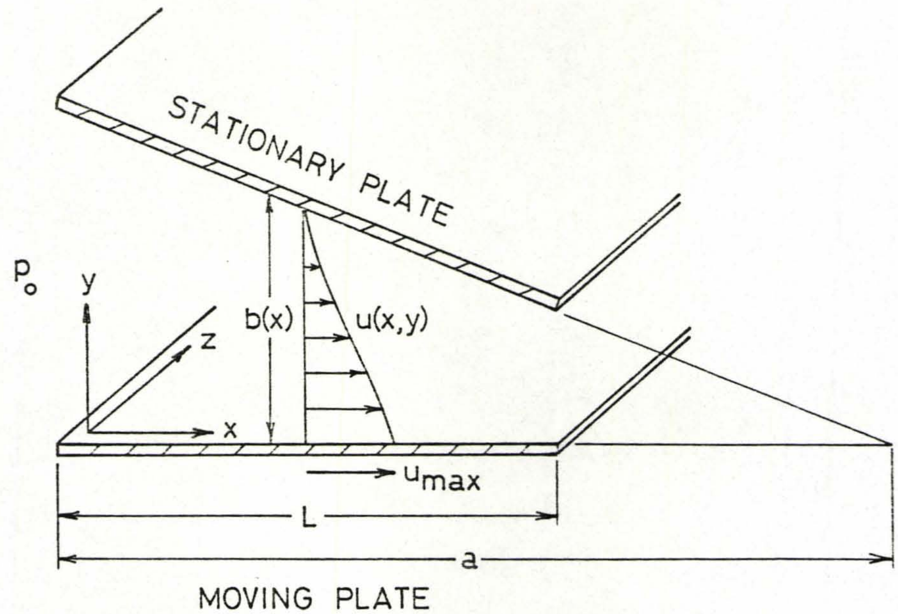

Fig. E-1. Drag flow between converging plates.

Schlichting (58) has obtained the following analytical expressions for the velocity profiles and the pressure distribution for drag flow of a Newtonian fluid between converging plates:

$$u(x,y) = u_{max}\left[1 - \frac{y}{b(x)}\right] - \frac{b(x)^2 p^I(x)}{2\eta} \cdot \frac{y}{b(x)}\left[1 - \frac{y}{b(x)}\right] \quad (E.31)$$

where $p^I(x) = \frac{dp(x)}{dx}$

$$p(x) = p_o + 6\eta \; u_{max} \frac{x(L-x)}{b(x)^2(2a-L)} \quad (E.32)$$

The analytical and finite difference solutions for the pressure distribution in the flow channel are compared in Table E-1. The finite difference grid has been divided into 25 steps in the X-direction and 50 steps in the Y-direction at the entrance of the channel.

Table D-1. Pressure distribution for drag flow of a Newtonian fluid between converging plates. $p_0 = 0$, $\eta = 200$ Pa·s, $u_{max} = 15$ cm/s, L = 10 cm, a = 20 cm, $b_0 = 0.025$ cm.

	p, MPa	
x, cm	Analytical	Finite differences
0	0	0
2	18.96	18.31
4	36.00	34.66
6	47.02	45.11
8	42.67	40.75
10	0	0

In the above table, the analytical and finite difference results differ by less than 4%.

APPENDIX F

PROGRAM LISTINGS

F.1 Drag Flow Between Parallel Plates

```
      PROGRAM TST (INPUT,OUTPUT,TAPE5=INPUT,TAPE6=OUTPUT)
C*********************************************************************
C                                                                    *
C     APPENDIX F.1  DRAG FLOW BETWEEN PARALLEL PLATES                *
C                                                                    *
C                   TO=130 C    TW1=160 C    TW2=160 C               *
C                                                                    *
C*********************************************************************
C
C     DIMENSION OF U1,U2,THETA,THETA1,THETA2,ETA,DUDY,ALPHA = M+1
C     DIMENSION OF DETADY,A,B,C,D,E,F,G,H,Q,S,T = M
C
C     M = NUMBER OF GRID DIVISIONS ALONG Y-AXIS
C     MX = INTERVAL AT WHICH VALUES ALONG Y-AXIS ARE PRINTED
C     TEMPO = FLUID TEMPERATURE AT CHANNEL INLET , K
C     TEMPW1 = WALL TEMPERATURE AT Y=0 , K
C     TEMPW2 = WALL TEMPERATURE AT Y=1 , K
C     TEMPM = MELTING TEMPERATURE OF POLYMER , K
C     PN = POWER-LAW INDEX , DIMENSIONLESS
C     UMAX = VELOCITY OF MOVING PLATE , CM/S
C     DX = DELTA X AT X=0 , DIMENSIONLESS
C     N = NUMBER OF GRID DIVISIONS ALONG X-AXIS
C     NA - DX IS INCREASED BY A FACTOR OF 10 AFTER THE NA-TH COLUMN
C     NB - DX IS INCREASED BY A FACTOR OF 10 AFTER THE NB-TH COLUMN
C     NX = INTERVAL AT WHICH VALUES ALONG X-AXIS ARE PRINTED
C     K = THERMAL CONDUCTIVITY OF FLUID , CAL/CM S K
C     DEN = DENSITY OF FLUID , G/CM3
C     CP = SPECIFIC HEAT OF FLUID , CAL/G K
C     RL = LENGTH OF CHANNEL , CM
C     RB = DISTANCE BETWEEN PLATES , CM
C
      REAL U1(101),U2(101),THETA(101),THETA1(101),THETA2(101),ETA(101)
      REAL DETADY(100),DUDY(101),ALPHA(101),A(100),B(100),C(100),D(100)
      REAL E(100),F(100),G(100),H(100),Q(100),S(100),T(100),K,NU1,NU2
      READ *,M,MX,TEMPO,TEMPW1,TEMPW2,TEMPM,PN,UMAX,DX,N,NA,NB,NX,K,
     1DEN,CP,RL,RB
      PRINT 100
  100 FORMAT(≠1≠,10X,≠COUETTE FLOW WITH CONVECTIVE TERM  POWER LAW FLUID
     1≠/)
      PRINT 101
  101 FORMAT(≠ ≠,12X,≠TEMPERATURE DEPENDENT VISCOSITY≠//)
      PRINT 102,M,TEMPO,TEMPW1,TEMPW2
  102 FORMAT(≠ ≠,10X,≠M=≠,I4,3X,≠TEMPO=≠,F6.1,≠ K≠,3X,≠TEMPW1=≠,
     1F6.1,≠ K≠,3X,≠TEMPW2=≠,F6.1,≠ K≠/)
      PRINT 103,PN,UMAX,K
  103 FORMAT(≠ ≠,10X,≠POWER LAW INDEX=≠,F5.3,3X,≠UMAX=≠,F4.1,≠ CM/SEC≠,
     13X,≠K=≠,F7.5,≠ CAL/CM SEC K≠/)
      PRINT 104,DEN,CP,RL,RB
  104 FORMAT(≠ ≠,10X,≠DENSITY=≠,F5.3,≠ G/CM3≠,3X,≠CP=≠,F4.2,≠ CAL/G K≠
     1,3X,≠L=≠,F4.1,≠ CM≠,3X,≠B=≠,F4.2,≠ CM≠/)
      XL=K*RL/DEN/CP/UMAX/RB**2
      PRINT 105,DX,XL
  105 FORMAT(≠ ≠,10X,≠DX=≠,F6.4,3X,≠X AT L=≠,F7.5/)
      PRINT 106,DX*10.,NA*DX
  106 FORMAT(≠ ≠,10X,≠DX=≠,F6.4,≠ AFTER X=≠,F6.3//)
      NO=0
      MI=M+1
      MJ=M-1
      MK=M-2
      DY=1./M
C
C     PRINT INITIAL VELOCITY AND TEMPERATURE PROFILES
C
      X=0.
      PRINT 108,NO,X
  108 FORMAT(≠ ≠,10X,≠N=≠,I4,3X,≠X=≠,F4.2/)
      PRINT 109
  109 FORMAT(≠ ≠,14X,≠Y≠,8X,≠U(Y)≠,4X,≠U(Y)*UMAX≠,4X,≠THETA(Y)≠,4X,
     1≠TEMP(Y)≠/)
      Y=0.
      DO 1 I=1,MI
      U1(I)=Y
      THETA1(I)=THETA(I)=1.
      Y=Y+DY
    1 CONTINUE
      Y=0.
```

```
      DO 2 I=1,MI,MX
      TEMP=THETA1(I)*(TEMP0-TEMPW1)+TEMPW1
      PRINT 110,Y,U1(I),U1(I)*UMAX,THETA1(I),TEMP
110   FORMAT(≠ ≠,F16.3,F11.4,F12.4,F12.4,F11.1)
      Y=Y+MX*DY
2     CONTINUE
      U2(1)=0.
      U2(MI)=1.
      THETA2(1)=0.
      THETA2(MI)=(TEMPW2-TEMPW1)/(TEMP0-TEMPW1)
      LL=0
      DO 26 LA=1,N
      IF(LA.EQ.NA+1) GO TO 3
      GO TO 4
3     DX=DX*10.
      NX=NX/10
4     CONTINUE
      IF(LA.EQ.NB+1) GO TO 5
      GO TO 6
5     DX=DX*10.
      NX=NX/10
6     CONTINUE
      LB=0
7     CONTINUE
      LB=LB+1
      IF(LB.EQ.40) GO TO 27
C
C     SOLVE SET OF ENERGY EQS.(4.19)
C
      DUDY(1)=(2.*U1(4)-9.*U1(3)+18.*U1(2)-11.*U1(1))/6./DY
      DUDY(2)=(-U1(4)+6.*U1(3)-3.*U1(2)-2.*U1(1))/6./DY
      DO 8 I=3,MJ
      DUDY(I)=(-U1(I+2)+8.*U1(I+1)-8.*U1(I-1)+U1(I-2))/12./DY
8     CONTINUE
      DUDY(M)=(2.*U1(MI)+3.*U1(M)-6.*U1(MJ)+U1(MK))/6./DY
      DUDY(MI)=(11.*U1(MI)-18.*U1(M)+9.*U1(MJ)-2.*U1(M-2))/6./DY
      DO 10 I=1,MI
      ALPHA(I)=2.*DY**2/DX*U1(I)
      TEMP=THETA1(I)*(TEMP0-TEMPW1)+TEMPW1
      ETA(I)=282000.*EXP(-.024*PN*(TEMP-TEMPM))*(ABS(DUDY(I)*UMAX
     1/RB))**(PN-1.)
10    CONTINUE
      BETA=2.3901*10.**(-8)*UMAX**2/(TEMP0-TEMPW1)/K
      B(2)=ALPHA(2)+2.
      C(2)=-1.
      E(2)=(ALPHA(2)-2.)*THETA(2)
      F(2)=THETA(3)
      G(2)=2.*DY**2*BETA*ETA(2)*DUDY(2)**2+THETA(1)+THETA2(1)
      H(2)=E(2)+F(2)+G(2)
      DO 11 I=3,MJ
      A(I)=-1.
      B(I)=ALPHA(I)+2.
      C(I)=-1.
      D(I)=THETA(I-1)
      E(I)=(ALPHA(I)-2.)*THETA(I)
      F(I)=THETA(I+1)
      G(I)=2.*DY**2*BETA*ETA(I)*DUDY(I)**2
      H(I)=D(I)+E(I)+F(I)+G(I)
11    CONTINUE
      A(M)=-1.
      B(M)=ALPHA(M)+2.
      D(M)=THETA(M-1)
      E(M)=(ALPHA(M)-2.)*THETA(M)
      G(M)=2.*DY**2*BETA*ETA(M)*DUDY(M)**2+THETA(MI)+THETA2(MI)
      H(M)=D(M)+E(M)+G(M)
      S(2)=B(2)
      T(2)=H(2)/S(2)
      DO 12 I=3,M
      Q(I-1)=C(I-1)/S(I-1)
      S(I)=B(I)-A(I)*Q(I-1)
      T(I)=(H(I)-A(I)*T(I-1))/S(I)
12    CONTINUE
      THETA2(M)=T(M)
      L=MJ
      DO 13 I=2,MJ
      THETA2(L)=T(L)-Q(L)*THETA2(L+1)
13    CONTINUE
C
C     SOLVE SET OF MOMENTUM EQS.(4.14)
C
      DO 14 I=1,MI
      TEMP=THETA2(I)*(TEMP0-TEMPW1)+TEMPW1
      ETA(I)=282000.*EXP(-.024*PN*(TEMP-TEMPM))*(ABS(DUDY(I)*UMAX
     1/RB))**(PN-1.)
```

```
14    CONTINUE
      DETADY(2)=(-ETA(4)+6.*ETA(3)-3.*ETA(2)-2.*ETA(1))/6./DY
      ALPHA(2)=0.5*DY*DETADY(2)/ETA(2)
      DO 15 I=3,MJ
      DETADY(I)=(-ETA(I+2)+8.*ETA(I+1)-8.*ETA(I-1)+ETA(I-2))/12./DY
      ALPHA(I)=0.5*DY*DETADY(I)/ETA(I)
15    CONTINUE
      DETADY(M)=(2.*ETA(MI)+3.*ETA(M)-6.*ETA(MJ)+ETA(M-2))/6./DY
      ALPHA(M)=0.5*DY*DETADY(M)/ETA(M)
      B(2)=-2.
      C(2)=ALPHA(2)+1.
      H(2)=(ALPHA(2)-1.)*U1(1)
      DO 16 I=3,MJ
      A(I)=-ALPHA(I)+1.
      B(I)=-2.
      C(I)=ALPHA(I)+1.
      H(I)=0.
16    CONTINUE
      A(M)=-ALPHA(M)+1.
      B(M)=-2.
      H(M)=-(ALPHA(M)+1.)*U1(MI)
      S(2)=B(2)
      T(2)=H(2)/S(2)
      DO 17 I=3,M
      Q(I-1)=C(I-1)/S(I-1)
      S(I)=B(I)-A(I)*Q(I-1)
      T(I)=(H(I)-A(I)*T(I-1))/S(I)
17    CONTINUE
      U2(M)=T(M)
      L=MJ
      DO 18 I=2,MJ
      U2(L)=T(L)-Q(L)*U2(L+1)
18    CONTINUE
C
C     CHECK U2 AND THETA2 FOR CONVERGENCE
C
      DO 19 I=2,M
      IF(ABS(U2(I)-U1(I)).GE..001) GO TO 20
      IF(ABS(THETA2(I)-THETA1(I)).GE..001) GO TO 20
19    CONTINUE
      GO TO 22
20    CONTINUE
      DO 21 I=1,MI
      U1(I)=U2(I)
      THETA1(I)=THETA2(I)
21    CONTINUE
      GO TO 7
22    CONTINUE
      X=X+DX
      IF(LL-NX.NE.0) GO TO 25
      LL=0
C
C      PRINT VELOCITY,TEMPERATURE AND VISCOSITY PROFILES
C
      PRINT 111,LA,X
111   FORMAT(≠1≠,10X,≠N=≠,I6,3X,≠X=≠,F7.4/)
      PRINT 112
112   FORMAT(≠ ≠,14X,≠Y≠,8X,≠U(Y)≠,4X,≠U(Y)*UMAX≠,4X,≠THETA(Y)≠,4X,
     1≠TEMP(Y)≠,3X,≠ETA  (POISE)≠/)
      Y=0.
      DO 23 I=1,MI,MX
      TEMP=THETA2(I)*(TEMP0-TEMPW1)+TEMPW1
      PRINT 113,Y,U2(I),U2(I)*UMAX,THETA2(I),TEMP,ETA(I)
113   FORMAT(≠ ≠,F16.3,F11.4,F12.4,F12.4,F11.1,F12.1)
      Y=Y+MX*DY
23    CONTINUE
C
C     CALCULATE BULK TEMPERATURE AND LOCAL NUSSELT NUMBERS
C
      AREA1=AREA2=0.
      DO 24 I=3,MI,2
      A1=(THETA2(I-2)*U2(I-2)+4.*THETA2(I-1)*U2(I-1)+THETA2(I)*U2(I))
     1*DY/3.
      A2=(U2(I-2)+4.*U2(I-1)+U2(I))*DY/3.
      AREA1=AREA1+A1
      AREA2=AREA2+A2
24    CONTINUE
      THETAB=AREA1/AREA2
      DTHDY1=(2.*THETA2(4)-9.*THETA2(3)+18.*THETA2(2)-11.*THETA2(1))
     1/6./DY
      DTHDY2=(11.*THETA2(MI)-18.*THETA2(M)+9.*THETA2(MJ)-2.*THETA2(MK))
     1/6./DY
      NU1=DTHDY1/THETAB
```

```
      NU2=-DTHDY2/(THETAB-THETA2(MI))
      PRINT 114,THETAB,THETAB*(TEMP0-TEMPW1)+TEMPW1
114   FORMAT(≠-≠,10X,≠THETABULK=≠,F7.4,3X,≠BULK TEMP=≠,F6.1,≠ K≠/)
      PRINT 115,NU1,NU2
115   FORMAT(≠ ≠,10X,≠LOCAL NUSSELT NO AT M=1 =≠,F7.2,3X,≠AT M=MI =≠
     1,F7.2/)
      PRINT 116,LB
116   FORMAT(≠ ≠,10X,≠NO OF ITERATIONS =≠,I3)
25    CONTINUE
      DO 26 I=1,MI
      U1(I)=U2(I)
      THETA(I)=THETA1(I)=THETA2(I)
26    CONTINUE
      GO TO 28
27    PRINT 117,LA
117   FORMAT(≠-≠,10X,≠PROGRAM STOPPED AT N=≠,I4)
28    STOP
      END
```

COUETTE FLOW WITH CONVECTIVE TERM POWER LAW FLUID
TEMPERATURE DEPENDENT VISCOSITY

M= 60 TEMPC= 403.0 K TEMPW1= 433.0 K TEMPW2= 433.0 K

POWER LAW INDEX= .453 UMAX=15.0 CM/SEC K= .00061 CAL/CM SEC K

DENSITY= .794 G/CM3 CP= .60 CAL/G K L= 5.0 CM B= .25 CM

DX= .0001 X AT L= .00683

DX= .0010 AFTER X= .100

N= 0 X=0.00

Y	U(Y)	U(Y)*UMAX	THETA(Y)	TEMP(Y)
0.000	0.0000	0.0000	1.0000	403.0
.050	.0500	.7500	1.0000	403.0
.100	.1000	1.5000	1.0000	403.0
.150	.1500	2.2500	1.0000	403.0
.200	.2000	3.0000	1.0000	403.0
.250	.2500	3.7500	1.0000	403.0
.300	.3000	4.5000	1.0000	403.0
.350	.3500	5.2500	1.0000	403.0
.400	.4000	6.0000	1.0000	403.0
.450	.4500	6.7500	1.0000	403.0
.500	.5000	7.5000	1.0000	403.0
.550	.5500	8.2500	1.0000	403.0
.600	.6000	9.0000	1.0000	403.0
.650	.6500	9.7500	1.0000	403.0
.700	.7000	10.5000	1.0000	403.0
.750	.7500	11.2500	1.0000	403.0
.800	.8000	12.0000	1.0000	403.0
.850	.8500	12.7500	1.0000	403.0
.900	.9000	13.5000	1.0000	403.0
.950	.9500	14.2500	1.0000	403.0
1.000	1.0000	15.0000	1.0000	403.0

N= 500 X= .0500

Y	U(Y)	U(Y)*UMAX	THETA(Y)	TEMP(Y)	ETA (POISE)
0.000	0.0000	0.0000	0.0000	433.0	20948.9
.050	.0506	.7594	-.0528	434.6	20166.8
.100	.1029	1.5437	-.0900	435.7	19636.2
.150	.1563	2.3449	-.1119	436.4	19330.1
.200	.2103	3.1544	-.1193	436.6	19228.7
.250	.2643	3.9642	-.1136	436.4	19308.3
.300	.3178	4.7675	-.0971	435.9	19541.5
.350	.3706	5.5536	-.0722	435.2	19996.2
.400	.4223	6.3340	-.0420	434.3	20334.6
.450	.4728	7.0920	-.0097	433.3	20813.8
.500	.5222	7.8326	.0214	432.4	21287.0
.550	.5705	8.5577	.0485	431.5	21707.3
.600	.6180	9.2703	.0691	430.9	22032.0
.650	.6650	9.9745	.0814	430.6	22227.6
.700	.7117	10.6748	.0846	430.5	22277.0
.750	.7584	11.3756	.0786	430.6	22180.8
.800	.8055	12.0820	.0649	431.1	21961.5
.850	.8531	12.7967	.0460	431.6	21662.0
.900	.9015	13.5219	.0255	432.2	21342.4
.950	.9505	14.2574	.0083	432.8	21076.7
1.000	1.0000	15.0000	0.0000	433.0	20948.1

THETABULK= .0209 BULK TEMP= 432.4 K

LOCAL NUSSELT NO AT M=1 = -57.83 AT M=MI = 1.69

NO OF ITERATIONS = 2

N= 100 X= .0100

Y	U(Y)	U(Y)*UMAX	THETA(Y)	TEMP(Y)	ETA (POISE)
0.000	0.0000	0.0000	0.0000	433.0	16985.3
.050	.0715	1.0721	.0548	431.4	17673.8
.100	.1396	2.0933	.1336	429.0	18710.1
.150	.2034	3.0512	.2311	426.1	20076.7
.200	.2627	3.9398	.3399	422.3	21719.1
.250	.3173	4.7599	.4515	419.5	23540.8
.300	.3678	5.5177	.5575	416.3	25410.5
.350	.4146	6.2226	.6512	413.5	27184.0
.400	.4590	6.8853	.7284	411.1	28735.8
.450	.5011	7.5162	.7877	409.4	29985.5
.500	.5416	8.1247	.8299	408.1	30965.0
.550	.5812	8.7183	.8566	407.3	31503.2
.600	.6202	9.3037	.8694	406.9	31793.0
.650	.6591	9.8866	.8676	407.0	31754.2
.700	.6983	10.4739	.8477	407.6	31307.1
.750	.7383	11.0746	.8026	408.9	30313.3
.800	.7802	11.7024	.7227	411.3	28625.2
.850	.8252	12.3777	.5991	415.0	26189.8
.900	.8752	13.1287	.4287	420.1	23161.4
.950	.9327	13.9909	.2206	426.4	19927.2
1.000	1.0000	15.0000	0.0000	433.0	16984.2

THETABULK= .6108 BULK TEMP= 414.7 K

LOCAL NUSSELT NO AT M=1 = 1.37 AT M=MI = 7.03

NO OF ITERATIONS = 2

N= 1000 X= .1000

Y	U(Y)	U(Y)*UMAX	THETA(Y)	TEMP(Y)	ETA (POISE)
0.000	0.0000	0.0000	0.0000	433.0	23513.8
.050	.0417	.6253	-.0998	436.0	21854.7
.100	.0863	1.2942	-.1576	438.6	20544.3
.150	.1336	2.0036	-.2629	440.9	19460.6
.200	.1833	2.7490	-.3254	442.8	18606.0
.250	.2350	3.5250	-.3748	444.2	17956.2
.300	.2884	4.3253	-.4114	445.3	17490.0
.350	.3429	5.1432	-.4357	446.1	17188.3
.400	.3981	5.9720	-.4482	446.4	17034.0
.450	.4537	6.8050	-.4501	446.5	17011.8
.500	.5091	7.6361	-.4424	446.3	17107.3
.550	.5640	8.4601	-.4262	445.8	17308.2
.600	.6182	9.2723	-.4027	445.1	17603.7
.650	.6713	10.0689	-.3729	444.2	17986.0
.700	.7231	10.8471	-.3374	443.1	18450.6
.750	.7736	11.6043	-.2967	441.9	18998.0
.800	.8226	12.3383	-.2509	440.5	19635.0
.850	.8698	13.0470	-.1993	439.0	20375.9
.900	.9152	13.7285	-.1412	437.2	21244.3
.950	.9587	14.3803	-.0753	435.3	22274.5
1.000	1.0000	15.0000	0.0000	433.0	23513.1

THETABULK= -.2855 BULK TEMP= 441.6 K

LOCAL NUSSELT NO AT M=1 = 7.39 AT M=MI = 5.64

NO OF ITERATIONS = 1

N= 1050 X= .1500

Y	U(Y)	U(Y)*UMAX	THETA(Y)	TEMP(Y)	ETA (POISE)
0.000	0.0000	0.0000	0.0000	433.0	24572.0
.050	.0387	.5804	-.1167	436.5	22592.8
.100	.0806	1.2092	-.2226	439.7	20935.1
.150	.1257	1.8850	-.3169	442.5	19561.3
.200	.1737	2.6050	-.3990	445.0	18439.9
.250	.2244	3.3654	-.4682	447.0	17544.2
.300	.2774	4.1607	-.5242	448.7	16852.5
.350	.3323	4.9846	-.5666	450.0	16346.7
.400	.3887	5.8299	-.5954	450.9	16012.6
.450	.4459	6.6885	-.6106	451.3	15839.2
.500	.5035	7.5524	-.6124	451.4	15818.3
.550	.5609	8.4134	-.6014	451.0	15944.9
.600	.6176	9.2637	-.5779	450.3	16216.8
.650	.6731	10.0962	-.5426	449.3	16634.6
.700	.7270	10.9045	-.4959	447.9	17202.6
.750	.7789	11.6831	-.4384	446.2	17928.6
.800	.8285	12.4273	-.3706	444.1	18825.0
.850	.8756	13.1336	-.2927	441.8	19909.4
.900	.9199	13.7990	-.2049	439.1	21205.8
.950	.9614	14.4216	-.1074	436.2	22746.2
1.000	1.0000	15.0000	0.0000	433.0	24571.6

THETABULK= -.3995 BULK TEMP= 445.0 K

LOCAL NUSSELT NO AT M=1 = 6.10 AT M=MI = 5.62

NO OF ITERATIONS = 2

N= 1100 X= .2000

Y	U(Y)	U(Y)*UMAX	THETA(Y)	TEMP(Y)	ETA (POISE)
0.000	0.0000	0.0000	0.0000	433.0	24976.2
.050	.0376	.5646	-.1228	436.7	22863.6
.100	.0786	1.1790	-.2352	440.1	21086.9
.150	.1228	1.8426	-.3364	443.1	19606.2
.200	.1702	2.5531	-.4256	445.8	18388.2
.250	.2205	3.3073	-.5020	448.1	17405.2
.300	.2733	4.1002	-.5649	449.9	16634.7
.350	.3284	4.9256	-.6140	451.4	16058.6
.400	.3851	5.7765	-.6487	452.5	15663.1
.450	.4429	6.6441	-.6689	453.1	15438.0
.500	.5013	7.5198	-.6744	453.2	15376.9
.550	.5596	8.3944	-.6655	453.0	15476.9
.600	.6173	9.2588	-.6422	452.3	15738.2
.650	.6736	10.1047	-.6050	451.2	16164.9
.700	.7283	10.9242	-.5544	449.6	16764.5
.750	.7807	11.7108	-.4909	447.7	17548.3
.800	.8306	12.4589	-.4150	445.5	18532.3
.850	.8776	13.1643	-.3274	442.8	19737.1
.900	.9216	13.8240	-.2286	439.9	21189.4
.950	.9624	14.4362	-.1193	436.6	22922.0
1.000	1.0000	15.0000	0.0000	433.0	24976.1

THETABULK= -.4414 BULK TEMP= 446.2 K

LOCAL NUSSELT NO AT M=1 = 5.79 AT M=MI = 5.63

NO OF ITERATIONS = 1

F.2 Poiseuille Flow Between Parallal Plates

```
      PROGRAM TST (INPUT,OUTPUT,TAPE5=INPUT,TAPE6=OUTPUT)
C****************************************************************************
C                                                                          *
C     APPENDIX F.2  POISEUILLE FLOW BETWEEN PARALLEL PLATES                *
C                                                                          *
C                   T0=130 C    TW1=160 C    TW2=160 C                     *
C                                                                          *
C****************************************************************************
C
C     DIMENSION OF U1,U2,THETA,THETA1,THETA2,ETA,DUDY,ALPHA,BETA = M+1
C     DIMENSION OF DETADY,A,B,C,D,E,F,G,H,Q,S,T,W = M
C     DIMENSION OF Z = M+2
C
C     M = NUMBER OF GRID DIVISIONS ALONG Y-AXIS
C     MX = INTERVAL AT WHICH VALUES ALONG Y-AXIS ARE PRINTED
C     TEMP0 = FLUID TEMPERATURE AT CHANNEL INLET , K
C     TEMPW1 = WALL TEMPERATURE AT Y=0 , K
C     TEMPW2 = WALL TEMPERATURE AT Y=1 , K
C     TEMPM = MELTING TEMPERATURE OF POLYMER , K
C     PN = POWER-LAW INDEX , DIMENSIONLESS
C     UAVG = AVERAGE VELOCITY OF FLUID , CM/S
C     P0 = FLUID PRESSURE AT CHANNEL INLET , DYNE/CM2
C     DX = DELTA X AT X=0 , DIMENSIONLESS
C     N = NUMBER OF GRID DIVISIONS ALONG X-AXIS
C     NA - DX IS INCREASED BY A FACTOR OF 10 AFTER THE NA-TH COLUMN
C     NB - DX IS INCREASED BY A FACTOR OF 10 AFTER THE NB-TH COLUMN
C     NX = INTERVAL AT WHICH VALUES ALONG X-AXIS ARE PRINTED
C     K = THERMAL CONDUCTIVITY OF FLUID , CAL/CM S K
C     DEN = DENSITY OF FLUID , G/CM3
C     CP = SPECIFIC HEAT OF FLUID , CAL/G K
C     RL = LENGTH OF CHANNEL , CM
C     RB = DISTANCE BETWEEN PLATES , CM
C
C****************************************************************************
      REAL U1(201),U2(201),THETA(201),THETA1(201),THETA2(201),ETA(201)
      REAL DETADY(200),DUDY(201),ALPHA(201),BETA(201),A(200),B(200)
      REAL C(200),D(200),E(200),F(200),G(200),H(200),Q(200),S(200)
      REAL T(200),W(200),Z(202),K,NU1,NU2
      READ *,M,MX,TEMP0,TEMPW1,TEMPW2,TEMPM,PN,UAVG,P0,DX,N,NA,NB,NX,K
     1,DEN,CP,RL,RB
      PRINT 100
100   FORMAT(≠1≠,10X,≠FLOW BETWEEN PARALLEL PLATES WITH CONVECTIVE TERM≠
     1/)
      PRINT 101
101   FORMAT(≠ ≠,10X,≠POWER LAW FLUID - TEMPERATURE DEPENDENT VISCOSITY≠
     1//)
      PRINT 102,M,TEMP0,TEMPW1,TEMPW2
102   FORMAT(≠ ≠,10X,≠M=≠,I4,3X,≠TEMP0=≠,F6.1,≠ K≠,3X,≠TEMPW1=≠,
     1F6.1,≠ K≠,3X,≠TEMPW2=≠,F6.1,≠ K≠/)
      PRINT 103,PN,UAVG,K
103   FORMAT(≠ ≠,10X,≠POWER LAW INDEX=≠,F5.3,3X,≠UAVG=≠,F4.1,≠ CM/SEC≠,
     13X,≠K=≠,F7.5,≠ CAL/CM SEC K≠/)
      PRINT 104,DEN,CP,RL,RB
104   FORMAT(≠ ≠,10X,≠DENSITY=≠,F5.3,≠ G/CM3≠,3X,≠CP=≠,F4.2,≠ CAL/G K≠
     1,3X,≠L=≠,F4.1,≠ CM≠,3X,≠B=≠,F4.2,≠ CM≠/)
      XL=K*RL/DEN/CP/UAVG/RB**2
      PRINT 105,DX,XL
105   FORMAT(≠ ≠,10X,≠DX=≠,F6.4,3X,≠X AT L=≠,F7.5/)
      PRINT 106,DX*10.,NA*DX
106   FORMAT(≠ ≠,10X,≠DX=≠,F6.4,≠ AFTER X=≠,F5.2/)
      PRINT 107,DX*100.,NA*DX+(NB-NA)*DX*10.
107   FORMAT(≠ ≠,10X,≠DX=≠,F6.4,≠ AFTER X=≠,F5.2//)
      N0=0
      MI=M+1
      MJ=M-1
      MK=M-2
      DY=1./M
      P=P0/DEN/UAVG**2
C
C     PRINT INITIAL VELOCITY AND TEMPERATURE PROFILES
C
      X=0.
      PRINT 108,N0,X
108   FORMAT(≠ ≠,10X,≠N=≠,I4,3X,≠X=≠,F4.2/)
      PRINT 109
109   FORMAT(≠ ≠,14X,≠Y≠,8X,≠U(Y)≠,4X,≠U(Y)*UAVG≠,4X,≠THETA(Y)≠,4X,
     1≠TEMP(Y)≠/)
```

```
      V=(PN+1.)/PN
      Y=0.
      DO 1 I=1,MI
      U1(I)=-2.**V*(V+1.)/V*(ABS(Y-.5))**V+(V+1.)/V
      THETA1(I)=THETA(I)=1.
      Y=Y+DY
1     CONTINUE
      Y=0.
      DO 2 I=1,MI,MX
      TEMP=THETA1(I)*(TEMP0-TEMPW1)+TEMPW1
      PRINT 110,Y,U1(I),U1(I)*UAVG,THETA1(I),TEMP
110   FORMAT(≠ ≠,F16.3,F11.4,F12.4,F12.4,F11.1)
      Y=Y+MX*DY
2     CONTINUE
      U2(1)=U2(MI)=0.
      THETA2(1)=0.
      THETA2(MI)=(TEMPW2-TEMPW1)/(TEMP0-TEMPW1)
      LL=0
      DO 34 LA=1,N
      IF(LA.EQ.NA+1) GO TO 3
      GO TO 4
3     DX=DX*10.
      NX=NX/10
4     CONTINUE
      IF(LA.EQ.NB+1) GO TO 5
      GO TO 6
5     DX=DX*10.
      NX=NX/10
6     CONTINUE
      LB=0
7     CONTINUE
      LB=LB+1
      IF(LB.EQ.40) GO TO 35
C
C     SOLVE SET OF ENERGY EQS.(5.25)
C
      DUDY(1)=(2.*U1(4)-9.*U1(3)+18.*U1(2)-11.*U1(1))/6./DY
      DUDY(2)=(-U1(4)+6.*U1(3)-3.*U1(2)-2.*U1(1))/6./DY
      DO 8 I=3,MJ
      DUDY(I)=(-U1(I+2)+8.*U1(I+1)-8.*U1(I-1)+U1(I-2))/12./DY
8     CONTINUE
      DUDY(M)=(2.*U1(MI)+3.*U1(M)-6.*U1(MJ)+U1(MK))/6./DY
      DUDY(MI)=(11.*U1(MI)-18.*U1(M)+9.*U1(MJ)-2.*U1(MK))/6./DY
      DO 10 I=1,MI
      TEMP=THETA1(I)*(TEMP0-TEMPW1)+TEMPW1
      IF(ABS(DUDY(I)*UAVG/RB).LT.1.) GO TO 9
      ETA(I)=282000.*EXP(-.024*PN*(TEMP-TEMPM))*(ABS(DUDY(I)*UAVG
     1/RB))**(PN-1.)
      ALPHA(I)=2.*DY**2/DX*U1(I)
      BETA(I)=2.3901*10.**(-8)*ETA(I)*UAVG**2/(TEMP0-TEMPW1)/K
     1*DUDY(I)**2
      GO TO 10
9     CONTINUE
      ETA(I)=282000.*EXP(-.024*PN*(TEMP-TEMPM))
      ALPHA(I)=2.*DY**2/DX*U1(I)
      BETA(I)=2.3901*10.**(-8)*ETA(I)*UAVG**2/(TEMP0-TEMPW1)/K
     1*DUDY(I)**2
10    CONTINUE
      B(2)=ALPHA(2)+2.
      C(2)=-1.
      E(2)=(ALPHA(2)-2.)*THETA(2)
      F(2)=THETA(3)
      G(2)=2.*DY**2*BETA(2)+THETA(1)
      H(2)=E(2)+F(2)+G(2)
      DO 11 I=3,MJ
      A(I)=-1.
      B(I)=ALPHA(I)+2.
      C(I)=-1.
      D(I)=THETA(I-1)
      E(I)=(ALPHA(I)-2.)*THETA(I)
      F(I)=THETA(I+1)
      G(I)=2.*DY**2*BETA(I)
      H(I)=D(I)+E(I)+F(I)+G(I)
11    CONTINUE
      A(M)=-1.
      B(M)=ALPHA(M)+2.
      D(M)=THETA(MJ)
      E(M)=(ALPHA(M)-2.)*THETA(M)
      G(M)=2.*DY**2*BETA(M)+THETA(MI)+THETA2(MI)
      H(M)=D(M)+E(M)+G(M)
      S(2)=B(2)
      T(2)=H(2)/S(2)
      DO 12 I=3,M
      Q(I-1)=C(I-1)/S(I-1)
      S(I)=B(I)-A(I)*Q(I-1)
      T(I)=(H(I)-A(I)*T(I-1))/S(I)
```

```
12    CONTINUE
      THETA2(M)=T(M)
      L=MJ
      DO 13 I=2,MJ
      THETA2(L)=T(L)-Q(L)*THETA2(L+1)
13    CONTINUE
C
C     SOLVE SET OF CONTINUITY AND MOMENTUM EQS.(5.19)
C
      DO 15 I=1,MI
      TEMP=THETA2(I)*(TEMPO-TEMPW1)+TEMPW1
      IF(ABS(DUDY(I)*UAVG/RB).LT.1.) GO TO 14
      ETA(I)=282000.*EXP(-.024*PN*(TEMP-TEMPM))*(ABS(DUDY(I)*UAVG
     1/RB))**(PN-1.)
      GO TO 15
14    CONTINUE
      ETA(I)=282000.*EXP(-.024*PN*(TEMP-TEMPM))
15    CONTINUE
      DETADY(2)=(-ETA(4)+6.*ETA(3)-3.*ETA(2)-2.*ETA(1))/6./DY
      ALPHA(2)=0.5*DY*DETADY(2)/ETA(2)
      BETA(2)=DY**2/DX*K/ETA(2)/CP
      DO 16 I=3,MJ
      IF(ABS(DUDY(I+1)*UAVG/RB).LE.1.) GO TO 17
      DETADY(I)=(-ETA(I+2)+8.*ETA(I+1)-8.*ETA(I-1)+ETA(I-2))/12./DY
      ALPHA(I)=0.5*DY*DETADY(I)/ETA(I)
      BETA(I)=DY**2/DX*K/ETA(I)/CP
16    CONTINUE
17    CONTINUE
      DETADY(I)=(2.*ETA(I+1)+3.*ETA(I)-6.*ETA(I-1)+ETA(I-2))/6./DY
      ALPHA(I)=0.5*DY*DETADY(I)/ETA(I)
      BETA(I)=DY**2/DX*K/ETA(I)/CP
      DETADY(I+1)=(11.*ETA(I+1)-18.*ETA(I)+9.*ETA(I-1)-2.*ETA(I-2))
     1/6./DY/2.
      ALPHA(I+1)=0.5*DY*DETADY(I+1)/ETA(I+1)
      BETA(I+1)=DY**2/DX*K/ETA(I+1)/CP
      IA=I+2
      DO 18 I=IA,MI
      IF(ABS(DUDY(I+1)*UAVG/RB).GE.1.) GO TO 19
      DETADY(I)=0.
      ALPHA(I)=0.
      BETA(I)=DY**2/DX*K/ETA(I)/CP
18    CONTINUE
19    CONTINUE
      DETADY(I)=(2.*ETA(I+3)-9.*ETA(I+2)+18.*ETA(I+1)-11.*ETA(I))/6.
     1/DY/2.
      ALPHA(I)=0.5*DY*DETADY(I)/ETA(I)
      BETA(I)=DY**2/DX*K/ETA(I)/CP
      DETADY(I+1)=(-ETA(I+3)+6.*ETA(I+2)-3.*ETA(I+1)-2.*ETA(I))/6./DY
      ALPHA(I+1)=0.5*DY*DETADY(I+1)/ETA(I+1)
      BETA(I+1)=DY**2/DX*K/ETA(I+1)/CP
      IA=I+2
      DO 20 I=IA,MJ
      DETADY(I)=(-ETA(I+2)+8.*ETA(I+1)-8.*ETA(I-1)+ETA(I-2))/12./DY
      ALPHA(I)=0.5*DY*DETADY(I)/ETA(I)
      BETA(I)=DY**2/DX*K/ETA(I)/CP
20    CONTINUE
      DETADY(M)=(2.*ETA(MI)+3.*ETA(M)-6.*ETA(MJ)+ETA(MK))/6./DY
      ALPHA(M)=0.5*DY*DETADY(M)/ETA(M)
      BETA(M)=DY**2/DX*K/ETA(M)/CP
      B(2)=-2.
      C(2)=ALPHA(2)+1.
      W(2)=-BETA(2)
      H(2)=-BETA(2)*P
      DO 21 I=3,MJ
      A(I)=-ALPHA(I)+1.
      B(I)=-2.
      C(I)=ALPHA(I)+1.
      W(I)=-BETA(I)
      H(I)=-BETA(I)*P
21    CONTINUE
      A(M)=-ALPHA(M)+1.
      B(M)=-2.
      W(M)=-BETA(M)
      H(M)=-BETA(M)*P
      DO 22 I=2,MK,2
      Z(I)=4.
      Z(I+1)=2.
22    CONTINUE
      Z(M)=4.
      Z(MI)=0.
      Z(M+2)=3.*M
      DO 23 I=3,M
      SS=-A(I)/B(I-1)
      B(I)=B(I)+C(I-1)*SS
      W(I)=W(I)+W(I-1)*SS
      H(I)=H(I)+H(I-1)*SS
```

```
23    CONTINUE
      L=MJ
      DO 24 I=3,M
      SS=-C(L)/B(L+1)
      W(L)=W(L)+W(L+1)*SS
      H(L)=H(L)+H(L+1)*SS
24    CONTINUE
      DO 25 I=2,M
      SS=-Z(I)/B(I)
      Z(MI)=Z(MI)+W(I)*SS
      Z(M+2)=Z(M+2)+H(I)*SS
25    CONTINUE
      P1=Z(M+2)/Z(M+1)
      DO 26 I=2,M
      U2(I)=(H(I)-W(I)*P1)/B(I)
26    CONTINUE
C
C     CHECK U2 AND THETA2 FOR CONVERGENCE
C
      DO 27 I=2,M
      IF(ABS(U2(I)-U1(I)).GE.0.001) GO TO 28
      IF(ABS(THETA2(I)-THETA1(I)).GE.0.001) GO TO 28
27    CONTINUE
      GO TO 30
28    CONTINUE
      DO 29 I=1,MI
      U1(I)=U2(I)
      THETA1(I)=THETA2(I)
29    CONTINUE
      GO TO 7
30    CONTINUE
      X=X+DX
      IF(LL-NX.NE.0) GO TO 33
      LL=0
C
C      PRINT VELOCITY,TEMPERATURE AND VISCOSITY PROFILES
C
      PRINT 111,LA,X
111   FORMAT(≠1≠,10X,≠N=≠,I6,3X,≠X=≠,F7.4/)
      PRINT 112
112   FORMAT(≠ ≠,14X,≠Y≠,8X,≠U(Y)≠,4X,≠U(Y)*UAVG≠,4X,≠THETA(Y)≠,4X,
     1≠TEMP(Y)≠,3X,≠ETA (POISE)≠/)
      Y=0.
      DO 31 I=1,MI,MX
      TEMP=THETA2(I)*(TEMP0-TEMPW1)+TEMPW1
      PRINT 113,Y,U2(I),U2(I)*UAVG,THETA2(I),TEMP,ETA(I)
113   FORMAT(≠ ≠,F16.3,F11.4,F 12.4,F12.4,F11.1,F12.1)
      Y=Y+MX*DY
31    CONTINUE
C
C     CALCULATE BULK TEMPERATURE AND LOCAL NUSSELT NUMBERS
C
      AREA1=AREA2=0.
      DO 32 I=3,MI,2
      A1=(THETA2(I-2)*U2(I-2)+4.*THETA2(I-1)*U2(I-1)+THETA2(I)*U2(I))
     1*DY/3.
      A2=(U2(I-2)+4.*U2(I-1)+U2(I))*DY/3.
      AREA1=AREA1+A1
      AREA2=AREA2+A2
32    CONTINUE
      THETAB=AREA1/AREA2
      DTHDY1=(2.*THETA2(4)-9.*THETA2(3)+18.*THETA2(2)-11.*THETA2(1))
     1/6./DY
      DTHDY2=(11.*THETA2(MI)-18.*THETA2(M)+9.*THETA2(MJ)-2.*THETA2(MK))
     1/6./DY
      NU1=DTHDY1/THETAB
      NU2=-DTHDY2/(THETAB-THETA2(MI))
      PRINT 114,P1,P1*DEN*UAVG**2+P0
114   FORMAT(≠-≠,10X,≠PRESSURE=≠,F13.0,3X,≠=≠,F16.0,≠ DYNE/CM2≠/)
      PRINT 115,THETAB,THETAB*(TEMP0-TEMPW1)+TEMPW1
115   FORMAT(≠ ≠,10X,≠THETABULK=≠,F7.4,3X,≠BULK TEMP=≠,F6.1,≠ K≠/)
      PRINT 116,NU1,NU2
116   FORMAT(≠ ≠,10X,≠LOCAL NUSSELT NO AT M=1 =≠,F7.2,3X,≠AT M=MI =≠
     1,F7.2/)
      PRINT 117,LB
117   FORMAT(≠ ≠,10X,≠NO OF ITERATIONS =≠,I3)
33    CONTINUE
      P=P1
      DO 34 I=1,MI
      U1(I)=U2(I)
      THETA(I)=THETA1(I)=THETA2(I)
34    CONTINUE
      GO TO 36
35    PRINT 118,LA
118   FORMAT(≠-≠,10X,≠PROGRAM STOPPED AT N=≠,I4)
36    STOP
      END
```

FLOW BETWEEN PARALLEL PLATES WITH CONVECTIVE TERM

POWER LAW FLUID - TEMPERATURE DEPENDENT VISCOSITY

M= 100   TEMP0= 403.0 K   TEMPW1= 433.0 K   TEMPW2= 433.0 K

POWER LAW INDEX= .453   UAVG=15.0 CM/SEC   K= .00061 CAL/CM SEC K

DENSITY= .794 G/CM3   CP= .60 CAL/G K   L= 5.0 CM   B= .25 CM

DX= .0001   X AT L= .00683

DX= .0010 AFTER X= .10

DX= .0100 AFTER X= .30

N= 0   X=0.00

Y	U(Y)	U(Y)*UAVG	THETA(Y)	TEMP(Y)
0.000	0.0000	0.0000	1.0000	403.0
.050	.3762	5.6425	1.0000	403.0
.100	.6705	10.0580	1.0000	403.0
.150	.8939	13.4090	1.0000	403.0
.200	1.0569	15.8539	1.0000	403.0
.250	1.1698	17.5465	1.0000	403.0
.300	1.2424	18.6353	1.0000	403.0
.350	1.2842	19.2627	1.0000	403.0
.400	1.3043	19.5638	1.0000	403.0
.450	1.3110	19.6643	1.0000	403.0
.500	1.3118	19.6765	1.0000	403.0
.550	1.3110	19.6643	1.0000	403.0
.600	1.3043	19.5638	1.0000	403.0
.650	1.2842	19.2627	1.0000	403.0
.700	1.2424	18.6353	1.0000	403.0
.750	1.1698	17.5465	1.0000	403.0
.800	1.0569	15.8539	1.0000	403.0
.850	.8939	13.4090	1.0000	403.0
.900	.6705	10.0580	1.0000	403.0
.950	.3762	5.6425	1.0000	403.0
1.000	.0000	.0000	1.0000	403.0

N= 200   X= .0200

Y	U(Y)	U(Y)*UAVG	THETA(Y)	TEMP(Y)	ETA (POISE)
0.000	0.0000	0.0000	0.0000	433.0	6688.9
.050	.3933	5.8994	-.2212	439.6	6480.6
.100	.7216	10.8246	-.1897	438.7	7647.4
.150	.9514	14.2709	-.0069	433.2	10256.9
.200	1.0949	16.4235	.2312	426.1	14672.6
.250	1.1736	17.6796	.4597	419.2	21562.7
.300	1.2249	18.3741	.6462	413.6	32298.0
.350	1.2487	18.7299	.7815	409.6	50419.8
.400	1.2591	18.8871	.8689	406.9	87607.0
.450	1.2624	18.9366	.9166	405.5	215493.2
.500	1.2630	18.9444	.9316	405.1	265482.2
.550	1.2624	18.9366	.9166	405.5	215493.2
.600	1.2591	18.8871	.8689	406.9	87607.0
.650	1.2487	18.7299	.7815	409.6	50419.8
.700	1.2249	18.3741	.6462	413.6	32298.0
.750	1.1736	17.6796	.4597	419.2	21562.7
.800	1.0949	16.4235	.2312	426.1	14672.6
.850	.9514	14.2709	-.0069	433.2	10256.9
.900	.7216	10.8246	-.1897	438.7	7647.4
.950	.3933	5.8994	-.2212	439.6	6480.6
1.000	0.0000	0.0000	0.0000	433.0	6688.9

PRESSURE= -2251799. = -402283870. DYNE/CM2

THETABULK= .5171   BULK TEMP= 417.5 K

LOCAL NUSSELT NO AT M=1 = -14.40   AT M=MI = -14.40

NO OF ITERATIONS = 2

N= 1000 X= .1000

Y	U(Y)	U(Y)*UAVG	THETA(Y)	TEMP(Y)	ETA (POISE)
0.000	0.0000	0.0000	0.0000	433.0	7727.8
.050	.3205	4.8068	-.3972	444.9	6592.2
.100	.6304	9.4567	-.5946	450.8	6594.0
.150	.8863	13.2950	-.6362	452.1	7520.2
.200	1.0717	16.0749	-.5790	450.4	9441.4
.250	1.1925	17.8875	-.4734	447.2	12698.2
.300	1.2642	18.9623	-.3559	443.7	18095.8
.350	1.3022	19.5332	-.2496	440.5	27659.2
.400	1.3193	19.7886	-.1676	438.0	47944.2
.450	1.3246	19.8697	-.1167	436.5	117951.1
.500	1.3254	19.8804	-.0995	436.0	189663.0
.550	1.3246	19.8697	-.1167	436.5	117951.1
.600	1.3193	19.7886	-.1676	438.0	47944.2
.650	1.3022	19.5332	-.2496	440.5	27659.2
.700	1.2642	18.9623	-.3559	443.7	18095.8
.750	1.1925	17.8875	-.4734	447.2	12698.2
.800	1.0717	16.0749	-.5790	450.4	9441.4
.850	.8863	13.2950	-.6362	452.1	7520.2
.900	.6304	9.4567	-.5946	450.8	6594.0
.950	.3205	4.8068	-.3972	444.9	6592.2
1.000	0.0000	0.0000	0.0000	433.0	7727.8

PRESSURE= -10081091. = -1800965112. DYNE/CM2

THETABULK= -.3468 BULK TEMP= 443.4 K

LOCAL NUSSELT NO AT M=1 = 29.09 AT M=MI = 29.09

NO OF ITERATIONS = 2

N= 1100 X= .2000

Y	U(Y)	U(Y)*UAVG	THETA(Y)	TEMP(Y)	ETA (POISE)
0.000	0.0000	0.0000	0.0000	433.0	8368.1
.050	.2843	4.2651	-.4748	447.2	6750.1
.100	.5783	8.6741	-.7779	456.3	6256.5
.150	.8411	12.6171	-.9354	461.1	6563.9
.200	1.0478	15.7164	-.9885	462.7	7610.3
.250	1.1930	17.8944	-.9792	462.4	9546.9
.300	1.2848	19.2715	-.9409	461.2	12844.1
.350	1.3361	20.0421	-.8963	459.9	18762.7
.400	1.3601	20.4015	-.8585	458.8	31442.7
.450	1.3679	20.5189	-.8342	458.0	74204.5
.500	1.3689	20.5333	-.8260	457.8	149650.3
.550	1.3679	20.5189	-.8342	458.0	74204.5
.600	1.3601	20.4015	-.8585	458.8	31442.7
.650	1.3361	20.0421	-.8963	459.9	18762.7
.700	1.2848	19.2715	-.9409	461.2	12844.1
.750	1.1930	17.8944	-.9792	462.4	9546.9
.800	1.0478	15.7164	-.9885	462.7	7610.3
.850	.8411	12.6171	-.9354	461.1	6563.9
.900	.5733	8.6741	-.7779	456.3	6256.5
.950	.2843	4.2651	-.4748	447.2	6750.1
1.000	0.0000	0.0000	0.0000	433.0	8368.1

PRESSURE= -19069571. = -3406778870. DYNE/CM2

THETABULK= -.8856 BULK TEMP= 459.6 K

LOCAL NUSSELT NO AT M=1 = 12.71 AT M=MI = 12.71

NO OF ITERATIONS = 2

N= 1200 X= .3000

Y	U(Y)	U(Y)*UAVG	THETA(Y)	TEMP(Y)	ETA (POISE)
0.000	0.0000	0.0000	0.0000	433.0	8704.5
.050	.2679	4.0178	-.5100	446.3	6844.7
.100	.5532	3.2965	-.8610	458.8	6127.8
.150	.8180	12.2699	-1.0719	465.2	6185.2
.200	1.0342	15.5129	-1.1769	468.3	6906.8
.250	1.1916	17.8742	-1.2135	469.4	8380.6
.300	1.2942	19.4135	-1.2133	469.4	10967.0
.350	1.3531	20.2965	-1.1984	469.0	15675.4
.400	1.3811	20.7162	-1.1820	468.5	25851.8
.450	1.3904	20.8553	-1.1706	468.1	60192.5
.500	1.3915	20.8721	-1.1666	468.0	133913.7
.550	1.3904	20.8553	-1.1706	468.1	60192.5
.600	1.3811	20.7162	-1.1820	468.5	25851.8
.650	1.3531	20.2965	-1.1984	469.0	15675.4
.700	1.2942	19.4135	-1.2133	469.4	10967.0
.750	1.1916	17.8742	-1.2135	469.4	8380.6
.800	1.0342	15.5129	-1.1769	468.3	6906.8
.850	.8130	12.2699	-1.0719	465.2	6185.2
.900	.5532	8.2965	-.8610	458.8	6127.8
.950	.2679	4.0178	-.5100	446.3	6844.7
1.000	0.0000	0.0000	0.0000	433.0	8704.5

PRESSURE= -27634603. = -4936921813. DYNE/CM2

THETABULK=-1.1416 BULK TEMP= 467.2 K

LOCAL NUSSELT NO AT M=1 = 10.34 AT M=MI = 10.34

NO OF ITERATIONS = 2

N= 1210 X= .4000

Y	U(Y)	U(Y)*UAVG	THETA(Y)	TEMP(Y)	ETA (POISE)
0.000	0.0000	0.0000	0.0000	433.0	8861.0
.050	.2605	3.9081	-.5262	446.8	6887.9
.100	.5419	8.1263	-.8991	460.0	6072.4
.150	.8072	12.1079	-1.1345	467.0	6024.7
.200	1.0276	15.4135	-1.2637	470.9	6614.6
.250	1.1906	17.8593	-1.3221	472.7	7904.8
.300	1.2984	19.4761	-1.3402	473.2	10213.1
.350	1.3609	20.4142	-1.3396	473.2	14452.2
.400	1.3909	20.8639	-1.3335	473.0	23664.4
.450	1.4009	21.0137	-1.3283	472.8	54862.4
.500	1.4021	21.0319	-1.3264	472.8	127112.1
.550	1.4009	21.0137	-1.3283	472.8	54862.4
.600	1.3909	20.8639	-1.3335	473.0	23664.4
.650	1.3609	20.4142	-1.3396	473.2	14452.2
.700	1.2984	19.4761	-1.3402	473.2	10213.1
.750	1.1906	17.8593	-1.3221	472.7	7904.8
.800	1.0276	15.4135	-1.2637	470.9	6614.6
.850	.8072	12.1079	-1.1345	467.0	6024.7
.900	.5419	8.1263	-.8991	460.0	6072.4
.950	.2605	3.9081	-.5262	446.8	6887.9
1.000	0.0000	0.0000	0.0000	433.0	8861.0

PRESSURE= -36002227. = -6431797869. DYNE/CM2

THETABULK=-1.2621 BULK TEMP= 470.9 K

LOCAL NUSSELT NO AT M=1 = 9.55 AT M=MI = 9.55

NO OF ITERATIONS = 2

F.3 Poiseuille Flow Through a Tube with Circular Cross-section

```
      PROGRAM TST (INPUT,OUTPUT,TAPE5=INPUT,TAPE6=OUTPUT)
C*********************************************************************
C                                                                    *
C     APPENDIX F.3  POISEUILLE FLOW THROUGH A TUBE WITH CIRCULAR     *
C                   CROSS-SECTION                                    *
C                                                                    *
C                   T0=130 C    TW=160 C                             *
C                                                                    *
C*********************************************************************
C
C     DIMENSION OF U1,U2,THETA,THETA1,THETA2,ETA,DUDR = M+1
C     DIMENSION OF DETADR,ALPHA,BETA,GAMMA,A,B,C,D,E,F,G,H,Q,S,T,W = M
C     DIMENSION OF X = M+2
C
C     M = NUMBER OF GRID DIVISIONS ALONG R-AXIS
C     MX = INTERVAL AT WHICH VALUES ALONG R-AXIS ARE PRINTED
C     TEMP0 = FLUID TEMPERATURE AT TUBE INLET , K
C     TEMPW = WALL TEMPERATURE , K
C     TEMPM = MELTING TEMPERATURE OF POLYMER , K
C     PN = POWER-LAW INDEX , DIMENSIONLESS
C     UAVG = AVERAGE VELOCITY OF FLUID , CM/S
C     P0 = FLUID PRESSURE AT TUBE INLET , DYNE/CM2
C     DZ = DELTA X AT Z=0 , DIMENSIONLESS
C     N = NUMBER OF GRID DIVISIONS ALONG Z-AXIS
C     NA - DZ IS INCREASED BY A FACTOR OF 10 AFTER THE NA-TH COLUMN
C     NB - DZ IS INCREASED BY A FACTOR OF 10 AFTER THE NB-TH COLUMN
C     NX = INTERVAL AT WHICH VALUES ALONG Z-AXIS ARE PRINTED
C     K = THERMAL CONDUCTIVITY OF FLUID , CAL/CM S K
C     DEN = DENSITY OF FLUID , G/CM3
C     CP = SPECIFIC HEAT OF FLUID , CAL/G K
C     RL = LENGTH OF TUBE , CM
C     RA = INSIDE RADIUS OF TUBE , CM
C
      REAL U1(101),U2(101),THETA(101),THETA1(101),THETA2(101),ETA(101)
      REAL DETADR(100),DUDR(101),ALPHA(100),BETA(100),GAMMA(100)
      REAL A(100),B(100),C(100),D(100),E(100),F(100),G(100),H(100)
      REAL Q(100),S(100),T(100),W(100),X(102),K,NU
      READ *,M,MX,TEMP0,TEMPW,TEMPM,PN,UAVG,P0,DZ,N,NA,NB,NX,K,DEN,
     1CP,RL,RA
      PRINT 100
  100 FORMAT(≠1≠,10X,≠FLOW IN A CIRCULAR TUBE WITH CONVECTIVE TERM≠/)
      PRINT 101
  101 FORMAT(≠ ≠,10X,≠POWER LAW FLUID - TEMPERATURE DEPENDENT VISCOSITY≠
     1//)
      PRINT 102,M,TEMP0,TEMPW,TEMPM
  102 FORMAT(≠ ≠,10X,≠M=≠,I4,3X,≠TEMP0=≠,F6.1,≠ K≠,3X,≠TEMPW=≠,
     1F6.1,≠ K≠,3X,≠TEMPM=≠,F6.1,≠ K≠/)
      PRINT 103,PN,UAVG,K
  103 FORMAT(≠ ≠,10X,≠POWER LAW INDEX=≠,F5.3,3X,≠UAVG=≠,F4.1,≠ CM/SEC≠,
     13X,≠K=≠,F7.5,≠ CAL/CM SEC K≠/)
      PRINT 104,DEN,CP,RL,RA
  104 FORMAT(≠ ≠,10X,≠DENSITY=≠,F5.3,≠ G/CM3≠,3X,≠CP=≠,F4.2,≠ CAL/G K≠
     1,3X,≠L=≠,F4.1,≠ CM≠,3X,≠A=≠,F5.3,≠ CM≠/)
      ZL=K*RL/DEN/CP/UAVG/RA**2
      PRINT 105,DZ,ZL
  105 FORMAT(≠ ≠,10X,≠DZ=≠,F6.4,3X,≠Z AT L=≠,F7.5/)
      PRINT 106,DZ*10.,NA*DZ
  106 FORMAT(≠ ≠,10X,≠DZ=≠,F6.4,≠ AFTER Z=≠,F5.2/)
      PRINT 107,DZ*100.,NA*DZ+(NB-NA)*DZ*10.
  107 FORMAT(≠ ≠,10X,≠DZ=≠,F6.4,≠ AFTER Z=≠,F5.2//)
      N0=0
      MI=M+1
      MJ=M-1
      MK=M-2
      DR=1./M
      P=P0/DEN/UAVG**2
C
C     PRINT INITIAL VELOCITY AND TEMPERATURE PROFILES
C
      Z=0.
      PRINT 108,N0,Z
  108 FORMAT(≠ ≠,10X,≠N=≠,I4,3X,≠Z=≠,F4.2/)
      PRINT 109
  109 FORMAT(≠ ≠,14X,≠R≠,3X,≠U(R)≠,4X,≠U(R)*UAVG≠,4X,≠THETA(R)≠,4X,
     1≠TEMP(R)≠/)
      V=(PN+1.)/PN
      R=0.
```

```
      DO 1 I=1,MI
      U1(I)=-(V+2.)/V*R**V+(V+2.)/V
      THETA(I)=THETA1(I)=1.
      R=R+DR
1     CONTINUE
      R=0.
      DO 2 I=1,MI,MX
      TEMP=THETA1(I)*(TEMPO-TEMPW)+TEMPW
      PRINT 110,R,U1(I),U1(I)*UAVG,THETA1(I),TEMP
110   FORMAT(≠ ≠,F16.3,F11.4,F12.4,F12.4,F11.1)
      R=R+DR*MX
2     CONTINUE
      U2(MI)=0.
      THETA2(MI)=0.
      LL=0
      DO 32 LA=1,N
      IF(LA.EQ.NA+1) GO TO 3
      GO TO 4
3     DZ=DZ*10.
      NX=NX/10
4     CONTINUE
      IF(LA.EQ.NB+1) GO TO 5
      GO TO 6
5     DZ=DZ*10.
      NX=NX/10
6     CONTINUE
      LB=0
7     CONTINUE
      LB=LB+1
      IF(LB.EQ.40) GO TO 33
C
C     SOLVE SET OF ENERGY EQS.(6.32)
C
      DUDR(1)=0.
      DUDR(2)=(-U1(4)+6.*U1(3)-3.*U1(2)-2.*U1(1))/6./DR
      DO 8 I=3,MJ
      DUDR(I)=(-U1(I+2)+8.*U1(I+1)-8.*U1(I-1)+U1(I-2))/12./DR
8     CONTINUE
      DUDR(M)=(2.*U1(MI)+3.*U1(M)-6.*U1(MJ)+U1(MK))/6./DR
      DUDR(MI)=(11.*U1(MI)-18.*U1(M)+9.*U1(MJ)-2.*U1(MK))/6./DR
      ALPHA(1)=2.*U1(1)*DR**2/DZ
      R=0.
      DO 10 I=2,M
      ALPHA(I)=2.*U1(I)*DR**2/DZ
      BETA(I)=DR/2./R
      TEMP=THETA1(I)*(TEMPO-TEMPW)+TEMPW
      IF(ABS(DUDR(I)*UAVG/RA).LT.1.) GO TO 9
      ETA(I)=282000.*EXP(-.024*PN*(TEMP-TEMPM))*(ABS(DUDR(I)*UAVG
     1/RA))**(PN-1.)
      GAMMA(I)=2.3901*10.**(-8)*ETA(I)/K*UAVG**2/(TEMPO-TEMPW)
     1*DUDR(I)**2
      GO TO 10
9     CONTINUE
      ETA(I)=282000.*EXP(-.024*PN*(TEMP-TEMPM))
      GAMMA(I)=2.3901*10.**(-8)*ETA(I)/K*UAVG**2/(TEMPO-TEMPW)
     1*DUDR(I)**2
10    CONTINUE
      B(1)=ALPHA(1)/2.+2.
      C(1)=-2.
      E(1)=(ALPHA(1)/2.-2.)*THETA(1)
      F(1)=2.*THETA(2)
      H(1)=E(1)+F(1)
      DO 11 I=2,MJ
      A(I)=BETA(I)-1.
      B(I)=ALPHA(I)+2.
      C(I)=-BETA(I)-1.
      D(I)=(-BETA(I)+1.)*THETA(I-1)
      E(I)=(ALPHA(I)-2.)*THETA(I)
      F(I)=(BETA(I)+1.)*THETA(I+1)
      G(I)=2.*DR**2*GAMMA(I)
      H(I)=D(I)+E(I)+F(I)+G(I)
11    CONTINUE
      A(M)=BETA(M)-1.
      B(M)=ALPHA(M)+2.
      D(M)=(-BETA(M)+1.)*THETA(MJ)
      E(M)=(ALPHA(M)-2.)*THETA(M)
      G(M)=2.*DR**2*GAMMA(M)+(BETA(M)+1.)*THETA(MI)
      H(M)=D(M)+E(M)+G(M)
      S(1)=B(1)
      T(1)=H(1)/S(1)
      DO 12 I=2,M
      Q(I-1)=C(I-1)/S(I-1)
      S(I)=B(I)-A(I)*Q(I-1)
      T(I)=(H(I)-A(I)*T(I-1))/S(I)
12    CONTINUE
```

```
      THETA2(M)=T(M)
      L=MJ
      DO 13 I=1,MJ
      THETA2(L)=T(L)-Q(L)*THETA2(L+1)
      L=L-1
13    CONTINUE
C
C     SOLVE SET OF CONTINUITY AND MOMENTUM EQS.(6.25)
C
      DO 15 I=1,MI
      TEMP=THETA2(I)*(TEMP0-TEMPW)+TEMPW
      IF(ABS(DUDR(I)*UAVG/RA).LT.1.) GO TO 14
      ETA(I)=282000.*EXP(-.024*PN*(TEMP-TEMPM))*(ABS(DUDR(I)*UAVG
     1/RA))**(PN-1.)
      GO TO 15
14    CONTINUE
      ETA(I)=282000.*EXP(-.024*PN*(TEMP-TEMPM))
15    CONTINUE
      BETA(1)=K/ETA(1)/CP*DR**2/DZ
      R=0.
      DO 16 I=2,MJ
      IF(ABS(DUDR(I+1)*UAVG/RA).GT.1.) GO TO 17
      ALPHA(I)=DR/2./R
      BETA(I)=K/ETA(I)/CP*DR**2/DZ
16    CONTINUE
17    CONTINUE
      DETADR(I)=(2.*ETA(I+3)-9.*ETA(I+2)+18.*ETA(I+1)-11.*ETA(I))/6.
     1/DR/2.
      ALPHA(I)=DR/2./R+DETADR(I)*DR/ETA(I)/2.
      BETA(I)=K/ETA(I)/CP*DR**2/DZ
      R=R+DR
      DETADR(I+1)=(-ETA(I+3)+6.*ETA(I+2)-3.*ETA(I+1)-2.*ETA(I))/6./DR
      ALPHA(I+1)=DR/2./R+DETADR(I+1)*DR/ETA(I+1)/2.
      BETA(I+1)=K/ETA(I+1)/CP*DR**2/DZ
      IA=I+2
      DO 18 I=IA,MJ
      R=R+DR
      DETADR(I)=(-ETA(I+2)+8.*ETA(I+1)-8.*ETA(I-1)+ETA(I-2))/12./DR
      ALPHA(I)=DR/2./R+DETADR(I)*DR/ETA(I)/2.
      BETA(I)=K/ETA(I)/CP*DR**2/DZ
18    CONTINUE
      R=R+DR
      DETADR(M)=(2.*ETA(MI)+3.*ETA(M)-6.*ETA(MJ)+ETA(MK))/6./DR
      ALPHA(M)=DR/2./R+DETADR(M)*DR/ETA(M)/2.
      BETA(M)=K/ETA(M)/CP*DR**2/DZ
      B(1)=-2.
      C(1)=2.
      W(1)=-BETA(1)/2.
      H(1)=-BETA(1)/2.*P
      DO 19 I=2,MJ
      A(I)=-ALPHA(I)+1.
      B(I)=-2.
      C(I)=ALPHA(I)+1.
      W(I)=-BETA(I)
      H(I)=-BETA(I)*P
19    CONTINUE
      A(M)=-ALPHA(M)+1.
      B(M)=-2.
      W(M)=-BETA(M)
      H(M)=-BETA(M)*P
      X(1)=0.
      R=DR
      DO 20 I=2,MK,2
      X(I)=4.*R
      R=R+DR
      X(I+1)=2.*R
      R=R+DR
20    CONTINUE
      X(M)=4.*R
      X(MI)=0.
      X(M+2)=1.5*M
      DO 21 I=2,M
      SS=-A(I)/B(I-1)
      B(I)=B(I)+C(I-1)*SS
      W(I)=W(I)+W(I-1)*SS
      H(I)=H(I)+H(I-1)*SS
21    CONTINUE
      L=MJ
      DO 22 I=2,M
      SS=-C(L)/B(L+1)
      W(L)=W(L)+W(L+1)*SS
      H(L)=H(L)+H(L+1)*SS
      L=L-1
22    CONTINUE
```

```
      DO 23 I=1,M
      SS=-X(I)/B(I)
      X(MI)=X(MI)+W(I)*SS
      X(M+2)=X(M+2)+H(I)*SS
 23   CONTINUE
      P1=X(M+2)/X(MI)
      DO 24 I=1,M
      U2(I)=(H(I)-W(I)*P1)/B(I)
 24   CONTINUE
C
C     CHECK U2 AND THETA2 FOR CONVERGENCE
C
      DO 25 I=1,M
      IF(ABS(U2(I)-U1(I)).GE.0.001) GO TO 26
      IF(ABS(THETA2(I)-THETA1(I)).GE.0.001) GO TO 26
 25   CONTINUE
      GO TO 28
 26   CONTINUE
      DO 27 I=1,MI
      U1(I)=U2(I)
      THETA1(I)=THETA2(I)
 27   CONTINUE
      GO TO 7
 28   CONTINUE
      Z=Z+DZ
      IF(LL-NX.NE.0) GO TO 31
      LL=0
C
C      PRINT VELOCITY,TEMPERATURE AND VISCOSITY PROFILES
C
      PRINT 111,LA,Z
 111  FORMAT(≠1≠,10X,≠N=≠,I6,3X,≠Z=≠,F7.4/)
      PRINT 112
 112  FORMAT(≠ ≠,14X,≠R≠,8X,≠U(R)≠,4X,≠U(R)*UAVG≠,4X,≠THETA(R)≠,4X,
     1≠TEMP(R)≠,3X,≠ETA (POISE)≠/)
      R=0.
      DO 29 I=1,MI,MX
      TEMP=THETA2(I)*(TEMP0-TEMPW)+TEMPW
      PRINT 113,R,U2(I),U2(I)*UAVG,THETA2(I),TEMP,ETA(I)
 113  FORMAT(≠ ≠,F16.3,F11.4,F12.4,F12.4,F11.1,F12.1)
      R=R+DR*MX
 29   CONTINUE
C
C     CALCULATE BULK TEMPERATURE AND LOCAL NUSSELT NUMBER
C
      AREA1=AREA2=0.
      R=0.
      DO 30 I=3,MI,2
      A1=(THETA2(I-2)*U2(I-2)*R+4.*THETA2(I-1)*U2(I-1)*(R+DR)
     1+THETA2(I)*U2(I)*(R+2.*DR))*DR/3.
      A2=(U2(I-2)*R+4.*U2(I-1)*(R+DR)+U2(I)*(R+2.*DR))*DR/3.
      R=R+2.*DR
      AREA1=AREA1+A1
      AREA2=AREA2+A2
 30   CONTINUE
      THETAB=AREA1/AREA2
      DTHDR=(11.*THETA2(MI)-18.*THETA2(M)+9.*THETA2(MJ)-2.*THETA2(MK))
     1/6./DR
      NU=-2.*DTHDR/THETAB
      PRINT 114,P1,P1*DEN*UAVG**2+P0
 114  FORMAT(≠-≠,10X,≠PRESSURE=≠,F13.0,3X,≠=≠,F16.0,≠ DYNE/CM2≠/)
      PRINT 115,THETAB,THETAB*(TEMP0-TEMPW)+TEMPW
 115  FORMAT(≠ ≠,10X,≠THETABULK=≠,F9.4,3X,≠BULK TEMP=≠,F7.1,≠ K≠/)
      PRINT 116,NU
 116  FORMAT(≠ ≠,10X,≠LOCAL NUSSELT NO AT R=1 =≠,F7.2/)
      PRINT 117,LB
 117  FORMAT(≠ ≠,10X,≠NO OF ITERATIONS =≠,I3)
 31   CONTINUE
      P=P1
      DO 32 I=1,MI
      U1(I)=U2(I)
      THETA(I)=THETA1(I)=THETA2(I)
 32   CONTINUE
      GO TO 34
 33   PRINT 118,LA
 118  FORMAT(≠-≠,10X,≠PROGRAM STOPPED AT N=≠,I4)
 34   STOP
      END
```

FLOW IN A CIRCULAR TUBE WITH CONVECTIVE TERM

POWER LAW FLUID - TEMPERATURE DEPENDENT VISCOSITY

M= 50 TEMPC= 403.0 K TEMPW= 433.0 K TEMPM= 399.5 K

POWER LAW INDEX= .453 UAVG= 15.0 CM/SEC K= .00061 CAL/CM SEC K

DENSITY= .794 G/CM3 CP= .60 CAL/G K L= 5.0 CM A= .125 CM

DZ= .0004 Z AT L= .02732

DZ= .0040 AFTER Z= .40

DZ= .0400 AFTER Z= 1.20

N= 0 Z=0.00

R	U(R)	U(R)*UAVG	THETA(R)	TEMP(R)
0.000	1.6235	24.3531	1.0000	403.0
.100	1.6225	24.3360	1.0000	403.0
.200	1.6142	24.2136	1.0000	403.0
.300	1.5894	23.8409	1.0000	403.0
.400	1.5376	23.0643	1.0000	403.0
.500	1.4478	21.7167	1.0000	403.0
.600	1.3081	19.6218	1.0000	403.0
.700	1.1064	16.5959	1.0000	403.0
.800	.8299	12.4485	1.0000	403.0
.900	.4656	6.9836	1.0000	403.0
1.000	.0000	.0000	1.0000	403.0

N= 200 Z= .0600

R	U(R)	U(R)*UAVG	THETA(R)	TEMP(R)	ETA (POISE)
0.000	1.5442	23.1637	.8654	407.0	259811.5
.100	1.5437	23.1554	.8472	407.6	195862.9
.200	1.5398	23.0974	.7894	409.3	78481.0
.300	1.5274	22.9117	.6843	412.5	44482.1
.400	1.4990	22.4850	.5235	417.3	27969.9
.500	1.4423	21.6344	.3053	423.8	18251.1
.600	1.3373	20.0600	.0459	431.6	12143.5
.700	1.1542	17.3132	-.2086	439.3	8386.6
.800	.8610	12.9154	-.3731	444.2	6334.2
.900	.4550	6.8251	-.3345	443.0	5643.8
1.000	0.0000	0.0000	0.0000	433.0	6321.3

PRESSURE= -4774063. = -852886345. DYNE/CM2

THETABULK= .1413 BULK TEMP= 428.8 K

LOCAL NUSSELT NO AT R=1 = -70.12

NO OF ITERATIONS = 2

N= 1000 Z= .4000

R	U(R)	U(R)*UAVG	THETA(R)	TEMP(R)	ETA (POISE)
0.000	1.7629	26.4431	-.7848	456.5	151671.6
.100	1.7618	26.4263	-.7987	457.0	68210.2
.200	1.7525	26.2869	-.8394	458.2	28712.0
.300	1.7235	25.8532	-.9030	460.1	16797.6
.400	1.6601	24.9014	-.9801	462.4	11222.9
.500	1.5437	23.1559	-1.0528	464.6	8132.4
.600	1.3552	20.3280	-1.0909	465.7	6346.6
.700	1.0826	16.2385	-1.0507	464.5	5421.3
.800	.7355	11.0318	-.8801	459.4	5215.1
.900	.3548	5.3221	-.5349	449.0	5799.0
1.000	0.0000	0.0000	0.0000	433.0	7507.5

PRESSURE= -20933100. = -3739698343. DYNE/CM2

THETABULK= -.9493 BULK TEMP= 461.5 K

LOCAL NUSSELT NO AT R=1 = 13.16

NO OF ITERATIONS = 2

N= 1100 Z= .8000

R	U(R)	U(R)*UAVG	THETA(R)	TEMP(R)	ETA (POISE)
0.000	1.8636	27.9545	-1.4738	477.2	121144.5
.100	1.8621	27.9308	-1.4776	477.3	44627.0
.200	1.8487	27.7309	-1.4884	477.7	19134.6
.300	1.8082	27.1227	-1.5029	478.1	11576.7
.400	1.7227	25.8403	-1.5126	478.4	8113.9
.500	1.5742	23.6125	-1.5005	478.0	6247.2
.600	1.3489	20.2332	-1.4391	476.2	5236.4
.700	1.0465	15.6971	-1.2908	471.7	4834.4
.800	.6898	10.3466	-1.0158	463.5	5013.3
.900	.3243	4.8651	-.5863	450.6	5923.8
1.000	0.0000	0.0000	0.0000	433.0	7957.7

PRESSURE= -39509161. = -7058311577. DYNE/CM2

THETABULK= -1.3458 BULK TEMP= 473.4 K

LOCAL NUSSELT NO AT R=1 = 9.78

NO OF ITERATIONS = 2

N= 1200 Z= 1.2000

R	U(R)	U(R)*UAVG	THETA(R)	TEMP(R)	ETA (POISE)
0.000	1.8928	28.3921	-1.6550	482.6	114194.6
.100	1.8911	28.3661	-1.6560	482.7	40159.8
.200	1.8764	28.1466	-1.6585	482.8	17205.1
.300	1.8322	27.4823	-1.6596	482.8	10505.1
.400	1.7398	26.0972	-1.6510	482.5	7459.6
.500	1.5817	23.7258	-1.6161	481.5	5638.6
.600	1.3461	20.1918	-1.5281	478.8	4988.4
.700	1.0361	15.5408	-1.3515	473.5	4700.4
.800	.6775	10.1626	-1.0498	464.5	4969.4
.900	.3165	4.7475	-.5990	451.0	5962.4
1.000	0.0000	0.0000	0.0000	433.0	8083.6

PRESSURE= -57596903. = -10289686656. DYNE/CM2

THETABULK= -1.4510 BULK TEMP= 476.5 K

LOCAL NUSSELT NO AT R=1 = 9.18

NO OF ITERATIONS = 1

N= 1210 Z= 1.6000

R	U(R)	U(R)*UAVG	THETA(R)	TEMP(R)	ETA (POISE)
0.000	1.9007	28.5101	-1.7029	484.1	112422.8
.100	1.8989	28.4834	-1.7032	484.1	39011.4
.200	1.8839	28.2584	-1.7035	484.1	16729.9
.300	1.8386	27.5785	-1.7010	484.0	10240.3
.400	1.7443	26.1651	-1.6674	483.6	7297.2
.500	1.5836	23.7547	-1.6464	482.4	5736.5
.600	1.3453	20.1795	-1.5513	479.5	4926.2
.700	1.0333	15.4938	-1.3672	474.0	4666.7
.800	.6743	10.1143	-1.0585	464.8	4956.5
.900	.3145	4.7170	-.6023	451.1	5972.8
1.000	0.0000	0.0000	0.0000	433.0	8117.0

PRESSURE= -75554498. = -13497811000. DYNE/CM2

THETABULK= -1.4788 BULK TEMP= 477.4 K

LOCAL NUSSELT NO AT R=1 = 9.04

NO OF ITERATIONS = 2

F.4 Drag Flow Between Converging Plates

```
      PROGRAM TST (INPUT,OUTPUT,TAPE5=INPUT,TAPE6=OUTPUT)
C*********************************************************************
C                                                                    *
C     APPENDIX F.4  DRAG FLOW BETWEEN CONVERGING PLATES              *
C                                                                    *
C                   T0=130 C    TW1=160 C    TW2=160 C               *
C                                                                    *
C*********************************************************************
C
C     DIMENSION OF A,B,C,E,PA,PB,THETA1,THETA2,U1,U2,Z = MX
C     DIMENSION OF F = LX*LX
C     DIMENSION OF G,PR = LX
C     DIMENSION OF Q,S,T,V,DETADY,ALPHA,BETA,GAMMA,DELTA = KA
C     DIMENSION OF THETAP,THETAQ,ETA,DVDY = KA+1
C     DIMENSION OF ZZ = LX+2,LX
C
C     KA = M-1 = NUMBER OF GRID POINTS (NOT INCLUDING END POINTS) ALONG
C                Y-AXIS AT X=0
C     LX = N+1 = NUMBER OF PRIMARY GRID POINTS ALONG X-AXIS AT Y=0
C     MX = TOTAL NUMBER OF PRIMARY GRID POINTS
C     M = NUMBER OF GRID DIVISIONS ALONG Y-AXIS AT X=0
C     N = NUMBER OF PRIMARY GRID DIVISIONS ALONG X-AXIS AT Y=0
C     LZ = NUMBER OF SECONDARY GRID DIVISIONS WITHIN 1 PRIMARY GRID
C          DIVISION ALONG X-AXIS
C     TEMP0 = FLUID TEMPERATURE AT CHANNEL INLET , K
C     TEMPW1 = WALL TEMPERATURE AT Y=0 , K
C     TEMPW2 = WALL TEMPERATURE AT Y=B(X) , K
C     TEMPM = MELTING TEMPERATURE OF POLYMER , K
C     U0 = VELOCITY OF MOVING PLATE , CM/S
C     PN = POWER-LAW INDEX , DIMENSIONLESS
C     K = THERMAL CONDUCTIVITY OF FLUID , CAL/CM S K
C     DEN = DENSITY OF FLUID , G/CM3
C     CP = SPECIFIC HEAT OF FLUID , CAL/G K
C     RL = LENGTH OF CHANNEL , CM
C     RB = DISTANCE BETWEEN PLATES AT X=0 , CM
C     RBL = DISTANCE BETWEEN PLATES AT X=L , CM
C
      REAL A(949),B(949),C(949),E(949),F(676),G(26),PA(949),PB(949)
      REAL PR(26),Q(49),S(49),T(49),THETA1(949),THETA2(949),THETAP(50)
      REAL THETAQ(50),U1(949),U2(949),V(49),Z(949),ZZ(26,26),ETA(50)
      REAL DETADY(49),DVDY(50),ALPHA(49),BETA(49),GAMMA(49),DELTA(49)
      REAL K,NU1,NU2
      READ *,KA,LX,MX,M,N,LZ,TEMP0,TEMPW1,TEMPW2,TEMPM,U0,PN,K,DEN,CP
     1,RL,RB,RBL
      PRINT 100
100   FORMAT(≠1≠,10X,≠THE LUBRICATION PROBLEM - POWER LAW FLUID≠/)
      PRINT 101
101   FORMAT(≠ ≠,10X,≠TEMPERATURE DEPENDENT VISCOSITY≠/)
      PRINT 102
102   FORMAT(≠ ≠,10X,≠FINITE DIFFERENCES SOLUTION≠//)
      PRINT 103,TEMP0,TEMPW1,TEMPW2,TEMPM
103   FORMAT(≠ ≠,10X,≠TEMP0=≠,F6.1,≠ K≠,3X,≠TEMPW1=≠,F6.1,≠ K≠,3X,
     1≠TEMPW2=≠,F6.1,≠ K≠,3X,≠TEMPM=≠,F6.1,≠ K≠/)
      PRINT 104,U0,K,DEN
104   FORMAT(≠ ≠,10X,≠U0=≠,F7.2,≠ CM/SEC≠,3X,≠K=≠,F7.5,≠ CAL/CM SEC K≠
     1,3X,≠DENSITY=≠,F5.3,≠ G/CM3≠/)
      PRINT 105,PN,CP,RL
105   FORMAT(≠ ≠,10X,≠POWER LAW INDEX=≠,F5.3,3X,≠CP=≠,F4.1,≠ CAL/G K≠
     1,3X,≠L=≠,F5.1,≠ CM≠/)
      PRINT 106,M,N,LZ,RB,RBL
106   FORMAT(≠ ≠,10X,≠M=≠,I3,3X,≠N=≠,I3,3X,≠LZ=≠,I4,3X,≠B AT 0=≠,F5.3,
     1≠ CM≠,3X,≠B AT L=≠,F6.4,≠ CM≠//)
      PRINT 107
107   FORMAT(≠ ≠,31X,≠SOLUTION≠//)
      XL=K*RL/DEN/CP/U0/RB**2
      DX=XL/N
      DY=1./M
      DO 2 I=1,LX
      DO 1 L=1,KJ
      U1(J)=(KJ+1.-L)/(KJ+1.)
      THETA1(J)=0.
      J=J+1
1     CONTINUE
      KJ=KJ-1
2     CONTINUE
      DO 46 IJK=1,5
      PRINT 108,IJK
```

```
108   FORMAT(≠ ≠,10X,≠ITERATION≠,I3//)
C
C     SOLVE SET OF CONTINUITY AND MOMENTUM EQS.(7.19)
C
      KK=KA
      KJ=KA
      DO 5 IK=1,LX
      CALL CALBET(J,KJ,DY,DX,U0,RB,PN,K,CP,TEMP0,TEMPW1,TEMPW2,TEMPM
     1,U1,DVDY,THETA1,DETADY,ETA,ALPHA,BETA)
      I=1
      A(J)=0.
      B(J)=-2.
      C(J)=BETA(I)+1.
      PA(J)=ALPHA(I)
      PB(J)=-ALPHA(I)
      E(J)=BETA(I)-1.
      JI=J+1
      IF(JI.EQ.KK) GO TO 4
      KKJ=KK-1
      DO 3 J=JI,KKJ
      I=I+1
      A(J)=-BETA(I)+1.
      B(J)=-2.
      C(J)=BETA(I)+1.
      PA(J)=ALPHA(I)
      PB(J)=-ALPHA(I)
      E(J)=0.
3     CONTINUE
4     CONTINUE
      I=I+1
      J=J+1
      A(J)=-BETA(I)+1.
      B(J)=-2.
      C(J)=0.
      PA(J)=ALPHA(I)
      PB(J)=-ALPHA(I)
      E(J)=0.
      J=J+1
      KJ=KJ-1
      KK=KK+KJ
      IF(KK.GT.MX) GO TO 7
      IF(J.EQ.KK) GO TO 6
5     CONTINUE
      GO TO 7
6     CONTINUE
      CALL CALBET(J,KJ,DY,DX,U0,RB,PN,K,CP,TEMP0,TEMPW1,TEMPW2,TEMPM
     1,U1,DVDY,THETA1,DETADY,ETA,ALPHA,BETA)
      A(J)=0.
      B(J)=-2.
      C(J)=0.
      PA(J)=ALPHA(1)
      PB(J)=-ALPHA(1)
      E(J)=BETA(1)-1.
7     CONTINUE
      DO 8 I=1,KA
      PA(I)=0.
8     CONTINUE
      MXB=MX-2*KA+2*LX-3
      MXA=MX-KA+LX-1
      KKI=MXB+1
      DO 9 I=KKI,MXA
      PB(I)=0.
9     CONTINUE
      KKI=MXA+1
      DO 10 I=KKI,MX
      PA(I)=0.
10    CONTINUE
      DO 11 J=1,MX
      Z(J)=2.
11    CONTINUE
      DO 12 I=1,LX
      DO 12 J=1,LX
      ZZ(I,J)=0.
12    CONTINUE
      I=LXI=LX+1
      DO 13 J=1,LX
      ZZ(I,J)=-2.*M
      ZZ(I+1,J)=-1.
13    CONTINUE
      DO 14 J=2,MX
      IF(A(J).EQ.0.) GO TO 14
      SS=-A(J)/B(J-1)
      B(J)=B(J)+C(J-1)*SS
      PA(J)=PA(J)+PA(J-1)*SS
      PB(J)=PB(J)+PB(J-1)*SS
```

```
      E(J)=E(J)+E(J-1)*SS
 14   CONTINUE
      L=MX-1
      DO 16 J=2,MX
      IF(C(L).EQ.0.) GO TO 15
      SS=-C(L)/B(L+1)
      PA(L)=PA(L)+PA(L+1)*SS
      PB(L)=PB(L)+PB(L+1)*SS
      E(L)=E(L)+E(L+1)*SS
 15   CONTINUE
      L=L-1
 16   CONTINUE
      J=1
      KK=KA
      KJ=KA
      LX2=LX+2
      DO 17 L=1,MXB
      SS=-Z(L)/B(L)
      ZZ(J,J)=ZZ(J,J)+PA(L)*SS
      ZZ(J+1,J)=ZZ(J+1,J)+PB(L)*SS
      ZZ(LX2,J)=ZZ(LX2,J)+E(L)*SS
      IF(L-KK.NE.0) GO TO 17
      J=J+1
      KJ=KJ-1
      KK=KK+KJ
 17   CONTINUE
      KKI=MXB+1
      DO 18 L=KKI,MXA
      SS=-Z(L)/B(L)
      ZZ(J,J)=ZZ(J,J)+PA(L)*SS
      ZZ(LX2,J)=ZZ(LX2,J)+E(L)*SS
 18   CONTINUE
      KKI=MXA+1
      J=J+1
      DO 19 L=KKI,MX
      SS=-Z(L)/B(L)
      ZZ(J,J)=ZZ(J,J)+PB(L)*SS
      ZZ(LX2,J)=ZZ(LX2,J)+E(L)*SS
 19   CONTINUE
      L=1
      DO 20 I=2,LXI
      DO 20 J=1,LX
      F(L)=ZZ(I,J)
      L=L+1
 20   CONTINUE
      I=I+1
      DO 21 J=1,LX
      G(J)=ZZ(I,J)
 21   CONTINUE
      CALL SIMQ(F,G,LX,KS)
      KK=KA
      KJ=KA
      DO 22 L=1,KA
      PT=G(1)*PB(L)
      U2(L)=(E(L)-PT)/B(L)
 22   CONTINUE
      J=1
      KKI=KK+1
      KJ=KJ-1
      KK=KK+KJ
      DO 23 L=KKI,MXA
      PT=G(J)*PA(L)+G(J+1)*PB(L)
      U2(L)=(E(L)-PT)/B(L)
      IF(L-KK.NE.0) GO TO 23
      J=J+1
      KJ=KJ-1
      KK=KK+KJ
 23   CONTINUE
      KKI=MXA+1
      DO 24 L=KKI,MX
      PT=G(J)*PB(L)
      U2(L)=(E(L)-PT)/B(L)
 24   CONTINUE
      PR(1)=PR(LX)=0.
      LXJ=LX-1
      DO 25 I=2,LXJ
      PR(I)=G(I-1)
 25   CONTINUE
      UAVG=G(LX)
C
C     PRINT INITIAL VELOCITY AND TEMPERATURE PROFILES
C
      PRINT 109,UAVG
 109  FORMAT(≠ ≠,10X,≠COLUMN  1≠,3X,≠X=0.≠,5X,≠UAVG=≠,F7.4/)
      PRINT 110
 110  FORMAT(≠ ≠,14X,≠Y≠,8X,≠U(Y)≠,5X,≠U(Y)*U0≠,5X,≠THETA(Y)≠,5X,
     1≠TEMP(Y)≠/)
```

```
      Y=0.
      THETA0=1.
      PRINT 111,Y,1.,U0,THETA0,TEMP0
111   FORMAT(≠ ≠,F16.3,F11.4,F12.4,F12.4,F11.1,≠ K≠)
      KJ=KA
      DO 26 I=1,KJ
      Y=Y+DY
      THETAP(I)=THETA2(I)=1.
      TEMP=THETAP(I)*(TEMP0-TEMPW1)+TEMPW1
      PRINT 112,Y,U2(I),U2(I)*U0,THETAP(I),TEMP
112   FORMAT(≠ ≠,F16.3,F11.4,F12.4,F12.4,F11.1,≠ K≠)
26    CONTINUE
      Y=Y+DY
      THETAP(KJ+1)=1.
      PRINT 113,Y,0.,0.,THETAP(KJ+1),TEMP0
113   FORMAT(≠ ≠,F16.3,F11.4,F12.4,F12.4,F11.1,≠ K≠//)
C
C     SOLVE SET OF ENERGY EQS.(7.26) AT SECONDARY COLUMNS
C
      THETAQ(KJ+1)=(TEMPW2-TEMPW1)/(TEMP0-TEMPW1)
      DO 43 LL=2,LX
      LZJ=LZ-1
      LB=0
      DO 32 L=1,LZJ
      LB=LB+1
      J=JA
      KJJ=KJ-1
      DO 27 I=1,KJJ
      V(I)=U2(J)+L*(U2(J+KJ)-U2(J))/LZ
      THETAQ(I)=THETA1(J)+L*(THETA1(J+KJ)-THETA1(J))/LZ
      J=J+1
27    CONTINUE
      V(KJ)=U2(J)-L*U2(J)/LZ
      THETAQ(KJ)=THETA1(J)-L*THETA1(J)/LZ
      DVDY(1)=(V(2)-1.)/2./DY
      DO 28 I=2,KJJ
      DVDY(I)=(V(I+1)-V(I-1))/2./DY
28    CONTINUE
      DVDY(KJ)=-V(KJJ)*LZ/(2.*LZ-L)/DY
      DO 31 I=1,KJ
      TEMP=THETAQ(I)*(TEMP0-TEMPW1)+TEMPW1
      IF(ABS(DVDY(I)*U0/RB).LT.1.) GO TO 29
      ETA(I)=282000.*EXP(-.024*PN*(TEMP-TEMPM))*(ABS(DVDY(I)*U0
     1/RB))**(PN-1.)
      GO TO 30
29    CONTINUE
      ETA(I)=282000.*EXP(-.024*PN*(TEMP-TEMPM))
30    CONTINUE
      GAMMA(I)=2.*DY**2*LZ/DX*V(I)
      DELTA(I)=2.3901*10.**(-8)*ETA(I)/K*U0**2/(TEMP0-TEMPW1)*DVDY(I)**2
31    CONTINUE
      CA=1.-(L-1.)/LZ
      DA=1.-1.*L/LZ
      CALL GAUSS(KJ,DY,CA,DA,THETA0,A,B,C,E,F,PA,PB,Z,Q,S,T
     1,THETAP,THETAQ,GAMMA,DELTA)
      IF(IJK.NE.5) GO TO 32
      IF(LL.GT.3) GO TO 32
      IF(LB-10.NE.0) GO TO 32
      LB=0
C
C     CALCULATE BULK TEMPERATURE AND LOCAL NUSSELT NUMBER (AT Y=0) AT
C     SECONDARY COLUMNS
C
      AREA1=0.
      AREA2=DY/2.
      DO 50 I=1,KJ
      A1=THETAQ(I)*V(I)*DY
      A2=V(I)*DY
      AREA1=AREA1+A1
      AREA2=AREA2+A2
50    CONTINUE
      THETAB=AREA1/AREA2
      DTHDY1=(2.*THETAQ(3)-9.*THETAQ(2)+18.*THETAQ(1))/6./DY
      NU1=DTHDY1/THETAB
C
C     PRINT VELOCITY AND TEMPERATURE PROFILES AT SECONDARY COLUMNS
C
      PRINT 200,L
200   FORMAT(≠ ≠,10X,≠SECONDARY COLUMN≠,I4/)
      PRINT 201
201   FORMAT(≠ ≠,14X,≠Y≠,8X,≠U(Y)≠,5X,≠U(Y)*U0≠,5X,≠THETA(Y)≠,5X,
     1≠TEMP(Y)≠/)
      Y=0.
      PRINT 202,Y,1.,U0,THETA0,TEMPW1
202   FORMAT(≠ ≠,F16.3,F11.4,F12.4,F12.4,F11.1,≠ K≠)
```

```
      DO 51 I=1,KJ
      Y=Y+DY
      TEMP=THETAQ(I)*(TEMP0-TEMPW1)+TEMPW1
      PRINT 203,Y,V(I),V(I)*U0,THETAQ(I),TEMP
203   FORMAT(≠ ≠,F16.3,F11.4,F12.4,F12.4,F11.1,≠ K≠)
51    CONTINUE
      Y=Y+DY*(LZ-L)/LZ
      PRINT 204,Y,0.,0.,THETAQ(KJ+1),TEMPW2
204   FORMAT(≠ ≠,F16.3,F11.4,F12.4,F12.4,F11.1,≠ K≠/)
      PRINT 205,THETAB,THETAB*(TEMP0-TEMPW1)+TEMPW1
205   FORMAT(≠ ≠,10X,≠THETABULK=≠,F7.4,3X,≠BULK TEMP=≠,F6.1,≠ K≠/)
      PRINT 206,NU1
206   FORMAT(≠ ≠,10X,≠LOCAL NUSSELT NO AT Y=0 =≠,F7.2//)
32    CONTINUE
C
C     SOLVE SET OF ENERGY EQS.(7.26) AT PRIMARY COLUMNS
C
      KJ=KJ-1
      J=JA
      DVDY0=(2.*U2(J+2)-9.*U2(J+1)+18.*U2(J)-11.)/6./DY
      DVDY(1)=(-U2(J+2)+6.*U2(J+1)-3.*U2(J)-2.)/6./DY
      J=J+1
      DVDY(2)=(-U2(J+2)+8.*U2(J+1)-8.*U2(J-1)+1.)/12./DY
      KJK=KJ-2
      DO 33 I=3,KJK
      J=J+1
      DVDY(I)=(-U2(J+2)+8.*U2(J+1)-8.*U2(J-1)+U2(J-2))/12./DY
33    CONTINUE
      J=J+1
      KJJ=KJ-1
      DVDY(KJJ)=(8.*U2(J+1)-6.*U2(J-1)+U2(J-2))/12./DY
      DVDY(KJ)=(3.*U2(J+1)-6.*U2(J)+U2(J-1))/6./DY
      KJI=KJ+1
      DVDY(KJI)=(-18.*U2(J+1)+9.*U2(J)-2.*U2(J-1))/6./DY
      IF(ABS(DVDY0*U0/RB).LT.1.) GO TO 34
      ETA0=282000.*EXP(-.024*PN*(TEMPW1-TEMPM))*(ABS(DVDY0*U0
     1/RB))**(PN-1.)
      GO TO 35
34    CONTINUE
      ETA0=282000.*EXP(-.024*PN*(TEMPW1-TEMPM))
35    CONTINUE
      J=JA
      DO 38 I=1,KJ
      TEMP=THETA1(J)*(TEMP0-TEMPW1)+TEMPW1
      IF(ABS(DVDY(I)*U0/RB).LT.1.) GO TO 36
      ETA(I)=282000.*EXP(-.024*PN*(TEMP-TEMPM))*(ABS(DVDY(I)*U0
     1/RB))**(PN-1.)
      GO TO 37
36    CONTINUE
      ETA(I)=282000.*EXP(-.024*PN*(TEMP-TEMPM))
37    CONTINUE
      GAMMA(I)=2.*DY**2*LZ/DX*U2(J)
      DELTA(I)=2.3901*10.**(-8)*ETA(I)/K*U0**2/(TEMP0-TEMPW1)*DVDY(I)**2
      J=J+1
38    CONTINUE
      IF(ABS(DVDY(KJI)*U0/RB).LT.1.) GO TO 39
      ETA(KJI)=282000.*EXP(-.024*PN*(TEMPW2-TEMPM))*(ABS(DVDY(KJI)*U0
     1/RB))**(PN-1.)
      GO TO 40
39    CONTINUE
      ETA(KJI)=282000.*EXP(-.024*PN*(TEMPW2-TEMPM))
40    CONTINUE
      CA=1.
      DA=1.
      THETAQ(KJ+1)=(TEMPW2-TEMPW1)/(TEMP0-TEMPW1)
      CALL GAUSS(KJ,DY,CA,DA,THETA0,A,B,C,E,F,PA,PB,Z,Q,S,T
     1,THETAP,THETAQ,GAMMA,DELTA)
C
C     PRINT VELOCITY,TEMPERATURE AND VISCOSITY PROFILES AT PRIMARY
C     COLUMNS
C
      PRINT 114,LL,XL*(LL-1.)/N
114   FORMAT(≠ ≠,10X,≠COLUMN≠,I3,3X,≠X=≠,F6.4/)
      PRINT 115
115   FORMAT(≠ ≠,14X,≠Y≠,8X,≠U(Y)≠,5X,≠U(Y)*U0≠,5X,≠THETA(Y)≠,5X,
     1≠TEMP(Y)≠,4X,≠ETA (POISE)≠/)
      Y=0.
      PRINT 116,Y,1.,U0,THETA0,TEMPW1,ETA0
116   FORMAT(≠ ≠,F16.3,F11.4,F12.4,F12.4,F11.1,≠ K≠,F12.1)
      J=JA
      DO 41 I=1,KJ
      Y=Y+DY
      THETA2(J)=THETAQ(I)
      TEMP=THETA2(J)*(TEMP0-TEMPW1)+TEMPW1
      PRINT 117,Y,U2(J),U2(J)*U0,THETA2(J),TEMP,ETA(I)
117   FORMAT(≠ ≠,F16.3,F11.4,F12.4,F12.4,F11.1,≠ K≠,F12.1)
```

```
      J=J+1
41    CONTINUE
      Y=Y+DY
      PRINT 118,Y,0.,0.,THETAQ(KJ+1),TEMPW2,ETA(KJI)
118   FORMAT(≠ ≠,F16.3,F11.4,F12.4,F12.4,F11.1,≠ K≠,F12.1/)
C
C     CALCULATE BULK TEMPERATURE AND LOCAL NUSSELT NUMBERS AT PRIMARY
C     COLUMNS
C
      AREA1=0.
      AREA2=DY/2.
      J=JA
      DO 42 I=1,KJ
      A1=THETA2(J)*U2(J)*DY
      A2=U2(J)*DY
      AREA1=AREA1+A1
      AREA2=AREA2+A2
      J=J+1
42    CONTINUE
      THETAB=AREA1/AREA2
      DTHDY1=(2.*THETAQ(3)-9.*THETAQ(2)+18.*THETAQ(1))/6./DY
      DTHDY2=(11.*THETAQ(KJ+1)-18.*THETAQ(KJ)+9.*THETAQ(KJJ)-2.
     1*THETAQ(KJ-2))/6./DY
      NU1=DTHDY1/THETAB
      NU2=-DTHDY2/(THETAB-THETAQ(KJI))
      PRINT 119,THETAB,THETAB*(TEMPC-TEMPW1)+TEMPW1
119   FORMAT(≠ ≠,10X,≠THETABULK=≠,F7.4,3X,≠BULK TEMP=≠,F6.1,≠ K≠/)
      PRINT 120,NU1,NU2
120   FORMAT(≠ ≠,10X,≠LOCAL NUSSELT NO AT Y=0 =≠,F7.2,3X,
     1≠AT Y=H =≠,F7.2/)
      PRA=PR(LL)*DEN*U0**2
      PRB=PRA*1.4479*10.**(-5)
      PRINT 121,PR(LL),PRA,PRB
121   FORMAT(≠ ≠,10X,≠PRESSURE=≠,F11.0,3X,≠=≠,F13.0,≠ DYNE/CM2≠,3X,≠=≠,
     1F7.0,≠ PSI≠//)
43    CONTINUE
C
C     CHECK U2 AND THETA2 FOR CONVERGENCE
C
      DO 44 I=1,MX
      IF(ABS(U2(I)-U1(I)).GE..001) GO TO 45
      IF(ABS(THETA2(I)-THETA1(I)).GE..001) GO TO 45
44    CONTINUE
      GO TO 47
45    CONTINUE
      DO 46 I=1,MX
      U1(I)=U2(I)
      THETA1(I)=THETA2(I)
46    CONTINUE
47    CONTINUE
      STOP
      END
```

```
      SUBROUTINE CALBET(JA,KJ,DY,DX,U0,RB,PN,K,CP,TEMP0,TEMPW1,TEMPW2
     1,TEMPM,U,DUDY,THETA,DETADY,ETA,ALPHA,BETA)
C
C     THIS SUBROUTINE CALCULATES ALPHA AND BETA USED IN SOLVING THE
C     SET OF CONTINUITY AND MOMENTUM EQS.(7.19)
C
      REAL U(1),DUDY(1),THETA(1),DETADY(1),ETA(1),ALPHA(1),BETA(1),K
      J=JA
      KJI=KJ+1
      KJJ=KJ-1
      KJK=KJ-2
      DUDY0=(2.*U(J+2)-9.*U(J+1)+18.*U(J)-11.)/6./DY
      DUDY(1)=(-U(J+2)+6.*U(J+1)-3.*U(J)-2.)/6./DY
      J=J+1
      DUDY(2)=(-U(J+2)+8.*U(J+1)-8.*U(J-1)+1.)/12./DY
      J=J+1
      DO 1 I=3,KJK
      DUDY(I)=(-U(J+2)+8.*U(J+1)-8.*U(J-1)+U(J-2))/12./DY
      J=J+1
1     CONTINUE
      DUDY(KJJ)=(8.*U(J+1)-8.*U(J-1)+U(J-2))/12./DY
      J=J+1
      DUDY(KJ)=(3.*U(J)-6.*U(J-1)+U(J-2))/6./DY
      DUDY(KJI)=(-18.*U(J)+9.*U(J-1)-2.*U(J-2))/6./DY
      IF(ABS(DUDY0*U0/RB).LT.1.) GO TO 2
      ETA0=282000.*EXP(-.024*PN*(TEMPW1-TEMPM))*(ABS(DUDY0*U0
     1/RB))**(PN-1.)
      GO TO 3
2     CONTINUE
      ETA0=282000.*EXP(-.024*PN*(TEMPW1-TEMPM))
3     CONTINUE
      J=JA
      DO 5 I=1,KJ
      TEMP=THETA(J)*(TEMP0-TEMPW1)+TEMPW1
      J=J+1
      IF(ABS(DUDY(I)*U0/RB).LT.1.) GO TO 4
      ETA(I)=282000.*EXP(-.024*PN*(TEMP-TEMPM))*(ABS(DUDY(I)*U0
     1/RB))**(PN-1.)
      GO TO 5
4     CONTINUE
      ETA(I)=282000.*EXP(-.024*PN*(TEMP-TEMPM))
5     CONTINUE
      IF(ABS(DUDY(KJI)*U0/RB).LT.1.) GO TO 6
      ETA(KJI)=282000.*EXP(-.024*PN*(TEMPW2-TEMPM))*(ABS(DUDY(KJI)*U0
     1/RB))**(PN-1.)
      GO TO 7
6     CONTINUE
      ETA(KJI)=282000.*EXP(-.024*PN*(TEMPW2-TEMPM))
7     CONTINUE
      IF(ABS(DUDY0*U0/RB).GT.1.) GO TO 8
      IA=1
      IF(ABS(DUDY(1)*U0/RB).LE.1.) GO TO 12
8     CONTINUE
      I=1
      IF(ABS(DUDY(2)*U0/RB).LE.1.) GO TO 11
      DETADY(1)=(ETA(2)-ETA0)/2./DY
9     CONTINUE
      IA=I+1
      DO 10 I=IA,KJJ
      IF(ABS(DUDY(I+1)*U0/RB).LE.1.) GO TO 11
      DETADY(I)=(ETA(I+1)-ETA(I-1))/2./DY
10    CONTINUE
      DETADY(KJ)=(ETA(KJI)-ETA(KJJ))/2./DY
      GO TO 16
11    CONTINUE
      DETADY(I)=(ETA(I+1)-ETA(I-1))/2./DY
      IF(ABS(DUDY(I+2)*U0/RB).LT.1.) GO TO 12
      I=I+1
      DETADY(I)=0.
      GO TO 9
12    CONTINUE
      DETADY(I+1)=(3.*ETA(I+1)-4.*ETA(I)+ETA(I-1))/2./DY/2.
      IA=I+2
13    CONTINUE
      DO 14 I=IA,KJ
      IF(ABS(DUDY(I+1)*U0/RB).GT.1.) GO TO 15
      DETADY(I)=0.
14    CONTINUE
      GO TO 16
15    CONTINUE
      DETADY(I)=(-ETA(I+2)+4.*ETA(I+1)-3.*ETA(I))/2./DY/2.
      GO TO 9
16    CONTINUE
      DO 17 I=1,KJ
      ALPHA(I)=K/ETA(I)/CP*DY**2/DX
      BETA(I)=DETADY(I)*DY/2./ETA(I)
17    CONTINUE
      RETURN
      END
```

```
      SUBROUTINE GAUSS(KJ,DY,CA,DA,THETA0,A,B,C,D,E,F,G,H,Q,S,T,THETA
     1,THETA2,GAMMA,DELTA)
C
C     THIS SUBROUTINE SOLVES THE TRIDIAGONAL SYSTEM OF ENERGY
C     EQS.(7.26) USING THOMAS≠ METHOD
C
      REAL A(1),B(1),C(1),D(1),E(1),F(1),G(1),H(1),Q(1),S(1),T(1)
      REAL THETA(1),THETA2(1),GAMMA(1),DELTA(1)
      B(1)=GAMMA(1)+2.
      C(1)=-1.
      E(1)=(GAMMA(1)-2.)*THETA(1)
      F(1)=THETA(2)
      G(1)=2.*DY**2*DELTA(1)+THETA0
      H(1)=E(1)+F(1)+G(1)
      KJJ=KJ-1
      DO 1 I=2,KJJ
      A(I)=-1.
      B(I)=GAMMA(I)+2.
      C(I)=-1.
      D(I)=THETA(I-1)
      E(I)=(GAMMA(I)-2.)*THETA(I)
      F(I)=THETA(I+1)
      G(I)=2.*DY**2*DELTA(I)
      H(I)=D(I)+E(I)+F(I)+G(I)
    1 CONTINUE
      CB=CA+1.
      DB=DA+1.
      A(KJ)=-1./DB
      B(KJ)=GAMMA(KJ)/2.+1./DA
      D(KJ)=THETA(KJJ)/CB
      E(KJ)=(GAMMA(KJ)/2.-1./CA)*THETA(KJ)
      G(KJ)=DY**2*DELTA(KJ)+THETA(KJ+1)/CA/CB+THETA2(KJ+1)/DA/DB
      H(KJ)=D(KJ)+E(KJ)+G(KJ)
      S(1)=B(1)
      T(1)=H(1)/S(1)
      DO 2 I=2,KJ
      Q(I-1)=C(I-1)/S(I-1)
      S(I)=B(I)-A(I)*Q(I-1)
      T(I)=(H(I)-A(I)*T(I-1))/S(I)
    2 CONTINUE
      THETA2(KJ)=T(KJ)
      L=KJJ
      DO 3 I=2,KJ
      THETA2(L)=T(L)-Q(L)*THETA2(L+1)
      L=L-1
    3 CONTINUE
      THETA0=0.
      KJI=KJ+1
      DO 4 I=1,KJI
      THETA(I)=THETA2(I)
    4 CONTINUE
      RETURN
      END
```

THE LUBFICATION PROBLEM - POWER LAW FLUID

TEMPERATURE DEPENDENT VISCOSITY

FINITE DIFFERENCES SOLUTION

TEMPO= 403.0 K TEMPW1= 433.0 K TEMPW2= 433.0 K TEMPM= 399.5 K

U0= 15.00 CM/SEC K= .00061 CAL/CM SEC K DENSITY= .794 G/CM3

POWER LAW INDEX= .453 CP= .6 CAL/G K L= 10.0 CM

M= 50 N= 25 LZ= 100 B AT 0= .025 CM B AT L= .0125 CM

SOLUTION

ITERATION 5

COLUMN 1 X=0. UAVG= .3467

Y	U(Y)	U(Y)*U0	THETA(Y)	TEMP(Y)
0.000	1.0000	15.0000	1.0000	403.0 K
.020	.9494	14.2407	1.0000	403.0 K
.040	.9097	13.6458	1.0000	403.0 K
.060	.8721	13.0815	1.0000	403.0 K
.080	.8353	12.5301	1.0000	403.0 K
.100	.7995	11.9930	1.0000	403.0 K
.120	.7647	11.4709	1.0000	403.0 K
.140	.7309	10.9633	1.0000	403.0 K
.160	.6980	10.4702	1.0000	403.0 K
.180	.6661	9.9913	1.0000	403.0 K
.200	.6351	9.5264	1.0000	403.0 K
.220	.6050	9.0753	1.0000	403.0 K
.240	.5759	8.6378	1.0000	403.0 K
.260	.5476	8.2136	1.0000	403.0 K
.280	.5202	7.8025	1.0000	403.0 K
.300	.4936	7.4044	1.0000	403.0 K
.320	.4679	7.0190	1.0000	403.0 K
.340	.4431	6.6461	1.0000	403.0 K
.360	.4190	6.2856	1.0000	403.0 K
.380	.3958	5.9371	1.0000	403.0 K
.400	.3734	5.6005	1.0000	403.0 K
.420	.3517	5.2755	1.0000	403.0 K
.440	.3308	4.9621	1.0000	403.0 K
.460	.3107	4.6599	1.0000	403.0 K
.480	.2912	4.3687	1.0000	403.0 K
.500	.2726	4.0884	1.0000	403.0 K
.520	.2546	3.8187	1.0000	403.0 K
.540	.2373	3.5594	1.0000	403.0 K
.560	.2207	3.3103	1.0000	403.0 K
.580	.2046	3.0713	1.0000	403.0 K
.600	.1895	2.8421	1.0000	403.0 K
.620	.1748	2.6225	1.0000	403.0 K
.640	.1608	2.4123	1.0000	403.0 K
.660	.1474	2.2114	1.0000	403.0 K
.680	.1346	2.0194	1.0000	403.0 K
.700	.1224	1.8362	1.0000	403.0 K
.720	.1108	1.6617	1.0000	403.0 K
.740	.0997	1.4956	1.0000	403.0 K
.760	.0892	1.3378	1.0000	403.0 K
.780	.0792	1.1879	1.0000	403.0 K
.800	.0697	1.0460	1.0000	403.0 K
.820	.0608	.9117	1.0000	403.0 K
.840	.0523	.7849	1.0000	403.0 K
.860	.0444	.6655	1.0000	403.0 K
.880	.0369	.5532	1.0000	403.0 K
.900	.0299	.4480	1.0000	403.0 K
.920	.0233	.3497	1.0000	403.0 K
.940	.0172	.2583	1.0000	403.0 K
.960	.0116	.1740	1.0000	403.0 K
.980	.0063	.0939	1.0000	403.0 K
1.000	0.0000	0.0000	1.0000	403.0 K

COLUMN 6 X= .2732

Y	U(Y)	U(Y)*U0	THETA(Y)	TEMP(Y)	ETA (POISE)
0.000	1.0000	15.0000	0.0000	433.0 K	4286.5
.020	.9640	14.4607	-.0235	433.7 K	4273.7
.040	.9284	13.9263	-.0454	434.4 K	4266.2
.060	.8932	13.3975	-.0657	435.0 K	4264.0
.080	.8583	12.8749	-.0844	435.5 K	4267.0
.100	.8239	12.3591	-.1017	436.0 K	4275.1
.120	.7900	11.8507	-.1174	436.5 K	4288.4
.140	.7567	11.3501	-.1318	437.0 K	4306.5
.160	.7239	10.8580	-.1447	437.3 K	4329.8
.180	.6917	10.3748	-.1563	437.7 K	4358.0
.200	.6601	9.9008	-.1666	438.0 K	4391.1
.220	.6291	9.4364	-.1756	438.3 K	4429.1
.240	.5988	8.9821	-.1834	438.5 K	4472.2
.260	.5692	8.5380	-.1900	438.7 K	4520.2
.280	.5403	8.1045	-.1955	438.9 K	4573.3
.300	.5121	7.6817	-.1998	439.0 K	4631.6
.320	.4847	7.2699	-.2031	439.1 K	4695.0
.340	.4580	6.8693	-.2054	439.2 K	4763.7
.360	.4320	6.4798	-.2067	439.2 K	4837.8
.380	.4068	6.1017	-.2070	439.2 K	4917.5
.400	.3823	5.7350	-.2065	439.2 K	5002.8
.420	.3587	5.3798	-.2051	439.2 K	5093.9
.440	.3357	5.0359	-.2029	439.1 K	5190.9
.460	.3136	4.7034	-.1996	439.0 K	5294.2
.480	.2922	4.3823	-.1961	438.9 K	5403.9
.500	.2715	4.0725	-.1916	438.7 K	5520.1
.520	.2516	3.7738	-.1865	438.6 K	5643.3
.540	.2324	3.4863	-.1807	438.4 K	5773.6
.560	.2140	3.2096	-.1743	438.2 K	5911.4
.580	.1963	2.9438	-.1673	438.0 K	6057.0
.600	.1792	2.6886	-.1598	437.8 K	6210.8
.620	.1629	2.4439	-.1518	437.6 K	6373.2
.640	.1473	2.2094	-.1433	437.3 K	6544.6
.660	.1323	1.9850	-.1343	437.0 K	6725.5
.680	.1180	1.7705	-.1249	436.7 K	6916.5
.700	.1044	1.5657	-.1151	436.5 K	7118.1
.720	.0914	1.3703	-.1049	436.1 K	7331.1
.740	.0789	1.1842	-.0944	435.8 K	7556.1
.760	.0671	1.0071	-.0835	435.5 K	7794.0
.780	.0559	.8387	-.0724	435.2 K	8045.7
.800	.0453	.6789	-.0609	434.8 K	8312.3
.820	.0352	.5274	-.0492	434.5 K	8594.9
.840	.0256	.3840	-.0372	434.1 K	8894.9
.860	.0166	.2484	-.0250	433.8 K	9214.0
.880	.0080	.1205	-.0126	433.4 K	9554.0
.900	0.0000	0.0000	0.0000	433.0 K	9916.9

THETABULK= -.1385 BULK TEMP= 437.2 K

LOCAL NUSSELT NO AT Y=0 = 8.78 AT Y=H = 4.58

PRESSURE= 1386045. = 247616938. DYNE/CM2 = 3585. PSI

COLUMN 11   X= .5463

Y	U(Y)	U(Y)*U0	THETA(Y)	TEMP(Y)	ETA (POISE)
0.000	1.0000	15.0000	0.0000	433.0 K	4511.8
.020	.9672	14.5075	-.0218	433.7 K	4486.5
.040	.9344	14.0165	-.0422	434.3 K	4466.1
.060	.9019	13.5278	-.0612	434.8 K	4450.4
.080	.8694	13.0416	-.0788	435.4 K	4439.5
.100	.8372	12.5586	-.0950	435.8 K	4433.1
.120	.8053	12.0793	-.1098	436.3 K	4431.2
.140	.7736	11.6040	-.1234	436.7 K	4433.5
.160	.7422	11.1333	-.1356	437.1 K	4440.7
.180	.7112	10.6676	-.1466	437.4 K	4452.0
.200	.6805	10.2073	-.1563	437.7 K	4467.5
.220	.6502	9.7528	-.1648	437.9 K	4487.3
.240	.6203	9.3043	-.1720	438.2 K	4511.3
.260	.5908	8.8624	-.1781	438.3 K	4539.5
.280	.5618	8.4273	-.1830	438.5 K	4572.0
.300	.5333	7.9992	-.1866	438.6 K	4608.7
.320	.5052	7.5785	-.1895	438.7 K	4649.6
.340	.4777	7.1654	-.1912	438.7 K	4694.8
.360	.4507	6.7601	-.1918	438.8 K	4744.3
.380	.4242	6.3628	-.1914	438.7 K	4798.2
.400	.3982	5.9737	-.1900	438.7 K	4856.4
.420	.3729	5.5930	-.1877	438.6 K	4919.1
.440	.3480	5.2207	-.1844	438.5 K	4986.4
.460	.3238	4.8570	-.1803	438.4 K	5058.3
.480	.3001	4.5019	-.1753	438.3 K	5134.8
.500	.2770	4.1556	-.1694	438.1 K	5216.1
.520	.2545	3.8180	-.1628	437.9 K	5302.4
.540	.2326	3.4892	-.1554	437.7 K	5393.7
.560	.2113	3.1693	-.1472	437.4 K	5490.1
.580	.1905	2.8581	-.1383	437.1 K	5591.7
.600	.1704	2.5557	-.1287	436.9 K	5698.8
.620	.1508	2.2620	-.1184	436.6 K	5811.5
.640	.1318	1.9771	-.1075	436.2 K	5929.9
.660	.1134	1.7007	-.0960	435.9 K	6054.3
.680	.0955	1.4329	-.0838	435.5 K	6184.8
.700	.0782	1.1736	-.0712	435.1 K	6321.6
.720	.0615	.9226	-.0579	434.7 K	6464.9
.740	.0453	.6799	-.0442	434.3 K	6615.0
.760	.0297	.4453	-.0299	433.9 K	6772.2
.780	.0146	.2187	-.0152	433.5 K	6936.6
.800	0.0000	0.0000	0.0000	433.0 K	7108.7

THETABULK= -.1282   BULK TEMP= 436.8 K

LOCAL NUSSELT NO AT Y=0 =   6.78   AT Y=H =   6.00

PRESSURE=   2402252.   =   429162326. DYNE/CM2   = 6214. PSI

COLUMN 16   X= .8195

Y	U(Y)	U(Y)*U0	THETA(Y)	TEMP(Y)	ETA (POISE)
0.000	1.0000	15.0000	0.0000	433.0 K	5006.4
.020	.9727	14.5899	-.0196	433.6 K	4943.8
.040	.9450	14.1753	-.0381	434.1 K	4885.9
.060	.9171	13.7565	-.0554	434.7 K	4832.3
.080	.8889	13.3337	-.0717	435.1 K	4783.0
.100	.8605	12.9072	-.0868	435.6 K	4738.0
.120	.8318	12.4773	-.1007	436.0 K	4697.2
.140	.8030	12.0443	-.1135	436.4 K	4660.3
.160	.7739	11.6086	-.1252	436.8 K	4627.5
.180	.7447	11.1704	-.1356	437.1 K	4598.6
.200	.7153	10.7300	-.1449	437.3 K	4573.5
.220	.6859	10.2879	-.1531	437.6 K	4552.3
.240	.6563	9.8443	-.1600	437.8 K	4534.7
.260	.6266	9.3996	-.1658	438.0 K	4520.9
.280	.5969	8.9541	-.1704	438.1 K	4510.8
.300	.5672	8.5081	-.1738	438.2 K	4504.3
.320	.5375	8.0621	-.1760	438.3 K	4501.5
.340	.5078	7.6163	-.1770	438.3 K	4502.3
.360	.4781	7.1711	-.1769	438.3 K	4506.6
.380	.4485	6.7268	-.1756	438.3 K	4514.6
.400	.4189	6.2837	-.1731	438.2 K	4526.3
.420	.3895	5.8423	-.1695	438.1 K	4541.5
.440	.3602	5.4028	-.1646	437.9 K	4560.5
.460	.3310	4.9655	-.1587	437.8 K	4583.1
.480	.3021	4.5308	-.1515	437.5 K	4609.5
.500	.2733	4.0990	-.1433	437.3 K	4639.6
.520	.2447	3.6703	-.1339	437.0 K	4673.6
.540	.2163	3.2452	-.1234	436.7 K	4711.4
.560	.1882	2.8237	-.1117	436.4 K	4753.2
.580	.1604	2.4063	-.0990	436.0 K	4799.0
.600	.1329	1.9931	-.0851	435.6 K	4848.9
.620	.1056	1.5845	-.0702	435.1 K	4902.9
.640	.0787	1.1807	-.0542	434.6 K	4961.3
.660	.0521	.7819	-.0372	434.1 K	5023.9
.680	.0259	.3882	-.0191	433.6 K	5091.1
.700	0.0000	0.0000	0.0000	433.0 K	5162.8

THETABULK= -.1176   BULK TEMP= 436.5 K

LOCAL NUSSELT NO AT Y=0 =   8.55   AT Y=H =   8.33

PRESSURE=   2932476.   =   523836853. DYNE/CM2   =   7585. PSI

COLUMN 21   X=1.0926

Y	U(Y)	U(Y)*U0	THETA(Y)	TEMP(Y)	ETA (POISE)
0.000	1.0000	15.0000	0.0000	433.0 K	6366.7
.020	.9820	14.7301	-.0168	433.5 K	6150.3
.040	.9630	14.4456	-.0329	434.0 K	5946.9
.060	.9431	14.1462	-.0484	434.5 K	5755.8
.080	.9221	13.8315	-.0632	434.9 K	5576.1
.100	.9001	13.5012	-.0772	435.3 K	5407.2
.120	.8770	13.1549	-.0903	435.7 K	5248.7
.140	.8526	12.7923	-.1026	436.1 K	5099.9
.160	.8275	12.4132	-.1140	436.4 K	4960.4
.180	.8012	12.0174	-.1244	436.7 K	4829.7
.200	.7736	11.6045	-.1337	437.0 K	4707.5
.220	.7450	11.1746	-.1420	437.3 K	4593.4
.240	.7152	10.7274	-.1490	437.5 K	4487.2
.260	.6842	10.2630	-.1549	437.6 K	4388.4
.280	.6521	9.7813	-.1594	437.8 K	4297.0
.300	.6188	9.2824	-.1626	437.9 K	4212.6
.320	.5844	8.7664	-.1644	437.9 K	4135.0
.340	.5489	8.2336	-.1646	437.9 K	4064.1
.360	.5123	7.6841	-.1633	437.9 K	3999.8
.380	.4746	7.1184	-.1604	437.8 K	3941.8
.400	.4358	6.5368	-.1557	437.7 K	3890.2
.420	.3960	5.9398	-.1493	437.5 K	3844.9
.440	.3552	5.3281	-.1410	437.2 K	3805.8
.460	.3135	4.7022	-.1308	436.9 K	3772.9
.480	.2709	4.0631	-.1186	436.6 K	3746.1
.500	.2274	3.4114	-.1044	436.1 K	3725.6
.520	.1832	2.7461	-.0880	435.6 K	3711.4
.540	.1383	2.0742	-.0694	435.1 K	3703.5
.560	.0927	1.3907	-.0486	434.5 K	3702.0
.580	.0466	.6990	-.0255	433.8 K	3707.2
.600	0.0000	0.0000	0.0000	433.0 K	3718.9

THETABULK= -.1073   BULK TEMP= 436.2 K

LOCAL NUSSELT NO AT Y=0 =   7.95   AT Y=H =   12.43

PRESSURE=   2500850.   =   446776834. DYNE/CM2   =   6469. PSI

COLUMN 26   X=1.3658

Y	U(Y)	U(Y)*U0	THETA(Y)	TEMP(Y)	ETA (POISE)
0.000	1.0000	15.0000	0.0000	433.0 K	14160.4
.020	.9957	14.9362	-.0137	433.4 K	13283.5
.040	.9908	14.8614	-.0272	433.8 K	11853.9
.060	.9845	14.7672	-.0407	434.2 K	10246.5
.080	.9762	14.6437	-.0540	434.6 K	8788.4
.100	.9656	14.4836	-.0670	435.0 K	7690.4
.120	.9524	14.2859	-.0797	435.4 K	6890.3
.140	.9366	14.0494	-.0920	435.8 K	6255.7
.160	.9181	13.7713	-.1037	436.1 K	5722.8
.180	.8965	13.4482	-.1147	436.4 K	5268.8
.200	.8718	13.0767	-.1249	436.7 K	4878.3
.220	.8436	12.6537	-.1340	437.0 K	4539.6
.240	.8117	12.1757	-.1419	437.3 K	4243.9
.260	.7760	11.6395	-.1484	437.5 K	3984.6
.280	.7361	11.0422	-.1533	437.6 K	3756.8
.300	.6921	10.3811	-.1561	437.7 K	3556.2
.320	.6436	9.6536	-.1567	437.7 K	3379.8
.340	.5905	8.8577	-.1548	437.6 K	3224.9
.360	.5328	7.9920	-.1499	437.5 K	3089.6
.380	.4704	7.0556	-.1417	437.3 K	2972.0
.400	.4032	6.0481	-.1298	436.9 K	2871.1
.420	.3314	4.9703	-.1138	436.4 K	2785.7
.440	.2549	3.8236	-.0933	435.8 K	2715.2
.460	.1740	2.6105	-.0677	435.0 K	2659.0
.480	.0890	1.3344	-.0366	434.1 K	2616.9
.500	0.0000	0.0000	0.0000	433.0 K	2588.2

THETABULK= -.0980   BULK TEMP= 435.9 K

LOCAL NUSSELT NO AT Y=0 =   6.98   AT Y=H =   20.35

PRESSURE=   0.   =   0. DYNE/CM2   =   0. PSI .